Understanding and exploring the phenotypic and genetic variation in a model system *Brachypodium distachyon* under abiotic stress

A thesis submitted to Aberystwyth University for the degree of Doctor of Philosophy in Biological Sciences

Kritika Bhardwaj

24.08.2022

IBERS
Athrofa y Gwyddorau Biolegol, Amgylcheddol a Gwledig
Institute of Biological, Environmental and Rural Sciences

National Plant PHENOMICS Centre

ACKNOWLEDGEMENTS

Aberystwyth University funded the current research, AberDoc and President's scholarship award and the Rank Prize Funds- Covid19 disruption in response to hardship caused by the restrictions imposed due to the pandemic. I want to thank the National Phenomics Centre for sharing the preliminary data in the collaborative project.

Firstly, I am incredibly grateful and would like to express my sincere gratitude to my supervisor Dr Maurice Bosch for his patience and unconditional trust. He not only allowed me to be a part of his lab but also promoted my personal and professional development during this journey. I also thank Professor John Doonan for his help, explanations, and inspiring conversations.

I want to thank Agnieszka Gladala-Kostarz, Marina Muñoz Triviño, Rosario Iacono, Ludi Wang, José Carli, Rakesh Bhatia, Candida Nibau, Emma Timms-Taravella, Samantha Gill, Simon Betts and Sue Dalton for creating a supportive and productive work environment in the office and lab. Special thanks to Giovanni Sanfratello, Odin Morón García, Gina Garzon Martinez, and Chandra Bhan for their friendship and support in statistical tool guidance. I am highly thankful to Fiona Corke for her contribution to the experimental setup and her patience in answering my questions. Immense gratitude to Tom Thomas, Andrew Tavarella, and Rob Darby for their invaluable knowledge and research assistance.

Living in Aberystwyth would not have been possible without the student community, making this journey an unforgettable experience. Antonella, Ben, and Rhiannon for the time together, support, and parties. A special thanks to Lukasz, an incredible person and a fantastic partner in crime. His continuous support cheered me up from time to time and helped me get through the most challenging moments of my thesis writing.

Last but not least, thanks to my beautiful family for their encouragement and my younger sibling Ritika for giving me the strength to finish this goal.

THESIS WORD COUNT

54590

DECLARATION

This work has not previously been accepted in substance for any degree and is not being concurrently submitted in candidature for any degree.

Signed (Candidate)

Date 24.08.2022

STATEMENT 1

This thesis is the result of my investigations, except where otherwise stated. Other sources are acknowledged by footnotes giving explicit references. A bibliography is appended.

Signed (Candidate)

Date 24.08.2022

STATEMENT 2

I hereby give consent for my thesis, if accepted, to be available for photocopying and inter-library loan, and for the title and summary to be made available to outside organisations.

Signed (Candidate)

Date 24.08.2022

SUMMARY

With the unpredictable environmental change, negative phenotypic plasticity in agriculture is one of the significant challenges to overcome by enhancing food security and productivity globally. Nutrient limitation is one of the significant abiotic stresses faced by plants which causes numerous alterations in plant morphology, physiology and reproductive growth and is poorly understood for crop improvement. This study aims to provide information on how nutrient limitation affects the growth and development of the model grass *Brachypodium distachyon*.

In particular, the first part of the research focuses on the screening and selecting nutrients (NPKB) and their dose-response (20%, 4%, and 0%) in above and below-ground measurements showing a significant decrease under nitrate and phosphate limitation. More detailed analysis, including total monosaccharide and enzymatic sugar release, showed significant reduction after the nutrient limitation stress in both the accessions of Brachypodium. Furthermore, I explored 17 Brachypodium genotypes to assess the tolerant and susceptible parental combination in response to nutrient limitations. Iraqi and Turkish genotypes suggest potential parents with the available RIL populations for studying detailed analysis in future. Seven significant QTLs were found where the two major QTLs were located on chromosomes 3 and 1 under nutrient limitation colocalising with the VERNALIZATION1 and VERNALIZATION2 loci identified as flowering regulators in the domesticated cereal crops. The results further suggest that the potential genes identified in the study will decipher the molecular basis of nutrient tolerance in Brachypodium.

The overexpression of pectin methylesterase inhibitor (PMEI-OE) showed a significant increase in gene expression compared to wild-type. PMEI_1 and PMEI_3 lines reduced significant pectin methylesterase activity suggesting the inhibitory effect of PMEI-OE. However, PMEI-OE lines significantly increased the saccharification efficiency in PMEI_1, PMEI_2, and PMEI_3 under Hoagland (control) whereas showing recalcitrance under nutrient treatment.

Table of content

List of figures

List of Tables

Chapter 1 : General introduction

1.1 Introduction

Biomass from agricultural residues of cereals (e.g., wheat and rice straw) and dedicated bioenergy crops, including Miscanthus, represent significant renewable resources to produce bioenergy and bioproducts. In the next decade, reducing the dependency on fossil fuels and producing biomolecules, bioenergy, and biomaterials from plant biomass is a substantial challenge. Unlike fossil sources, creating energy from renewable sources has a lower increase in the total amount of CO_2 in the atmosphere than fossil fuels. Thus their use could contribute to slowing down the effects of global warming. A renewable energy source, able to completely replace fossil sources, has to satisfy the needs for the current usage and future energy demand and the production of chemicals and materials.

One of our challenges is developing a system to effectively exploit biomass as a source of organic carbon. In this regard, attention has focused on the use of plant biomass. Biomass is the largest reservoir of organic carbon on Earth that could be used as a source of molecules for the production of fuels and chemicals while reducing carbon emissions dramatically. Human history and the development of our society are strictly connected to the history of the Poaceae family (grasses) and their cultivation over time (Piperno *et al*., 2007). Meanwhile, the world population is estimated to rapidly increase to more than 9,100 million by 2050, impairing environmental sustainability by putting a strain on the planet's life-support and contributing to environmental degradation and resource depletion (Godfray *et al*., 2010; Wilson *et al*., 2019).

In addition, agricultural production will increase by 70% to satisfy the anticipated demand for food. These required increases in the production of our food will be obstructed by global

climate change. Plants will increasingly be subjected to a wide range of abiotic and biotic stresses during their lifecycle, affecting their yield and production. Such agricultural losses will threaten food security on a worldwide scale. By providing staple food for the vast majority of humanity and food for the grazing animals from which society derives most of its protein, they shaped the cultural history of humans. Nutrient stress is a type of abiotic stress that may result from the presence of the element's excess concentrations or its lower availability. The impact of low nutrient availability in biomass crops experienced with cell-wall consistency traits will affect the lower-grade agricultural land. Developing tolerance to nutrient stress in crop plants can help expand agriculture to unexplored harsh and nutrient-poor soils. Understanding the phenotypic and genotypic responses to environmental stresses, particularly in a period of predicted climate change, is a significant and essential challenge (FAO, 2019).

1.2 Selections for improved yield and biomass productivity

Selection criteria to improve crop yield and biomass quality growing on marginal lands are essential in production for energy, feed, and forage purposes. Moreover, crops like Miscanthus growing on marginal or broken lands can improve the soil quality and biomass yield production (Costa *et al*., 2019). Consequently, deficiencies in nutrients can decrease root growth and alter root morphology. Under this stress factor, plants disperse an essential portion of biomass to the roots. In comparison with regulation, plants under N stress have a more significant root: shoot ratio and shorter lateral branches. Plants grown in semi-arid and arid regions have a thick root system in the soil, which helps to efficiently absorb nutrients with a high influx of soil water (Merrill & Cornwell, 2005).

According to Hirel *et al*. (2007), it is possible to obtain more efficient genotypes by increasing the efficacy of absorption and/or intake. Some authors regard the ability of genotypes to grow, develop and replicate under stress conditions as low nutrient tolerance (de Oliveira Maia Júnior *et al*., 2020), and others as the efficiency of nutrient use (Fritsche-Neto *et al*., 2010). In both cases, the plant uses physiological and often anatomical mechanisms, resistance or efficacy, to escape stress or rapidly recover from its effects. In this context, three key strategies used by plants to deal with the unpredictable availability of resources have been identified:

1. Specialisation: a genotype is adapted to a particular environment (*Brachypodium*)
2. Generalisation: a genotype with moderate suitability for most environments (Arabidopsis, Miscanthus)
3. Phenotypic plasticity: environmental signals may interact with the genotype and promote the creation of alternative environments (*Triticum aestivum*)

According to Bradshaw (2006), phenotypic plasticity is strongly associated with yield stability; therefore, a desirable trait is not necessarily low plasticity (or high strength). The explanation is that yields of tolerant genotypes are typically moderate even under ideal growing conditions, which is interesting for crops under permanent stress in marginal regions. Thus, in areas with low availability of resources, the efficiency of these 'generalised' genotypes is greater. There is, however, no substantial yield increase under non-limiting environmental conditions. Because of this, many enhancement studies aim to improve plant efficiency, i.e., high phenotypic plasticity breeding genotypes.

Consequently, if plants are grown under limited cultivation conditions, they will use limited resources to produce adequate yields; however, yields will be high under optimum

conditions. The genetic regulation of both tolerance and efficiency of use is quantitative and includes several loci spread across different genome regions of crop organisms. Genetic variation within the trait population enables quantitative trait loci to be identified to recognise molecular markers linked to genes of interest and thus facilitate marker-assisted selection (Singh & Singh, 2015).

This introductory section summarises present knowledge on the phenological and biomass-related traits under low nutrient availability. This section will also describe, *Brachypodium distachyon,* a model system for cereal, forage, and bioenergy crops, as all the experimental work in the present research is performed using the model system.

1.3 *Brachypodium distachyon*: a model system for grasses

Model systems are essential resources for research, including genetics, ecology, and cell biology, comprise diverse accessions, are readily available and differ majorly from experimental organisms. Previous studies have therefore defined and accepted *Brachypodium* as a model plant for grasses (Poaceae) in plant biology and the evolution of grasses in temperate climates (JP Vogel, 2016; Scholthof *et al*., 2018; Coomey *et al*., 2020). In addition, the genus *Brachypodium* has been recognised as evolutionary closer to cereal crops such as wheat, rice, barley, and maize, making it the most suitable model system for to study of cereal biology (Draper *et al*., 2001). *Brachypodium distachyon* is considered in C3 plants where it underlies a less complex, smallest grass genome (Bd21 accession; 272 Mb) when compared with other grasses like sorghum (*Sorghum bicolour*; 730 Mb), goat grass (*Aegilops tauschii*; 4020 Mb) by International *Brachypodium* Initiative (J. P. Vogel *et al*., 2010). Thus, this suggests the Brachypodium genome's simplicity due to uniformly distributed, short intergenic distances on gene distribution (Gottlieb *et al*., 2013).

Brachypodium underlies the Pooideae subfamily group and is considered the most agronomical important C3 grass group is considered phylogenetically sister to a large clade of C3 grasses like cereal and forage crops which are found in temperate climates (Brkljacic *et al*., 2011; Mur *et al*., 2011). This close phylogenetic relationship with the Poaceae family suggested that the *Brachypodium* genome can be used for dissecting genomic studies in this group due to its C3 photosynthetic system and adaptation to temperate climates (Figure 1.4). Thus, distributing them to higher latitudes suggests a tremendous genetic diversity in the Brachypodium genus.

Moreover, *Brachypodium distachyon* and its close relative's *B*. *stacei* and *B*. *hybridum* have been identified as new resources focusing on improving biofuel grass production. Previous studies suggested that the three cytotypes should be treated as three different species: two diploids, each with an extra chromosome base number, *B. distachyon* (x = 5, 2n = 10) and *B. stacei* (x = 10, 2n = 20), and they are derived allotetraploid with larger genome size, *B. hybridum* (x = 5+10, 2n = 30) (Catalan *et al*., 2012). The species have similar DNA content but vary in chromosome number due to multiple centric fusion/fission events. Manzaneda et al. (2015) suggested that allotetraploids are better adapted to aridity than diploid *Brachypodium*. It has shown great adaptation to different environments and is therefore of interest to the degree of diversity of the different cytotypes. The native distribution of all three species is mainly spread around the Mediterranean with small genome size, thus suggesting a model plant genus for temperate grasses.

Brachypodium species consists of small chromosomes with a variable base number (ranging from 5 to 9), making it rare in the Pooideae compared to other grass species having smaller chromosome numbers with a base number of 7 (Draper *et al*., 2001). *Triticum aestivum*

(wheat) and other temperate cereals and most types of forage grass are closely associated with Brachypodium, making it a valuable model for a wide range of biological aspects of cool-season grass biology (Draper *et al*., 2001; Barrero *et al*., 2012; Cui *et al*., 2012; Figueroa *et al*.,2015; Zhong *et al*., 2015). Furthermore, it can be deduced that *B*. *distachyon* occupies an essential phylogenetic position. Therefore, mapping information from the genome can be used to locate colinear regions in the cereal genome.

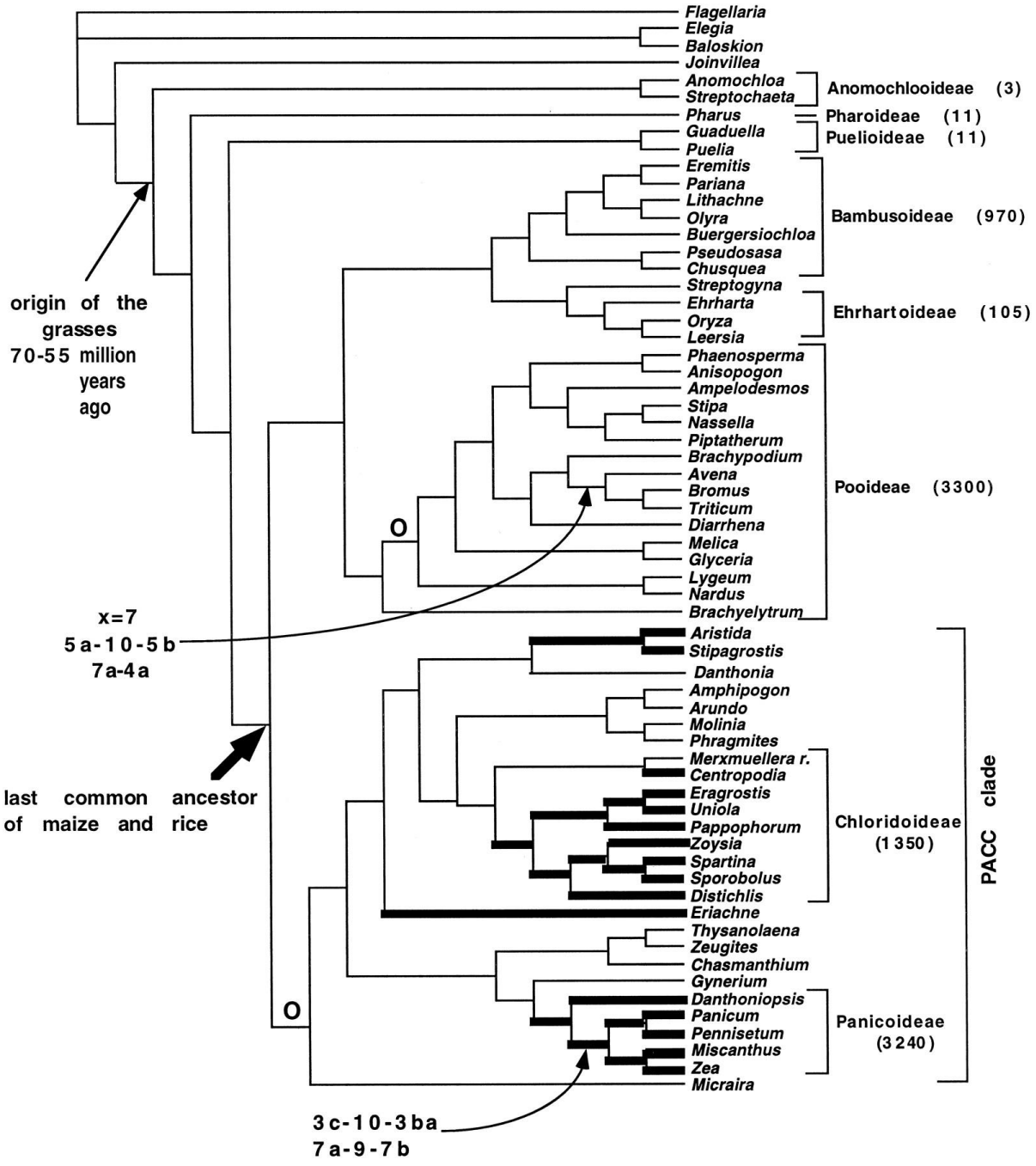

Figure 1-1: Phylogenetic relationship between grass family (Poaceae) members (EA Kellogg, 2001)

Natural diversity in *Brachypodium* wild accessions is another crucial resource required for a model system. One of the most powerful methods to attain biological diversity is creating recombinant lines segregating diverse alleles in different generations (Brkljacic *et al*., 2011). *Brachypodium* is a diploid, annual, perennial grass plant in temperate regions with varied

environments in its native and invasive ranges (Catalán P. *et al*., 2012). For many characteristics, including flowering time, vernalization responsiveness, and above-ground growth characteristics, significant natural variation has been found in *Brachypodium*. In comparative genomic approaches, the genome sequence of *Brachypodium* is used to help primary map characteristics in cereal crops (larger genome). In both tissue culture and greenhouse, it has the ability to expand, making the study more condensed. It is, therefore, a step forward in agricultural studies, both for discovering new genes and for the growth of new transgenic plants.

Abiotic stress has a significant effect on the production of food and feedstock crops of agricultural significance (*Brachypodium distachyon*) was first suggested in 2001 as a model system (Draper *et al*., 2001). It has all the desirable features of a model system, and a wide range of genetic and genomic instruments have already been created. From recent collection efforts, several hundred wild accessions are available; roughly 250 lines are described at *Brachypodium* resources (Garvin *et al*., 2008; Opanowicz, M *et al*., 2008; Mur *et al*., 2011). Consequently, *Brachypodium* serves as an essential model system with several interesting attributes for analysing plant-environmental interactions.

1.4 Abiotic stress and sustainable farming

Abiotic stresses cause an extensive loss to agricultural and biomass production as the world faces climate change and soil degradation, making today's agricultural food production increasingly unsustainable (Sheikh, 2006; Godfray *et al*., 2010; Tscharntke *et al*., 2012). Meanwhile, crops growing on abandoned, marginal lands (which are usually degraded agricultural soil) are often subjected to a range of abiotic stresses including water deficiency, flooding, temperature variation, and nutrient availability (Wang *et al*., 2003). Most of the marginal lands are of poor quality for agriculture and avoid competition. However, high yielding crops growing on these lands face the countenance of low nutrient availability, ultimately lowering the crop's yield under their threshold (Mehmood *et al*., 2017). The aim is to grow bioenergy crops on such grounds to optimise production practices.

Crops absorb water and plant nutrients from the soil as nutrients play a pivotal role in the plant's growth and metabolism. The root system is highly responsive to nutrient availability and distribution within the plant. Moreover, nutrients like potassium, nitrogen, phosphorus, and boron are essential for a plant's cell structure as these nutrients are potential growth-limiting in the natural environment and have unique physiological functions. This current scenario of nutrient limitation degrading sustainable agriculture has been further explained in the next section.

1.5 Principle of crop nutrition

Liebig's law or the law of the minimum, originally developed by Carl Sprengel (1840) and later popularized by Liebig & Playfair (1843), is applied to the biological populations and

ecosystem models for factors like mineral nutrients (Ploeg *et al*., 1999). It states that "Crop yields are proportional to the amount of the most limiting nutrient". This is because plant nutrients have specific and essential functions in metabolism which cannot replace each other. It is, therefore, crucial to focus on balanced nutrition and a healthy diet.

The law of the minimum is often demonstrated using a water barrel, with staves of different lengths and the barrel's capacity to hold water determined by the shortest stave. Similarly, crop yields are frequently affected by shortages of nutrients and water in the soil. Nutrients are classified into three sub-groups based on plant growth requirements:

- Macro or primary nutrients: nitrogen (N), phosphorous (P), and potassium (K)
- Major or secondary nutrients: calcium (Ca), magnesium (Mg), and sulphur (S)
- Micro-nutrients or trace elements: Chlorine (Cl), Iron (Fe), Manganese (Mn), boron (B), selenium (Se), zinc (Zn), copper (Cu), molybdenum (Mo) etc.

Yield responses to N, P, K and B are frequently observed and are often the most limiting factor to crop production. In the current study, nutrient stress has been previously exploited in the literature to investigate plant response to low soil fertility with a focus on yield quality (Gondwe et al., 2020). However, balanced nutrition of all plant nutrients is required to obtain the maximum yield. Therefore, the development of nutrient-resistant crops with enhanced soil resource acquisition is an important strategic goal for global agriculture (Vance et al., 2003; Lynch & Lynch, 2007). The research will focus on different low nutrient stress application strategies for quantitative trait loci (QTL) identification in recombinant inbred line populations of Brachypodium to ultimately enhance the productivity of grasses by assessing phenotypic traits. In the following paragraphs, I will discuss nutrient stressors (NPKB) and their role in a plant's development and growth.

1.5.1 Nitrogen stress

Nitrogen (N) is a naturally occurring mineral nutrient and is derived from the Greek word Nitron implying "saltpetre forming". It is present in all living forms is present in various chemical structures, and is an essential nutrient for plant growth (Schlegel *et al*., 2005; Fageria & Moreira, 2011). N use involves uptake, assimilation, translocation, recycling and remobilisation. 1.5% of the plant's dry weight is usually comprised of N derived from the atmosphere. N cannot be consumed by plants in this form and therefore involves three different ways:

- Biological fixation of N_2 to ammonia via rhizobacterium.
- Atmospheric fixation via lightening and photochemical conversions of N_2 to a nitrate.
- Haber-Bosch industrial fixation of N_2 to produce ammonia.

N is a crucial constituent of amino acids as it is vital for building blocks of proteins and an essential constituent of chlorophyll. Its compounds make up about 40-50% of the total protoplasm dry matter and about 1.5% of the total dry weight of plants (Figure 1-1). Mostly, roots absorb N from the soil and leaves and stems can take it up in small quantities from the atmosphere (X. Li *et al*., 2013).

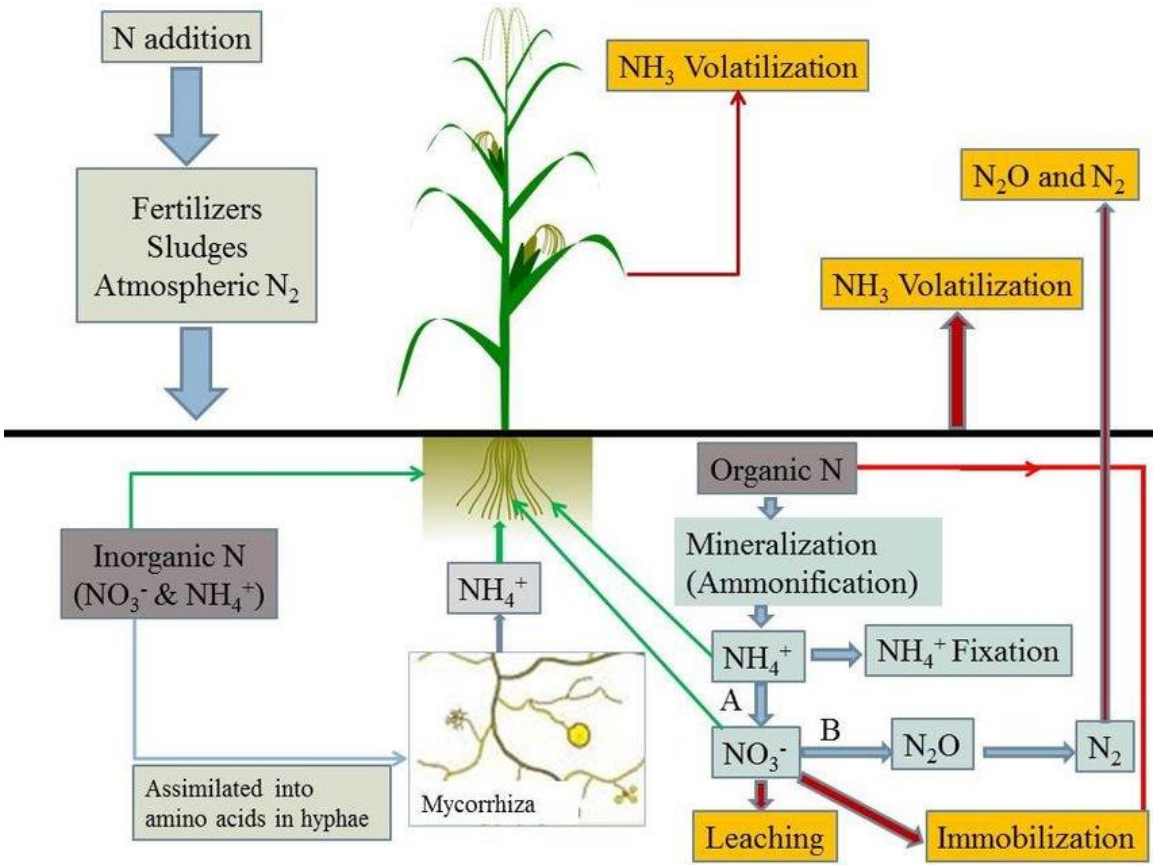

Figure 1-2: Basic scheme of inorganic and organic nitrogen uptake in plants in a simplified and modified version (M Seleiman, 2014)

N has been found as a limiting nutrient for fast growth in many agricultural settings. Although highly abundant (approximately 78% by volume) in the atmosphere but N is highly mobile (nitrate form) in most agricultural soils (JP Lynch, 2013). The abundance of N is often a limiting factor in plant growth in natural habitats as well as in agricultural production. Too little nitrogen application directly decreases crop yield, while excess N also causes adverse effects on plants, and this problem continues to focus on crop production (Leghari *et al*., 2016).

Most commonly, N stress in terms of deficiency contributes to chlorosis, stunted development, small leaves, slow growth, reduced shoot and early flowering (de Bang *et al*., 2021). Nitrogen-deficient plants may also show a purple appearance from an accumulation

of anthocyanin pigments on the roots, petioles and underside of leaves. N limitation decreases crop photosynthesis by reducing the leaf area development and leaf photosynthesis rate by accelerating leaf senescence. It has been reported in previous literature that N limitation reallocates N from older to younger tissues leading to early senescence of the older, lower leaf tissue in plants, thus causing early mature plants (Blevins, 1989; Mengel *et al*., 2001). Root growth is better than shoot growth in plants under low N availability; however, the absolute number of roots is usually less when compared to fertile agricultural land. With prolonged N deficiency, primary root growth and total root length are inhibited, while mild deficiency leads to elongation of lateral roots and stimulation of lateral growth is suggested due to auxin dependency (de Bang *et al*., 2021; Gruber *et al*., 2013). Yield determining factors during the flowering stage under N stress are primarily affected in crop development due to early flowering. Additionally, resulting in the kernel and ear abortion, thus increasing leaf senescence and reducing ear weight and crop photosynthesis (Bänziger M. *et al*., 2000; Bianco *et al*., 2015; Perchlik *et al*., 2018). All the above studies suggest that N limitation can significantly affect the growth and yield of crops.

1.5.2 Phosphorous stress

P, the genetic "memory device" of all living organisms, is a crucial element of DNA and is an essential macronutrient for seed yield, plant structure, and hereditary transfer. It is present in the molecules such as phospholipids, sugar phosphates and nucleic acids (Starnes *et al*., 2008). The most comprehensive and least costly P source from the world's various phosphate deposits is produced by extracting and concentrating phosphate rock. P is an integral part of ATP, the plants' "energy unit". It is present in the structure of ATP form during photosynthesis and processes from the beginning of seedling growth through to the

development of grain and maturity. Plants absorb inorganic P in the form of the two orthophosphate ions (Pi) dihydrogen phosphate ($H_2PO_4^-$) or hydrogen phosphate (HPO_4^{2-}) present in the soil solution or attached to the complex clay-humic (Havlin *et al*., 2005). These negative ions are often used along with other positive ions in fertilisers. Plants can also absorb organic P compounds which are produced during metabolism in living beings (Marschner, 1986). Organic P represents up to 80% of the total P present in the soil (Condron & Tiessen, 2005). It is mainly present as inositol phosphates (phytate) and secondarily in the form of sugars, nucleic acids, and phospholipids. Phytates constitute phosphorus reserves stored in seeds, mostly ranging from phytic acid in cereals from 0.5 to 5.0% (Reddy *et al*., 1982; Greiner & I Egli, 2003).

P deficiency: A broad root system capable of exploring greater soil volume has been recognised as an essential plant adaptation to ensure that P is adequately absorbed (Lynch & Brown, 2001). P is highly mobile in plants, and when deficient can be translocated from old plant tissue into young, actively growing areas. Therefore, P is vital for the general plant growth, translocation of sugars and starch to storage organs maintains turgor pressure and reduces water loss. P deficiency in plants can be visually identified at the early vegetative stage as an abnormally dark green or reddish-purple colour around the edge of the lower plant leaves. Most P deficiencies are observed in low pH soils (less than 5) or fields with low soil phosphorus test values in early spring. Leaf tips appear burnt due to P deficiency, leaves are often spotted with necrotic tissue, loss of older leaves, stunted plant growth and the colour of leaves turn dark green than normal, seed dormancy rises, leaves and fruit fall prematurely. Soil plants are unable to take up other soil elements in excess of P and display tissue bleaching and chlorosis marked by yellowing between leaf veins (Aziz *et al*., 2015;

Malhotra et al., 2018). Plants generally respond to P deficiency by reducing the total plant biomass and distributing more resources towards root growth. This diversion of resources leads to an increase in the root biomass to aboveground biomass ratio. A suitable supply of P to the plants promotes precocity, the rigidity of the tissues and forage quality. P is necessary for root proliferation (Lynch & Brown, 2001) and boosts the development of the plant. It takes time for plants that lack P to mature and the fruits or seeds they carry are few and low in quality when they do. Plants that have access to adequate P have the potential to resist diseases because all their sections are well-formed and grow quickly. P is a critical component of a healthy fertility programme that results in crops that are more resilient to stress and thus less susceptible to disease infection (Gondwe *et al*., 2020).

1.5.3 Potassium stress

Studies have suggested that mineral nutrients play a significant role in plant stress resistance and K is an essential and most abundant cation in plants comprising 3-5% of its dry weight in plants (Amtmann *et al*., 2008; Cakmak, 2005; Marschner, 1986; Römheld & Kirkby, 2010). K is the second-largest absorbed nutrient by plants after N, and it plays a vital role in plant growth and metabolism under various abiotic and biotic stress conditions. It is a readily available macronutrient and is absorbed by plant roots in the form of K^+ and its transport is well studied at the physiological level. In-plant tissue, K is associated with the water relations and osmotic pressure of plant cells due to its high mobility. Furthermore, it is related to activating enzymes within the plant, influencing the development of protein, starch and adenosine triphosphate. ATP production can regulate the photosynthesis rate. K plays a significant role in membrane integrity and stability (Schlegel *et al*., 2005). The opening and closing of the stomata, which controls the exchange of water vapour, oxygen

and carbon dioxide, also helps to stabilise K. Therefore, K^+ channels present in the plasma membrane are the best-characterised plant transport system because of their accessibility to internal membranes and stronger currents.

Most notably, agricultural problems like K deficiency have deteriorating effects on crop production and their survival (Steingrobe & Claassen, 2000). Crops are susceptible to the increased light intensity in arid, and semi-arid lands and K deficiency further induces necrosis and chlorosis in the leaf. Plants exposed to low K produce higher reactive oxygen species (ROS) such as superoxide radicals, hydrogen peroxide, and singlet oxygen and inhibit plant growth and production. ROS production can be highly toxic for the plants causing membrane damage and chloroplast degradation leading to programmed cell death (Cakmak, 2005). It stunts plant growth and decreases yield if K is deficient or not supplied in appropriate quantities. Chlorosis along the edges of leaves is the most frequent symptom due to K deficiency (leaf margin scorching). In older leaves, this happens first, since K in the plant is very mobile. Slow and stunted growth would have plants missing K. In some crops, stems are poor and if K is deficient, lodging is normal. Because of K deficiency, the size of seeds and fruits and the quantity of their development are decreased. For enzyme activity, energy transfer, protein synthesis, osmoregulation, stoma movement, phloem transport, anion-cation balance and stress resistance, K is an important nutrient (M. Wang *et al*., 2013).

Under saline conditions, Na+ is also present at high concentrations, where the availability of K is essential to sustain the K^+/Na^+ ratio in plants. The Na^+ uptake must therefore be decreased, and the K uptake increases optimal plant growth (Wakeel, 2013), as a higher K^+/Na^+ ratio increases the plant's resistance (Hu & Schmidhalter, 2005). Therefore, an

increased Na+ uptake also needs to be transported to the shoot with an increased volume of K (Adolf *et al*., 2013).

Osmotic capacity and hydraulic conductivity of membrane regulation and improvements in plant water permeability play a significant role under K sufficiency. An aquaporin gene (channel proteins present in the plasma and intracellular membranes) expression is produced under conditions of drought stress, thus maintaining the water balance in the plants and is also predicted to play a significant role in K buffering. Liu *et al*. (2006) also disclosed a potential functional association between K^+ channel/transporters and water channels in rice. The mRNA expression levels of plasma membrane intrinsic proteins (PIPs) and K^+ channel/transporters responded similarly to K^+ starvation or water deprivation. The PIPs and K^+ channel-encoding genes transcription was activated by K^+ starvation and could be down-regulated by the water deficit induced by polyethene glycol (PEG) (Liu *et al*., 2006). Wang Y. *et al*. (2021) indicated that aquaporin activity is mainly affected by K^+ deficiency, resulting in root hydraulic conductance and leaf transpiration water supply. K is a major component of protein synthesis, activation of enzymes, pH gradient, upload of phloem, control of turgor strain, stomatal function and photosynthetic system. K^+ is also required in plants at high concentrations from the early vegetative development stage (Kant *et al*., 2002).

1.5.4 Boron stress

B is an essential micronutrient for crops, and the quantities required are small depending on the plant species, cultivar and variety (García-Sánchez *et al*., 2020). B exists as both water-soluble and insoluble forms in the intact tissues of higher plants. The bulk of the water-soluble B is found as boric acid in the apoplastic zone. Rhamnogalacturonan II (RG-II)

is associated with water-insoluble B, and the complex is widespread in larger plants. The B-RG-II complex structure shows that the complex is composed of boric acid and two monomeric RG-II chains. Boric acid binds to sugars and links two pectic polysaccharide chains through borate-diester bonding in the RG-II region, creating a network of pectic polysaccharides in the cell walls (Matoh, 1997). A complex with RG-II and the B-RG-II complex comprising two boric acid molecules, two Ca^{2+} molecules per two monomeric RG-II complex chains, is generated by B in the cell walls (Matoh, 1997), which further leads to plant growth and development.

Several studies indicated that B forms a gel-like structure comprised of polysaccharides secreted into the cell walls producing pectic polysaccharides (Marschner, 1986; Matoh & Kobayashi, 2002). B also functions in protein synthesis, hormonal regulation, phenol, phosphorous metabolism, and vegetative and reproductive growth including flowering, production, and harvest quality (Gimeno *et al*., 2012; García-Sánchez *et al*., 2020). B deficiency causes a substantial loss of productivity and quality of crops as it affects the young and growing parts of plants. B is arguably a more critical mineral nutrient than other micronutrients or traces elements. Boron's primary functions relate to the strength and growth of the cell wall, cell division, fruit and seeds development, sugar transport, and hormones. In plants, certain boron functions interact with those of K, P, N and Ca for optimum crop growth; balanced nutrition is fundamental.

Symptoms of B deficiency reflect the various functions boron performs in plant life, and symptoms vary significantly between plant species. B deficiency often is confused with other defects or disorders that cause distorted growth (such as infectious disease, frost or hormone damage). As B does not pass around the plant quickly, deficiency will likely be seen

first in the younger tissues (Dear, B.S. & Weir, 2004). B deficiency manifests as cambia sugar deficiency, stem tips, root tips, flowers and fruits (Blevins & Lukaszewski, 1998). Plants deficient in B have various visual signs, such as cell division in rising tips without cell differentiation that would otherwise lead to cells being stems, leaves, flowers, etc. Since B is involved in the division and growth of cells, its deficiency destroys vegetative growth tips consisting of the meristematic cell line. The development of lateral shoots, the tips of which may also be deformed or die, leaving a rosette on the plant called the 'witches broom' condition, directly affects the death of terminal buds. Typically, leaves become dense, have a coppery texture and become curled and brittle and hinder the growth of young leaves. B defective plant tissue also breaks down prematurely, causing brown flecks, necrotic patches, fruit and tubers to crack and corky areas (Matoh & Kobayashi, 2002). B deficiency hampers flowering and fruiting by retarding pollen germination and pollen tube growth processes. Moreover, B deficiency decreases fertility and, depending on the severity of the deficiency; fruit production becomes sluggish or non-existent. Often plants fail to set flowers, or they are aborted due to B deficiency if flowers can be arranged anyway and cause a common symptom of deformed flowers (Gupta *et al*., 2013).

1.6 Nutrient depletion and cell wall biomass

Crops suck up nutrients from the soil, and many of these nutrients are extracted or removed from the field when the crops are facing mechanical harvest. Some nutrients are returned to the field after harvesting crops by crop residues and other organic matter, which alone cannot provide optimum nutrients over time for sustainable crop yields

It is also vital to use energy-intensive fertilisers with both environmental and environmental impacts. Cell wall biomass-related characteristics of low nutrient conditions in crops need to

be known to increase crop yield and minimise environmental effects. The significance of the cell wall for biomass quality characteristics is well known. However, there is still a lack of understanding of how the individual or combined effects of nutrient stress affect cell wall quality characteristics in grasses.

Plant cell walls are composed of carbohydrate polymers (cellulose, hemicellulose, and pectin), lignin, and structural proteins in varying quantities. As it gives the cell shape and mechanical strength to combat turgor strain, the cell wall is of vital importance. In addition, the first line of protection against environmental pressures is the cell wall. Grasses constitute one of the essential flowering plant families, including all cereal crops and many necessary grazing animal feed and forage crops, and dedicated bioenergy crops. These grasse's biomass consists mainly of cell walls, usually 60-70% depending on the dry matter yield. The quality of the cell wall biomass in terms of its composition and cross-linkages determines to a large extent, the quality of grasses as feed for ruminants and feedstocks bio-refineries, respectively (Hatfield *et al*., 2017).

1.7 The Cell wall and its composition

At the metabolic stage, the cell wall of Brachypodium resembles the field grasses, such as cereal crops, various grazing animal feed and forage crops, and bio-energy crops. Moreover, in terms of its composition and cross-linkage, the nature of the cell wall biomass mainly depends on the developmental stage and further influences the consistency of grasses as feedstocks for ruminants, and bio-refineries, (Hatfield *et al*., 2017). Plant cell walls consist of, in varying amounts, carbohydrate polymers (cellulose, hemicellulose and pectin), lignin and structural proteins. The cell wall is of critical importance, as it gives the cell form and mechanical strength to fight turgor pressure and enacts as a major target of saccharification

in biofuel production. In addition, the cell wall also acts as a front line in the defence against abiotic and biotic stresses and thus makes Brachypodium an ideal crop for studying saccharification and abiotic stress-tolerant.

1.7.1 Primary Cell Wall

Polysaccharides are abundantly distributed in nature as structural components of the cell wall and as reserve carbohydrate material. The primary cell wall is comprised of cellulosic micro-fibrils embedded in a matrix of non-cellulosic polysaccharides (hemicelluloses and pectin) and structural glycoproteins. In addition, the layers deposited after the cell has stopped growing lead to the formation of a thick secondary cell wall internally situated to the primary cell wall (Theander and Aman 1984).

Significant compositional differences between grass and dicot cell walls have been known for some time. Primary cell walls of plants can be divided into two broad categories (N. C. Carpita & Gibeaut, 1993). Type I cell walls, found in dicots, non-commelinoid monocots, and gymnosperms, consist of cellulose fibres encased in a xyloglucan (XyG) network pectin and structural proteins. Type II cell walls found only in the commelinoid monocots (e.g., grasses, sedges, rushes, and gingers), are composed of cellulose fibres encased in glucuronoarabinoxylans (GAX), high levels of hydroxycinnamates, and very low levels of pectin and structural proteins. In addition, the cell walls of grasses (family Poaceae) and some related families in the order Poales contain significant quantities of mixed linkage glucans (MLG) (Smith BG & PJ Harris, 1999).

Cellulose

The cellulose content in primary cell walls is rather low (often below 20%) but it provides mechanical strength for load-bearing. Cellulose is the dominant and the most abundant

polysaccharide component by weight, in the grasses and is often touted as “the most abundant biopolymer on earth” (Ding & Himmel, 2006). Cellulose forms long fibres which group to form bundles called microfibrils. Each microfibril has a diameter of about 10 to 20 nm and can consist of up to 40 chains of cellulose. Hemicellulose, a branched polymer consisting of a mixture of primarily pentose sugars (xylose, arabinose) and some hexoses (mannose, galactose, glucose), covers the crystalline cellulose centre of a microfibril (mannose, galactose, glucose). Hemicellulose also forms covalent associations with lignin, a rigid aromatic polymer, in addition to cross-linking individual microfibrils (Figure 1-2).

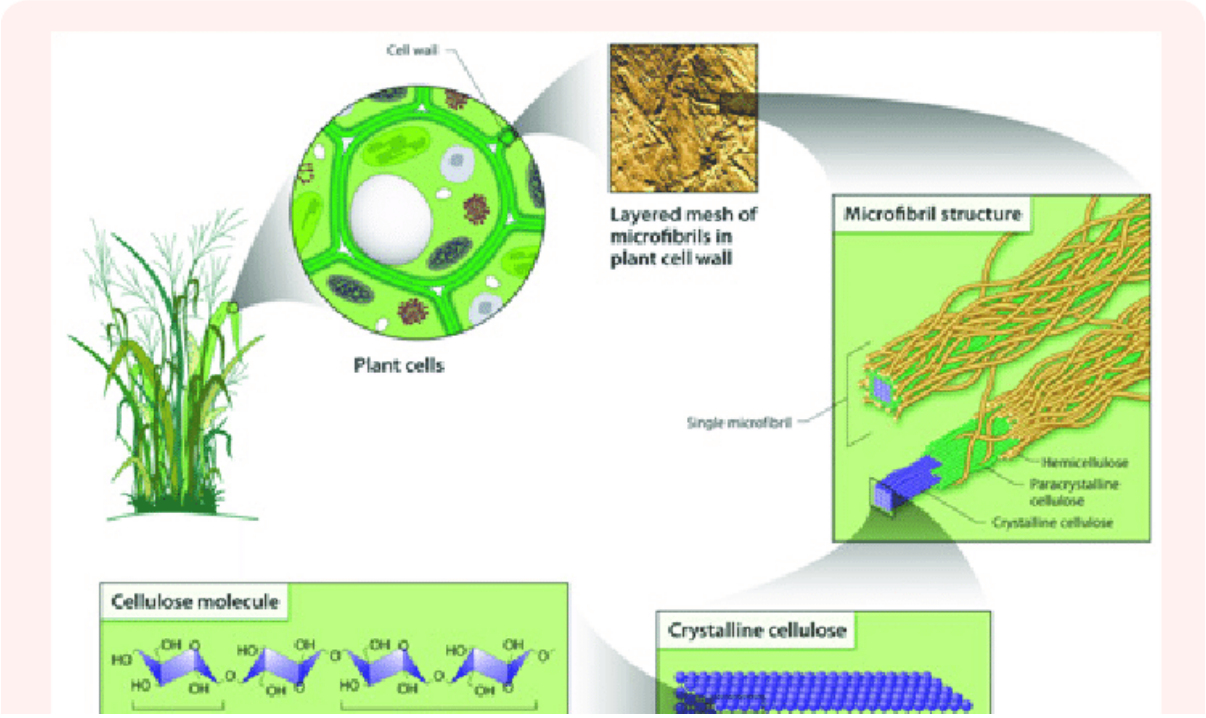

Figure 1-3: Diagrammatic representation of structures of cellulose in the plant cell wall and its hydrolysis (Meng et al., 2016)

Hemicellulose

Hemicelluloses are present along with cellulose in plant cell walls. It has an amorphous structure and provides little strength. Hemicelluloses include xylan, glucuronoxylan (GAX), arabinoxylan (ABX), and xyloglucan (XG).

Xylans are the major non-cellulosic polysaccharide in primary walls, constituting about 20% of the wall. These xylans usually contain many arabinose residues attached to the backbone and are known as arabinoxylans and glucuronoarabinoxylans (GAXs). GAX, the major hemicellulose in grass cell walls, is composed of a β1, 4-linked xylose backbone with single arabinose and glucuronic acid side chains primarily attached at the O-3 and O-2 positions, respectively (A Ebringerová, 2005). Several studies have suggested that most of the xylose and a portion of the arabinose in *Brachypodium* and other grasses are present in the hemicellulose glucuronoarabinoxylan fraction (N. C. Carpita & Gibeaut, 1993; N. Carpita *et al*., 2008; Vogel, 2008; Scheller & Ulvskov, 2010).

MLGs (also known as β-glucans) are unbranched homopolymers of glucose that are unusual and comprise both β1, 3- and β1, 4-linkages. MLGs are unique to the cell walls of grasses (Trethewey *et al*., 2005).

Pectin

Pectin is found in both the primary cell wall and middle lamella and is mostly composed of middle lamellas, unlike the cell wall. It is involved in the regulation of ion transport and wall porosity, the control of cell wall permeability, and the determination of the retention potential of water in relation to its charged nature. In particular, pectin is structurally and functionally the most complex polysaccharides in nature, and only constitutes 2–10% of the primary cell wall of grasses. It plays a vital role in plant growth, morphology, development, and plant defence (Mohnen, 2008).

Roughly 65% of pectin is homogalacturonan (HG,) which is a homopolymer of d-GalA linked in an α-1,4 configuration as shown in Figure 1-3. HG is partially methylesterified at the *O*-6 position and to a lesser extent acetylated at *O*-2 and *O*-3. There is evidence that contiguous

regions of unesterified HG interact via Ca^{2+} salt bridges in the wall (Mohnen, 2008; Harholt *et al*., 2010). RG-I constitutes 20–35% of pectin. Unlike HG and RG-II, it has a disaccharide repeat backbone of [4)-α-d-GalA-(1,2)-α-l-Rha-(1,]$_n$ in which the GalA residues are highly acetylated at *O*-2 or *O*-3 (Figure 1-3).

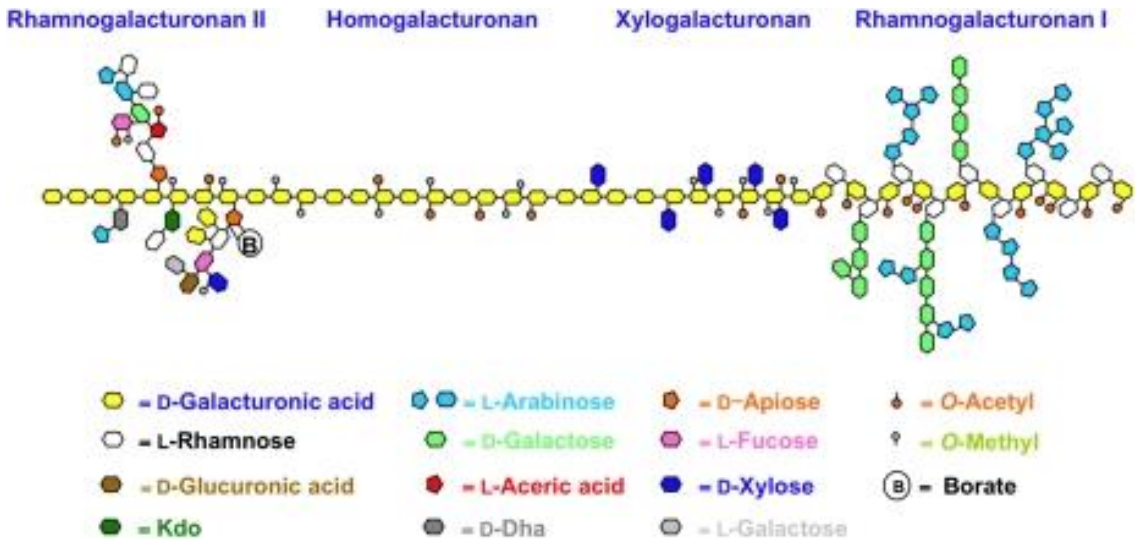

Figure 1-4: Schematic structure of pectin comprising the detailed composition of rhamnogalacturonan II, homogalacturonan, xylogalacturonan, and rhamnogalacturonan I (Harholt *et al*., 2010)

The RG-I backbone consists of alternating residues [→ 4)-alpha-GalA-(1 →2)-alpha-Rha-(1 →], and recorded values are as high as 100 repeats for segments composed of this disaccharide. In RG-I side chain length, high variation is observed. In the RG-I backbone, between 20-80% of all rhamnose residues are replaced with side chains. The length of side chains differs from monomeric residues to several (Gal). With several variants, either consisting of single or more residues, side chains are found and can be classified into type I and II arabinans, galactans and arabinogalactans. Arabinans consist of alpha-(1-5)-linked arabinose units that can be substituted by (1-2)-linked or (1-3)-linked side chains of arabinose. Galactans are composed of residues of β-(1→4)-linked Gal. In their binding form,

arabinogalactans (AG) vary with a β-(1 → 4)-linked galactan backbone replaced by Ara and/or Gal residues in Type I AG at O-3 and O-6 of the galactose residue, respectively. Type II arabinogalactans are composed of a β-(1 → 3)-linked backbone that may be branched with β-(1 → 6) Gal residues [1, 3]. Pectic polysaccharides are associated with Type I arabinogalactans. Type II arabinogalactans are part of Arabinogalactan proteins (AGPs), while Type II AG has indicated interactions between AGP and pectin (Mohnen, 2008). The structurally very complex part of Rhamnogalacturonan II (RG-II) is composed of a GalA backbone and substituted with rare sugars such as 2-O-methyl xylose, 2-O-methyl fucose and acetic acid. RG-II is present in all plants and usually has low levels, although there are exceptions in pumpkin and grape-derived wine. While RG-II is less frequently included in pectin studies than HG and RG-I, since decreased RG-II levels have been shown to have significant effects on inhibiting plant growth, it appears to be of key importance to plant growth (Mohnen, 2008). In several sources, such as apple, watermelon, onion, potato and pear, the existence of xylogalacturonan does not seem to be widespread (Ishii, T & T Matsunaga, 2001). The main role of pectin is to participate in these two roles along with the other polymers. It is particularly well known that HG and RG-II are involved in reinforcing the cell wall that is covalently cross-linked by a borate diester (T Ishii *et al*., 1996; O'Neill *et al*., 1996). Other than pure mechanical assistance, HG performs additional functions like plant pathogens also causing pectin degradation, and oligogalacturonides (alpha-1,4-linked GalUA oligomers). HG are well known to be part of a signalling cascade that senses pathogen attack degradation of the wall (Ridley *et al*., 2001; D'Ovidio *et al*., 2004; Kohorn *et al*., 2009).

1.7.2 Secondary Cell Wall

The incorporation of lignin in the secondary cell wall plays an important role in cell wall strengthening. Secondary cell walls are deposited inside of the primary cell walls and are prominent features of xylem, fibre and sclerenchyma. The typical grass secondary cell wall is largely composed of cellulose, glucuronoarabinoxylan (GAX), and lignin (Vogel J., 2008, 2008). Lignin is one of the main carbon components (~20%) of grass secondary walls. The secondary cell wall contains negligible amounts of pectin (~0.1%), minor structural proteins and MLGs, HCAs which are comprised of ferulic acid (FA) and para-coumaric acid (pCA) (~0.5%–1.5%) and a small proportion of water (~5%). Moreover, it is primarily made up of hundreds of layers of cellulose microfibrils (~35%–45%) embedded in GAXs (~40%–50%) which are covalently cross-linked with hydrophobic polyphenol lignin (~20%) (A Ebringerová, 2005; Vogel, 2008; Albersheim *et al*., 2010). Hemicellulose xylan is the primary source of acetate in dicot and grass walls, where 40-80% of the backbone xylosyl residues can be O-acetylated (Tadashi Ishii, 1997; de Oliveira Maia Júnior *et al*., 2020; Ralph *et al*., 2004; Pauly *et al*., 2013) In addition, the total number, architecture, and chemical composition of cell walls can vary greatly depending on the tissue, cell type, cell wall layer, developmental stage, and plant taxa (Pauly & Keegstra, 2010).

1.8 A phenotypic and genotypic view

Phenotype and genotype were first defined by Johannsen (1911) as “real things, the appearing types or sorts of organisms”, making all typeable phenomena in the organic world phenotypical. In this definition, a combination of all the morphological, physiological, anatomical, chemical, developmental, and behavioural characteristics representing the individual organisms can identify a visual or observable feature. Genotype is described as

the number of the total genes in a gamete or zygote of an individual. F1 generation developed from a monohybrid cross produces a heterozygote that differs in one point from another. Furthermore, a gene or an allele of genetic information is accumulated in the individual organisation of the genotype.

An individual organism occupies a point in the genotypic space that characterizes the full array of genotypes possible for that species. Combined with the environmental characteristics, this position determines an organism's phenotypic state within the overall space of possible phenotypes (Pieruschka & Poorter, 2012). Furthermore, an organism can affect the environment, creating a complex feedback relationship between genes, territories, and phenotypes (Houle *et al*., 2010). Unnatural selection of plants with desirable traits to achieve improved quality and higher yields for more disease-resistant plants. Due to the complexities of the physiological, biochemical, and genetic traits involved, increased resistance to abiotic stress was prolonged. The selection of agricultural favourable development characteristics, including plant height (cm), tiller number, spikelet on the main stem, number of leaves, vegetative biomass (fresh and dry weight), flowering period, resulting in altered habits, were therefore generally underscored by plants. The phenotypic measurements in the present study distinguishing the traits relevant to biofuel and food production are shown below in Table 1-1.

Table 1-1: Summary of phenotypic measured for both bioenergy/biofuel and cereal crop for food production traits in *Brachypodium* studied under abiotic stress conditions

Stage	*Phenotypic traits*
Vegetative (Biomass traits)	*Plant height (cm)*
	Tiller number
	Spikelet on the main stem
	Number of leaves
	Vegetative biomass (fresh and dry)
Spikelet (Cereal traits)	*Days of flowering*
	Ear weight (g)
	Number of fertile tillers
	Harvest index (HI)

Genotyping is the process by which we determine differences in the genotype or genetic information of an organism which can be followed down by genetic markers that can be used as probes or tags (Xu *et al*., 2016). Morphological markers represent genetic polymorphisms that are visible as differences in appearance, such as leaf size, plant height etc. During the 1980s and 1990s, several molecular markers based directly on traceable differences in the DNA sequence were developed. There are different types of markers termed as follows: restriction fragment length polymorphism (RFLPs), amplified fragment length polymorphism (AFLPs), random amplification of polymorphic DNA (RAPD), simple sequence repeat (SSRs), and single nucleotide polymorphism (SNPs).

1.9 The hypothesis of the present study

The purpose of the study will explore and deepen the scientific understanding of the phenotypic measurements of abiotic stressors, and the central working hypothesis was tested as follows:

- I hypothesised that phenological and biomass quality traits associated with nutrient limitation would be specie-specific in *Brachypodium distachyon* genotypes, i.e. tolerant and susceptible accessions
- I also hypothesised that PMEI-OE *Brachypodium* transgenic lines would show tolerance to abiotic stress compared to the wild-type (Bd21-3)

The summary of the chapters is described below:

Previous studies have advanced the development of high-throughput phenotyping and screening of complex traits associated with abiotic stress tolerance (Fahlgren *et al*., 2015). In chapter 2, available ABR6 and Bd21 accessions were grown under control and selected low nutrient dose-response. I conducted the screening based on morpho-physiological traits of above-ground and below-ground parameters of Brachypodium along with saccharification efficiency under selected N and P dose-response conditions.

Chapter 3 studies the Iraqi (Bd21) and Spanish (ABR6) accessions for more detailed phenotyping and flowering time measurement using partial high-throughput phenotyping facilities. Consequently, Chapter 4 deals with the phenotypic screening and ranking of Brachypodium genotypes to investigate N and P limitation adapted genotypes. Chapter 5 uses the available RIL population derived from ABR6 and Bd21 accessions to identify Quantitative trait loci (QTL) linked traits affected by nutrient limitation, followed by

candidate gene identification for flowering time. Chapter 6 uses the transgenic lines with overexpressing Pectin Methylesterase Inhibitor (PMEI-OE) to screen the positive lines, measure the expression of overexpressing gene, and PME-assay to confirm the selected lines. This was followed by phenotypic interaction under drought and nutrient limitation and saccharification efficiency estimation under chosen nutrients. Finally, a general discussion of the results is given, considering the implications, possible applications of this research and recommendations for future investigations.

Chapter 2 : Experimental evaluation of above and below-ground biomass in *Brachypodium distachyon* genotypes ABR6 and Bd21 under low nutrient dose-response

2.1 Introduction

The yield losses in cereal crops because of abiotic stress and the expected huge losses from climate change direct our urgent requirement for valuable traits to achieve food security. Plants are static and cannot escape from environmental stresses during their growth period. Additionally, there is an urgent need to accelerate plant breeding and mining of novel traits for increased yield potential and better adaptation to abiotic stresses to secure food availability and meet the future demand for agricultural production (Kamal *et al*., 2019). In contrast, the effect of temperature (high and cold), salinity, water (drought, flooding, submergence) and chemical factors (heavy metals) have been extensively studied in plants (Bita & Gerats, 2013; Hindhaugh *et al*., 2021). Cereal and biomass crops in agriculture face nutrient limitations limiting plant growth and productivity (Mehmood *et al*., 2017). Recently, a study has been performed using a natural genetic variation to understand drought and nutrient tolerance in root architecture in *Brachypodium* (Ingram *et al*., 2012; Pacheco-Villalobos & Hardtke, 2012).

Mineral nutrient limitation is considered one of these lands' most critical agricultural problems. Nutrient distribution in the soil is usually not homogenous, leading to nutrients on the upper layers, causing a change in root architecture due to nutrient stress conditions in the lower soil (López-Bucio *et al*., 2003). Excessive agricultural exploitation, contamination due to pollutants, drought or flooding, are characteristics that primarily determine the marginality of the lands that are not used for agriculture (Kang & Banga,

2013; Carlsson *et al*., 2017; Mehmood *et al*., 2017; Pancaldi & Trindade, 2020). The marginalization of soil caused by the above factors is often correlated with nutrient deficiencies in the soil. However, there is little or not much known in terms of above ground, below ground morphology and cell wall characteristics like saccharification efficiency under low nutrient dose-response. Nutrient uptake by plants can vary dependent on the availability of nutrient elements present in the soil, thus limiting the biomass quality of cereal and bioenergy crops. Sugar release by enzymatic hydrolysis is one of the most commonly used quality measures for grass biomass quality, as a forage and a bioenergy feedstock.

Macronutrients like nitrogen (N), phosphorous (P), and potassium (K) are necessary for plant growth, metabolism and development. However, micronutrients like boron (B) play a vital role in plant composition for cell wall synthesis by maintaining its structure. Previous studies suggested that the plant root system absorbs P and N in their inorganic forms i.e., P ($H2PO_4^-$) and nitrate (NO_3^-) or ammonium (NH_4^+) whereas B in the form of boric acid (H_3BO_3) (Bouain *et al*., 2019; Brdar-Jokanović , 2020). The nutrient limitation in the soil and low nutrient uptake via roots usually results in decreased vegetative growth, and low photosynthetic rate, thus altering root architecture (Ingram *et al*., 2012; Pacheco-Villalobos & Hardtke, 2012). Ogden *et al*. (2018) also suggested that plants develop nutrient specific phenotypes and reorganise the root system under low nutrient availability, resulting in plant growth inhibition. Plant root systems usually get exposed to spatial heterogeneity when exposed to low nutrient availability. Therefore, the characterization of morphological root architecture and root physiological adaptations become important traits to study the effects of inadequate nutrient availability (Jia *et al*., 2020).

Brachypodium develops a fasciculate root system without a cambium vascular system as the root first emerges from the base of the embryo inside the seed, followed by secondary root development. As illustrated in Figure 2-1, the root system is categorised as primary or crown roots, roots starting from the coleoptile node, known as coleoptile node roots, and roots starting from the leaf node, leaf node roots (Watt *et al.*, 2008). *Brachypodium* has been selected as a model species for essential crops like maize, wheat, barley and oats, and switchgrass biofuel crop (Bevan *et al.*, 2010). Draper *et al.* (2001) recommended *Brachypodium* as the first grass crop model as it has several properties that make it suitable.

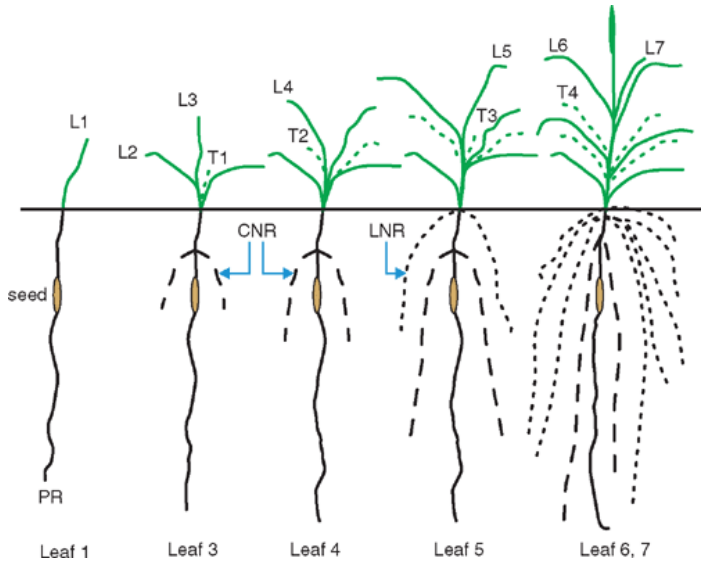

Figure 2-1: Demonstration of the root system and its stages in *Brachypodium distachyon* by Watt *et al*. (2008) where PR= primary root, CNR= coleoptile nodal root, LNR= leaf nodal root.

Therefore, root studies grown in different media using agar gel can help to improve screening for root phenotypes thereby. The differences in root length and development can be measured when different nutrient conditions are replicated. Differing root ideotypes were described by White *et al.* (2013) under P, K, and N deficient uptake in cereal crops (Figure 2-2). Furthermore, higher rooting densities in deeper soil layers are beneficial to access subsoil water and nitrogen due to its soluble nature commonly travelling down the soil profile (JP Lynch, 2013). The selection of nutrient-limited stress conditions would help us

focus on improving crop yield and nutrient uptake in early growth stages.

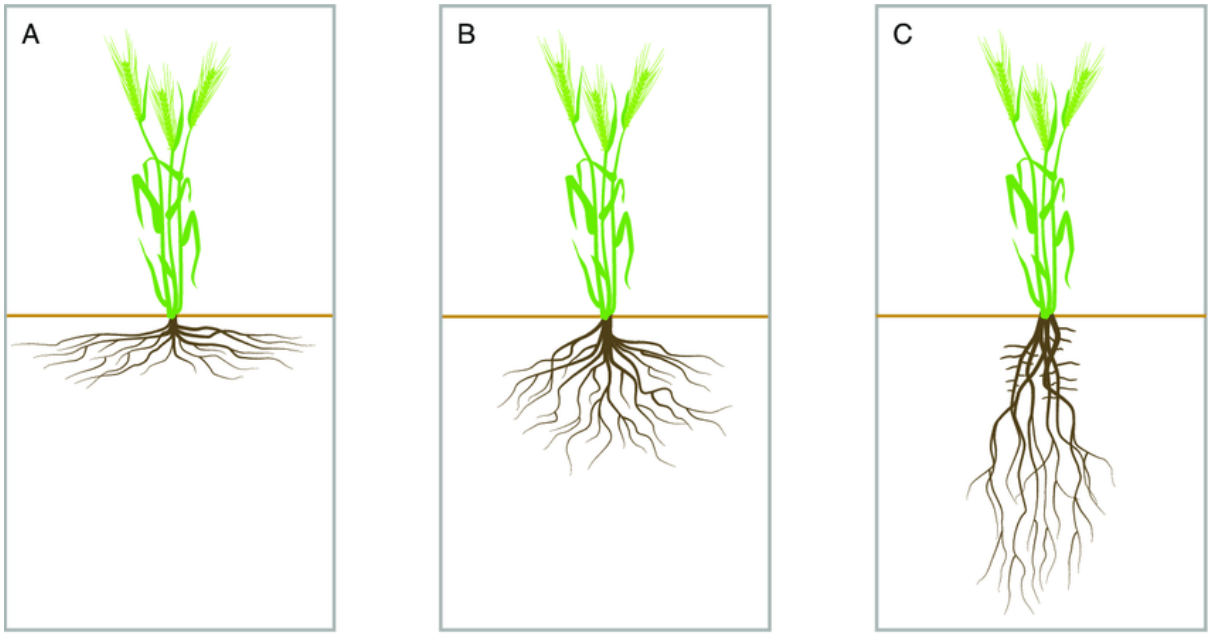

Figure 2-2: Root ideotypes for efficient acquisition of different nutrients explained by White *et al*. (2013) in cereal crops, (A) P, (B) K, (C) N

This chapter aims to unravel the implications and understand the phenotypic effect on the shoot and root traits grown in glasshouse and MS media to further understand how *Brachypodium* accessions adapt to reduced nutrient dose-response (NPKB). To achieve the objective and to use the advantages of the model specie *Brachypodium*, various

concentration effects of N, P, K, and B were examined. Differential shoot, root and cell-wall analysis such as total monosaccharide content and enzymatic sugar release under the nutrient response of the two parental genotypes ABR6 and Bd21 were used in this study. ABR6 and Bd21 accessions are the parents of a well-established recombinant inbred line (RIL) population which represents a powerful tool for the identification of genetic components that underpin important traits (Bettgenhaeuser, 2016). Consequently, an already existing RIL population from the above parental accession was studied under control and nutrient limitation (Chapter 5). This further involves the phenotypic above-ground and below-ground biomass study and selection of nutrient deficiency treatments. The presented knowledge will provide insights that may be transferred to related crop species like wheat and rice securing the rising global food demand for cereals by improving biomass yield and quality.

2.2 Materials and methods

Brachypodium distachyon accessions were used for plant growth for above-ground biomass measurements. ABR6 and Bd21 accessions obtained from IBERS, Aberystwyth University, were used during this experiment. Florets of both genotypes were peeled from the lemma and palea and transferred into 6 cm diameter pots in an ultralow nutrient substrate (Table 2-1) with a mixture of 40% silver sand/ 60% WI13 compost (Bulrush, Magherafelt, N Ireland, low nutrient compost). Individual seeds were placed in 1 cm deep holes covered lightly with soil so that each seed was just below the surface of the soil, and then watered with water containing insect pest control (GNAT OFF, Fungus). Plants were germinated in controlled greenhouse conditions operating at 16/8 h (day/night), at 20-21°C, under natural light supplemented with artificial light generated by 400 W sodium lamps) with 50%-60% relative

humidity. Temperature and humidity were further monitored using a Tinytag (Gemini Data Loggers). The experiment also helped us to understand different growth stages in two *Brachypodium* accessions with different geographical origins where Bd21 the Iraqi accession does not require vernalization while the Spanish accession (ABR6) requires a 6-week vernalization period to induce flowering (Garvin et al., 2008; Bettgenhaeuser *et al*., 2017). Therefore, vernalisation (4°C) was initiated for 6-weeks after germination to synchronise plant development in both the accessions and to induce the flowering process in ABR6. During this period, plants were covered with plastic lids to minimise exposure to air movement. Soil moisture was monitored weekly, and plants were watered when needed. After vernalisation, plants were transferred to the greenhouse in a controlled and monitored environment operated with 16/8 h photoperiod, at 21-22°C/18-20°C Day/night temperatures. To eliminate the influence of temperature and humidity on plant development between treatments, temperature and humidity were regulated throughout the experiment.

Table 2-1: Details specifying the chemical composition of Bulrush-compost that was used to grow plants

Parameter	Unit	Value
Density	g/l	264
pH		3.6
Conductivity	µs/cm	16
NH_4-N	mg/l	6.2
$N0_3$-N	mg/l	0.8
N (Total)	mg/l	7
Cl	mg/l	10.5
K	mg/l	1.2
Mg	mg/l	<0.2
Ca	mg/l	0.7
Na	mg/l	5.3
Fe	mg/l	0.13
P	mg/l	<1
Cu	mg/l	<0.01
Mn	mg/l	<0.01
Zn	mg/l	0.03
B	mg/l	<0.05
SO_4	mg/l	8.8

2.2.1 Nutrient composition

The nutrient solution was prepared according to (Hoagland & Arnon,1950) and Hoagland stock solutions with reduced NPKB solution reported in Appendix Table A2.1 and Appendix Table A2.2, respectively. Full Hoagland nutrient solution was used for before vernalisation followed by low nutrient dose-response. The selection low nutrient dose response was calculated by using five-fold dilution from 100% Hoagland solution (control) to attain 20% followed by five-fold-dilution from 20% to attain 4% low nutrient treatments. The solutions were prepared with slight modifications to the Hoagland recipe with substituting KCl and $NaNO_3$. From the above-mentioned stock solution different low nutrient dose (NPKB) concentrations were prepared and the solutions were finally brought to pH 6. This dilution

was generated to obtain a dynamic range of low nutrient dose-response effect for NPKB.

Table 2-2 shows the list of treatments used during this experiment.

Table 2-2: List of different nutrient treatments used during the nutrient stress experiments with ABR6 and Bd21 accessions of *Brachypodium*

Treatment	**Nutrient dose-response**
Hoagland full dose (Control)	Full/Optimum
N (Hoagland minus N dose-response)	N20% N4% N0%
P (Hoagland minus P dose-response)	P20% P4% P0%
K (Hoagland minus K dose-response)	K20% K4% K0%
B (Hoagland minus B dose-response)	B20% B4% B0%

2.2.2 Experimental design

After vernalization, the plants were randomly divided into 13 groups, each containing six ABR6 and Bd121 plants, and each to be exposed to one of the treatments as mentioned in Table 2-2. The plants were primed with full Hoagland solution (25 ml/pot) before vernalization for even growth and were treated the second time with nutrient-deprived Hoagland solution (25 ml/pot) after vernalization. The nutrient-deprived treatment was given once the seedlings had acclimatized two days in the glasshouse environment after the

vernalization period. This was followed by watering regularly when required for the next two weeks and phenotypic measurements of plants exposed to the above 13 treatments (n= 6) for each genotype for each of the treatments) were taken on day 14.

2.2.3 Above-ground phenotypic measurements

All plants were measured at the end of the experiment after 14 days i.e. after nutrient-deprived treatment during the vegetative plant growth. To understand the phenotypic differences between the treatments detailed measurements were taken as follows.

Plant height (cm): the height was measured at the end of the experiment and was measured from the bottom of the main stem to the last internode of the flowering branch.

Tiller number: total number of branches was counted excluding the main stem.

Leaf number: total number of leaves per plant was counted at the end of each treatment.

Spike number on the main stem: Spike present on the main stem were scored at the end of the experiment.

Fresh weight (g): this was determined after two week-stress treatment and the harvested aboveground biomass was instantly measured accurate to 0.05 g.

Dry weight (g): the samples used for fresh weight determination were oven-dried at 60 °C for 48 h until a stable weight was reached. The resulting weight was recorded as dry weight.

2.2.4 Chlorophyll content in plant biomass

Chlorophyll content (Chl a, Chl b, and total Chls) was measured by using a spectrophotometric method as reported by Lichtenthaler (1987). Leaf samples were harvested at the end of the experiment and freeze-dried at -80 °C. The samples were

immediately frozen by using liquid nitrogen and sample powder was weighed (10 mg) in plastic test tubes (15 ml) using a high precision balance (Sartorius, Mettler AK 160, 0.0001 g). A solution of 2 ml of 95% ethanol was added to the sample tube, which was wrapped with aluminium foil, vortexed and stored at 4 °C. After 24 h tubes were centrifuged for 15 minutes at 2500 rpm. Then, the supernatant was decanted into new glass tubes (5 ml) and stored in the dark at 4 °C. 2 ml of 95% ethanol solution was added to the remaining sample pellet, vortexed and stored in the dark at 4 °C. After 48 h, the new supernatant was collected into glass tubes for UV/VIS spectrophotometric measurement. The absorbance of 170 µl of sample extract was read at 648, and 664 nm against the same amount of blank (extractant solution, 95% ethanol) in a 96 well Half Area UV-Star Microplate 23 (Greiner Bio-One International GmbH, Austria). Chl a and Chl b content was calculated according to Lichtenthaler & Buschmann (2001). The whole extraction process was executed in low light conditions to reduce pigment degradation. The Chl a and Chl b content was determined according to the following formulas:

$$Chl\ a\ content\ (\mu g/ml)\ =\ (13.36 * A664)\ -(5.19 * A648)$$

$$Chl\ b\ content\ (\mu g/ml)\ =\ (27.43 * A648)\ -\ (8.12 * A664)$$

where A is the absorbance at that specified wavelength.

2.2.5 Root assay measurements

Media composition

The media was prepared using Murashige and Skoog (MS) as described by Gruber et al. (2013) with 0.1% Agar in the solution. The nutrient-deprived MS media was modified similar to the Hoagland solution by supplementing 1 mM $NaNO_3$ in potassium and 1M KCl in a nitrate deprived medium so as to balance the nitrate and potassium under reduced N and K treatment (Appendix Table A2.3- A2.5).

Root growth conditions

Brachypodium seeds of uniform size were selected and sterilised for an hour using 10% bleach (Domestos) followed by rinsing with sterile distilled water several times. It was made sure that the traces of bleach from the water were removed by checking the pH ranging from 5.6 - 6.0 of the water in which the seeds were imbibed. The seeds were left overnight in sterile water at 4 °C, and re-sterilisation with 10% bleach concentration with several rinsing steps was done the very next day. Under sterile conditions, the seeds were transferred onto round Petri dishes (90mm x 20 mm) with a half-strength nutritional MS medium for plant growth. The Petri plates were first placed in the refrigerator at 4 °C for two days to synchronize the germination rate and were then placed in growth chambers with a 16/8 h photoperiod at 23 °C.

Homogeneous seedlings (germinated caryopses) with a radicle were selected for each genotype and treatment (n=5) for the rest of the experiment. These seedlings were gently removed from the Petri dishes using forceps and transplanted individually. Root tips were aligned onto the square Petri-Plates (120 mm x 120 mm x 17 mm), which contained different deprived nutrient-dose medium (Appendix Table A2.5: A, B, C, D). The plates were placed vertically on the rack in the growth chamber, and root growth was measured every two days for the 10-day duration of the experiment by marking the position of the root tip on the back of the plate using a permanent marker Three biological replicates, i.e., three plates per genotype per treatment containing five seedlings were analysed for data analysis.

Image analysis of root traits

At the end of the experiment, the plates were scanned for two-dimensional image analysis and the root traits such as root length, and root length over time was measured using Image J software (Fiji, U.S.).

2.2.6 Biomass quality

OVERVIEW

This section will mainly characterise and discuss the *Brachypodium* cell wall carbohydrate composition by liquid chromatography, following acid and enzymatic hydrolysis of the cell wall material (CWM). Several forms of HPLC are useful for the separation of monosaccharides and oligosaccharides in cell wall hydrolysates. One of such forms, frequently abbreviated as HPAEC-PAD, consists of a high-performance anion-exchange chromatography (HPAEC) system coupled to a pulsed amperometric detector (PAD). HPAEC is a method to separate anionic analytes, yet cell wall monosaccharides are not anions in their common form. However, by using chromatographic eluents at high pH, carbohydrates may be ionised. The reason for this is that most cell wall monosaccharides have dissociation constants (p*Ka*) in the range 12–14 (e.g., Xyl: 12.15, Glc: 12.28, Gal: 12.39, Ara: 12.43) and are weak acids. As a result, at high pH values, the hydroxyl groups of these sugars are partially transformed into oxyanions and may be separated by anion-exchange mechanisms (Zhang & Lee, 2002). Most notably, the CarboPac series of columns has been specifically designed for carbohydrate anion-exchange chromatography (Dionex). Within this range, the CarboPac SA10 column has been developed to provide a fast and well-resolved separation for most monosaccharides and disaccharides in biofuel research and is packed with a hydrophobic, polymeric, porous resin, coated with a strong anion-exchange layer of latex nanobeads (Dionex, 2013). By using these column packing materials and high pH eluents,

cell wall carbohydrates are separated by interaction with quaternary ammonium cation functional groups and may be eluted in a single run where higher retention times correspond to lower pKa value (Corradini & Cavazza, 2012). PAD is considered superior since it provides advantages in terms of speed and sensitivity, with an excellent signal-to-noise ratio even at extremely low analyte concentrations, without requiring derivatisation (Swadesh, 2001). Detection of carbohydrates is achieved by measuring the electrical current generated by their oxidation at the surface of a gold electrode.

High sensitivity and lack of need for sample derivatisation represent the major advantages of HPAEC-PAD over other methods for carbohydrate detection and quantification. Additionally, no extensive sample preparation is required for analyte detection, since neutral or cationic sample components elute within the void volume of the column, and thus do not usually interfere with the analysis of the carbohydrate components of interest.

2.2.7 Cell wall material preparation

Stem materials were analysed in duplicates per each treatment- control, N20%, N4%, N0%, P20%, P4%, and P0% for both the genotypes. The harvested senesced biomass was collected and then freeze-dried. The dry biomass was milled by using a biomass grinding and loading robot (Labman Automation Ltd.). Stem biomass was then fractionated to an alcohol insoluble residue (AIR) according to a protocol adapted from (da Costa *et al*., 2014; Foster *et al*., 2010). For each sample, approximately 60-70 mg of dry milled biomass was weighed, and 1.5 ml of 70% ethanol was added. This was followed by the first incubation for 12 h in a shaking incubator set at 25 °C and 150 rpm and then twice for 30 min at 40 °C. Consequently, cell wall biomass (CWM) was extracted three times with 1.5 mL of chloroform/methanol solution (1:1 v/v) at 25 °C/ 150 rpm and finally twice with 500 mL of

acetone at 25 °C/ 150 rpm after which samples were air-dried for at least two days in a laminar fume hood at room temperature. Between each extraction, samples were thoroughly vortexed before incubation and centrifuged at 3,000 rpm for 10 min to aspirate the supernatant-containing extractives.

De-starching of extracted biomass was initiated by re-suspending the samples in 1 mL of 0.1 M sodium acetate buffer (pH 5) and heating them in a water bath at 80 °C for 20 min to induce starch gelatinisation. Samples were subsequently cooled to room temperature and centrifuged at 1000 rpm. After the supernatants were discarded, the pellet was washed twice with 1.5 mL of deionised water with resuspension, centrifugation and supernatant discarding. To inhibit microbial growth sodium azide was added at 0.0002% (w/v) and starch was removed by incubation with a saturating amount of type-I porcine α-amylase (Sigma-Aldrich; 47 units per 100 mg cell wall) in 0.5 mL of 0.1 M ammonium acetate buffer (pH 5). To ensure complete starch hydrolysis, samples were then placed in a shaking incubator set at 25 °C (150 rpm) for an extended incubation period of 48 h. α-amylase digestion was terminated by heating samples in the water bath for 15 min at 95 °C and samples were cooled at room temperature. The supernatant containing solubilised starch was aspirated, and the pellet was then washed three times in 1.5 mL of deionised water and twice with 1.5 mL of acetone, with centrifugation, vortexing and supernatant removal between each step. De-starched AIR was air-dried in a laminar flow bench until moisture content was ≤10%.

A Lugol staining test was performed by randomly selecting samples for the confirmation of the absence of starch residues in the biomass material (Barnes & Anderson, 2018). To perform the analysis, 2 mg of AIR samples were weighed, and 0.5 mL of Lugol's iodine solution was added. Samples were incubated for 5 minutes at room temperature,

centrifuged at 10,000 x g for 10 min to pellet residue, and the supernatant was removed without disturbing the pellet. The pellet was washed with 1 mL of deionised (DI) water, centrifuged, and the supernatant discarded as previously described, and the colour of the AIR sample was observed. Since no colour was seen in the AIR after de-starching, the samples were considered free from starch.

2.2.8 Determination of monosaccharide content

Composition analysis of previously prepared AIR samples was based on the procedure described by (Sluiter et al., 2012). Briefly, 10 mg of AIR samples were weighed into 10 mL Pyrex glass tubes, and 100 µl of 72% (w/w) H_2SO_4 was added. Tubes were capped with polypropylene caps and placed on a heating block set at 30 °C for 1 h. Samples were vortexed every 10 min. The acid hydrolysate was diluted to 4% (w/w) H_2SO_4 with 2.5 mL of deionised water, and samples were mixed by inversion to eliminate phase separation. Subsequently, tubes were sealed and placed in an autoclave at 121 °C for 1 h and then cooled to room temperature and centrifuged to produce a particulate-free supernatant. Stem samples were diluted ten-fold (1:10) by mixing 100 µl of each sample with 900 µl of deionised water followed by a hundred-fold (1:100) dilution by mixing 50 µl of the 1:10-diluted samples with 950 µl of a solution of 0.015 M KOH. Finally, 400 µl of the 1:100 diluted samples were transferred into 0.45 µm nylon filter vials (Thomson SINGLE StEP). Monosaccharide concentrations were determined using a Dionex ICS-5000 HPAEC system equipped with a pulsed amperometric detector (PAD) using a gold working electrode and an Ag/AgCl reference electrode. Monosaccharides were separated using the Dionex CarboPac SA10 column set at 45 °C and 1 mM KOH for isocratic elution, with a flow rate of 1.5 mL/min for 14 min and 25 µl injection volume. Sugar calibration standards for glucose, xylose,

arabinose, galactose, mannose, fructose, sucrose, cellobiose, and fucose were run using serial dilution concentration ranges of 20 µg/mL, 10 µg/mL, 5 µg/mL, 2.5 µg/mL and 1.25 µg/mL. A cellobiose standard was used as an indicator of incomplete hydrolysis. Chromeleon™ 7.2 Chromatography Data System (CDS) software was used for processing and analysing monosaccharide chromatograms. Finally, the content of each component was estimated as a percentage of cell wall biomass dry weight (Mns%) according to:

$$Mns\% = \frac{C_{Mns} \times V_R}{W_S} \times 100\%$$

Where: C_{Mns} - supernatant concentration (g/L) of the corresponding monosaccharide; V_R - reaction volume (L); W_S - sample weight (g).

2.2.9 Effect of nutrient stress on enzymatic saccharification efficiency

Biomass preparation includes oven-drying plant biomass at 45 °C until moisture content was ≤10%. Dry biomass was then milled with the use of a biomass grinding and loading robot (Labman Automation Ltd.). Biomass material was then fractionated to an alcohol insoluble residue (AIR) according to a protocol adapted from (da Costa *et al*., 2014; Foster et al., 2010) with some modifications. The digestibility of CWM from ABR6 and Bd21 accessions were determined following an approach consisting of the enzymatic hydrolysis of un-pretreated biomass, followed by HPAEC-PAD analysis of released sugars. Approximately 10 mg of CWM was weighed and enzymatic hydrolysis was achieved by using an enzyme cocktail consisting of a mixture of Cellulast (NS 50013; cellulase) and Novozyme 188 (NS 50010; β-glucosidase). Specifically, an incubation mixture was prepared and dispensed in such a way that per each CWM sample there were 997 µl of KOAc buffer at 0.025M (pH=5.6), 2.4 µl of Celluclast, and

0.6 µl of Novozyme 188, with added sodium azide at 0.04% (w/v) to inhibit microbial growth. To each tube 1 mL saccharification mixture was added. The saccharification mixture comprised the following composition:

- *0.957 mL of 0.025M Potassium acetate buffer (pH 5.6)*
- *0.0024 mL of cellulase from Trichoderma resesei (Cellulase, Sigma Aldrich, code C2730)*
- *0.0006 mL of β-glucosidase from Aspergillus niger (Novozyme 188, Novozyme, discontinued)*
- *0.040 mL of 1% sodium azide to repress bacterial growth*

The samples were incubated for 48 h in a shaking incubator at 50 °C/150 rpm. The samples were diluted after incubation with deionised water with a dilution factor of 1:100. Subsequently, 400 µl of these diluted samples were transferred to filter vials and analysed by HPAEC-PAD on an ICS-5000 ion chromatography system with a CarboPac SA10 column, operated at 45 °C with isocratic elution at a flow rate of 1.5mL/min. All samples were analysed in duplicate. Identification and supernatant concentrations of enzymatically released Ara, Glc and Xyl were determined using a standard curve prepared with a concentration gradient of the appropriate monosaccharide standards.

Saccharification efficiency:

$$Percentage\ Total\ Mns\ = \frac{Enz.Mns}{Total\ Mns} * 100$$

where: Enz. Mns is the amount of enzymatically released monosaccharide from the sample; Total Mns is the total amount of monosaccharide in the sample, previously determined by total acid hydrolysis of the cell wall.

2.2.10 Data analysis

Statistical analyses were performed by using R software (RStudio, 2021). The normality of data was verified by using the Shapiro test and Levene's test was used for homogeneity of

variances. A one-way analysis of variance was performed within each accession to compare the mean differences between treatments. Tukey HSD test (P=0.05) was used to determine the significance to compare the treatment means within each accession. Paired t-tests were used for pairwise comparison between accessions within each treatment.

2.3 Results

To understand the phenotypic behaviour and nutrient uptake under nutrient limiting conditions, a dose-response screening experiment was designed to attain insights into the phenotypic response to low nutrient dose stress in both ABR6 and Bd21 accession plants.

Low nutrient dose-response was selected for this experiment to recognize the unique ability of plants to adapt in response to nutrient availability in the soil. Images of both the genotypes, ABR6 and Bd21, under low nitrate (N), phosphate (P), potassium (K) and boron (B) dose-response are shown in Appendix Figure A2.1. A low nutrient dose has been reported to enable plants to reorganise themselves by affecting their biological processes related to plant growth and nutrient uptake under nutrient limitations (Swift *et al*., 2020). Therefore, this chapter focuses on improving our understanding of the phenotypic adaptations of ABR6 and Bd21 under low nutrient dose stress. The results will further enable us to underpin the detailed study on the largely unknown effect of nutrient limitation on biomass quality and yield of a model specie- Brachypodium.

2.3.1 Above-ground biomass

PLANT HEIGHT

Different doses of nutrient limitations showed another effect on plant height during the experiment in Bd21 genotypes (Figure 2-3 B). No significant effects were observed under K

and B dose-response in both ABR6 and Bd21 compared to the control-treated plants, except for a substantial increase in Bd21 plant height following K20% treatment. However, a significant reduction in plant height was observed in ABR6 under conditions of limiting N (N20%, $p<0.01$; N4%, $p<0.001$; N0%, $p<0.001$, respectively) and P0% ($p<0.001$) compared with the control, whereas no significant difference was observed in Bd21 (Figure 2-3 A).

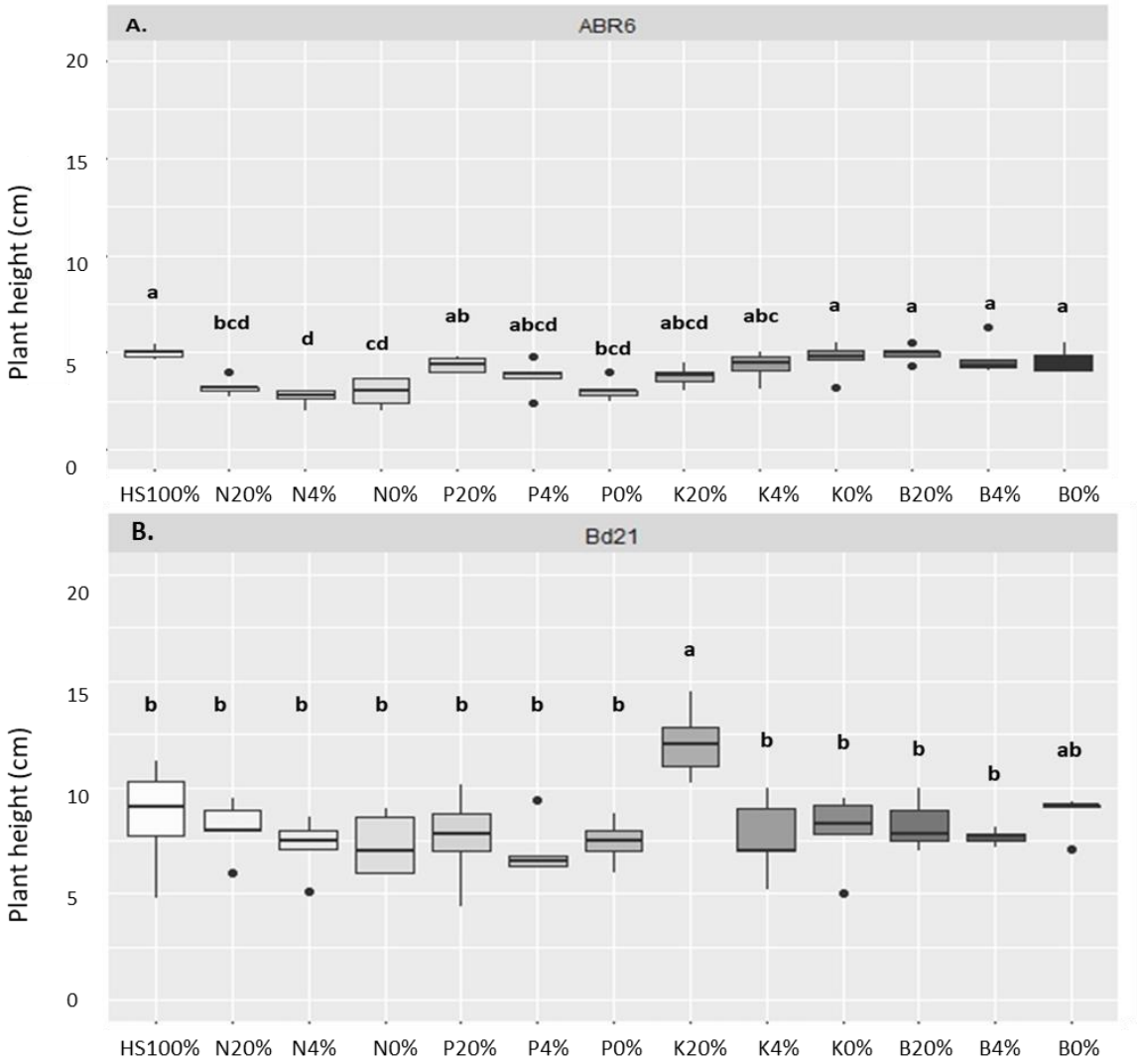

Figure 2-3: Plant height (cm) measurements A. ABR6, B. Bd21 in and ecotypes of *Brachypodium* under low nutrient dose-response. Control receiving full Hoagland solution (white). Boxes represent the mid two quartiles with the median drawn and lowercase letters show statistical significant values between the treatment by Tukey's test ($p=0.05$), n=5 replicates.

LEAF NUMBER

For both accessions, leaf numbers were not significantly affected by the K and B dose-response treatments compared with the control (Figure 2-3). However, limitations of N and P resulted in significant leaf number reductions for both ABR6 and Bd21, although no dose-response could be observed when comparing the 20%, 4% and 0% nutrient levels. For ABR6, the average reduction in leaf number was 42% following the limitation of P, whereas under the N limitation, this reduction was 50% compared to the control ($p<0.001$). Bd21 also showed a similar effect to ABR6 accession in leaf number except in P20%, which had no significant effect on leaf number, as shown in figures 2-3 A. A significant difference in leaf number under N dose-response by 44%, 48%, and 44% (N20%, $p=0.01$; N4%, $p=0.004$ and N0%, $p=0.01$) whereas P4% by 48% ($p=0.004$), and P0% by 46% ($p=0.007$) was found compared with the control (Figure 2.3 B).

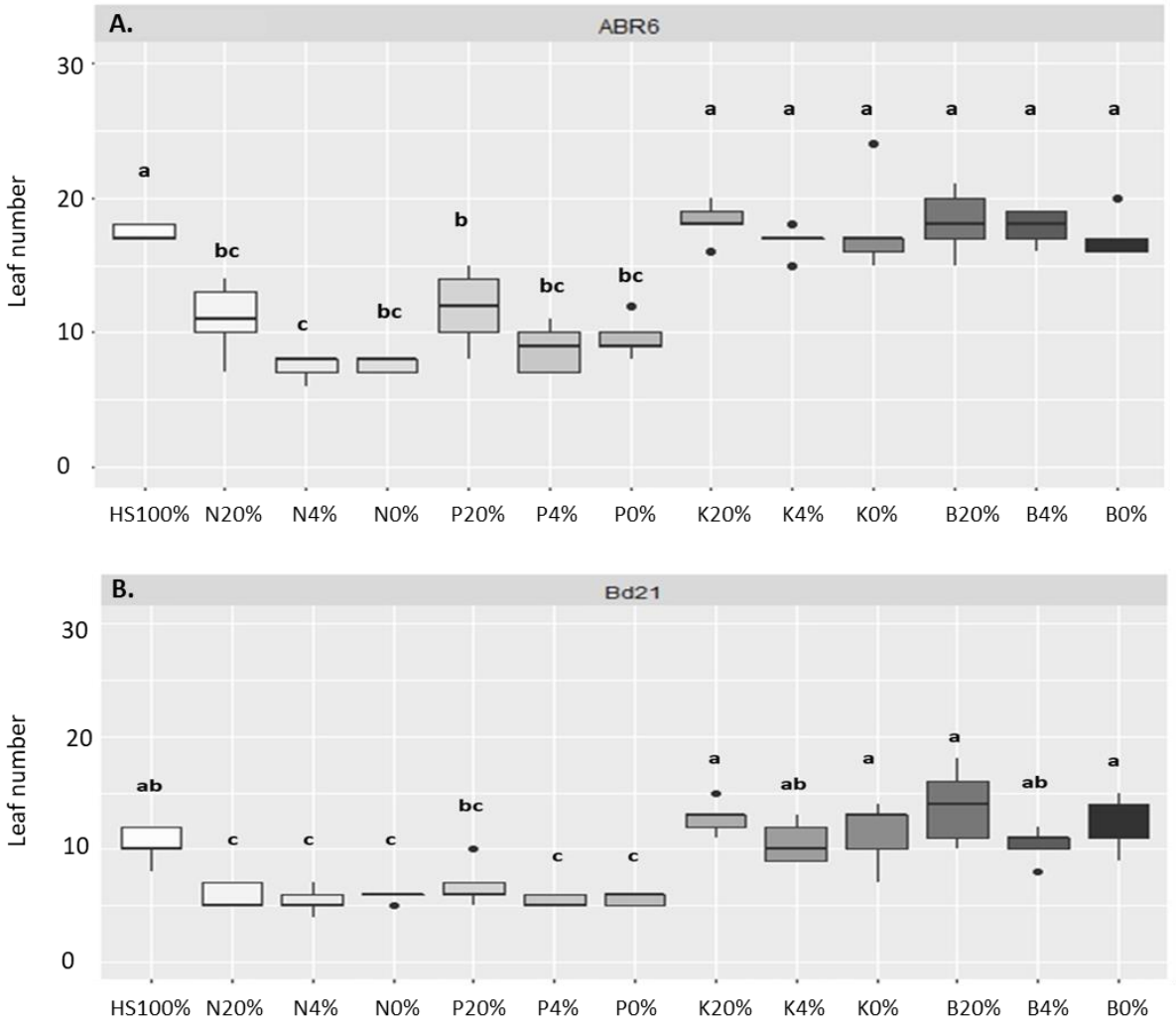

Figure 2-4: Leaf number A. ABR6, B. Bd21 in and ecotypes of *Brachypodium* under low nutrient dose-response. Control receiving full Hoagland solution (white). Boxes represent the mid two quartiles with the median drawn and lowercase letters show statistical significant values between the treatment by Tukey's test (p=0.05), n=5 replicates.

TILLER NUMBER

The tiller numbers were counted at the end of the experiment (after 14 days of nutrient stress treatment). N and P dose-response treatments significantly reduced the tiller number for both ABR6 and Bd21 ($p<0.001$). Nitrate stress (N20%, N4%, and N0%), P4%, and P0% showed the complete absence of tillers in Bd21 (Figure 2-5 B). Furthermore, B and K dose-response treatments did not significantly affect the tiller number in both the accessions compared to the control treatment, except for K20% in ABR6 (Figure 2-5 A).

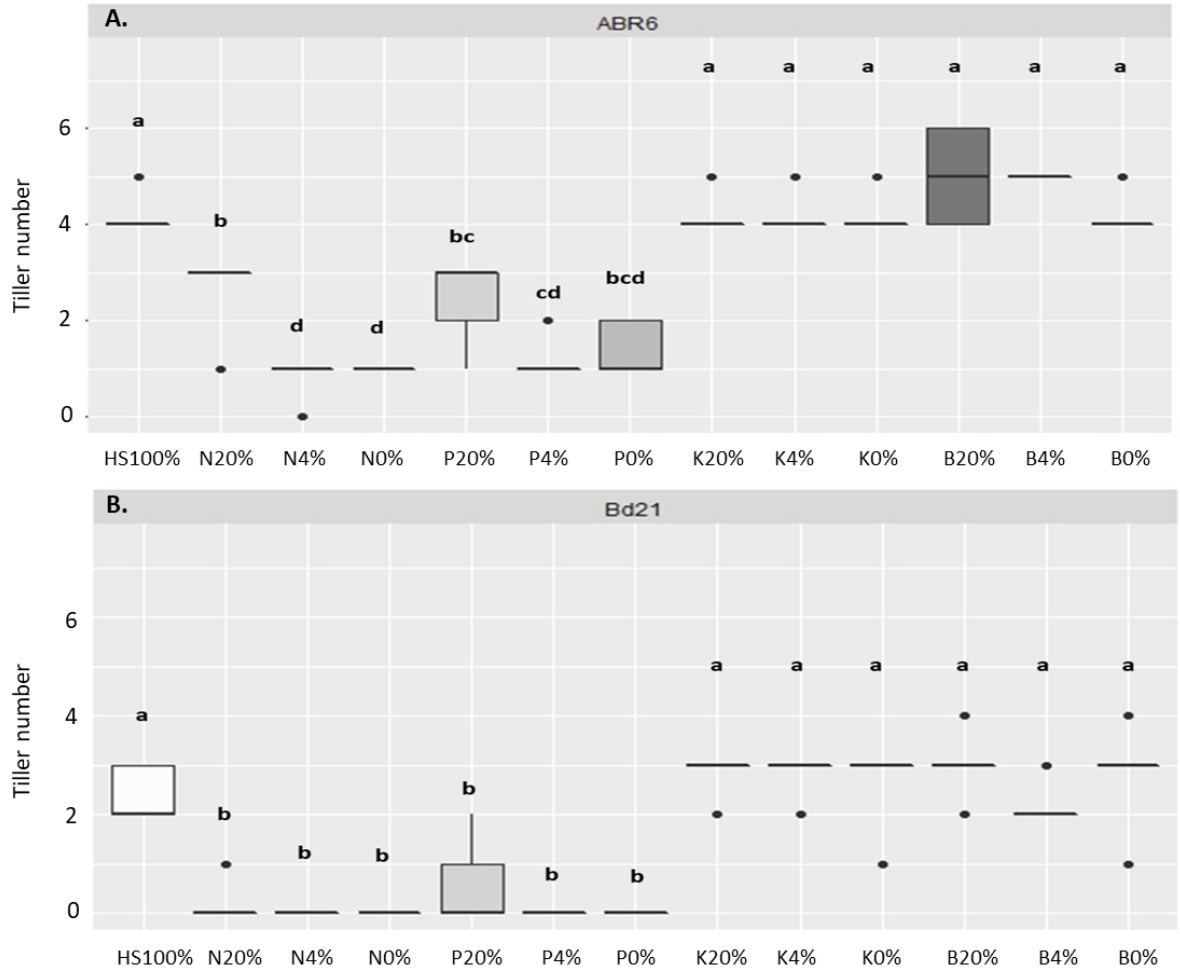

Figure 2-5: Tiller number A. ABR6, B. Bd21 in and ecotypes of *Brachypodium* under low nutrient dose-response. Control receiving full Hoagland solution (white). Boxes represent the mid two quartiles with the median drawn and lowercase letters show statistical significant values between the treatment by Tukey's test (p=0.05), n=5 replicates.

TOTAL SPIKE NUMBER

The plants were analysed at the senescence stage to determine if spikelet number was affected in the two parental accessions of *Brachypodium* across each nutrient-limiting treatment. Spike numbers present on the main stem also known as spikelet showed significantly reduced in both accessions following the P and N dose response treatments ($p<0.01$), although for Bd21 N20% and P20% treatments the reductions were not statistically significant (Figure 2-6 B). No significant effect on spikelet number was observed

for K and B treatments for both accessions, except for K20% showing a significant decrease in ABR6 (Figure 2-6 A).

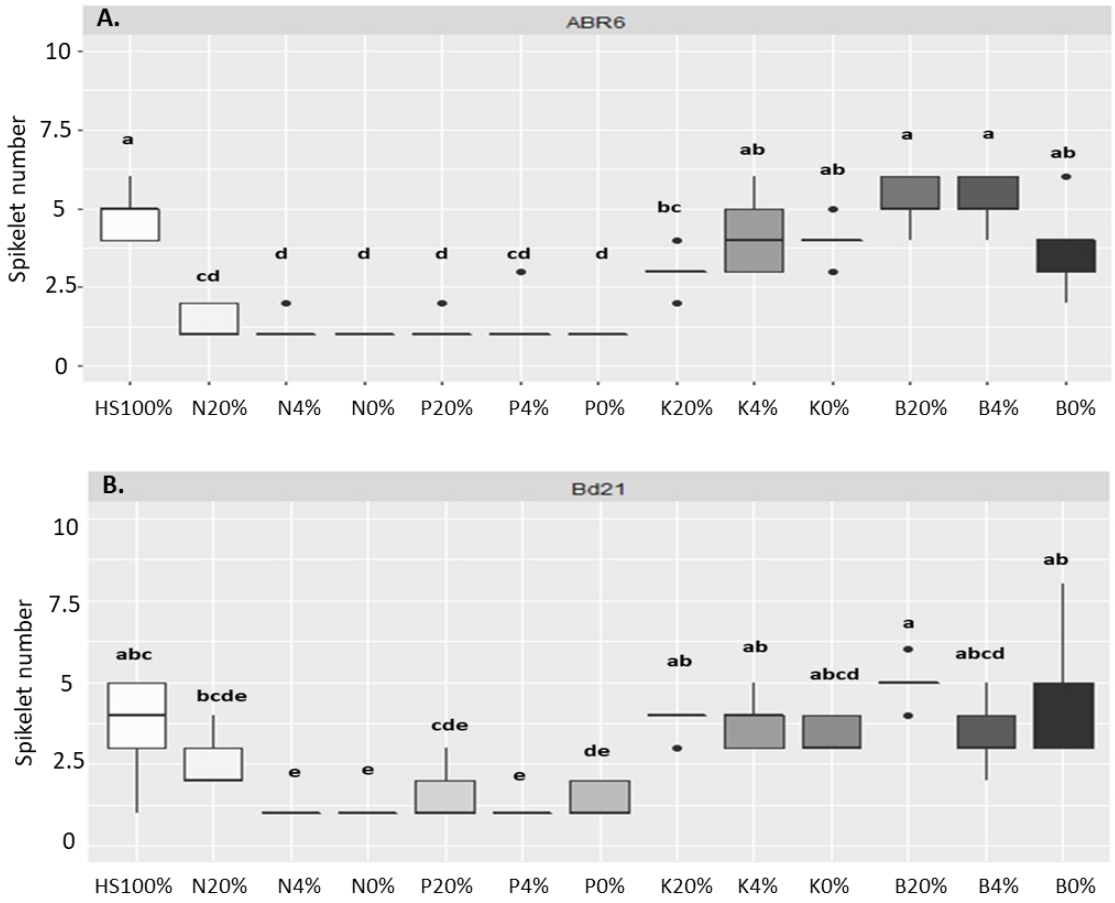

Figure 2-6: Spikelet number A. ABR6, B. Bd21 in and ecotypes of *Brachypodium* under low nutrient dose-response. Control receiving full Hoagland solution (white). Boxes represent the mid two quartiles with the median drawn and lowercase letters show statistical significant values between the treatment by Tukey's test (p=0.05), n=5 replicates.

FRESH WEIGHT

To determine the effect of nutrient stress treatments on aboveground biomass, the fresh weight of plants (leaf and stem material, without heads) was measured (Figure 2-7, n=3 per each treatment, both treatments). Fresh weight was distinctive in both the *Brachypodium* accessions and was measured and recorded at the end of the 2-week stress treatment and shown in Figure 2-7 (mean ± standard error).

A significant decrease ($p<0.01$) in fresh weight in all the selected nutrient dose-response treatments was found in ABR6 compared with the control (Figure 2-7 A). Based on average reduction for N dose- response treatments (N20%, N4%, N0%) showed the highest reduction in fresh biomass by 78% ($p<0.001$), followed by P, B and K dose- response treatments (75%, $p<0.001$;70%, $p<0.001$;52%, $p<0.01$) when compared to the control ABR6 plants. A similar trend was found in Bd21 accession with a significant reduction in fresh weight compared to the control except for B0% ($p=0.3$) treatment (Figure 2-7 B). The average results from nutrient dose-response in Bd21 suggested that N showed the highest reduction in fresh biomass by 74% ($p<0.001$) followed by P (74%, $p<0.001$), K (55%, $p<0.01$), and B (55%; B20%, B4%, $p=0.006$, respectively) compared with the control.

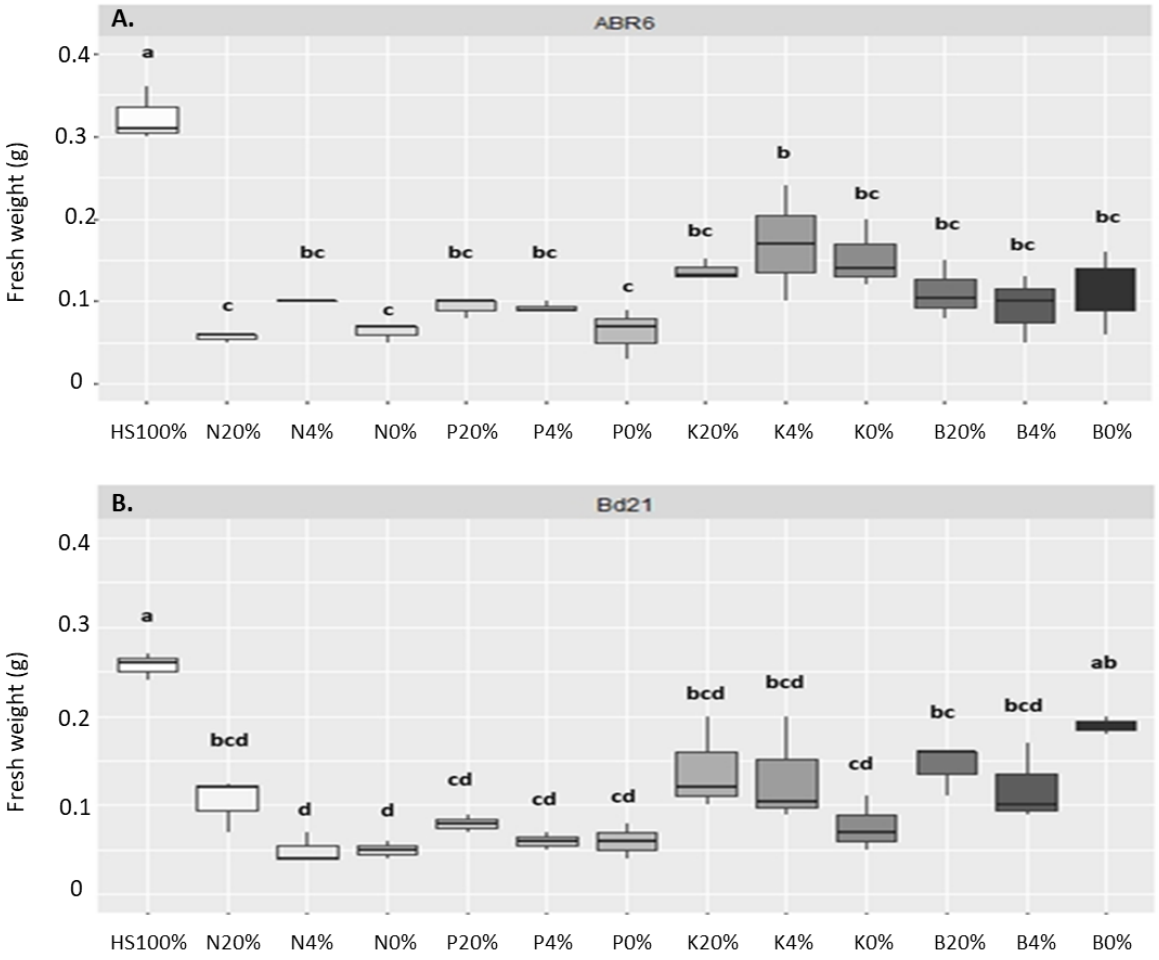

Figure 2-7: Fresh weight (g) A. ABR6, B. Bd21 in and ecotypes of *Brachypodium* under low nutrient dose-response. Control receiving full Hoagland solution (white). Boxes represent the mid two quartiles with the median drawn and lowercase letters show statistical significant values between the treatment by Tukey's test (p=0.05), n=3 replicates.

DRY WEIGHT

The dry biomass measurement showed no significant effect under N, P, and B treatments in ABR6 (Figure 2-8 A). However, a significant increase in dry biomass was almost doubling in K4% (p=0.004) and K20% (p=0.01) treatment compared with the control. Bd21 accession showed no significant effect on treated plants dry biomass compared to the control (Figure 2-8 B).

Comparing the different nutrient limitation treatments, experiencing N (Hoagland with N levels reduced to N20%, N4%, N0%) and P (Hoagland with P levels reduced to P20%, P4%, P0%) deficits had overall the most significant impact on plant growth and development in both Bd21 and ABR6 parental lines of *Brachypodium*.

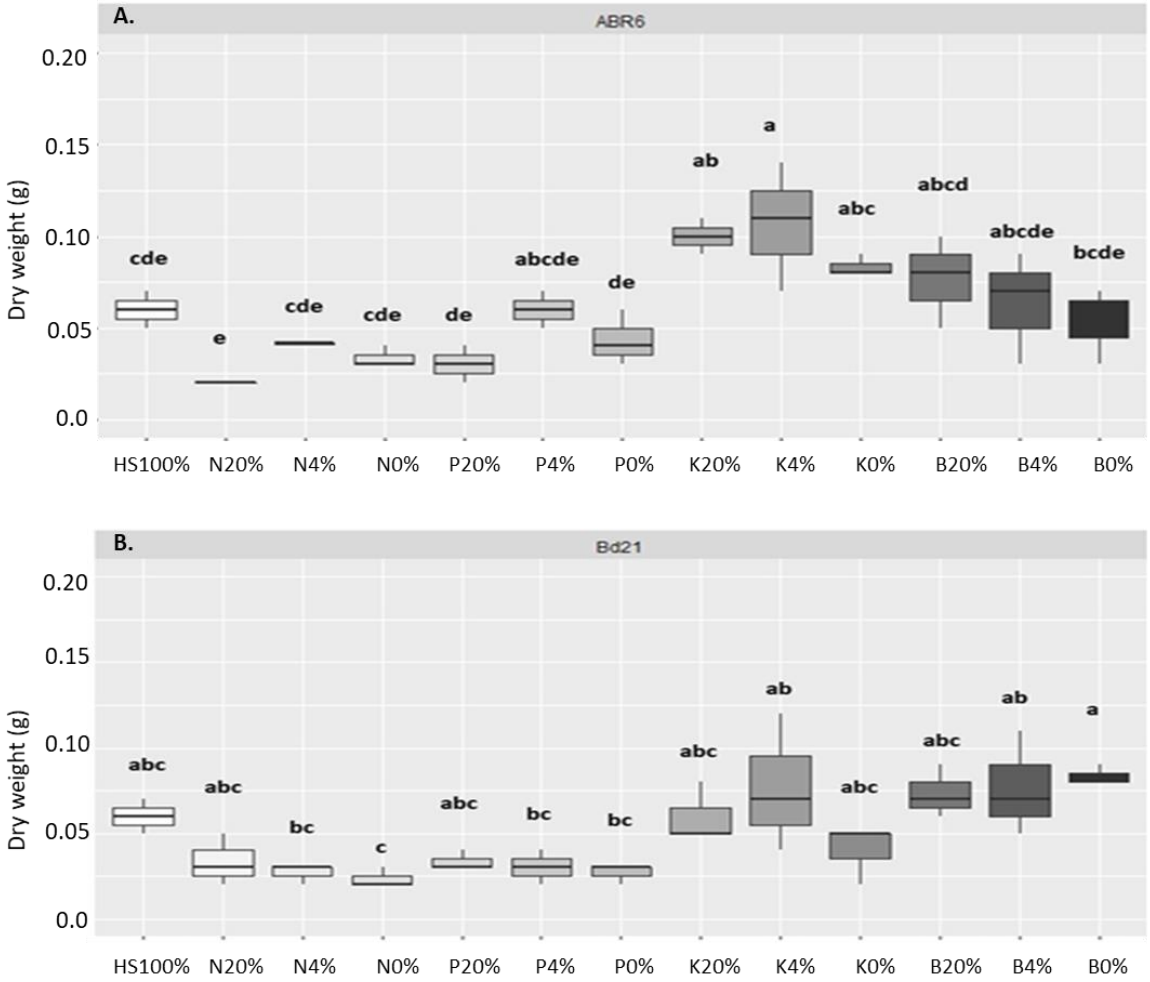

Figure 2-8: Dry weight (g) A. ABR6, B. Bd21 in and ecotypes of *Brachypodium* under low nutrient dose-response. Control receiving full Hoagland solution (white). Boxes represent the mid two quartiles with the median drawn and lowercase letters show statistical significant values between the treatment by Tukey's test (p=0.05), n=3 replicates.

2.3.2 Root traits under nutrient dose-response

To investigate the effect of nutrient limitation on root growth, root growth assays were carried out, and root length was measured as a proxy of below-ground development. This

method involved growing seedlings into full-nutrient growth media and then transplanting them on nutrient-deprived growth media to expose them to N, P, K, and B limiting conditions for ten days.

Seedlings exposed to low K and B concentrations in the growth media showed no significant difference in the total root length in the Brachypodium accessions compared to the control (Figure 2-9 C & D). The statistical analysis performed between the ABR6 and Bd21 under each treatment also showed no significant difference except in B4% ($p<0.05$). Reducing N levels to 20% and 4% did not affect root length in ABR6 and Bd21 compared with full nutrient control (Figure 2-9 A). However, N0% treatment showed a statistically significant reduction in root length compared with control plants in both accessions ($p<0.01$). In addition, there was a significant difference in root phenotypic length between ABR6 and Bd21 ecotypes ($p<0.01$) in response to N4%. Reducing P levels to 4% and 0% resulted in a significant reduction in root length in Bd21 (P4%, $p<0.01$; P0% $p<0.001$) while for ABR6 a considerable reduction was only observed for P0% ($p<0.001$) compared with the control (Figure 2-9 B). Moreover, a significant difference in root length between the two distinct ecotypes was found for P20% ($p<0.001$) and P4% ($p<0.05$) treatments, respectively.

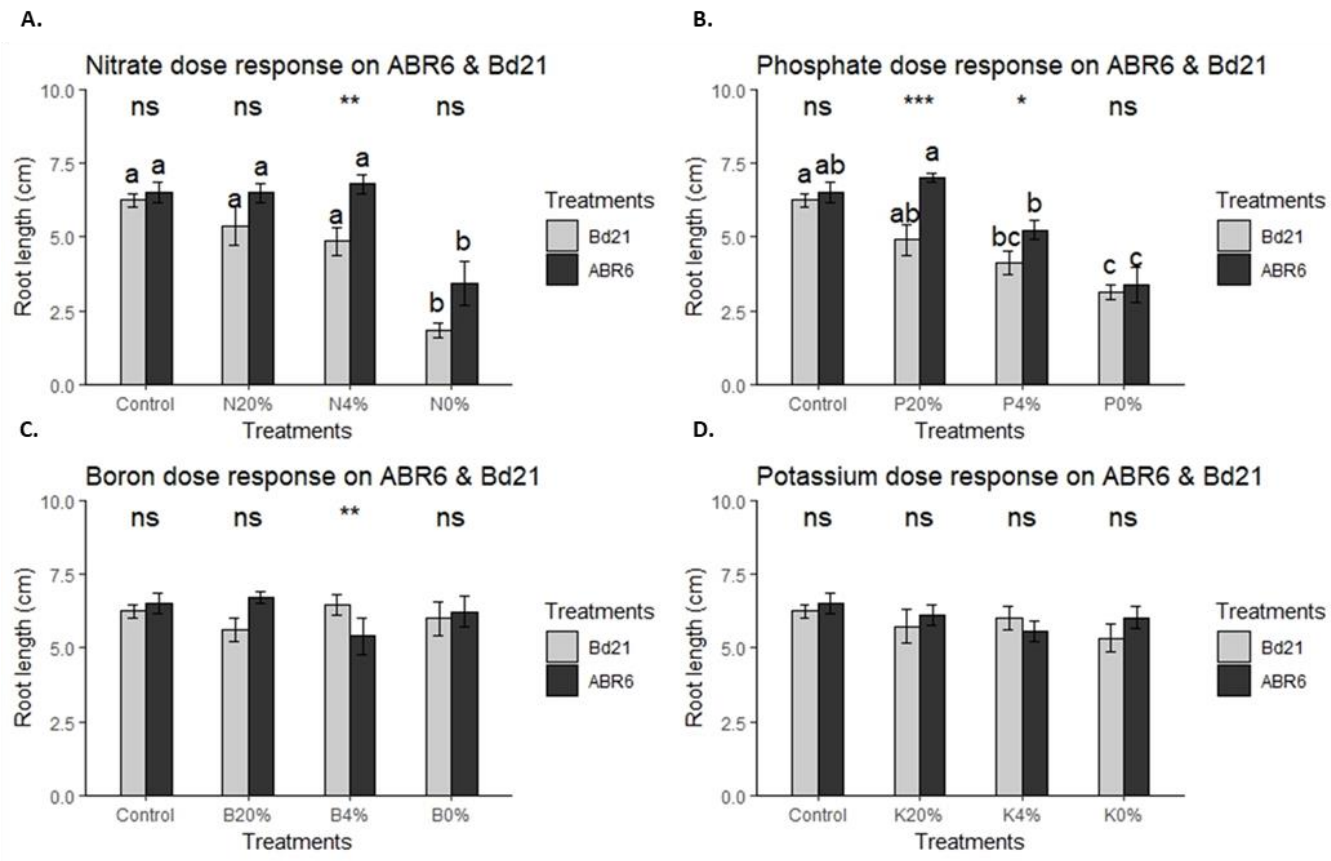

Figure 2-9: Root length measurement under different nutrient dose-response treatments in ABR6 and Bd21 ecotypes of *Brachypodium*. Letters indicate significant treatment differences at p<0.05, as determined by analysis of variance (ANOVA) and high significant difference (HSD) test. Paired t-test was used to compare treatment means between accessions. Significant codes indicate significant differences between the two accessions of *Brachypodium* for a given treatment, p<0.001 '***', p<0.01 '**', p<0.05 '*', 'ns'.

NITRATE AND PHOSPHATE DOSE-RESPONSE OVERTIME

As before, ABR6 and Bd21 accessions were grown on control media and transplanted to nutrient-deprived media as mentioned in section 2.3.2. The root length was marked every three days to allow assessment of root growth over time, as shown in Figures 2-10. To select a single, most representative root system we used Image J analysis as shown in figure 210 C and D. Bd21 plants appeared to have a wider and more branched root system (Figure 2-10 D) compared to that of ABR6 plants (Figure 2-10 C).

Progression of root growth was visualised under nitrate and phosphate dose-response treatments compared to control media, as shown in Figures 2-10 A & B. No significant effect

was observed in ABR6 on days 0, 3, and 6. However, a significant reduction in root length on day 9 in ABR6 seedlings was found under N0% ($p<0.001$) and P0% ($p<0.001$) compared to the control. For Bd21, no nitrate started showing a significant reduction in root length on day 6 (by 63%) when compared with the control. On day 9, Bd21 also showed a drastic significant reduction in root length under P4% by 34% ($p=0.05$), no phosphate by 50%, and no nitrate by 71% ($p<0.001$), respectively.

The results indicate that both N0% and P0% treatments significantly reduce root growth over time in both accessions.

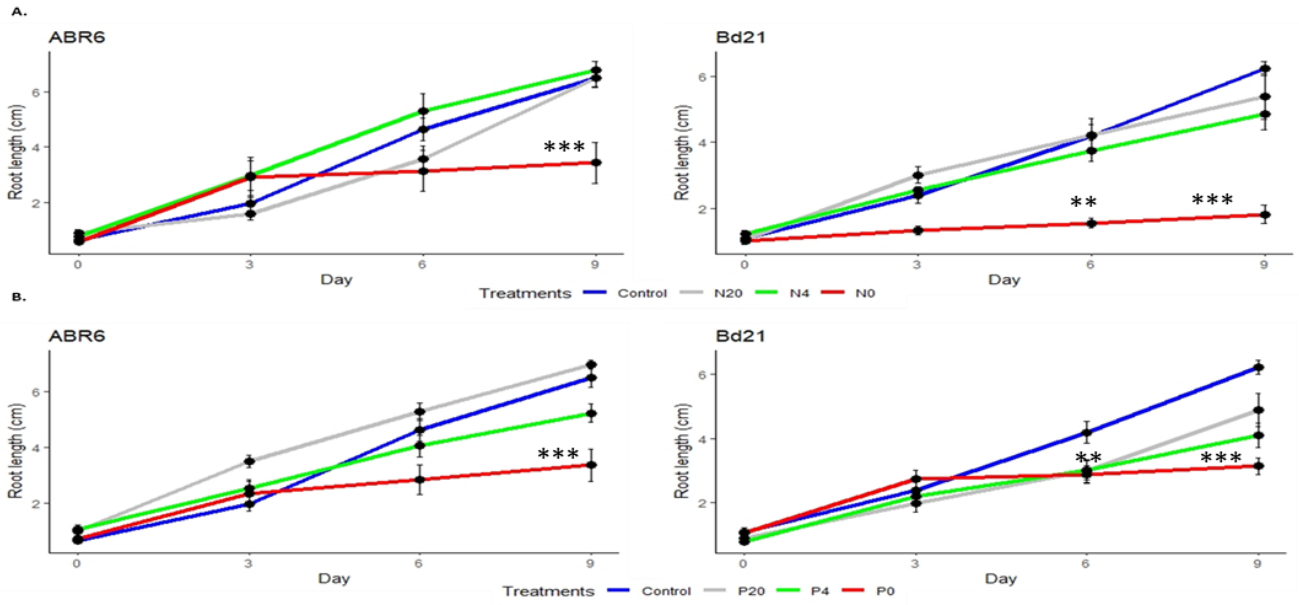

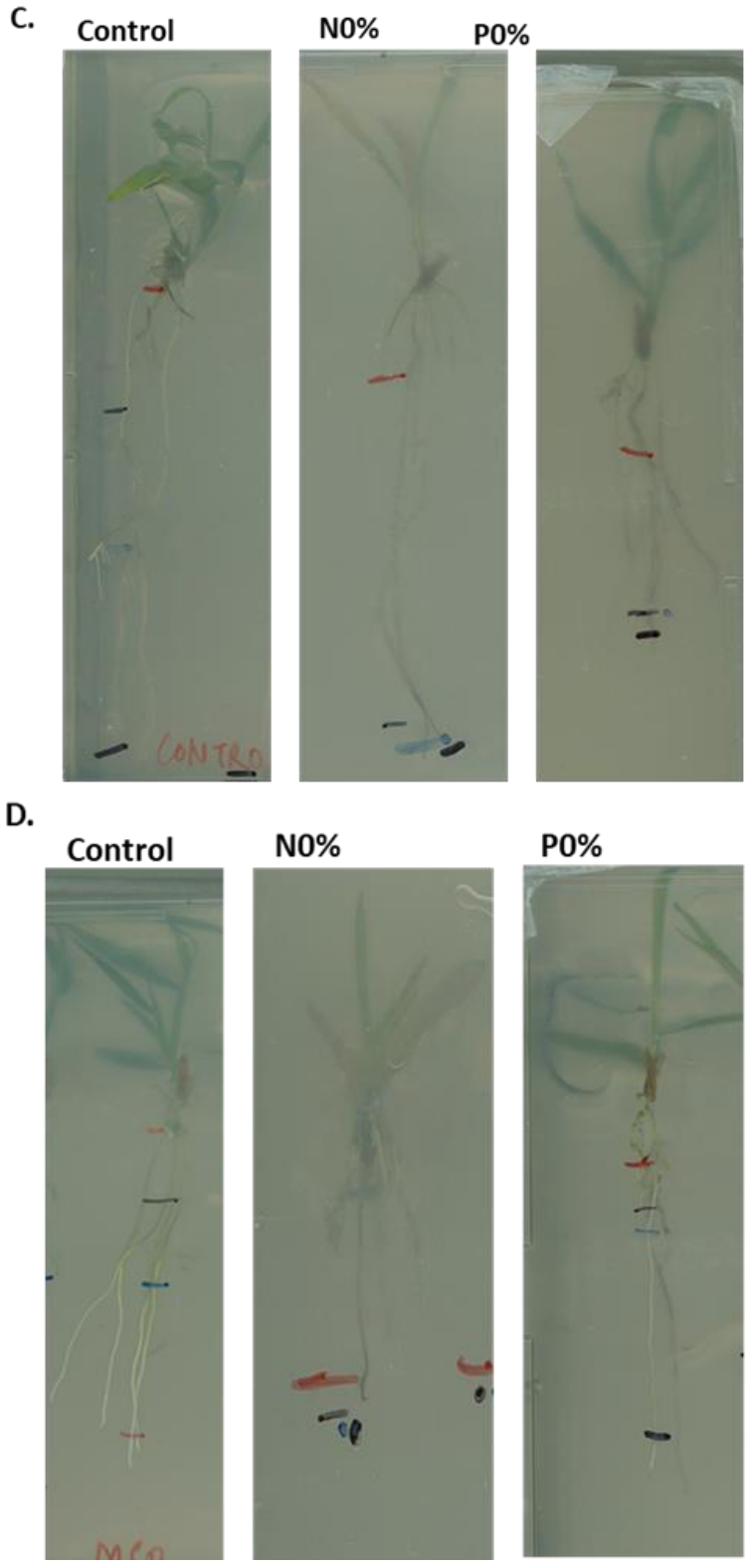

Figure 2-10: A & B: Cumulative root length measurement of *Brachypodium* genotypes ABR6 and Bd21 at an interval of 0, 3, 6 and 9 day on the nutrient deprived media over time under selected N (N20%, N4%, N0%) and P (P20%, P4%, P0%) dose-response treatments compared with the Hoagland by using Image J software (n=15). Asterik shows the significant difference

p<0.001 '***', p<0.01 '**'. Root image at 9 day after the transplanting the seeds in nutrient deprived N and P dose-response growth media C: ABR6, D: Bd21

2.3.3 Chlorophyll content

Chla and Chlb content was measured to understand the mechanisms of acclimatization of photosynthesis under different low nutrient stress conditions in ABR6 and Bd21 accessions. Previous results suggested that N and P limitations had a significant effect on the root phenotypic behaviour of both accessions (A. Ingram *et al*., 2012). Therefore, the above two nutrients were selected for further in detail study. The complete Hoagland control treatment for this experiment.

Nitrate dose-response resulted in a significant reduction in Chla content in ABR6 when compared to the control ($p<0.01$), whereas a substantial decrease in N20% ($p<0.001$) with no effect on N4% and N0% on levels of the primary reaction centres pigment was found in Bd21 accessions (Table 2.3). However, phosphate dose-response (P205, P4%, P0%) showed a significant rise in Chla in ABR6 accessions when compared to the control ($p<0.001$). P20% stress condition showed the highest Chla content in ABR6 ($p<0.001$; 10.5±0.7 mg g DW^{-1}) and Bd21 ($p<0.001$; 7.7±1.9 mg g DW^{-1}) leaves, whereas no significant effect was observed in P4%, and P0% in Bd21, compared with the control (Table 2.3).

Chlb content was significantly affected by nitrate dose-response in both the accessions of *Brachypodium*, with the lowest content found in the N0% ($p<0.001$) treatment (Table 2.3). P20% treated plants showed a statistically significant effect in ABR6 ecotypes compared to the control ($p<0.001$), and a significant reduction in P4% and P0% was found in ABR6 leaves. P20% treatment did not have a significant effect on levels of Chlb content ($p=0.5$) but did have a significant decrease in P4% and P0% ($p<0.001$) when compared to the control Bd21 accessions.

The ratio of chlorophyll a to b (Chla:b) of the N and P dose-response plants was significantly higher than the plants grown under control and Hoagland treatment in both the accessions. P4% treatment resulted in the highest Chl a:b ratio, increasing by 2.5-fold and 3-fold, respectively, in ABR6 and Bd21 *Brachypodium* accessions compared with their respective Hoagland controls (Table 2.3).

In conclusion, the results indicate that phosphate deficiency had a more enormous impact on the chlorophyll content of ABR6, following P4% and P0% treatments which increased Chl-a and decreased Chl-b content. In contrast, nitrate limitation resulted in an overall decrease in both Chl-a and Chl-b content in both the ecotypes compared to the control and Hoagland treatment. This further suggested that nutrient stress can act as a limiting factor for crop yields by reducing the photosynthetic rate, destruction of chlorophyll pigment-protein complex, and intrusion in chlorophyll synthesis (Ali et al., 2004; Yuan S. et., 2015).

Table 2-3: Chlorophyll content a and b measurement in different nitrate and phosphate dose-response in *Brachypodium* accessions

Leaf pigment related trait	Treatment	Accessions		One-way ANOVA comparison between ABR6 & Bd21
		ABR6	Bd21	
Chla mg g DW-1	Hoagland	5.39±2.1c	5.7±5.8bc	ns
	N20%	5.07±6de	4.3±5.6d	***
	N4%	4.94±4.6de	4.7±2.0bcd	*
	N0%	4.81±3.9e	4.6±4.4cd	*
	P20%	10.5±0.7a	7.7±1.9a	ns
	P4%	8.03±3.4b	5.9±2.1b	***
	P0%	8.23±9.2b	5.9±2.2b	**
Chlb mg g DW-1	Hoagland	5.2±1.6c	6.6±2.6a	**
	N20%	2.1±2.7e	1.95±1.5b	ns
	N4%	2.2±3.8e	2.2±3.1b	**
	N0%	1.9±1.8e	1.85±0.8b	ns
	P20%	11.9±1.9a	6.5±1.5a	***
	P4%	3.2±2.4d	2.14±0.2b	**
	P0%	3.4±1.9d	0.06±0.5b	ns
Chl a/b ratio	Hoagland	1.03±0.02c	0.88±0.12ns	ns
	N20%	2.44±0.03a	2.22±0.19ns	ns
	N4%	2.22±0.01b	2.33±0.01ns	**
	N0%	2.42±0.08a	2.48±0.01ns	ns
	P20%	0.89±0.02c	1.19±0.04ns	**
	P4%	2.49±0.02a	2.86±0.36ns	ns
	P0%	2.39±0.05ab	1.2±1.48ns	ns

Values are reported as mean ± standard error of the mean. Different letters within columns indicate significant treatment differences at $p<0.05$, as determined by analysis of variance (ANOVA) and high significant difference (HSD) test. Significant codes: $p<0.001$ '***', $p<0.01$ '**', $p<0.05$ '*'. N=3 replicates

2.3.4 Stem cell wall monosaccharide content

Stem cell wall monosaccharide content was characterised for nitrate and phosphate dose-response treatments for both genotypes through complete cell wall hydrolysis followed by HPAEC-PAD. Arabinose, galactose, glucose, mannose, and xylose were identified and quantified, as shown in Table 2.4. The analysis suggested that treatments induced significant differences in the abundance of the different monosaccharides in both the ecotypes of *Brachypodium*. Glucose content was significantly ($p<0.01$) lowered under N0% in Bd21 compared to the control stem samples. ABR6 accessions showed a significant reduction in glucose content in N0% ($p<0.001$), P0% ($p<0.001$), N4% ($p<0.01$), P4% ($p=0.01$) compared with the Hoagland treatment. The various treatments had significant effect on xylose content of Bd21 stem samples. However, the xylose content was significantly reduced ($p\leq0.01$) in ABR6 samples following nitrate and phosphate dose-response treatments (Table 2.4). Interestingly, arabinose content showed no significant difference in ABR6 accessions of *Brachypodium* however, Bd21 showed a significant reduction in arabinose content following no nitrate and phosphate treatments when compared with the Hoagland (control) treatment. Galactose content was not significantly affected by nutrient stress in both the ecotypes compared with the control.

Table 2-4: Total monosaccharide content quantified by HPAEC-PAD for each genotype ABR6 and Bd21 are presented as a percentage of cell wall material dry weight (%CWM). Statistical significance was performed, and a post-hoc Tukey's test (P≤0.05) was performed between the treatments

Genotype	Treatment	Glucose	Xylose	Arabinose	Galactose	Mannose
	Hoagland	36.3 ± 1.6a	12.7 ± 0.4b	2.9 ± 0.05a	0.63 ± 0.08	0.58 ± 0.03
	N20%	38 ± 0.06ab	15.9 ± 2.8ab	1.15 ± 0.1b	0.64 ± 0.01	0.60 ± 0.05
	N4%	36.5 ± 1.3a	19.8 ± 1.6a	1.3 ± 0.3ab	0.67 ± 0.06	0.59 ± 0.06
Bd21	N0%	41.2 ± 1.1b	19.7 ± 1.2a	1.3 ± 0.3b	0.75 ± 0.06	0.68 ± 0.03
	P20%	39.4 ±5.6ab	12.6 ± 0.5b	0.9 ± 0.07b	0.63 ± 0.01	0.62 ± 0.05
	P4%	35.4 ± 0.1a	17.1 ± 0.3ab	0.4 ± 0.2b	0.65 ± 0.01	0.60± 0.08
	P0%	40.6 ± 3.4b	19.1 ± 1.8ab	1.1 ± 0.01b	0.71 ± 0.1	0.67 ± 0.08
	Hoagland	40.48 ± 1.9a	27.5 ± 5.4abc	3.4 ± 0.4a	0.54 ± 0.01	0.46 ± 0.05
	N20%	41.8 ± 1.2ab	21 ± 0.6c	2.1 ± 0.1ab	0.56 ± 0.0	0.52 ± 0.1
	N4%	42.7 ± 0.6ab	9.5 ± 0.3d	1.7 ± 0.2ab	0.55 ± 0.09	0.52 ± 0.05
ABR6	N0%	46.7 ± 0.7b	32.1 ± 0.16a	1.7 ± 0.03ab	0.72 ± 0.1	0.59 ± 0.03
	P20%	41 ± 0.9ab	23.7 ± 0.05bc	3.3 ± 1.03a	0.55 ± 0.0	0.46 ± 0.08
	P4%	41.9 ± 1.7ab	25.2 ± 1.6abc	0.5 ±0.02b	0.58 ± 0.04	0.49 ± 0.03
	P0%	47 ± 1.8b	29.0 ± 2.4ab	2.6 ± 0.7ab	0.71 ± 0.08	0.60 ± 0.08

Values are reported as mean ± standard error of the mean, n=2 biological reps, and 3 technical replicates. Different letters within columns indicate significant differences between the treatments determined by analysis of variance (ANOVA) and significant difference Tukey's (HSD) test (P=0.05). No letters signify no significant difference found between the treatments.

2.3.5 Saccharification efficiency for stem samples

The enzymatic sugar release data presented in Table 2.5 shows the percentages of corresponding monosaccharide content released per cell wall dry weight unit. Enzymatic saccharification for nutrient dose treatment was assessed by extraction with enzymatic cocktail treatment followed by HPAEC-PAD. To calculate the enzymatic saccharification efficiency, the sugar release is expressed as a percentage of the available sugars. Since the total monosaccharide content was only determined for stem samples of ABR6 and Bd21 (Table 2-4), the enzymatically released monosaccharides (glucose, xylose and arabinose)

could only be calculated for stem samples of both the accessions (Table 2.5). All the samples are duplicates.

The glucose release efficiency was not significantly affected in Bd21 following the nutrient treatments, glucose release for ABR6 showed a significant reduction in N0% (22.5 ± 2.1, $p<0.01$) and P0% (21.9 ± 0.4, $p<0.01$) treatment when compared to the control plants (29.6 ± 0.6) (Table 2-5). Xylose release showed an opposite response in both accessions under treatment conditions. Bd21 showed with a significant increase in N20% (15.5 ± 4.6, $p<0.01$) and N4% (17.4 ± 1.3, $p<0.001$) compared to the control (Table 2-5). However, ABR6 plants showed a significant decrease in xylose release for N20%, N4% (12.8 ± 0.3, $p<0.01$; 6.7 ± 0.6, $p<0.001$) and P4%, P0% (13.4 ± 2.3, $p<0.01$; 13.2 ± 0.9, $p<0.001$) compared to control (22.5 ± 1.7), respectively (Table 2-5).

The efficiency of arabinose release was generally reduced in both ecotypes. However, this decrease was not significant for Bd21 under N and P dose treatment compared with the control (Table 2-5). While for ABR6 it was significantly reduced for all the N and P limitation dose treatments (0.6 ± 0.4, $p=0.01$; 0.5 ± 1.23, $p=0.001$; 0.2 ± 0.6, $p=0.001$, for N20, N4 and N0%) and (1.1 ± 0.7, $p=0.05$; 0.9 ± 0.1, $p=0.01$; 0.4 ± 0.15, $p=0.01$, for P20, P4, and P0%) compared with control (2.2 ± 1.8) (Table 2-5). The overall, results suggested that nutrient limitation had the strongest effect on the enzymatic sugar release from ABR6 stem samples.

Table 2-5: Enzymatic saccharification efficiency (%) for stem samples under nitrate and phosphate dose-response in both accessions of *Brachypodium*

***Brachypodium* accessions**	**Treatment**	**Glucose**	**Xylose**	**Arabinose**
Bd21	Hoagland	28.73± 0.9	8.7 ± 2.3c	0.6 ± 0.3ab
	N20%	27.46 ± 2.1	15.5 ± 4.6ab	0.1 ± 0.7ab
	N4%	27.46 ± 1.5	17.4 ± 1.3a	0.5 ± 1.4ab
	N0%	26.5 ± 0.4	13.8 ± 0.8abc	0.2 ± 0.2b
	P20%	28.3 ± 3.4	9.4 ± 1.0bc	0.5 ± 1.5ab
	P4%	29.6 ± 0.1	12.3 ± 1.1abc	0.9 ± 0.2a
	P0%	26.5 ± 0.7	13.1 ± 2.5abc	0.4 ± 0.8ab
ABR6	Hoagland	29.6 ± 0.6a	22.5 ± 1.7ab	2.2 ± 1.8a
	N20%	28.9 ± 0.19a	12.8 ± 0.3cd	0.6 ± 0.4bc
	N4%	26.8 ± 0.42a	6.7 ± 0.6d	0.5 ± 1.23bc
	N0%	22.5 ± 2.1ab	26.5 ± 2.2a	0.2 ± 0.6c
	P20%	24.8 ± 4.7a	15.6 ± 2.32bc	1.1 ± 0.7b
	P4%	26.42 ± 3.6a	13.4 ± 2.3c	0.9 ± 0.1bc
	P0%	21.9 ± 0.4ab	13.2 ± 0.9c	0.4 ± 0.15bc

Reported values as mean ± standard error of the mean, n=2 biological reps, and 3 technical replicates. Different letters within columns indicate significant differences between the treatments determined by analysis of variance (ANOVA) and significant differences in Tukey's (HSD) test ($P<0.05$). No letters signify no significant difference found between the treatments

2.4 Discussion

Nutrient limitation exhibits most vitally as a loss of yield or a yield gap (Kvakić *et al*., 2018), suggesting the requirement for an adequate supply of all essential nutrients for optimum yield and quality of cereals. The results obtained in this chapter portrayed a profound difference in above-ground and below-ground biomass between two *Brachypodium* accessions in control conditions but also in NPKB low nutrient dose response. Both ABR6 and Bd21 showed significance. It was also proposed that plants within the same species may respond differently regarding some phenotypical aspects (Bossdorf & Pigliucci, 2009; Murren & Pigliucci, 2005). However, in this study, no such differences were found as both

reduced nitrate and phosphate affected all the observed and measured morphological traits in the same manner. It is worth mentioning that plants' phenotypic and cell wall properties to nutrient limitation are broadly studied. *Brachypodium distachyon* is also known as core pooid as it is closely related to temperate cereals, fodder grasses, and amenity grasses, suggesting a co-linearity in gene organisation (Draper *et al*., 2001; D. Garvin *et al*., 2008; The International *Brachypodium* Initiative, 2010). All these characteristics make *Brachypodium* a model system as it is easy to grow with a relatively shorter life cycle and a small diploid genome that has been fully sequenced. In the present study, aerial stem biomass and biomass total of plant dry up under nitrate and phosphate dose-response deficiency in *Brachypodium* accessions. The decrease in the phenotypic traits and aerial biomass of both the accessions of *B*. *distachyon* is a deficit condition that has been studied in the reduction of leaf expansion, leaf area (Fredeen *et al*.,1989) and the number of leaves (J. Lynch *et al*., 1991) under nutrient stress. Similar results were obtained by Rosolem *et al*. (1994) on maize, by López-Bucio (2003) on Arabidopsis thaliana, Ciereszko et al. (2011a) and Yaseen & Malhi (2011) on wheat, for Ciereszko *et al*. (2011) on barley, by Poiré *et al*. (2014) on *B*. *distachyon*. However, there is minimal knowledge about the grass-to-species nutrient response.

Above-ground and root measurements respond differently to nutrient limitation

To determine the above-ground phenotypic measurements under nutrient limitation in *Brachypodium* accessions, ABR6 and Bd21 were vernalized and grown in control and reduced NPKB dose-response.

Nitrate treatment

Under N limitation, the present chapter showed a significant decrease in plant height, leaf number, tiller number, spikelet number, and fresh weight in the ABR6 ecotype. Furthermore, Bd21 plants again displayed substantial changes in a greater number of above-ground measurements in leaf number, tiller number, spikelet number and fresh weight, except no significant effect, was found in reduced N20% treatment in spikelet number of Bd21. Interestingly, no significant effect on plant height in response to low nitrate treatment was observed in the Bd21 genotype suggesting the ability of specific genotypes to respond to nutrient limitation due to natural variation found in *Brachypodium* species. For ABR6 and Bd21 accessions, overall dry weight showed no significant changes under nitrate limitation treatments. The potential physiological changes were maintained in root length measurement in low N deficient conditions. In this study, both ABR6 and Bd21 showed a significant reduction in root length in N0%. Similar results showed that Bd21 plants were highly responsive to low N, and a drastic decrease in root system architecture parameters was found (Ingram *et al*., 2012).

Phosphate treatment

No significant effect in plant height for ABR6 *Brachypodium* accession was found under reduced P20% and P4%; however, a substantial reduction in the height was observed in P0%. Whereas leaf number, tiller number, spikelet number, and fresh weight appeared to be lowered compared to the control under low P. Similar results were found in Bd21, where fewer leaf, tiller, and spikelet number along with fresh biomass was measured. However, no plant height reduction under low P was observed compared to the control. ABR6 and Bd21 showed no significant change in dry weight under P deficiency. Reduction in total plant biomass under P limitation decreased root growth rate in the present study. P is majorly

found in the upper layer of the soil, which is further immobilised with other molecules, thus proposing the varieties with deeper root systems show decreased P concentration and biomass when compared to the shallower root varieties in maize and bean plants (Bonser *et al*., 1996; Zhu *et al*., 2005). The diversion of the majority of the plant's resources towards the roots under phosphorous limitation (Zhu *et al*., 2005) could also explain the decrease in dry biomass of the leafy stem of *B*. *distachyon* in the present root architecture experiment. In the current study, both genotypes showed a relative reduction in root growth compared to the control under P scarcity. Appendix Figure A2.2 shows a diagrammatic representation of the treatment effect on both the *Brachypodium* accessions.

Potassium treatment

K is the third most essential macronutrient after N, and plants require P for their successful life cycle (Srinivasarao C. *et al*., 2016). K limitation induces physiological changes causing a reduction in plant biomass and root development with enhanced total root length in the wheat (Thornburg *et al*., 2020). This study explains K deficiency induced above and below-ground changes in both *Brachypodium* accessions. The results for fresh plant biomass showed a consistent finding with other studies where a reduction was observed. Interestingly, the control increased dry weight by K20% and K4% in the ABR6 genotype. K deficiency showed no significant change in root length in both the accessions. Similar results were suggested in a previous study where K deficiency delayed seminal root emergence but enhanced seminal root elongation and root length, further impacting root morphology and growth in wheat cultivars. In addition, the results in this study did not show a significant effect on plant height, leaf number, tiller number, spikelet number and root development between K limitation and control in ABR6 and Bd21, suggesting a short treatment time and

led to quick adaptations of *Brachypodium* plants due to K^+ channels and high-affinity transporters.

Potassium is essential in productivity by performing physiological functions; however, potassium deficiency probably activates a signalling mechanism leading to the translocation of mobile K^+ ions. Molecular and high-affinity transporters mechanisms are assumed to act better after sensing potassium deficient conditions, thus leading to adaptive responses and showing no effect in physiological measurements. This could be a possible reason why the hypothesis got rejected due to several signalling mechanisms, thus showing no effect on the growth of *Brachypodium* species under K dose-response. Overall, the study suggested potassium deficient plants enhance the K^+ transporters prominently, leading to a two-way relationship between potassium-nitrogen and regulating the translocation of nutrients.

Boron treatment

Boron (B) is an essential micronutrient for plant growth and the most important found in the field (Warington,1923; Gupta *et al*., 2013). In this study, no significant effect on all the measured parameters was found except fresh weight, where a reduction was found compared to the control in both the accessions. It has been studied that B interrelate with those nitrogen, phosphorus, and potassium in plants and acts as synergistic or antagonistic with other nutrients (Ahmad *et al*.,2012). Boron deficiency in wheat showed a reduction in leaf number and deformed leaf margin shape, however, no such morphological changes were found in the present study. M Brdar-Jokanović (2020) suggested that shoot root ratio increases under boron limitation, thus making the plants more susceptible to drought and nutritive imbalances. In wheat plants, the number of seeds per spike (Rerkasem & Jamjod, 2004) was relatively reduced however no significant change was found in this study. A

previous study suggested that dicots are more sensitive to boron limitation and insufficient B translocation leads to poor tomato, celery quantity and quality (Bellaloui & Brown, 1998). This is due to the high content of pectin found in dicots, thus leading to the formation of borate diester bonds with rhamnogalacturonan II in the cell wall.

Boron deficiency in early vegetative growth is much less readily inducible in wheat than in dicotyledons. The most rapid response to B deficiency in higher plants is the cessation of root elongation (Dugger, 1983; Marschner, 1986; Dell & Huang,1997), but this has rarely been seen in wheat. B deficiency didn't affect the primary root growth rate in ABR6 and Bd21 genotypes compared to the control in this study. However, low B reduces the primary root growth in Arabidopsis and trifoliate plants, indicating that B deficiency can inhibit root growth in dicots (González-Fontes *et al*., 2016; Liu Y. *et al*., 2019). This suggests that B limitation affects cell elongation in the growing tissues, and reduction of meristem size correlates with the inhibition of root growth (Martín-Rejano *et al*., 2011; Camacho-Cristóbal, 2015); however, this was not found in the present study. It has also been reported that B deficiency promotes the formation of higher low methyl esterified pectin to increase cell wall thickness which further affects the morphological development of the root system (Liu Y. *et al*., 2019). The possible reason for not showing any significant effect could be due to the readily available minimal amount of B present in the low nutrient bulrush compost and providing a coping mechanism in *Brachypodium* species. Hydroponics could have been an ideal technique and vital tool to fulfil the aim of investigation of low B dose-response treatment. This system enables to scope for careful abiotic stress induction at the root level by manipulating conditions of the nutrient solution (Citadirin *et al*., 2011).

Response of chlorophyll content to Nitrate and Phosphate deficiency

Both nitrogen and phosphorous limitation decreases the leaf chlorophyll content in maize plants, consequently suggesting leaf nitrogen is linearly related to leaf chlorophyll content as N plays a vital role in chlorophyll synthesis and crop growth (Cai *et al*., 2012; Wasaya A. *et al*., 2017). Here, the low N treatment decreased chlorophyll content in the ABR6 genotype, showing no significant effect in Bd21, suggesting different genotypes can differ in the linear correlation between the measured chlorophyll level and leaf nitrogen content (J. Zhang *et al*., 2000). Compared to the low N treatment used here, the low P treatment did not affect the Chlorophyll content in Bd21; however, an increase of 65% was found in the ABR6 genotype compared with the control. Chlorophyll b showed a significant reduction under N limitation in both the genotypes. The ratio Chla/ Chlb representing the thylakoid composition (Anderson *et al*., 1988) remains unchanged in Bd21 accessions in both N and P limitation treatment. A similar result was found in barley plants under N-deficiency (Bhaskar R. *et al*., 2003). However, a significant increase in the ratio was found in ABR6 genotype under both N and P reduced treatment.

Monosaccharide analysis

Previous studies have majorly focused on Arabidopsis for cell wall research; however, a vast number of agriculturally essential cereal crops' cell wall composition significantly varies from dicots. Therefore, this study studied cell wall composition analysis in *Brachypodium* accessions under nutrient limitations. Monosaccharide analysis was performed using the AIR samples with an acid treatment which further helped to determine the monomers released. The carbohydrates in *Brachypodium distachyon* can be divided into two groups based on abundance: major, including glucose (Glc), xylose (Xyl), arabinose (Ara), galactose (Gal); minor, including rhamnose (Rha), fucose (Fuc), and mannose (Man) (Rancour *et al*., 2012). In this study, results for Glu, Xyl, Ara, Gal and Man are presented.

The main building block of hemicellulose in grasses is xylan, which comprises a backbone of B (1-4) linked xylose residues. Mannans are another type of hemicellulose which is usually linked with mannose units (Scheller *et al*., 2010). This decrease in xylose and increase in mannose monomers is easier to break down by the enzymes or even if there is an increased amount of monomers. Glucose was released higher in both ABR6 and Bd21 accessions under nitrate and phosphate limitation, whereas xylose was reduced compared to the control. ABR6 and Bd21 accessions under low nutrient treatment showed an increase in glucose monomers in the hydrolysate, indicating an increase in cellulose or hemicellulose digestibility due to enhanced accessibility to enzyme degradation or an increase in cellulose constructed from glucose subunits. Several studies have suggested that grass secondary cell wall comprises a small fraction of xyloglucan, and therefore a reduction in xylose monomers was found in this study (Scheller *et al*., 2010).

Since galactose is associated chiefly with pectins and AGPs, which are less abundant in secondary cell walls (Tadashi Ishii, 1997), low Gal contents in stress treatments may be explained by the higher proportion of secondary cell walls after stress exposition.

Saccharification efficiency

Biomass refers to any biological material of organisms living or recently alive plant materials, including grasses, crops, and trees, microorganisms. More recently, grasses have been explored as biomass feedstocks for bioenergy production and biorefining into platform chemicals and value-added bio-based products. The inherent recalcitrance of lignocellulosic materials to deconstruction is the most crucial limitation of biomass biorefining's commercial viability and economic feasibility (Bhatia *et al*., 2017). Sugar release by enzymatic hydrolysis is one of the most used quality measures for grass biomass as a forage

and a bioenergy feedstock. Saccharification (i.e., enzymatic sugar release using an enzyme cocktail) was measured to estimate and evaluate the alteration of saccharification efficiency under nutrient limitation to understand the potential factors involved in improved efficiency (decker et al., 2009; (Studer *et al*., 2011).

In the present work, the efficiency of enzymatic conversion of cell wall material into fermentable monosaccharides was studied using ABR6 and Bd21 accessions of *Brachypodium* under nutrient limitation dose-response. Results indicated no significant effect in enzymatic glucose release in Bd21; however, a substantial decrease in ABR6 under N0% and P0% was found. Xylose showed a considerable increase in Bd21 accessions under low nitrate dose-response, whereas P20% significantly reduced ABR6 accessions. A significant reduction in arabinose for ABR6 accessions was found under low nitrate and phosphate availability, with no effect on Bd21 Brachypodium accessions. In conclusion, nutrient limitation reduced the enzymatic sugar release in ABR6 genotypes as no response was observed in Bd21 plants suggesting a species-specific effect. The possible explanation for lower saccharification after the nutrient stress treatment could be the higher lignin content observed in these plants, as it has previously been reported that lignin content, as well as lignin structure in cell walls, can have an impact on saccharification (Bouvier D'Yvoire *et al*., 2013; Chen & Dixon, 2007; Marriott *et al*., 2014; Studer *et al*., 2011). The study showed higher biomass recalcitrance in *Brachypodium* ABR6 accessions. This knowledge could impact the future breeding program to improve biomass quality in cereal and bioenergy crops growing in low nutrient conditions.

2.5 Conclusion

In conclusion, the results of this chapter showed a significant effect on nitrate and phosphate dose-response in above and below-ground biomass of both the *Brachypodium* accessions. Low nutrient stress conditions reduced the enzymatic sugar release in ABR6 genotypes as no response was observed in Bd21 plants suggesting a species-specific effect. In future, this chapter will also help to study the cell wall compositional alterations in Brachypodium stems in response to reduced nutrient dose treatment.

Chapter 3 : Low nutrient dose-response measurements using an automated irrigation platform reveal phenotypic variation in ABR6 and Bd21 *Brachypodium* genotypes

3.1 Introduction

One such high throughput system is the PlantScreen Phenotyping (Photon System Instruments, PSI) platform, which allows 2000 plants to be screened at a time by individually weighing and watering the pots. The plant's phenotype is dynamic and frequently erratic because it communicates with complex responses to endogenous and exogenous signals received under environmental stress conditions. Phenotyping collectively with genotyping facilitates the discovery of candidate gene(s) responsible for nutrient tolerance by dissecting and identifying QTL. This will correlate to the genetic data where identifying adaptive loci that control the above specific complex traits responsible will rapidly improve cereal crop production under low nutrient environmental conditions.

The present chapter focuses on investigating the morphological parameters as screening techniques for the dose-response of the four different nutrients with automated irrigation using the PSI platform. Although only two accessions are tested in this chapter, these phenotypic measurements under controlled environmental conditions will eventually help evaluate the accessions that are tolerant or resistant to the given nutrient stress. The results will help uncover genes that function for phenotypic traits in grasses for nutrient tolerance (Schwartz *et al*., 2010). Finally, the following study will assist in evaluating the parents using the conditions of the PSI platform, and the same setup will be used on a genetic basis by performing quantitative trait loci (QTL) analysis from a RIL population derived from ABR6 and Bd21 accessions nutrient-limited conditions (Chapter 4 & 5).

3.2 Materials and methods

3.2.1 Experimental setup and growth requirements

Brachypodium distachyon accessions ABR6 and Bd21 were selected and used in this study. The seeds were obtained from Aberystwyth University and the experiment was set up at the National Plant Phenomics Centre facilities (NPPC), Aberystwyth, U.K. The substrate used in the experiment comprised 40% silver sand/ 60% WI13 compost (Bulrush, Magherafelt, N Ireland, low nutrient compost) as detailed in Chapter 2. Each plant of both the accessions was sown in individual pots (6 cm diameter) which were filled with a uniform amount of compost. For the nutrient dose-response, the 2-week-old seedlings per each accession (n=6) were treated twice, once prior to vernalization and the second time after the vernalization as explained in Section 3.2.2. The vernalisation or cold exposure (6 weeks) was performed under controlled environment growth room conditions at 4 °C with 16/8h photoperiod. After 6 weeks of induced cold environment, the pots were transferred to the PSI system and automated irrigation during their vegetative growth period was maintained at the PSI system. The system was set at 22 °C (day) and 20 °C (night) with 18h photoperiod and irrigation were maintained above to 65% gravimetric water content daily by weight. The plants were grown at approximately 600 µmol m^2 s^{-1} (200W GreenPower LED). They were further transferred to a neighbouring glasshouse compartment from the PSI platform when the plants reached the senescence stage and the experiment was given the code: BdD022.

3.2.2 Nutrient dose-response

The experiment was performed to investigate the implications of a nutrient dose-response in *Brachypodium*. N, P, K, and B were selected as nutrients (treatment), and the solutions

were prepared as mentioned in Chapter 2. Each tray (40x40 cm) containing 20 pots was soaked with 500ml of nutrient-deprived treatment twice in the experiment (before and after vernalization). Twice nutrient-deprived treatment and automated water irrigation, when required under controlled environmental conditions, were the factors that differed from chapter 2 in the present study. The following different treatment solutions were used: a Hoagland's nutrient solution (control), a 20% of N (ammonium and nitrate-based) (N20%), a 4% of N (N4%), a N deprived solution (N0%) , a 20% of P (20%), a 4% of P (P4%), a P-depleted solution (P0%), a 20% of K (K20%), a 4% of K (K4%), K-depleted solution (K0%), a 20% of B (B20%), a 4% of B (B4%), and B-depleted solution (B0%), respectively (Table 3-1).

Table 3-1: Compost and treatments used in the experiment

Compost	Treatment	Abbreviation
	100% Hoagland	Control
WI13-low nutrient	Hoagland reduced N	N20%, N4%, N0%
	Hoagland reduced P	P20%, P4%, P0%
	Hoagland reduced K	K20%, K4%, K0%
	Hoagland reduced B	B20%, B4%, B0%

WI13= West Islands 13 Bulrush compost

3.2.3 Phenotypic measurements

The phenotypic measurements did not distinguish much from chapter 2 as all the measurements were taken by hand, and no integrated imaging facility was used in the present chapter. Plant height was measured from the soil to the awn of the tallest culm. Fertile tillers were scored based on the spikelet presence on the tillers. Plants were inspected daily, and the flowering time was scored as the number of days after sowing (DAS) and the day on which the first inflorescence or heading appeared. The day of

flowering was recorded for each plant in a pot. At maturity, each plant was harvested individually. Spikelet number was counted as the total number of spikelets on all tillers, and spikelets on just the main stem were counted and scored at the senescence stage. Plant vouchers were created after measuring the plant weight without the spikelet. The ear (seed) was harvested, and the total ear mass was weighed using small bags.

3.2.4 Statistical analysis

Statistical tests were performed using R software (Team, R, 2020). The data's normality was verified using the Shapiro test, and Levene's test was used for homogeneity of variances. 1-Way ANOVA was performed to detect treatment effect, and Tukey's test was used to compare the means.

3.3 Results

Phenotypic variation measurements in ABR6 and Bd21 accessions

Phenotypic traits were measured, and complete Hoagland treatment was considered a control. All the plants were measured for different phenotypic traits at the senescence stage. Photographs were taken with the front view and black background (Appendix 3.1). According to Levene's test, the results showed homogeneity of variances and had a normal distribution.

3.3.1 Plant height measurement

ABR6, which is a Spanish accession of *Brachypodium*, showed a significant increase in plant height following K4% ($p=0.004$), B20% ($p=0.02$) and B4% ($p<0.001$) treatments by 67%, 53% and 90%, respectively, compared with the control. However, no significant effect on plant

height was observed in N-deprived (N20%, N4%, N0%), and P-deprived (P20%, P4%, P0%) dose responses, as well as for K20%, K0%, and B0% treatments compared with the control (Figure 3.1. A).

Bd21, an Iraqi accession, also showed a significant increase (by 17%, $p=0.02$) in plant height following B20% treatment. However, a significant reduction in plant height was observed under P4% (21%, $p=0.005$), and P0% (25%, $p<0.001$), compared with the control (Figure 3.1. B). No significant difference was found in N-deprived (N20%, N4%, N0%) and K –deprived (K20%, K4%, K0%) dose responses as well as for P20%, B4% and B0%, respectively. The results suggest that, based on plant height measures, both accessions are relatively tolerant to N, K, and B limitations, but Bd21 is sensitive to P limitations. It is interesting to note that B20% resulted in an increase in plant height for both accessions.

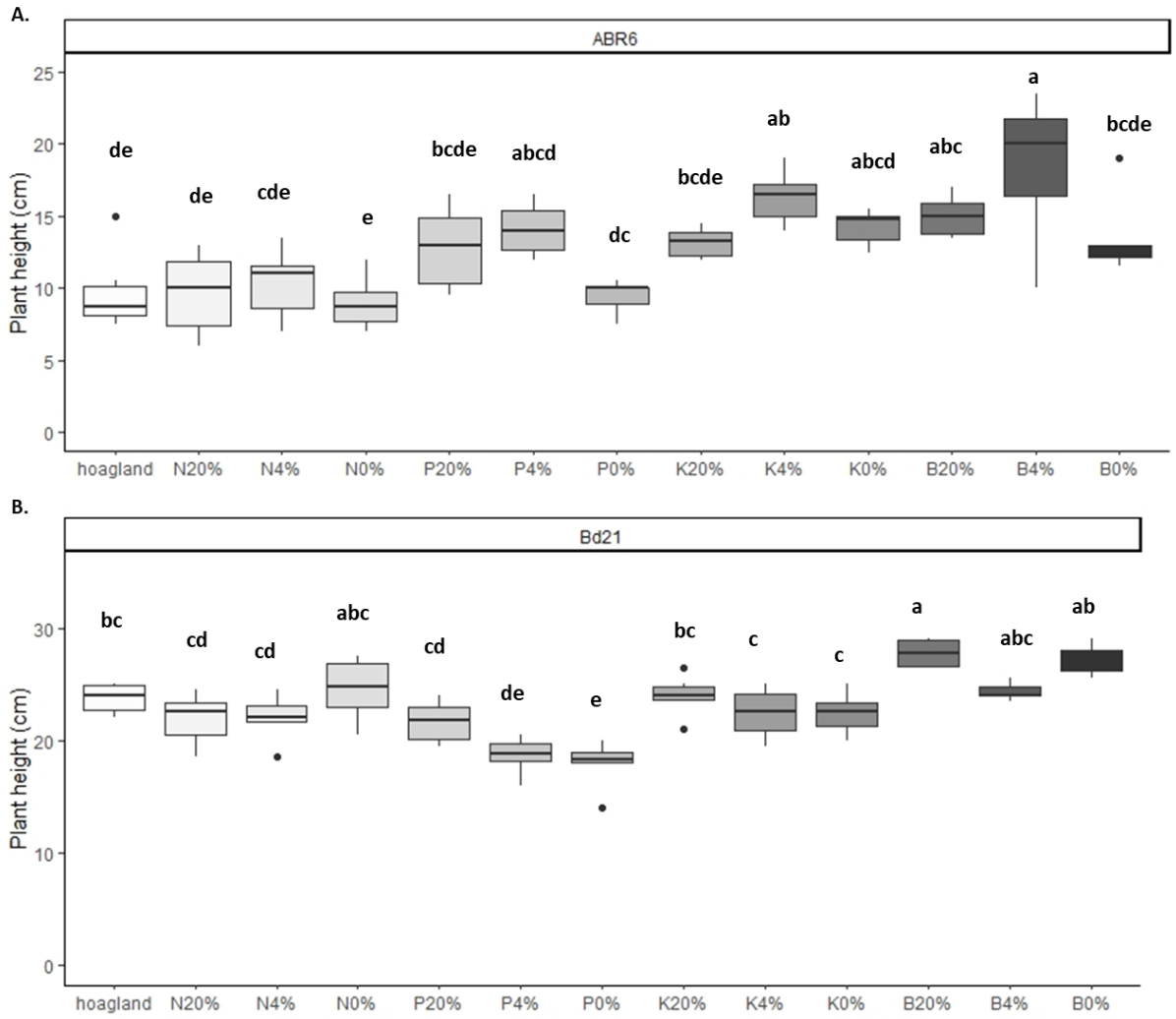

Figure 3 1: Boxplots represent plant height (cm) with mean height, standard deviation, and the maximum and minimum value. A. ABR6, B. Bd21 under various nutrient (NPKB) deprived conditions along with 100% Hoagland treatment (control). Means with same letter do not differ (Tukey's test, p=0.05). Letters show a significant difference in same accession between the treatments.

3.3.2 Fertile tillers

Tillering is a primitive characteristic of cereals, as it impacts the number of spikes and grain yield. Fertile tillers were counted for both the accessions as shown in Figure 3.2. ABR6 showed an overall significant decrease in fertile tillers for all nitrate (N20%= 51%, $p<0.001$; N4%= 82%, $p<0.01$; N0%= 79%, $p<0.001$, respectively) and potassium (K20%= 31%, $p=0.03$; K4%= 45%, $p<0.001$; K0%= 55%, $p<0.001$, respectively) dose-response treatments compared

with the control. Also, P4% (by 33%, p=0.01) and P0% (by 45%, p<0.001) treatments showed a significant reduction in fertile tillers when compared to the control (Figure 3.2. A).

For Bd21, the number of fertile tillers was only affected following treatment with N4% (65% reduction, p<0.001), N0% (70% reduction, p<0.001) and P0% (65% reduction, p<0.001). No difference in fertile tiller number was observed following both K and B dose response treatments (Figure 3.2. B). Together these results suggest that ABR6 is more sensitive than Bd21 to decreases in N, P and K when it comes to fertile tiller numbers.

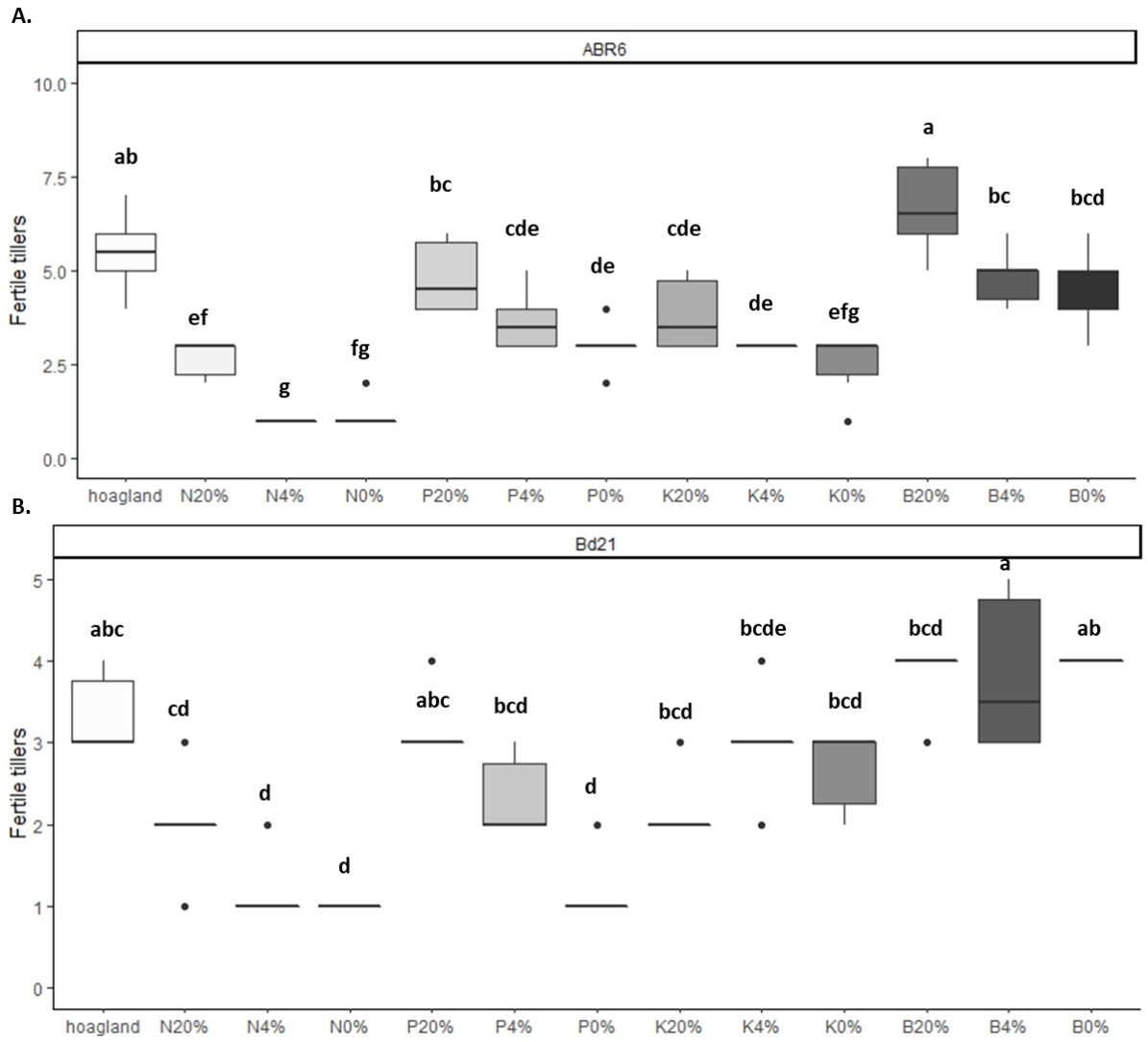

Figure 3 2: Boxplots representing fertile tiller number with mean tiller number, standard deviation, and the maximum and minimum value. A. ABR6, B. Bd21 under various nutrient (NPKB) deprived conditions along with 100% Hoagland treatment. Means (n=6) with the

same letter do not differ (Tukey's test, $p<0.05$). Letters show a significant difference in the same accession between the treatments.

3.3.3 Flowering time

Both the accessions (ABR6 and Bd21) differ considerably in flowering time and requirement for vernalization. Previous studies have suggested that Bd21 is extremely rapid at flowering, even without vernalization (Ream et al., 2014; Woods et al., 2016), whereas ABR6 does not flower without vernalization and usually requires 6 weeks of cold treatment. Therefore, as expected, ABR6 showed a much later flowering time (around 111 days) compared to Bd21 (76-days) under control conditions. For ABR6, a significant increase in flowering time was observed following P4% (91-days, p=0.004), P0% (94- days, p=0.04), K20% (92-days, p=0.007), K4% (89-days, p=0.001), K0% (91-days, p=0.005), and B4% (94-days, p=0.04) deprived nutrient conditions when compared with the control (111 days) (Figure 3.3. A). However, no significant effect on flowering time was found in Bd21 under the respective nutrient-deprived treatments compared to the control conditions (Figure 3.3. B).

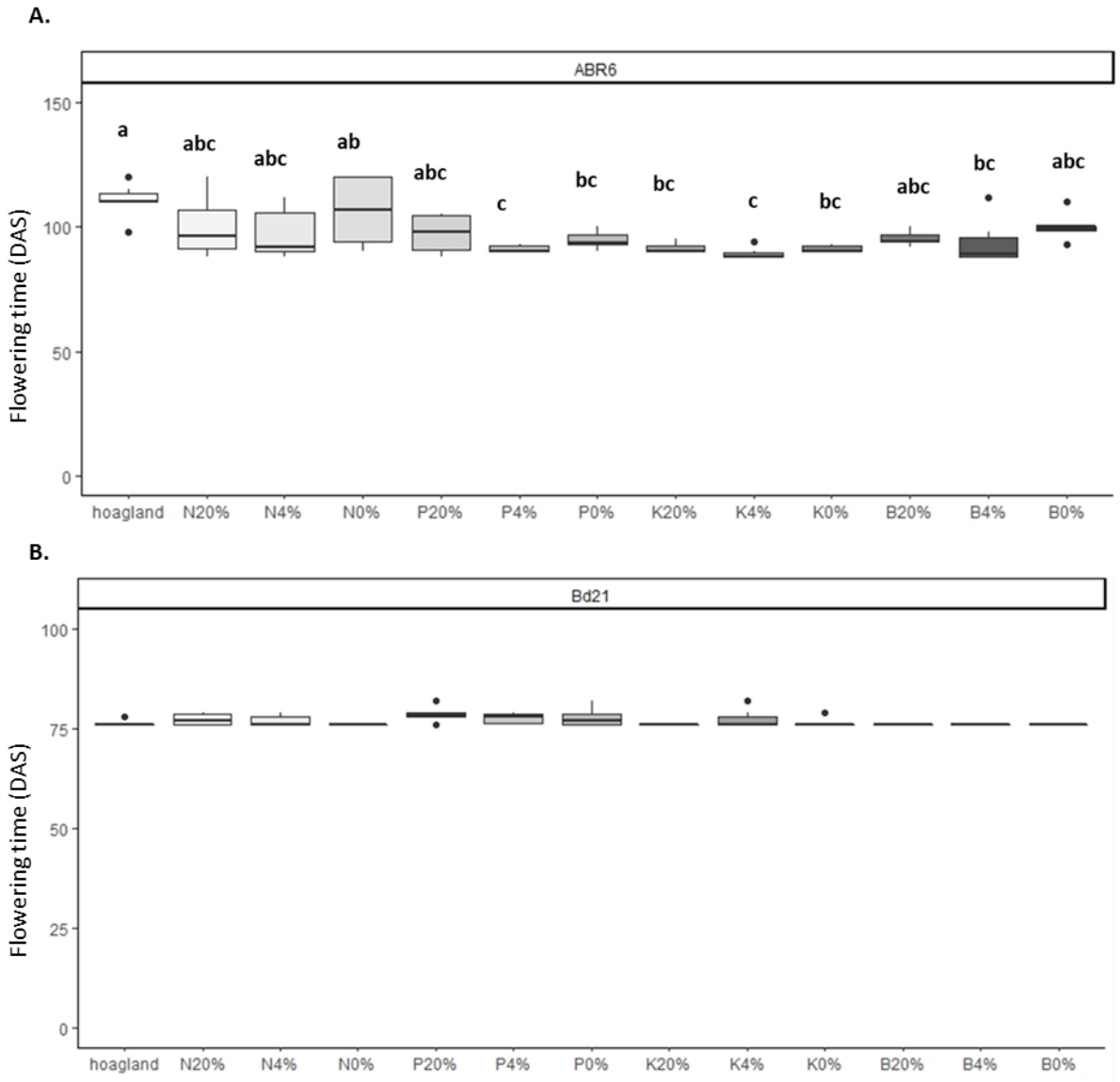

Figure 3-3: Boxplots representing flowering time (days from the emergence of spikes/heading) with mean flowering time, standard deviation, and the maximum and minimum value. A. ABR6, B.Bd21 under various nutrient (NPKB) deprived conditions along with 100% Hoagland treatment (control with WI13 low nutrient compost). Means (n=6) with no letter indicating no significant effect. Letters show a significant difference in same accession between the treatments (Tukey's test, p=0.05).

3.3.4 Spikelet number

Following the effects of nutrient stress at vegetative stage, spikelet number was measured at senescence stage. All N dose-response treatments resulted in a significant decrease in spikelet number compared with the control in ABR6: N20% by 53% ($p \leq 0.01$), N4% by 82%

(p<0.001), and N0% by 79% (p<0.001). Also, treatment with K4% and K0% resulted in a decrease in spikelet number (47%, p=0.04; 56%, p=0.01, respectively), respectively, compared with control (Figure 3.4. A).

On the other hand, Bd21 only showed a significant reduction in spikelet number following N4% and N0% treatments (61%, p<0.001 and 61%, p<0.001, respectively), and P0% (65%, p=0.03) compared with the control (Figure 3.4. B). No difference in the spikelet number was observed among K and B dose-response treatments in Bd21.

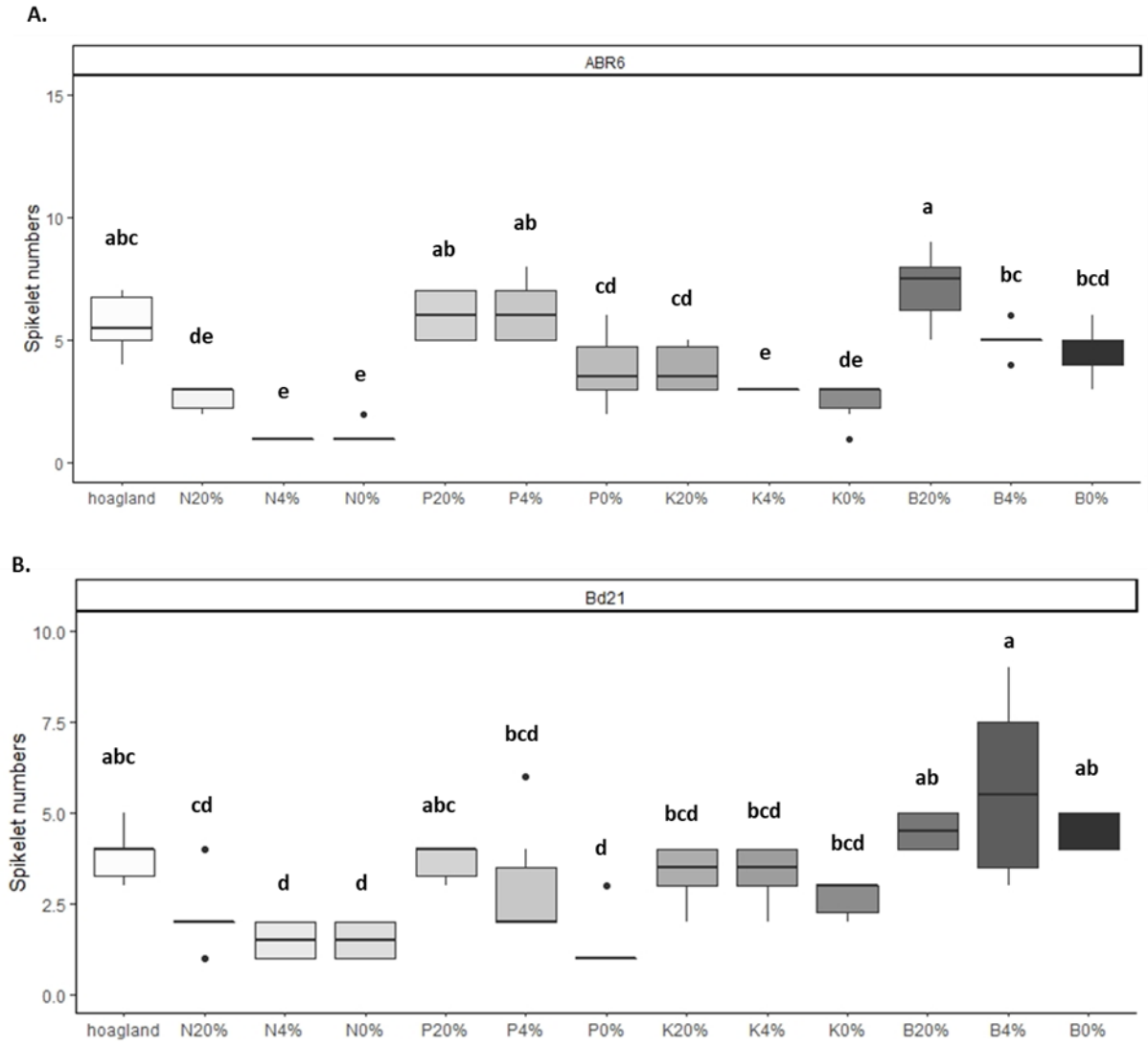

Figure 3 4: Boxplots representing total spikelet number with mean spikelet number, standard deviation, and the maximum and minimum value. A. ABR6, B. Bd21 under various nutrient (NPKB) deprived conditions along 100% Hoagland treatment (control with WI13 low nutrient compost). Means (n=6) with same letter do not differ (Tukey's test, p=0.05). Letters show a significant difference in same accession between the treatments.

3.3.5 Total spikelet on the main stem

The total number of spikelets on the main stem was scored at the senescence stage for each treatment. ABR6 showed no significant difference in nutrient (NPKB) deprived dose responses except for B4% which showed a significant increase by 59% (p=0.002) when compared with the control (Figure 3.5. A). However, Bd21 ecotypes showed a significant

reduction in spikelet formation on the main stem under N4% (49%, p<0.001), N0% (57%, p<0.001), and P0% (57%, p<0.001) whereas there was no significant difference for the other treatments compared with the control (Figure 3.5. B).

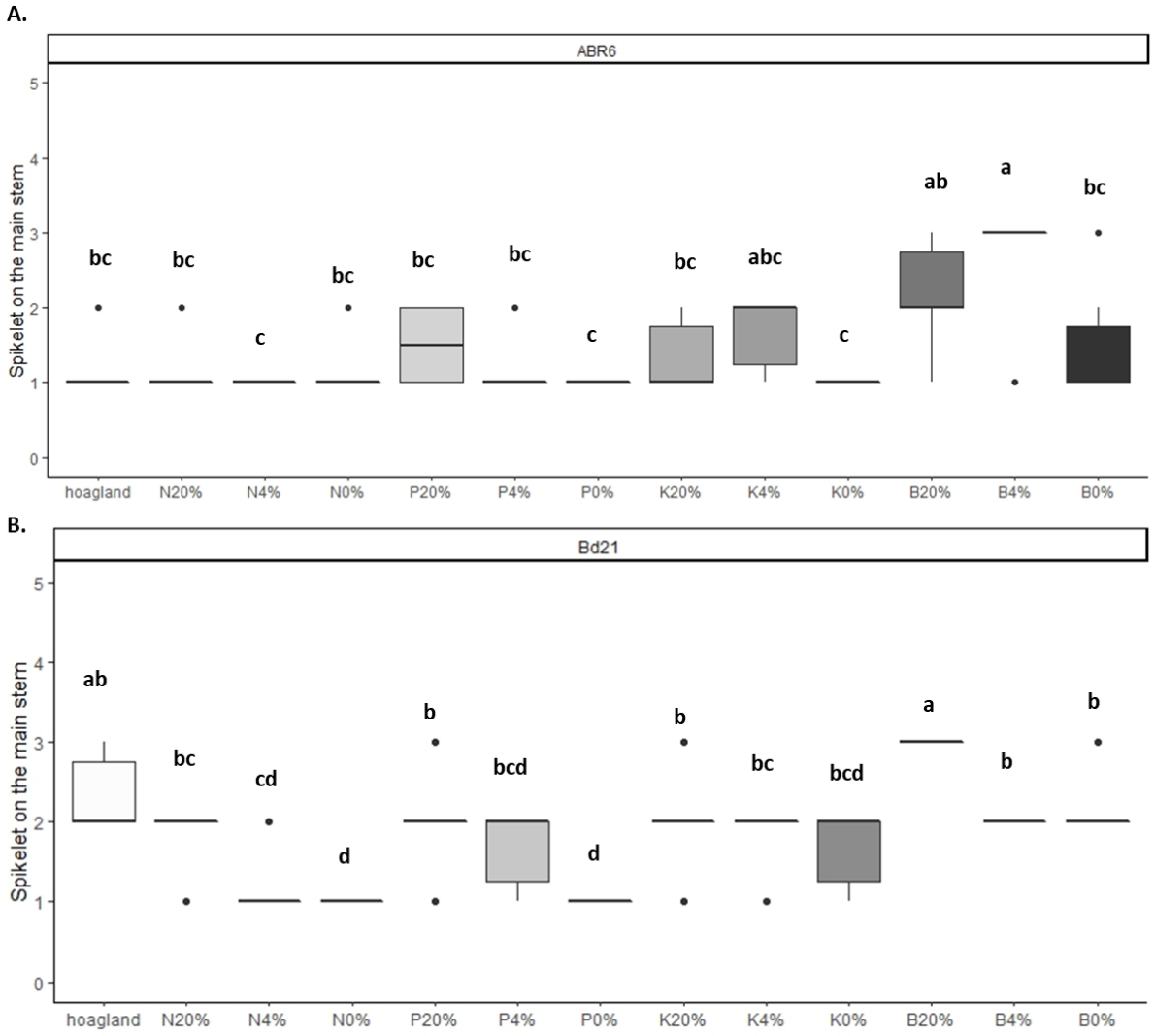

Figure 3 5: Boxplots representing spikelet number present on the main stem with mean spikelet on the main stem, standard deviation, and the maximum and minimum value. A. ABR6, B. Bd21 under various nutrient (NPKB) deprived conditions along with 100% Hoagland treatment (control with WI13 low nutrient compost). Means (n=6) with same letter do not differ (Tukey's test, p=0.05). Letters show a significant difference in same accession between the treatments.

3.3.6 Plant weight

Following the dose-response experiment, the above ground biomass was measured after harvesting the various plant samples of the two *Brachypodium* ecotypes. ABR6 showed a significant decrease in plant weight under N-deprivation (N20%=67%, p=0.02; N4%= 83%, p<0.001; N0%=86%, p<0.001) and K- deprived (K20%= 38%, p=0.03; K4%=41%, p=0.01; K0%= 62%, p=0.04) do as well as under P0% starvation (45%; p=0.003) compared with the control (Figure 3.7. A). On the other hand, a significant increase in plant biomass was observed under B20% (57%, p<0.001) and B4% (42%, p=0.01) treatments when compared to the control (Figure 3.6 A).

For Bd21, a significant reduction in plant biomass was observed under N, P, and K deprivation compared to the control. N deprived treatments showed a reduction which ranged from 58% to 77%, p<0.001. P4% (p<0.001) and P0% (p<0.001) showed a significant reduction by 56%, and 77%, respectively. K deprived dose response showed a significant decrease (p<0.001) ranging from 39% to 58%, respectively compared to the control (Figure 3.6 B). A significant increase in plant biomass was observed for B20% (30%, p=0.04). Overall, these results indicate that N, P and K treatments decreased and B20% treatment increased the biomass for both accessions.

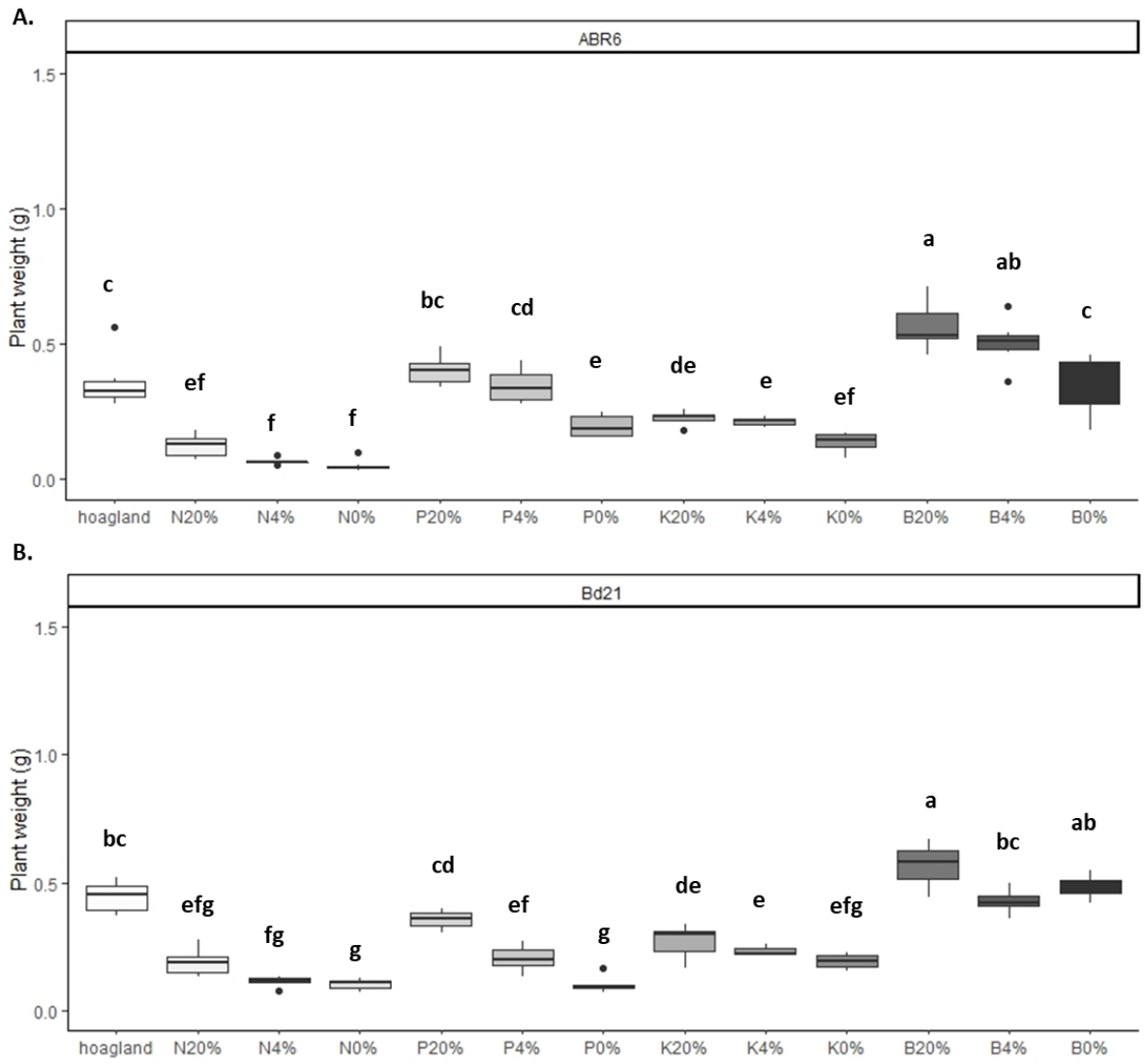

Figure 3 6: Boxplots representing plant weight (g) with mean plant weight, standard deviation, and the maximum and minimum value. A. ABR6, B. Bd21 under various nutrient (NPKB) deprived conditions along with 100% Hoagland treatment (control with WI13 low nutrient compost). Means (n=6) with same letter do not significantly differ (Tukey's test, p=0.05). Letters show a significant difference in same accession between the treatments.

3.3.7 Ear weight

The inflorescence was harvested from each plant and the total ear biomass (seed and the awns) were weighed (g) at the end of the experiment Interestingly, B20% and B4% showed a significant increase in ear weight (93%, $p<0.001$; 86%, $p<0.001$) in ABR6 accessions compared to the control (Figure 3.7. A). However, a significant reduction in ear weight in

ABR6 accessions was observed following N treatments (N20%= 61%, p=0.02; N4%= 76%, p=0.001; N0%=84%, p<0.001) compared to the control. No significant difference among P and K deprived dose- treatments was found (Figure 3.7 A).

Bd21 also showed a similar effect following B20% treatment with a significant 28% increase in ear weight compared with the control (p=0.02). Ear weight decreased significantly under N- deprived (N20%=65%, p<0.001; N4%=80%, p<0.001; N0%=85%, p<0.001), P- deprived (P4%= 58%, p<0.001, P0%= 81%, p<0.001) and K-deprived dose-responses (K20%=50%, p<0.001; K4%=58%, p<0.001; K0%=65%, p<0.001) compared to the control (Figure 3.8. B).

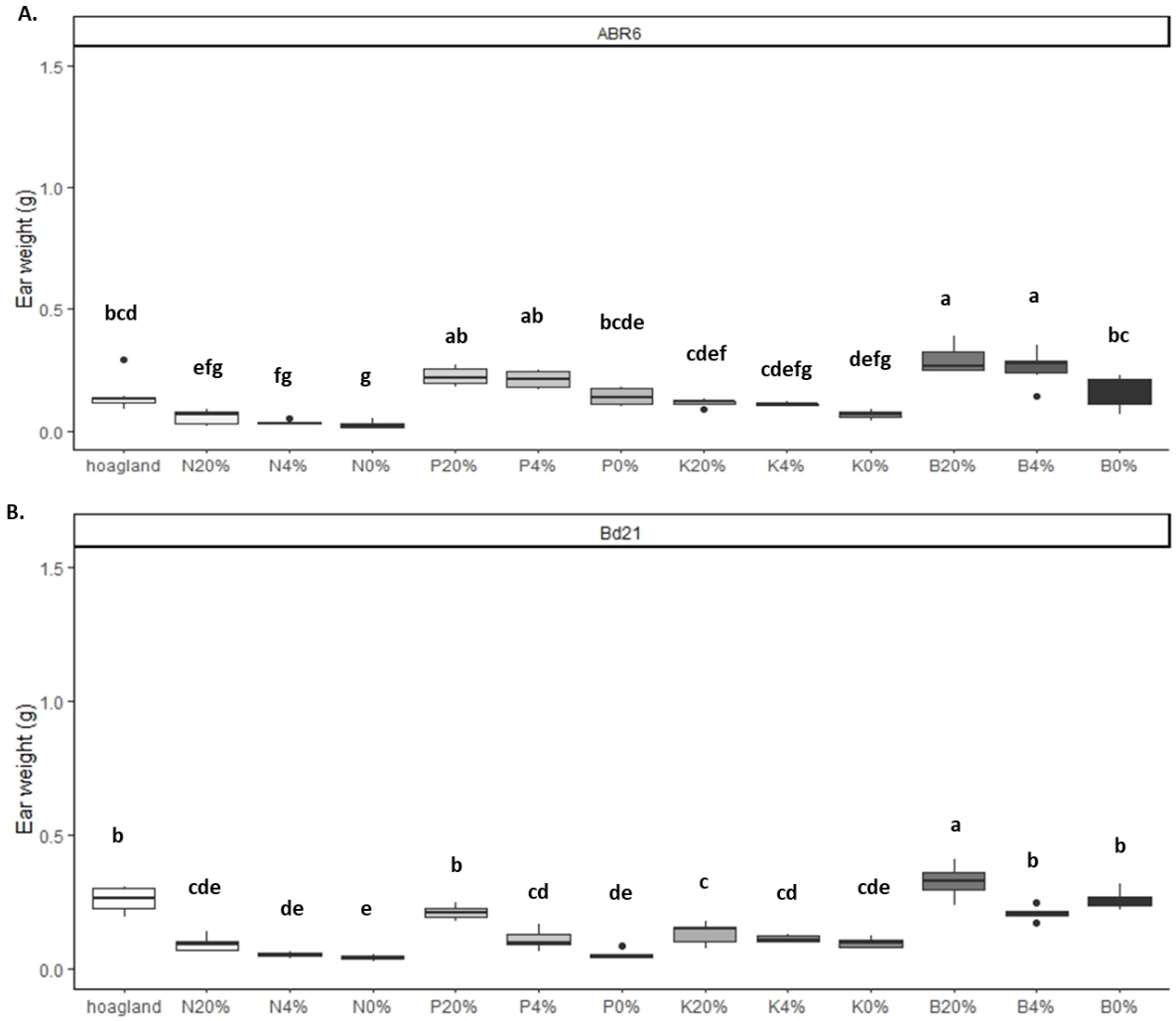

Figure 3 7: Boxplots representing ear weight (g) with mean ear weight, standard deviation, and the maximum and minimum value. A. ABR6, B. Bd21 under various nutrient (NPKB) deprived conditions along with 100% Hoagland treatment (control). Means (n=6) with same

letter do not differ (Tukey's test, p=0.05). Letters show a significant difference in the same accession between the treatments.

3.4 Discussion

Two methods can be performed to identify genetic components that underpin growth response to low nutrient availability. One of them is the comparison of the characterized mutants (induced variation) for a specific gene with their respective wild type. The second approach (used in this study) is based on quantitative trait loci (QTL) analysis (natural variation). Natural variation indeed delivers a structure to learn more about the adaptation of different traits that define the growth of plants to coinciding genetic changes and environmental variations. Therefore, the present study's objective was the determine traits that define growth variation among different *Brachypodium* accessions, depending on nutrient availability. This can be achieved by screening and selecting nutrient responsive geographical origin diverse accessions of *B. distachyon* selected from a core collection that was shown to maximize genetic diversity (Bettgenhaeuser, 2016).

Abiotic stresses cause a negative effect on the growth and development of cereal crops, thus reducing agricultural production globally (Myers *et al*., 2017; Wuebbles *et al*., 2017). Plants are exposed to various environmental stresses like drought, chilling, heat, and nutrient limitation, limiting their yield and productivity (Cakmak, 2005). Swift *et al*. (2020) suggested that an extreme variation, including toxicity and deficiency of nutrients, directly influences a significant increase or decrease in biomass and yield in cereal crops. The above-selected nutrients were used to understand the effects on the growth of ABR6 and Bd21 accessions of *Brachypodium* under limited nutrient dose-response which are majorly unknown. It was found that the two accessions exhibited differences in some of their phenotypic responses such as plant height, and flowering time when faced with conditions

of nutrient limitation. A prolonged cold treatment along with photoperiod allows plants to become competent to flower and this process is called vernalisation (Chouard, 1960). It has been suggested that the vernalisation response in wheat and barley is mostly due to allelic variation as they both are classified into spring and winter varieties (David L. *et al*., 2015). A regulatory loop of genes responsible for vernalisation is studied in grasses that involve VERNALIZATION1 (VRN1), VERNALIZATION2 (VRN2) and VERNALIZATION3 (VRN3), where VRN3 is often an orthologous gene to Flowering time (FT) (Yan *et al*., 2006; Greenup *et al*., 2009; Distelfeld *et al*., 2009; Distelfeld *et al*., 2012). VRN2 enacts as a flowering repressor when active and usually requires vernalisation requirement whereas VRN1 seems to suppress the activity of VRN2 after vernalisation (Woods & Amasino *et al*., 2015). *B. distachyon* is an excellent model system with extensive genetic, and natural variation resources with respect to flowering and vernalisation (Schwartz *et al*., 2010; Ream *et al*., 2014; Tyler *et al*., 2014). The need for vernalisation varies from different accessions where Bd21 accessions originating from northern Iraq only require 20 h long day's photoperiod without vernalisation requirement and tends to acquire rapid flowering cycling, low dormancy with low or no vernalisation requirements accession (Barrero *et al*., 2012). On the other hand, many other accessions are relatively late flowering and usually require cold treatment of seed or vernalisation of plants to flower. For instance, ABR6 originating from Spain requires 6-8 weeks of cold exposure from vegetative growth to initiate flowering (Schwartz *et al*., 2010; Ream *et al*., 2014).

Nitrate limitation in *Brachypodium* accessions

Nitrate often has a weak affinity to form surface complexes with soil minerals which leads to N losses by leaching of soil water. An indication of the growth is the amount of vegetative

mass-produced in the plants. Data on the aboveground biomass decreased markedly under N deficiency in both the *Brachypodium* accessions (ABR6 and Bd21). This further suggests the significance of N limiting nutrient for plant growth, which acts as a controlling element in biomass production and yield (Krapp *et al*., 2011; Ikram *et al*., 2012). ABR6 and Bd21 responded very similar to N dose-response treatments with a reduction in fertile tillers, spikelet numbers, plant weight and ear weight which is consistent with observations of reduction of biomass accumulation in Switchgrass under N limitation (Zhu *et al*., 2014). However, no significant effect was found in the plant height under a range of low N concentrations (N20%, N4%, N0%, respectively) in both the accessions. Similar effects were observed and demonstrated by Oscarson (2000) on wheat grown under limited N availability where the tiller spikes produced more grains per spikelet with increased N levels whereas a decrease in spikelet formation was observed under N limitation. N is the most vital nutrient in the flowering of plants and the most effective in the process of flowering plants. ABR6 accession of *Brachypodium* differed significantly in the time of flowering compared to Bd21, despite a 6 weeks vernalization period. Bd21 control plants flowered ~35 days earlier in comparison to ABR6 grown under control conditions (Figure 3-4). Kolář & Seňková (2008) suggested that the time of floral bud emergence in Arabidopsis is accelerated by low nutrient stress, but the response majorly depends on the genotype and day length. Both the accessions showed no significant effect in flowering time under N deprived conditions compared to the control (Figure 3-3). In addition, ABR6 accessions under N limitation delayed the floral appearance, however, no statistical effect was found (Figure 3-3 A). It has been suggested that climate change affects grass phenology and causes early flowering in increased temperature (Munson & Long, 2017). The results are contrary according to those (Schwartz & Amasino, 2013) where different N concentrations mostly delayed flowering

time, thus producing more leaves in *Brachypodium* accessions. Therefore, the results suggested that a low level of N limitation does not alter the habit of flowering but significantly reduces their spikelet formation, and ear weight and is intimately related to its growth and flowering behaviour in the present study.

Phosphate limited response in *Brachypodium* accessions

There was little effect of limited nutrient availability on plant height, especially in ABR6. For P limitation, P20% has no significant effect on any of the measured traits for both accessions. Bd21 seemed more sensitive to P limitation for plant height, spikelet numbers, and plant weight and ear weight measurements when compared to ABR6 while P limitation had a more profound effect on the number of fertile tillers and flowering time in ABR6. A decrease in shoot growth found in the present study in Bd21 under P starvation was also observed in beans (Thuynsma *et al*., 2016). Vance *et al*. (2003) suggested that a decrease in plant growth rate is a mechanism to safeguard the usage of P when its availability is severely limited. Shoot biomass was significantly reduced in both ABR6 and Bd21 *B*. *distachyon* under P deprived conditions, which has also been observed for *Brachiaria* forage grasses under conditions of P limitation (Louw-Gaume *et al*., 2010).

The number of spikes present on the main stem was affected the most under P deprived condition with a decrease in ear weight only in Bd21. The *Brachypodium* accessions are inherent in the natural variation and genetic architecture due to the varied geographic distribution of ABR6 and Bd21 ecotypes. With low nutrient availability, fewer fertile tillers were observed in both ABR6 and Bd21 accessions. To understand the growth and metabolism in black mustard plants P deficiency was induced which resulted in smaller flower buds (Eaton, 1952). The results showed a similar result in the present study which

suggested a fewer number of spikelet formations and reduced ear weight in Bd21 accessions under P deficiency. P deficiency showed no effect in flowering time in Bd21 in the present study. This agrees with the literature studied on soybeans which had little or no effect on the number of days of flowering (Howell,1954). With an exception in ABR6 plants where flowering time was accelerated under P deficiency.

Potassium limitation in parental *Brachypodium* accessions

Potassium is the most abundant macronutrient and occurs in cationic form required for plant development and it has been suggested that under K deficiency plants can show sensitivity to other environmental stresses (Cakmak, 2005; Shabala & Pottosin, 2014). Seeley (1950) suggested that in rose plants a fewer number of flowering shoots or fertile tillers was found under potassium deficiency and the present study had a similar effect on fertile tillers and spikelet formation under insufficient supply of K in ABR6 accession of *Brachypodium*. Aboveground biomass was significantly lowered in both ABR6 and Bd21 under potassium dose-response stress. In addition, plants activate defence mechanism and is tends to high energy demanding, therefore leading to the reduction in crops growth and yield (Zorb *et al*., 2019). The results were consistent with findings from dicots after potassium starving conditions in oilseed rape cultivar under potassium starving conditions (Pan *et al*., 2017). A reduction in biomass is associated with a reduction in tiller number in ABR6 accessions of *Brachypodium*. A possible explanation for this could be to increase in ionic equilibrium caused due to calcium and magnesium ions or sugar accumulation.

The literature suggests that potassium deficiency results in lower ear weight in soybean and cotton plants (Pan *et al*., 2017; Singh & Reddy, 2017; Hu *et al*., 2020). Indeed, in the present study similar results in Bd21 ecotypes were found which resulted a decrease in ear weight

under K induced dose-response. Potassium deficiency was also studied in sunflower plants where the growth and metabolism were majorly affected thus producing smaller flower buds due to potassium translocation in the plant (Eaton, 1952). Interestingly, under potassium limitation flowering time was accelerated significantly in ABR6 accessions. Similar results were found in cotton plants where early flowering was initiated under potassium deficiency (Pettigrew, 2008). Potassium deficiency causes premature senescence in cotton plants and thus causing increased growth processes (Li *et al*., 2012). However, K deficiency did not affect the number of days for flower initiation in Bd21 while, the development of floral bud formation was accelerated in ABR6 accessions of *Brachypodium* when compared to the control conditions.

Ultimately, potassium deficiency activates multiple parallel pathways within the cell and is regulated by Ca^{2+} ions, reactive oxygen species (ROS), and phytohormones like ABA. However, further studies need to be performed in order to understand the plant functioning especially under combined abiotic stress conditions.

Boron deficiency in *Brachypodium* accessions

B is an essential micronutrient and it's important for plant growth and development. In addition, the present study shows that low B stress suggested numerous changes in morphological changes which resulted in an increase in plant height, above-ground biomass and ear weight in both the accessions of *Brachypodium*. There are numerous reports in the literature on the effect of B deficiency on plant reproductive growth and development. Dell & Huang (1997) suggested that often reproductive growth is more sensitive to B deficiency than vegetative growth. The present research showed an acceleration in flowering time under B4% in ABR6 while no significant effect in Bd21 accession thus, suggesting that plants

may adapt to the B deficiency and therefore, shows no delay in floral development. Similar findings were reported by Brdar-Jokanović (2020) in wheat plants where prolonged deficiency was required as no phenotypic symptoms were observed under B deficiency.

The phenological effects were specie specific and suggested that nutrient limitation does not necessarily correspond to the reduction in flowering time thus suggesting activation of coping mechanism in short lifecycle of *Brachypodium*.

3.5 Chapter 2 versus chapter 3

Table 3-2: Similarities found in chapter 2 and chapter 3

Similarities	**Chapter 2 & chapter 3**
	ABR6 and Bd21
	Brachypodium genotypes
	Bulrush low nutrient compost used
	6 week vernalisation
	Phenotypic measurements by hand
	NPKB nutrient dose-response selected (20%, 4%, and 0%)

	N0% showed an increase in plant height in Bd21 ecotype

Table 3-3: Differences between chapter 2 and chapter 3

Chapter 2	**Chapter 3**
Glasshouse for plants growth	Automated PSI system used for plants growth
Irrigation manually when required	Irrigation using automated system when required
Full Hoagland (100%) solution given at seedling stage before vernalisation	No full Hoagland given before vernalisation
Once nutrient deprived treatment after vernalisation	Twice nutrient deprived treatment given i.e. before and after vernalisation
No flowering time measured	Flowering time measured showed no significant effect

3.6 Conclusion

The results confirm that amongst the deprived mineral nutrient treatments used in the experiment, N0% and P0% had the most significant effect on vegetative and reproductive growth in *Brachypodium*. ABR6 and Bd21 accessions of *Brachypodium* showed a considerable variation in response to nutrient limitation. Both the accessions were moderately tolerant to N limitation in plant height and flowering time. However, a drastic decrease in fertile tillers, above-ground biomass, ear weight and spikelet numbers were reduced under N dose-response in ABR6 and Bd21 accessions. P20% dose-response showed no effect on any measured phenotypic traits in both the accessions, whereas P4% and P0% showed an acceleration in days of flowering time in the ABR6 ecotype. Subsequently, the results suggested no significant effect on physiological responses under B limitation and it could be interesting to focus research in future on the reproductive growth by inducing prolonged low B conditions. Therefore, the results obtained from the present study will be suitable target traits for subsequent QTL analysis and candidate gene identification for low nutrient tolerance in the mapping population of *Brachypodium*.

Chapter 4 : Screening parental ecotypes of RIL population under nutrient-deprived conditions

4.1 Introduction

Brachypodium distachyon, also known as purple false brome, belonging to the Poaceae family, is found in a diverse native range of environments throughout temperate regions and emerged as a research model species for grasses (Opanowicz *et al*., 2008; Vain P., 2011; Garvin, 2015). Several studies have suggested that its natural diversity is widely spread across different habitats from the Mediterranean to the Indian subcontinent, mainly originating from northern Spain, France, Turkey, Slovenia, and Iraq (Garvin *et al*., 2008; Ozdemir *et al*., 2008; Filiz *et al*., 2009). Figure 4.1 shows the geographic distribution of *Brachypodium* with varying degrees of adaptation to changes in environmental conditions and genetic factors, which enacts a better potential for the species to overcome ecological changes (Draper *et al*.,2001; Luo *et al*., 2011). The construction of a mapping population is a requirement for identifying quantitative trait loci (QTLs) that influence a target trait. The most commonly used approach for QTL analysis by association mapping employs populations of RILs derived from a cross between parental lines showing differences in the trait of interest. To improve the chances of successfully identifying QTLs during analysis there are several considerations to take into account when designing an experiment.

Most importantly, the trait being studied should show measurable differences in the parental lines; secondly, the same plant lines used to construct the genotype data must be used for the phenotypic analysis (Collard *et al*., 2005). The recombinant inbred line (RIL) population is majorly used to identify QTLs in many crop species (Yano & Tuberosa, 2009). Different groups and crosses currently produce RIL populations between various accessions listed in Table 4-1. The screening of parental accessions of *Brachypodium* will help us obtain

RILs from divergent parental accessions and will lead to the molecular identification of QTL (Simon *et al*.,2008). Interestingly, hundreds of inbred accessions have been collected throughout the world to study molecular diversity based on their morphological traits under environmental conditions.

Aberystwyth University host an extensive *Brachypodium* germplasm collection with 38 ecotypes available. The research into *Brachypodium* focuses primarily on traits relevant to domesticated cereals, like wheat, barley, rice, and maize which feature complex genomes. The wide geographical distribution of *Brachypodium* has led to unlocking genetic diversity, which facilitates improved breeding programs and cereal genome studies.

.

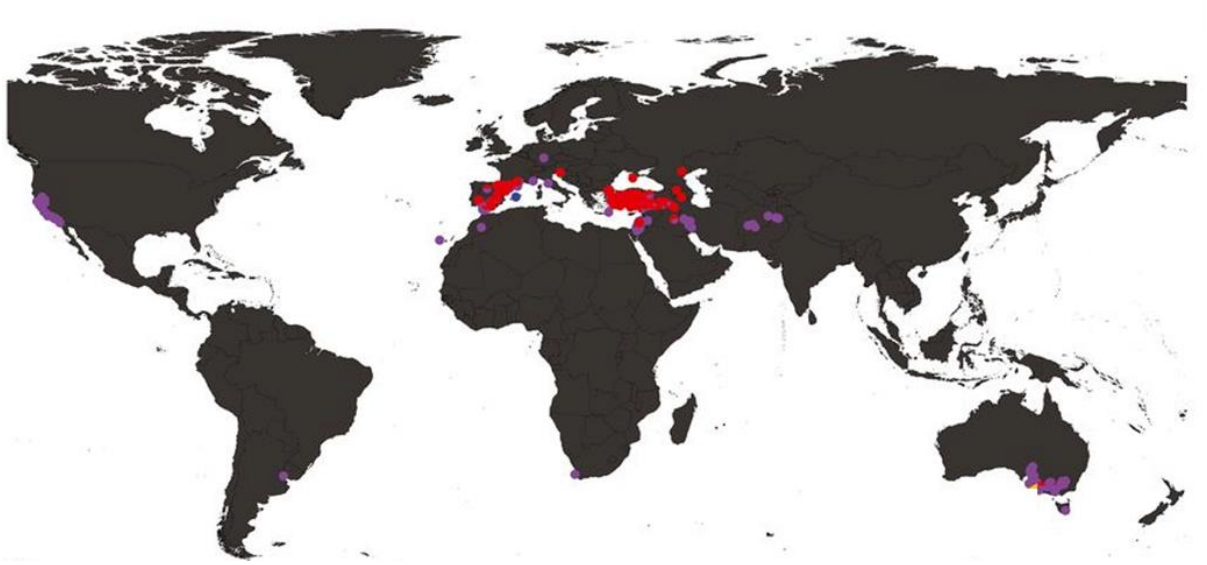

Figure 4-1: Geographic distribution of *Brachypodium* globally suggests the grass species' natural diversity. Pink= *B*. *distachyon*, blue = *B*. *stacei*, and purple= *B*. *hybridum* colour indicates areas corresponding to *Brachypodium* species distribution inferred from herbarium records, field observations, and germplasm collection passport data (Wilson B. P. *et al*., 2019)

RILs are the homozygous true-breeding population that allows the use of the same population over time without losing information derived from the selected accessions. The present chapter aims to screen the phenotypic characteristics of different parental *B*.

distachyon accessions with RIL populations. These accessions represent a range of genomic and phenotypic variations in the species under nutrient limitations (Appendix: Figure A4. 1). In particular, the investigation of several parental accessions for nutrient resistance and nutrient susceptibility was measured by ranking scores. This work lays the foundation for the future identification of critical genetic components of phenotypic traits and QTL for nutrient tolerance using RIL populations, as it represents the most practical means of accessing natural variation for genetic studies.

4.2 Materials and methods

4.2.1 Plant material and vernalisation conditions

Seventeen *Brachypodium* parental accessions of RIL populations with different geographic origins were used in this experiment. Table 4-1 shows the list of *Brachypodium* ecotypes sourced across Europe and the Mediterranean from a range of biological niches. The experiment was conducted under controlled environmental conditions and plants were grown in a glasshouse 16/8h; 21-22 °C/18-20 °C Day/night-controlled environment and were grown in bulrush compost (composition in section 2.2). The glasshouse was fitted with automatic vents and an extractor fan to help reduce variance caused due to environmental factors. The genotypes chosen were representative of different morphotypes and had vernalisation requirements for flowering. Draper *et al*. (2001) suggested that a cold room space for vernalization was required to induce flowering. Whereas, a long day length was sufficient for Bd2-3, Bd3-1, and Bd21 to successfully induce flowering (J. Vogel, 2016). Thus, all the accessions were vernalised for 7.5 weeks (5 °C cold treatment) and a full nutrient solution was given before vernalisation (100% Hoagland or control) for even growth (25ml/pot). N and P were selected as nutrients (treatment) and the solutions were prepared

as mentioned in Chapter 2. Each tray (40x40 cm) containing 20 pots was soaked with 500ml of selected nutrient-deprived solution treatment after they came out of vernalization. The following different treatment solutions were used: a Hoagland's nutrient solution (control), N deprived solution (ammonium and nitrate-based) (N0%), and a P-depleted solution (P0%). Plants were watered when required, and measurements were made after 10-day nutrient-deprived treatment.

Table 4-1: Table listing the *Brachypodium* ecotypes from different countries that were included in the screen with the parents of RIL population available, stage, and institution (Filiz *et al*., 2009; Vogel *et al*., 2009)

Ecotypes	Country of origin	Population	Generation	Institution where RILs generated
ABR6	Spain (lowland)	ABR6 x Bd21	F8	Aberyswyth University and The Sainsbury Laboratory
Adi-9	Spain	Koz-3 x Bd1-1	F6:7	University of Wisconsin, Madison
Bd1-1	Turkey	Ron-2 x Bd1-1	F5:6	University of Wisconsin, Madison
Bd2-3	Iraq (lowlands)	Koz-3 x Bd29-1	F5:6	University of Wisconsin, Madison
Bd3-1	Iraq	Bd21 x Bd1-1	F8	USDA-ARS
Bd21	Iraq (unknown)	Bd2-3 x Bd21	Unknown	USDA-ARS
Bd21-3	Iraq	Bd3-1 x Bd21	Unknown	USDA-ARS
Bd29-1	Iraq	Bd21 x Bd30-1	F8	USDA-ARS
Bd30-1	Turkey	Bd2-3 x Bd3-1	Unknown	USDA-ARS
BdTR10h	Turkey	Bd3-1 x Bd1-1	Unknown	USDA-ARS
BdTR11f	Turkey	Bd21 x Bd29-1	F5:6	University of Wisconsin, Madison
BdTR13k	Turkey	Bd21 x BdTR1-1f	F3	
Foz-1	Spain	Bd21 x Bd3-1	F6	INRA Versailles
Jer-1	Spain (lowlands)	Bd3-1 x Bd21	F6	INRA Versailles
Koz-3	Turkey (highlands)			
Luc-1	Spain (highlands)	Adi-9 x Bd3-1	F2	INRA Versailles
Tek-4	Turkey (lowlands)	Luc1 x Foz1	F3	The Sainsbury Laboratory
		Luc1 x Jer1	F3	The Sainsbury Laboratory
		BdTR13k x Bd21	F6	CSIRO
		BdTR10h x Tek-4	F4	CSIRO

4.2.2 Experimental setup and growth measurements

Seedlings (n=12) were grown for each of the 17 parental accessions for all three treatments. Representative samples for each genotype and treatment were photographed from the front view against a black background and a measuring scale (Appendix Figure A4.2).

Phenotypic characterisation was conducted in the glasshouse and plant height and leaf number were measured at the end of the experiment, followed by harvesting the plants for fresh and dry biomass (day 10 of the nutrient-deprived treatment, n=6). The remaining plants (n=6) were left in the glasshouse to attain the senescence stage to determine spikelet morphology by estimating the number, weight and length of the spikelet present on the main stem.

4.2.3 Relative growth rate

Plant height was measured one day before the nutrient-deprived treatment and was termed as 0 d. After the treatment, the plant height was measured on 3 d, 6 d, and 9 d, respectively.

The relative growth rate (RGR, cm cm^{-1} day^{-1}) was calculated (Chen *et al*., 2001) as follows:

$$RGR = \left(\frac{\ln PHt\ (d2 - d1)}{3}\right)$$

Where, RGR= Relative growth rate, PHt= Plant height (cm)

4.2.4 Biomass measurements

For fresh biomass calculation, plants were harvested and the fresh weight (FW) of the shoot was measured immediately at the end of the experiment as mentioned in section 4.2.1. All the plants (n=6/accession) were then placed in an oven at 65 °C for 3 days and dry weight was recorded. Plant water content was calculated as follows:

$$PWC\% = \frac{FW - DW}{FW} * 100$$

where, PWC= plant water content, FW= Fresh weight (g), DW= Dry weight (g)

4.2.5 Data analysis

Data were analysed using statistical software in R version 3.2.1 (R Team, 2020). Statistical significance was indicated as follows: * $p<0.05$; **, $p<0.01$; ***, $p<0.001$. Data were analyzed with ANOVA one way and Tukey's HSD test at the 0.05 level of significance to determine posthoc pairwise comparison.

4.3 Results

4.3.1. Imaging and morphological measurements

For morphological analysis, *Brachypodium* accessions that were previously collected from different locations (Table 4-1) available at IBERS, Aberystwyth, were measured under nutrient-deprived conditions. The photographs were taken at the end of the experiment and are shown in Appendix Figure A4.2.

PLANT HEIGHT

After ten days of treatment, the plant height was measured from the base of the soil and ranged from 15.8 to 45 cm for Hoagland treatment, 14.8 to 43 cm for N0%, and 13.4 to 34.6 cm for P0%, respectively. Statistical analysis was performed within the accessions between the treatments to observe the nutrient limitation effect on the *Brachypodium* accessions, as shown in Table 4.2. N0% and P0% treatments showed no statistical difference in plant height for 12 out of the 17 accessions (ABR6, Adi-9, Bd21, Bd21-3, Bd29-1, Bd30-1, BdTR10h, BdTR11F, BdTR13k, Foz, Jer, Luc-1) when compared to the control (100% Hoagland solution; Table 4-2). However, when compared with control, plant height measures for the remaining five genotypes suggested an apparent variation in size and stature for these ecotypes following no nitrate and/or no phosphate conditions. Bd1-1 ($p<0.001$), Bd2-3 ($p<0.001$), and

Tek-4 (p=0.03) showed a significant decrease in plant height by 18%, 26%, 27%, respectively under N0% compared with the control. P0% treatment resulted in a significant reduction in Bd1-1 (12%, p=0.02), Bd2-3 (17%, p=0.01), Bd3-1 (30%, p=0.009,), Koz-3 (30%, p<0.001), and Tek-4 (14%, p=0.01) accessions compared with the control (Figure 4-2).

Table 4-2: Growth related measurements of *Brachypodium* parental accessions (mean± SE, n=6). Letters indicate a significant difference between the treatments within the *Brachypodium* parental accessions of RIL populations

Brachypodium accessions	Treatment	Plant height (cm)	Leaf number	Fresh biomass (g)	Dry biomass (g)	PWC (%)
	Hoagland	18.1±0.4a	6.1±0.9a	0.63±0.05a	0.27±0.02a	56.0±1.0a
ABR6	N0%	18.4±0.4a	7.7±0.7a	0.31±0.05b	0.16±0.02b	53.2±1.6a
	P0%	18.9±0.9a	7.5±0.9a	0.49±0.07ab	0.20±0.02ab	59.0±2.1a
Adi-9	Hoagland	20.9±0.8a	5.5±0.2a	0.89±0.07a	0.41±0.05a	54.7±3.1a
	N0%	20.5±1.3a	5.2±0.2a	0.40±0.03b	0.17±0.01b	55.3±0.7a
	P0%	21.5±1.2a	5.0±0.0a	0.44±0.04b	0.19±0.02b	58.0±1.1a
Bd21	Hoagland	31.4±0.5a	5.0±0.0a	0.69±0.13a	0.37±0.12a	50.5±6.2a
	N0%	32.0±1.9a	5.7±0.5a	0.44±0.08ab	0.23±0.04a	57.1±1.5a
	P0%	32.7±1.7a	5.8±0.4a	0.30±0.04b	0.13±0.02a	55.7±3.4a
Bd1-1	Hoagland	18.1±0.5a	8.3±0.3a	1.16±0.05a	0.42±0.01a	63.3±1.1a
	N0%	14.8±0.6b	6.3±0.9ab	0.43±0.06b	0.17±0.04b	61.6±2.7a
	P0%	15.9±0.4b	5.7±0.3b	0.54±0.03b	0.19±0.01b	64.7±2.1a
Bd2-3	Hoagland	33.5±0.5a	3.8±0.2ab	1.1±0.18a	0.41±0.04a	63.2±1.8a
	N0%	24.5±0.4b	3.0±0.0b	0.16±0.01b	0.06±0.00c	60.5±2.1a
	P0%	27.7±2.1b	4.0±0.4a	0.51±0.06b	0.19±0.02b	61.1±0.5a
	Hoagland	32.7±2.1a	4.7±0.3a	1.28±0.22a	0.58±0.13a	53.0±9.7ab
Bd21-3	N0%	31.5±1.8a	5.3±0.2a	0.18±0.01b	0.05±0.00b	72.8±3.6a
	P0%	30.1±1.4a	5.0±0.0a	0.49±0.07b	0.10±0.01b	45.9±4.6b
	Hoagland	16.7±0.3a	5.2±0.4a	0.63±0.02a	0.27±0.01a	57.9±0.6a
Bd29-1	N0%	17.0±0.4a	4.0±0.3a	0.37±0.04b	0.15±0.02b	58.3±0.7a
	P0%	16.1±0.3a	5.3±0.8a	0.39±0.05ab	0.16±0.02b	58.0±1.8a
	Hoagland	44.6±2.4a	7.2±0.5a	0.89±0.13a	0.36±0.06a	58.5±1.6a
Bd3-1	N0%	43.0±1.6a	8.2±0.5a	0.45±0.04b	0.23±0.02b	49.5±1.2b
	P0%	34.6±2.0b	5.5±0.2b	0.33±0.03b	0.16±0.01b	52.5±1.9b
	Hoagland	15.8±0.8ab	4.8±0.8a	0.62±0.05a	0.24±0.02a	62.0±1.1a
Bd30-1	N0%	17.4±0.7a	6.0±0.4a	0.33±0.02b	0.15±0.02b	55.2±1.1b
	P0%	14.3±0.7b	4.3±0.3a	0.31±0.08b	0.12±0.03b	59.4±1.2a
	Hoagland	23.6±0.7a	4.2±0.4a	0.58±0.07a	0.24±0.03a	58.4±0.6a
BdTR10h	N0%	24.5±0.7a	4.5±0.3a	0.39±0.01b	0.19±0.00a	52.0±2.6b
	P0%	23.4±1.3a	5.0±0.6a	0.21±0.03c	0.10±0.02b	51.2±1.3b
	Hoagland	22.2±1.1a	2.7±0.2a	0.59±0.04a	0.26±0.02a	58.4±0.4a
BdTR11F	N0%	21.8±0.8a	3.2±0.2a	0.41±0.06ab	0.19±0.02ab	50.8±4.6a
	P0%	22.6±1.2a	2.8±0.2a	0.33±0.05b	0.14±0.02b	55.1±3.2a
	Hoagland	21.1±1.0a	6.3±0.6a	0.69±0.08a	0.31±0.03a	55.3±1.8a
BdTR13k	N0%	20.7±1.3a	4.5±0.3b	0.50±0.04ab	0.22±0.02b	56.3±0.8a
	P0%	21.9±0.6a	5.0±0.0ab	0.47±0.04b	0.20±0.02b	56.9±2.5a
	Hoagland	20.0±1.6a	5.5±0.6ab	1.71±0.34a	0.42±0.04a	71.0±4.1a
Foz-1	N0%	18.2±1.2a	7.0±0.3a	0.4±0.03b	0.17±0.02b	58.0±0.9b
	P0%	21.6±1.2a	4.0±0.4b	0.56±0.03b	0.22±0.01b	60.1±0.6b
	Hoagland	18.0±0.9a	5.2±0.6a	0.75±0.05a	0.3±0.02ab	58.5±1.8a
Jer	N0%	17.8±0.7a	5.5±0.7a	0.45±0.07b	0.17±0.03b	63.8±1.5a
	P0%	18.8±1.0a	5.5±0.7a	0.79±0.06a	0.35±0.05a	56.6±4.3a
Koz-3	Hoagland	19.1±0.8a	4.2±0.3b	0.72±0.07a	0.32±0.03a	55.2±0.7a

	N0%	19.6±1.0a	5.5±0.5a	0.39±0.01b	0.18±0.00b	55.1±1.1a
	P0%	13.4±0.9b	2.3±0.2c	0.13±0.02c	0.06±0.00c	56.3±2.1a
	Hoagland	17.7±0.5a	6.0±0.4a	0.76±0.06a	0.30±0.03a	60.0±2.0a
Luc-1	N0%	16.0±1.3a	5.2±0.6a	0.45±0.04b	0.20±0.02b	55.6±1.8a
	P0%	17.7±0.6a	4.7±0.5a	0.66±0.03ab	0.30±0.0a	56.9±0.7a
	Hoagland	21.1±0.7a	7.3±0.5a	0.86±0.07a	0.31±0.03a	64.2±2.6a
Tek-4	N0%	18.6±0.8b	5.0±0.2b	0.52±0.01b	0.21±0.0b	60.2±0.9a
	P0%	18.1±0.3b	5.8±0.3b	0.41±0.06b	0.15±0.02b	61.7±1.6a

A ranking of parental accessions of the RIL populations was performed to understand and determine the phenotypic traits of the parental lines in different environments, i.e., reduced nutrient treatment. Figures 4-2 suggested an interaction between genotype and environment (G x E) which further confirmed that a genotype performing superior in one environment might perform less well in a different environment (Assmann, 2013; Juenger, 2013).

Rankings were based on the difference in plant height after nutrient treatments (N0% and P0%) with those of control treatments. Bd21 and Bd30-1 were the most susceptible accessions under N0% and P0%, respectively, while Bd21-3 and Luc-1 were the most resistant accessions under N0% and P0%, respectively. These results suggest that among the ecotypes tested in this experiment, Bd21-3 and Luc-1 are the more tolerant in terms of plant height traits under nitrate and phosphate-deprived conditions, respectively (Appendix 4.2).

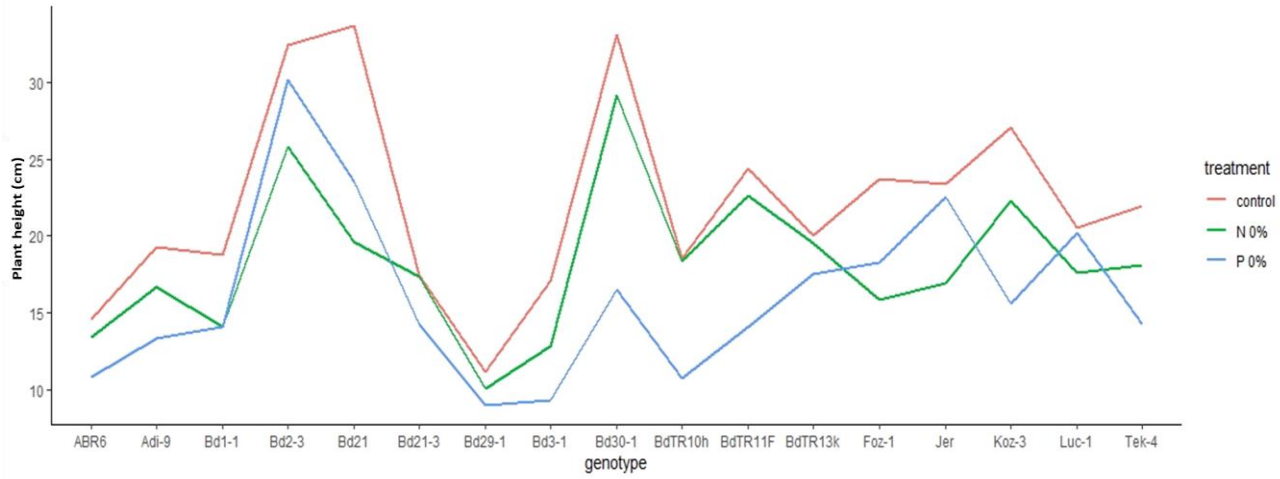

Figure 4-2: Plot for mean (n=6) plant height value under control (red), N0% (green), and P0% (blue) treatment in all the selected ecotypes of *Brachypodium distachyon*.

RELATIVE GROWTH RATE

The relative growth rate was estimated to measure the growth rate based on the plant height along with the time period under different nutrient-deprived conditions (Table 4-3). The results showed that on day 3 a significant decrease in growth rate could only be observed for Tek-4 (p=0.003) under N0% and Bd3-1 (p=0.007) and Tek-4 (p=0.02) under P0% conditions compared with the control (Table 4-3).

On day 6 a significant decrease in relative growth rate under N0% was again observed for Tek-4 (p=0.04). However, a significant increase was found in Bd21 (p=0.005) accession in N0% compared with the control. Under P0%, Bd3-1 (p<0.001), Foz-1 (p=0.01), and Koz-3 (p=0.03) showed a significant reduction in relative growth rate when compared to the control plants. As previously seen for N0%, Bd21 (p=0.007) showed again a significant increase in growth rate was under P0% compared with the control (Table 4-3).

Day 9 measurements showed a significant relative growth rate reduction in only Tek-4 (p=0.01) under N0%, however, an increase was observed in BdTR10h (p=0.02) under N0% compared with the control. In contrast, P0% resulted a significant reduction in Bd21

(p=0.03), Bd3-1 (p<0.001), and Tek-4 (p=0.006) accessions compared to the control (Table 4-3).

Table 4-3: RGR calculated at 3, 6, and 9 days after the treatment under control, N0%, and P0% conditions. Letters of significance indicate differences between the mean with each accession (Tukey's test, $p<0.05$). Mean ± SE (n=6)

Brachypodium accessions	Treatment	RGR (day3)	RGR (day6)	RGR (day9)
	Hoagland	0.036±0.0a	0.036±0.0a	0.036±0.0a
ABR6	N0%	0.041±0.0a	0.035±0.0a	0.035±0.0a
	P0%	0.041±0.0a	0.035±0.0a	0.035±0.0a
Adi-9	Hoagland	0.033±0.0a	0.033±0.0a	0.033±0.0a
	N0%	0.032±0.0a	0.035±0.0a	0.035±0.0a
	P0%	0.032±0.0a	0.034±0.0a	0.034±0.0a
Bd21	Hoagland	0.045±0.0a	0.049±0.0b	0.06±0.0a
	N0%	0.048±0.0a	0.057±0.0a	0.058±0.0ab
	P0%	0.049±0.0a	0.056±0.0a	0.056±0.0b
Bd1-1	Hoagland	0.042±0.0a	0.036±0.0a	0.036±0.0a
	N0%	0.037±0.0a	0.033±0.0a	0.033±0.0a
	P0%	0.035±0.0a	0.036±0.0a	0.036±0.0a
Bd2-3	Hoagland	0.044±0.0a	0.042±0.0a	0.042±0.0a
	N0%	0.040±0.0a	0.039±0.0a	0.039±0.0a
	P0%	0.041±0.0a	0.040±0.0a	0.040±0.0a
	Hoagland	0.047±0.0a	0.075±0.0a	0.045±0.0a
Bd21-3	N0%	0.044±0.0a	0.048±0.0a	0.048±0.0a
	P0%	0.046±0.0a	0.047±0.0a	0.047±0.0a
	Hoagland	0.029±0.0a	0.030±0.0a	0.030±0.0a
Bd29-1	N0%	0.028±0.0a	0.033±0.0a	0.033±0.0a
	P0%	0.031±0.0a	0.030±0.0a	0.030±0.0a
	Hoagland	0.061±0.0a	0.066±0.0a	0.066±0.0a
Bd3-1	N0%	0.055±0.0ab	0.063±0.0a	0.063±0.0a
	P0%	0.047±0.0b	0.049±0.0b	0.049±0.0b
	Hoagland	0.023±0.0a	0.023±0.0a	0.023±0.0a
Bd30-1	N0%	0.026±0.0a	0.023±0.0a	0.023±0.0a
	P0%	0.022±0.0a	0.021±0.0a	0.021±0.0a
	Hoagland	0.035±0.0a	0.035±0.0a	0.034±0.0b
BdTR10h	N0%	0.035±0.0a	0.034±0.0a	0.040±0.0a
	P0%	0.035±0.0a	0.033±0.0a	0.036±0.0ab
	Hoagland	0.040±0.0a	0.039±0.0a	0.037±0.0a
BdTR11F	N0%	0.046±0.0a	0.042±0.0a	0.046±0.0a
	P0%	0.039±0.0a	0.036±0.0a	0.039±0.0a
	Hoagland	0.037±0.0a	0.039±0.0a	0.037±0.0a
BdTR13k	N0%	0.035±0.0a	0.036±0.0a	0.038±0.0a
	P0%	0.036±0.0a	0.035±0.0a	0.039±0.0a
	Hoagland	0.033±0.0a	0.035±0.0a	0.033±0.0a
Foz-1	N0%	0.034±0.0a	0.032±0.0ab	0.028±0.0a
	P0%	0.029±0.0a	0.030±0.0b	0.031±0.0a
	Hoagland	0.033±0.0ab	0.033±0.0a	0.036±0.0a
Jer	N0%	0.030±0.0b	0.031±0.0a	0.036±0.0a
	P0%	0.038±0.0a	0.034±0.0a	0.037±0.0a
	Hoagland	0.032±0.0a	0.036±0.0a	0.032±0.0a
Koz-3	N0%	0.031±0.0a	0.033±0.0ab	0.031±0.0a
	P0%	0.034±0.0a	0.030±0.0b	0.029±0.0a
	Hoagland	0.032±0.0a	0.033±0.0a	0.030±0.0a
Luc-1	N0%	0.029±0.0a	0.033±0.0a	0.030±0.0a
	P0%	0.031±0.0a	0.029±0.0a	0.028±0.0a
	Hoagland	0.039±0.0a	0.037±0.0a	0.033±0.0a
Tek-4	N0%	0.032±0.0b	0.034±0.0b	0.029±0.0b
	P0%	0.031±0.0b	0.035±0.0ab	0.028±0.0b

LEAF NUMBER

Leaf number was scored after nutrient-deprived treatments on day 10. The natural variation amongst different *Brachypodium* accessions resulted in different leaf numbers for each accession. Therefore, statistical analysis was performed within the accessions between the treatments. N0% treatment showed a significant reduction in leaf number for BdTR13k ($p=0.01$), and Tek-4 ($p=0.001$) while a significant increase was found in Koz-3 ($p\leq0.05$) compared with the control (Table 4.2). The remaining fourteen ecotypes showed no statistical difference in leaf number in response to no nitrate conditions when compared to the control. Only three *Brachypodium* ecotypes showed a significant decrease in leaf number following P0% treatment, Bd1-1 ($p=0.01$), Koz-3 ($p<0.001$), and Tek-4 ($p=0.03$) compared with the control (Table 4.2). The leaf number scoring suggested that reducing nutrient availability only once was not enough to stress the plants as leaf number was not significantly affected in most ecotypes (Figure 4.3).

Leaf number ranking suggested that Tek-4 was the most susceptible and Koz-3 the most tolerant accession under N0% as shown in Figure 4.3. Interestingly, Koz-3 was the most affected ecotype found in P0% with ABR6 the most resistant with the maximum number of leaves found after the P treatment (Appendix A4.2).

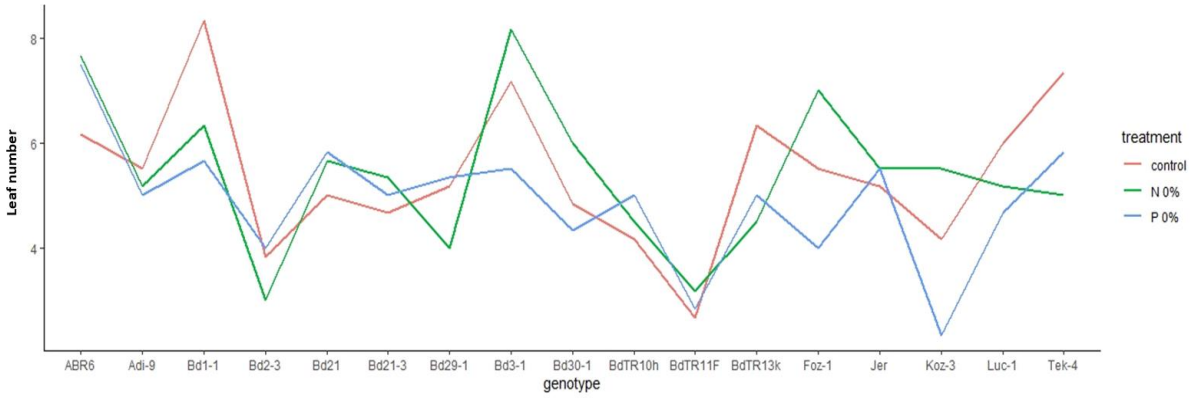

Figure 4-3: Plot for the mean (n=6) leaf number value under control (red), N0% (green), and P0% (blue) treatment in all the selected ecotypes of *Brachypodium* distachyon

FRESH WEIGHT

No nitrate showed a negative effect on fresh biomass of ABR6 (51%, p=0.003), Adi-9 (55%, p<0.001), Bd1-1 (63%, p<0.001), Bd2-3 (85%, p<0.001), Bd21-3 (85%, p<0.001), Bd29-1 (41%, p<0.001), Bd3-1 (49%, p<0.01), Bd30-1 (47%, p=0.005), BdTR10h (33%, p=0.03), Foz-1 (77%, p<0.001), Jer (40%, p=0.02), Koz-3 (46%, p<0.001), Luc-1 (41%, p=0.02), and Tek-4 (40%, p<0.001) *Brachypodium* ecotypes compared to the control conditions (Figure 4.4). Interestingly, only three accessions (Bd21, BdTR11F, and BdTR13k) showed no significant effect compared with the control (Table 4-2).

P0% showed a significant decrease in fresh biomass of Adi-9 (51%, p<0.001), Bd21 (57%, p=0.02), Bd1-1 (53%, p<0.001), Bd2-3 (54%, p<0.01), Bd21-3 (62%, p<0.001), Bd3-1 (63%, p<0.001), Bd30-1 (50%, p=0.002), BdTR10h (64%, p<0.001), BdTR11F (44%, p=0.008), BdTR13k (32%, p=0.03), Foz-1 (67%, p<0.001), Koz-3 (82%, p<0.001), and Tek-4 (52%, p<0.001) compared with the control (Figure 4.4). Interestingly, Spanish ecotypes, ABR6, Luc-1, and Jer showed no statistically significant reduction in fresh biomass weight under phosphate deprived conditions compared with the control (Table 4-2).

The ranking of ecotypes under N0% and P0% deprived conditions suggested Bd2-3 a as the most susceptible ecotype. Interestingly, BdTR13k and Jer were found to be the most resistant ecotype under both nutrient-deprived conditions, suggesting that the experimental nutrient limitation stress conditions had no impact on the fresh biomass weight of the Turkish and Spanish ecotype (Appendix Table A4.2).

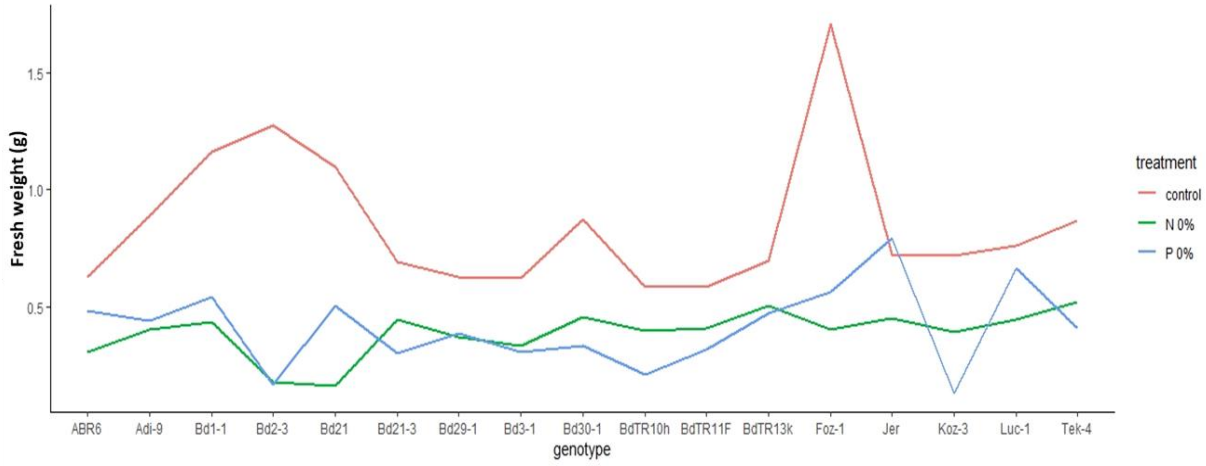

Figure 4-4: Plot for average (n=6) fresh weight under control (red), N0% (green), and P0% (blue) treatment in all the selected ecotypes of *Brachypodium distachyon*

DRY WEIGHT

Dry weight biomass fell in the range of 0.24 to 0.58 g in control conditions, 0.05 to 0.23 g in N0%, and 0.06 to 0.35 g in P0% conditions (Table 4-2). N0% reduced the dry weight accumulation in thirteen ecotypes when compared with the control (Table 4.2): ABR6 (41%, p=0.006), Adi-9 (58%, p<0.001), Bd1-1 (60%, p<0.001), Bd2-3 (85%, p<0.001), Bd21-3 (91%, p<0.001), Bd29-1 (44%, p<0.001), Bd3-1 (36%, p=0.03), Bd30-1 (38%, p=0.02), BdTR13k (29%, p=0.03), Foz-1 (60%, p<0.001), Koz-3 (44%, p<0.001), Luc-1 (33%, p=0.02), and Tek-4 (32%, p=0.01) (Figure 4-5).

P0% treatment on the other hand showed a significant decrease in dry biomass weight in thirteen ecotypes when compared with control (Table 4.2): Adi-9 (54%, p<0.001), Bd1-1

(55%, p<0.001), Bd2-3 (54%, p<0.001), Bd21-3 (83%, p=0.001), Bd29-1 (41%, p<0.001), Bd3-1 (56%, p=0.002), Bd30-1 (50%, p=0.003), BdTR10h (58%, p<0.001), BDTR11F (46%, p=0.003), BdTR13k (35%, p=0.01), Foz-1 (48%, p<0.001), Koz-3 (81%, p<0.001), and Tek-4 (52%, p<0.001) (Figure 4-5).

Dry biomass under no nitrate and phosphate conditions had the most severe impact on Jer and Koz-3 , respectively, when ranked based on differences between treatments and control. BdTR10h and Bd2-3 ecotypes were the most tolerant under N0% and P0%, respectively (Appendix Table 4.2).

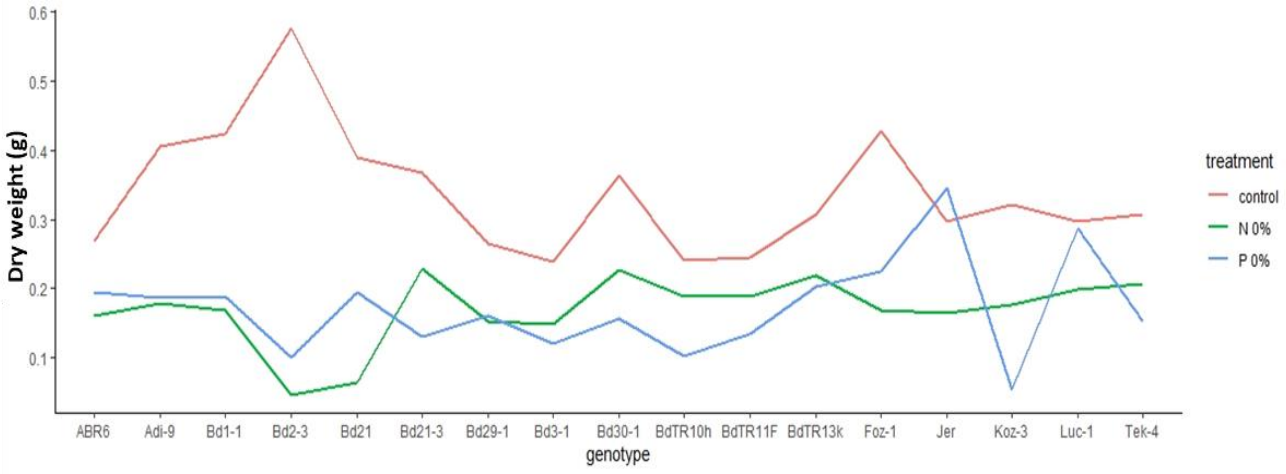

Figure 4-5: Plot for mean (n=6) dry weight under control (red), N0% (green), and P0% (blue) treatment in all the selected ecotypes of *Brachypodium* distachyon

PLANT WATER CONTENT

PWC was measured based on fresh and dry biomass for all the treatments and statistical analysis was performed within the accessions, between the treatments. Bd3-1 (p=0.004), Bd30-1 (p=0.002), BdTR10h (p=0.04; p=0.02), and Foz-1 (p=0.006, P0%=0.02) showed a significant reduction in PWC under N0% compared with the control. P0% also showed a significant decrease in PWC in Bd3-1 (p=0.05), BdTR10h (p=0.02), and Foz-1 (p=0.02)

compared with the control (Table 4-2). No significant effect on PWC was found for the other ecotypes.

4.3.2. Spikelet morphology

It is vital to comprehend the impact of low nutrient stress conditions on spikelet development and yield in *Brachypodium*.

SPIKELET NUMBER

Spikelet number on the main stem was counted for all the accessions of *Brachypodium* under 100% Hoagland, N0%, and P0% conditions. A reduction in spikelet number was observed for ten ecotypes in N0% and eleven ecotypes in P0% compared with the control. Adi-9 ($p=0.004$), Bd1-1 ($p<0.001$), Bd21 ($p=0.04$), Bd2-3 ($p<0.001$), Bd30-1 ($p<0.001$), BdTR10h ($p=0.04$), BdTR11F ($P=0.004$), BdTR13k ($p=0.004$), Foz-1 ($p<0.001$), and Jer ($p=0.002$) showed a significant decrease in under N0% compared to the control (Table 4.4).

P0% treatment resulted in a significant decrease in spike number in ABR6 ($p=0.04$), Adi-9 ($p=0.02$), Bd21 ($p=0.04$), Bd21-3 ($p<0.001$), Bd3-1 ($p<0.001$), Bd30-1($p<0.001$), BdTR10h ($p<0.001$), BdTR11F ($p<0.001$), BdTR13k ($p=0.004$), Jer ($p=0.002$), and Koz-3 ($p=0.003$) compared to the control (Table 4-4).

Table 4-4: Spikelet number, weight and length at senescence stage of *Brachypodium* parental accessions. Mean± SE, (n=6). Letters indicate a significant difference between the treatments within the *Brachypodium* accessions

Brachypodium accessions	Treatment	Spikelet on m.s.	Spikelet weight (g)	Spikelet length (cm)
	Hoagland	2.3±0.33a	0.06±0.0a	3.8±0.13a
ABR6	N0%	1.7±0.22ab	0.08±0.0a	2.8±0.13b
	P0%	1.3±0.22b	0.05±0.0a	2.7±0.21b
Adi-9	Hoagland	3.0±0.0a	0.08±0.0a	3.9±0.07a
	N0%	2.2±0.2b	0.07±0.0ab	2.8±0.11b
	P0%	2.3±0.2b	0.06±0.0b	2.8±0.15b
Bd21	Hoagland	2.5±0.2a	0.08±0.0a	3.95±0.26a
	N0%	2.0±0.0b	0.05±0.0a	2.5±0.12b
	P0%	2.0±0.0b	0.05±0.0a	2.6±0.07b
Bd1-1	Hoagland	3.7±0.2a	0.05±0.0ab	3.6±0.11a
	N0%	1.7±0.4b	0.03±0.0b	2.1±0.4b
	P0%	2.7±0.2ab	0.06±0.0a	3.0±0.2ab
Bd2-3	Hoagland	2.8±0.3a	0.10±0.0a	4.1±0.1a
	N0%	1.0±0.0b	0.04±0.0b	2.5±0.1b
	P0%	2.7±0.3a	0.07±0.0ab	3.8±0.2a
	Hoagland	3.3±0.2a	0.12±0.0a	5.0±0.15a
Bd21-3	N0%	2.9±0.2a	0.09±0.0ab	4.1±0.17b
	P0%	1.8±0.17b	0.07±0.0b	3.15±0.17c
	Hoagland	2.8±0.2a	0.04±0.0a	3.4±0.08a
Bd29-1	N0%	2.3±0.2a	0.04±0.0a	3.0±0.13ab
	P0%	2.2±0.2a	0.04±0.0a	2.9±0.08b
	Hoagland	2.8±0.2a	0.11±0.0a	5.5±0.21a
Bd3-1	N0%	3.0±0.0a	0.09±0.0b	4.2±0.14b
	P0%	1.8±0.2b	0.07±0.0b	3.0±0.11c
	Hoagland	3.5±0.2a	0.06±0.0a	4.3±0.04a
Bd30-1	N0%	1.7±0.2b	0.06±0.0a	2.92±0.12b
	P0%	1.0±0.0c	0.05±0.0a	2.6±0.07c
	Hoagland	2.5±0.2a	0.08±0.0a	2.8±0.12a
BdTR10h	N0%	2.0±0.0b	0.06±0.0a	2.5±0.06a
	P0%	1.0±0.oc	0.04±0.0b	1.8±0.1b
	Hoagland	3.0±0.0a	0.09±0.0a	3.92±0.12a
BdTR11F	N0%	2.3±0.2b	0.08±0.0b	3.5±0.09b
	P0%	2.0±0.0b	0.05±0.0c	2.9±0.06c
	Hoagland	2.7±0.2a	0.06±0.0a	3.9±0.23a
BdTR13k	N0%	2.0±0.0b	0.07±0.0a	3.6±0.14a
	P0%	2.0±0.0b	0.07±0.0a	3.6±0.11a
	Hoagland	2.5±0.2a	0.09±0.0a	3.8±0.1a
Foz-1	N0%	1.0±0.0b	0.03±0.0b	2.8±0.07b
	P0%	1.7±0.3ab	0.07±0.0a	3.7±0.2a
	Hoagland	2.8±0.2a	0.06±0.0a	4.4±0.16a
Jer	N0%	1.7±0.2b	0.06±0.0a	3.4±0.09b
	P0%	1.7±0.2b	0.03±0.0a	3.2±0.08b
	Hoagland	3.2±0.3a	0.07±0.0a	3.9±0.14a
Koz-3	N0%	2.3±0.2ab	0.05±0.0ab	3.3±0.12b
	P0%	1.8±0.16b	0.04±0.0b	3.45±0.1ab
	Hoagland	2.3±0.2a	0.08±0.0a	3.1±0.19a
Luc-1	N0%	2.0±0.0a	0.06±0.0a	3.2±0.18a
	P0%	1.8±0.2a	0.07±0.0a	3.4±0.08a
	Hoagland	3.2±0.3a	0.11±0.0a	4.1±0.14a
Tek-4	N0%	2.3±0.2a	0.06±0.0b	3.6±0.13b
	P0%	2.7±0.2a	0.04±0.0b	3.35±0.1b

Plots for spikelet number on the main stem across reduced nitrate and phosphate treatment along with control are shown in Figure 4.6. The data on spikelet number is the average values of six each parental accessions of RIL population under each treatment. Ranking was calculated by standardising the treatment values from the control and ranking was performed for all the parental accessions of the RIL populations based on change in spikelet number. Bd21 and ABR6 are the most susceptible ecotypes for the spikelet number measured trait under reduced nitrate and phosphate treatment, whereas Bd30-1 and Bd21 are the most resistant ecotypes found under N0% and P0%, respectively (Appendix: Table 4.1).

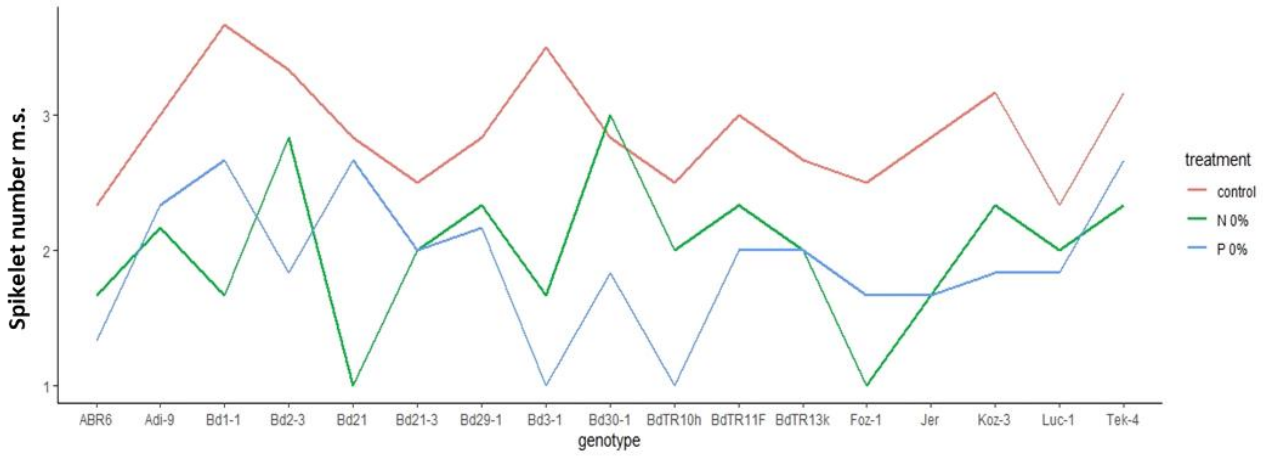

Figure 4-6: Plot for spikelet number on the main stem under control (red), N0% (green), and P0% (blue) treatment in all the selected ecotypes of *Brachypodium distachyon*

SPIKELET LENGTH

Spikelet length was measured from the node of the spikelet to the awn at the senescence stage. No nitrate resulted in a significant decrease in spikelet length in ABR6 ($p \leq 0.05$), Adi-9 ($p<0.001$), Bd21 ($p<0.001$), Bd1-1 ($p<0.01$), Bd21-3 ($p<0.01$), Bd3-1 ($p<0.001$), Bd30-1 ($p<0.001$), BdTR11F ($p=0.01$), Foz-1 ($p=0.01$), Jer ($p<0.001$), Koz-3 ($p=0.01$), Koz-3 ($p=0.01$), and Tek-4 ($p=0.03$) compared to the control. Whereas for no phosphate treatment a smaller

spikelet length was observed in ABR6 (p=0.01), Adi-9 (p<0.001), Bd21 (p<0.001), Bd21-3 (p<0.001), Bd3-1 (p<0.001), Bd30-1 (p<0.001), BdTR10h (p<0.001), BdTR11F (p<0.001), Foz-1 (p<0.001), and Jer (p<0.001) when compared to the control (Table 4.4). Figure 4.7 showed spikelet length measured across reduced nitrate and phosphate treatment along with control. Ranking of seventeen ecotypes under nutrient deprived conditions was measured and Luc-1 was the most notable resistant accession in both N0% and P0% conditions. Bd1-1 and Bd30-1 were the most susceptible ecotypes under N0% and P0% in spikelet length trait (Appendix: Table 4.1).

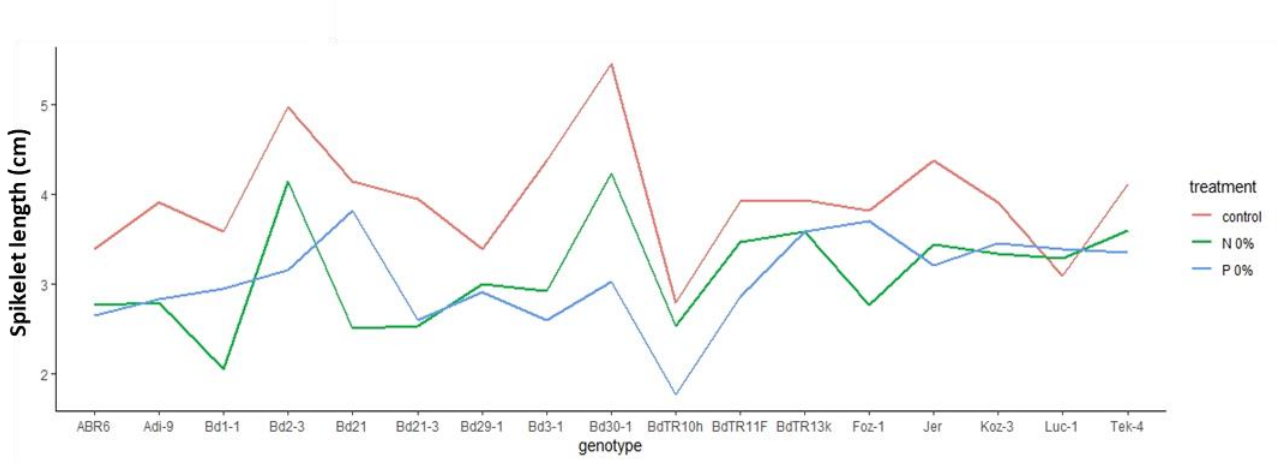

Figure 4-7: Plot for average (n=6) spikelet length (cm) under control (red), N0% (green), and P0% (blue) treatment in all the selected seventeen ecotypes of *Brachypodium distachyon*

SPIKELET WEIGHT

Another important trait of the plant is the weight of the seed produced; therefore the harvested spikelet from the main stem was weighed after measuring the length of all *Brachypodium* accessions (Figure 4.8). N0% treatment showed a significant reduction in spikelet weight in Bd2-3 (p<0.001), Bd3-1 (p=0.03), BdTR11F (p=0.04), Foz-1 (p<0.001), and Tek (p<0.001) compared to the control (Table 4-4). For P0% treatment a significant reduction was observed for Adi-9 (p<0.01), Bd21-3 (p=0.002), Bd3-1 (p<0.001), BdTR10h

(p<0.001), BdTR11F (p<0.001), Koz-3 (p=0.04), and Tek (p<0.001) compared to the control (Table 4). The ranking of parental accessions under N0%, and P0% nutrient-deprived conditions. Ranking of the grain weight showed that N0% and P0% treatments affected the grain weight in Foz-1 and Tek-4 *Brachypodium* accessions while ABR6 and Bd1-1 the least (Appendix: Table 4.1).

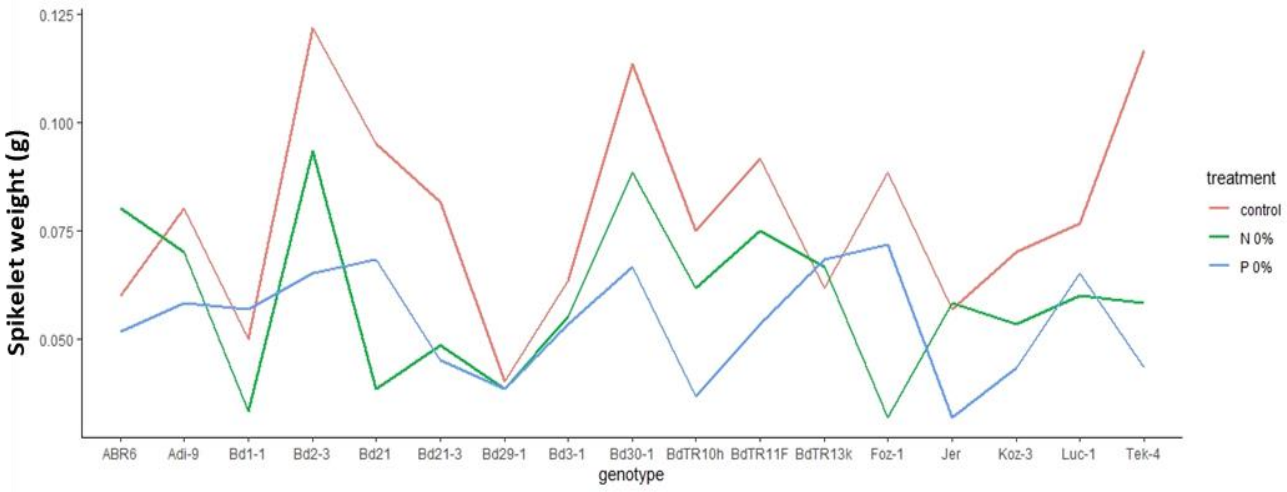

Figure 4-8: Plot for average (n=6) spikelet weight (g) under control (red), N0% (green), and P0% (blue) treatment in all the selected seventeen ecotypes of *Brachypodium distachyon*

4.3.3. Principal component analysis (PCA)

To understand the relation between the genetic variations of each genotype of *Brachypodium* under nutrient limitation, a principal component analysis (PCA) was performed. The PCA dataset revealed that the first component was explaining 48% of the total variability (Figure 4-9). The plot of the PCA scores on 17 geographically distinct genotypes was able to partially separate plants grown under nitrate and phosphate limiting conditions. Interestingly, Bd21 (Iraq) showed higher PC1 value under nitrate stress conditions whereas Jer (Spain) showed higher PC2 value (Figure 4-9).

In conclusion, looking at the PCA score plot suggests that the data points are all over the place thus clustering both component under N0% and P0%, respectively.

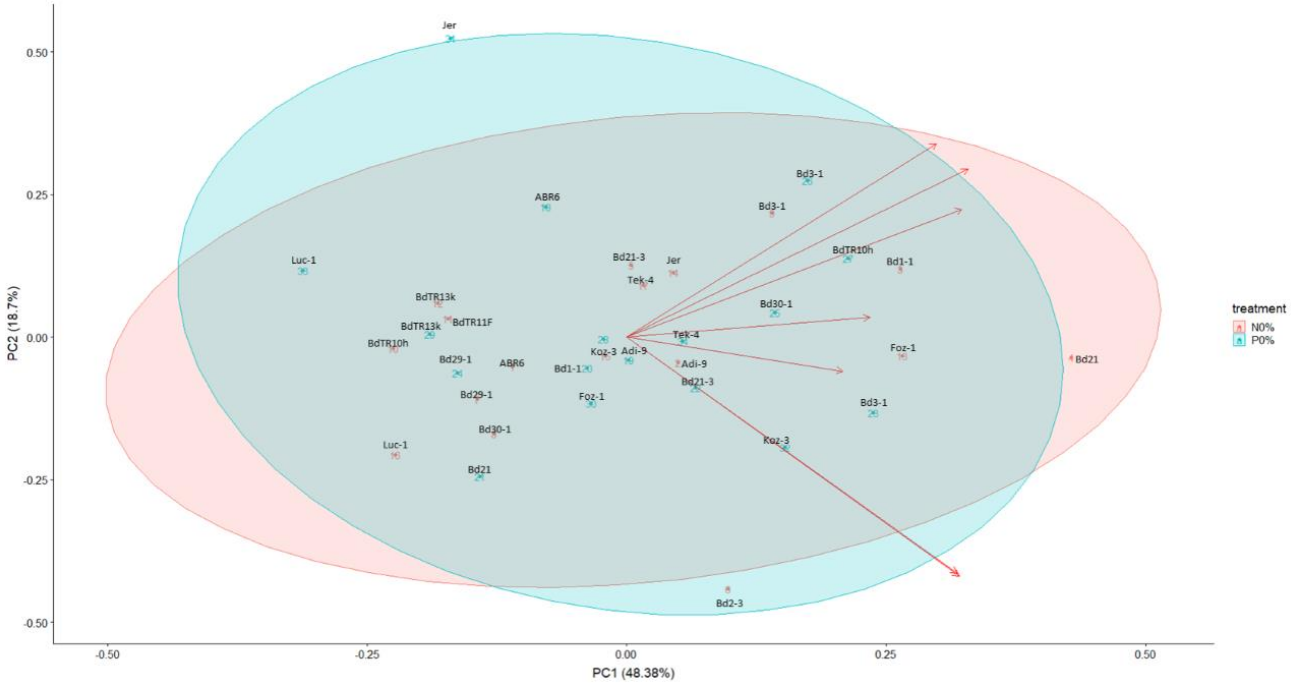

Figure 4-9: Principal Component Analysis (PCA) results for selected parental B. distachyon accessions of RIL population under N and P limitation PC1 expanding most of the variation by 48%, PC2: the second most variation by 18.7% under two dimensions

4.4 Discussion

The main objective of this study was to carry out a robust natural accessions screening using nutrient-deprived treatments, which would subsequently allow the selection of the key parental plants with their existing RIL population for detailed studies. The genetic components that govern traits in different ecotypes represent the outcome of adaptation arising from selecting those traits that allow better-adapted populations to reproduce more successfully (higher fitness) than less well-adapted populations. For instance, one ecotype of a plant species may be able to increase plant growth at the vegetative and reproductive stage, whereas another ecotype lacks this characteristic, thus showing variation within the assessed phenotypic traits (Gifford *et al*., 2013).

The present study evaluated the selected accessions for more detailed phenotypic characterisation in response to nutrient limitation environments (N and P) to help identify superior and stable genotypes. Therefore, providing more robust breeding results and insights into the genetic basis to exploit these phenotypic differences to identify genetic loci (Bergelson & Roux, 2010; Eeuwijk *et al*., 2010). Several phenotypic traits at the vegetative and reproductive stage were measured and screening was performed in *B*. *distachyon* ecotypes resulting in significant differences to classify the tolerant and susceptible accessions in response to nutrient limitation (Pacheco-Villalobos & Hardtke, 2012) studied natural variation within *Brachypodium* in terms of root architecture. The PCA study suggested that some parental accessions of *Brachypodium* showed variation and it would be helpful to distinguish further and understand the genetic causes (Appendix: Figure 4.5). Thereby, the large phenotypic variation of *Brachypodium* in response to nutrient limitation was studied in the chapter to better understand identifying QTLs and genes important for the complex trait under nutrient limitation conditions.

Growth measurements

The above experimental approach allowed for screening and discrimination of several ecotypes based on the morphological behaviour under a low nutrient environment. A wide range of natural variations in response to nutrient stress was found amongst the *Brachypodium* ecotypes. Plant height was increased (though not significantly) under nutrient-deprived conditions in Bd21 lines with an increased relative growth rate between day 3 and day 6. Two accessions (Bd2-3 and Bd3-1) showed a significantly stunted growth under reduced nitrate and phosphate treatment. The same accessions of *Brachypodium* have been previously reported where they have been the most susceptible with the

reductions in leaf water content and Fv/Fm under water stress conditions (Luo *et al*., 2011). Della Coletta *et al* (2019) also suggested that the Bd2-3 genotype was more susceptible to wheat stem rust or *P*. *graminis* f. sp. *tritici*. by using bulked segregant analysis. The focus of their study was on biotic stress, whereas I wanted to gain insight into overall resistance and susceptibility levels by scoring the accessions.

Significant differences were found in leaf number among the accessions under nitrate and phosphate limitation. Interestingly, Koz-3 (Turkish accession) showed to be tolerant under no nitrate, regardless of its sensitivity to reduced phosphate stress. However, no obvious differences were found in leaf number under water deficit stress in *Brachypodium* accessions (Luo *et al*., 2011). Previous studies that have been carried out on different *Brachypodium* accessions tended to focus on overexpression of the gene in Brachypodium and tobacco plants showed resistance to drought stress (Vogel *et al*., 2009, Wang *et al*., 2016). The amount of biomass produced was a commonly measured trait at the vegetative phase for cereal grasses and is of great value. Reduction biomass in Iraqi and Turkish accessions was observed under nitrate and phosphate limitation in the present study. The reduction of biomass in Sorghum has also been reported under nitrogen limitation conditions (Makino & Ueno, 2018). The Turkish lines, BdTR13k and BdTR10h both were able to withstand the imposed nutrient limitation stress resulting in above-ground fresh and dry weight biomass that was similar to the under-control conditions.

Spikelet morphology

Previous studies have suggested that flowering time is an important trait to consider and late-flowering produces greater yields (Schwartz *et al*., 2010; Bettgenhaeuser *et al*., 2017). All *Brachypodium* accessions received six weeks of vernalisation however, this study does not involve the flowering time scoring but involves other reproductive traits measurement like spikelet morphology under nitrate and phosphate limitation. Flowering time is a complex trait majorly regulated by vernalisation and photoperiod controlling environment before spikelet formation. Therefore, flowering time was not measured in the present study due to the extensive variation in flowering time across *Brachypodium* accessions.

Previously, natural variation has been majorly used to study vernalization time period and flowering in Turkish or latest flowering *Brachypodium* accessions indicating that flowering might be controlled by multiple loci or alleles (Schwartz *et al*., 2010). The spikelet morphology was measured at the senescence stage where spikelet number, length and weight were measured for all the selected *Brachypodium* parental accessions of RIL population. The variation was observed in both the resistant and susceptible accessions under reduced nutrient responses (Figures 4.2- 4.8).

Reduced nitrate treatment suggested Bd3-1, Luc-1, and ABR6 plants were the most susceptible to the spikelet morphology measurements. Ingram et al. (2012) also showed in the study that the root system architecture for Bd3-1 is resistant under N limitation. Bd2-3, Bd1-1, and Foz-1 were the most susceptible accessions when treated with reduced nitrate. Bd2-3 (Iraq) and BdTR11F (Turkey) were the most resistant genotypes for spikelet number, weight and length under reduced phosphate treatment. However, ABR6, Koz-3, and Bd29-1 showed a significant reduction in measured spikelet traits on low phosphate treatment. Natural tolerance of *Brachypodium* to stresses like heat, chilling, high salinity, drought etc.

plays a substantial role in identifying efficient mechanisms in cultivated cereals (Girin *et al*.,2014). The degeneration of spikelet morphology also occurred under heat stress conditions in rice seedlings (Wang Y. *et al*., 2019). Previous studies have suggested that cold, salinity and drought stresses cause a significant impact on spikelet morphology, thus, dropping the yield for major crops (Mahajan & Tuteja, 2005; Khan *et al*., 2016; Beyaz, 2020). Spearman correlation coefficients showed a significant positive correlation in all the measured phenotypic traits under nutrient limitations (Appendix Figure 4.4).

Principle Component Analysis (PCA) was performed to investigate the phenotypic variation between the parental accessions of RIL populations in response to N and P limitations (Figure 4-9). The results also showed a variation in the parental ABR6 and Bd21 accessions of *Brachypodium* under nutrient limitation (Figure 4-9). The data suggested high variability in Iraqi, Spanish, and Turkish genotypes as the data was all over under low nitrate and phosphate conditions.

4.5 Conclusion

Overall, future studies based on fresh weight (Bd29-1 x Koz-3), spikelet number (Bd30-1 x Bd21) and spikelet weight (BdTR13k x Bd21) suggest tolerant x susceptible genotypes under nutrient limitation. The above parental genotypes showed sufficiently large phenotypic variation under nutrient limitation, thus suggesting potential parents with RIL populations available for studying detailed analysis. The present study comprehended that Turkish and Iraqi *Brachypodium* genotypes were ideal for exploring the RIL population derived from the above combinations under low nitrate and phosphate limitations.

Interestingly, the ABR6 x Bd21 Brachypodium population has since been published by Bettgenhaeuser *et al*. (2017) to identify genetic loci associated with flowering time and due

to its prevalence in the scientific community and availability of F8 generation of this particular existing RIL population at Aberystwyth University more detailed analysis was performed (Appendix Table A4.1). However, ABR6 x Bd21 parental genotypes were an intriguing combination for further study. The selected candidate parental genotypes are geographically distinct and showed a higher phenotypic variation under nutrient limitation. Therefore, the above mapping population was chosen for phenotyping and identifying QTL in the RIL population derived from ABR6 and Bd21 in response to nutrient limitation. A further detailed research needs to be performed on all the selected *Brachypodium* bi-parental populations to identify and choose ideal genotypes. The study could then be used to develop specific populations to further implement in future studies to establish the current knowledge of nutrient limitation response.

Chapter 5 : Using *Brachypodium* ABR6 x Bd21 derived RILs to identify QTLs for response to low nutrient availability

5.1 Introduction

Dissecting the natural genetic variation requires quantitative trait locus (QTL) analysis to identify chromosomal loci, each carrying one or more genes controlling these complex traits (Cobb *et al*., 2013). Genetic crop improvement can be achieved by calculating the recombination rates between the molecular markers on the genetic map and functional gene localization. The variation in gene sequence between different individuals contributes to their phenotypic differences (Cleveland & Deeb *et al*., 2012). These differences in sequence can be analysed further, allowing us to characterize each individual accordingly and be used to select favourable traits (Bekeko & Mulualem, 2016).

Many agriculturally important traits, such as flowering time, and grain yield, are quantitative traits, and such traits are often affected by multiple genes known as quantitative trait loci (QTLs). To enhance agricultural production, we need to bridge genotype and phenotype; linking the genomic data to different levels of phenomics data will allow advances in crop genetics to be fully utilized (Großkinsky & Svensgaard, 2015). However, confirming a candidate gene as the casual gene underlying a QTL ultimately rests on complimenting the phenotypic QTL analysis with statistical procedures to link these two types of information—the phenotypic data, recorded as trait measurements, and genotypic data. QTL for nutrient tolerance have been reported in two major cereal crops: wheat (Hussain *et al*., 2017) and rice (Jewel *et al*.,2019). Furthermore, QTL mapping for nutrient stress resistance is vital for bioenergy and forage crops to improve their productivity when grown under nutrient-limiting conditions.

5.1.1 Quantitative traits and QTL mapping

A QTL is a gene locus or region responsible for a particular quantitative phenotype of interest. These can encompass any number of linked genes within the same QTL region or multiple QTLs linked to the same phenotypic trait. These include the generation of mapping populations, genetic markers to construct linkage maps and QTL analysis for linking markers to phenotype. In order to link a phenotype to a genotype, firstly, a population of individuals is required to show diversity or segregate for the trait of interest, such as a low nutrient response.

Phenotypic traits are usually controlled either by many genes with minor effects termed polygenic inheritance or by single genes with significant effects known as monogenic inheritance. However, understanding complex trait variation, such as nutrient resistance/tolerance or yield, has proven difficult, as the genetic architecture of these essential traits often involves many loci of minor effects that may interact with each other, as well as with the environment (Collard & Mackill, 2008; Buckler *et al*., 2009; Schuster, 2011). These quantitative traits associated with many loci containing gene(s) on a chromosome are denominated as QTLs. They are the summation of their effects and their interaction with the environment that determines the individual's phenotype (Falconer and Mackay, 1996).

Quantitative trait values often show a continuous distribution that indicates the presence of many genes contributing to or underlying the trait. Therefore, a given trait's distribution of phenotypic values is often normally distributed. For example, grain yields exhibit a wide range from low to high yield depending on the presence of the responsible genes (as well as variation in the environment). Genes controlling quantitative traits interact with each other

(epistasis), and the expression of these traits is often influenced by environmental conditions (Falconer and Mackay, 1996). Quantitative traits have been targets of crop improvement for yield, quality and pest resistance. Understanding the influences of genes and environment on quantitative traits is a significant challenge in biological studies. Enhanced understanding of these traits leads to utilizing them to benefit the scientific community (Bernardo, 2008).

QTL mapping is often performed on populations developed from two parents (bi-parental mapping populations) that possess different traits of interest. The variation of the respective trait(s) and also a variation of their genetic background enhances the chance of detection of polymorphic markers and QTL in the RIL population. Careful measurement of the phenotype(s) of interest must be done before the phenotype can be correlated to genetic elements (called markers) on the chromosome required for QTL mapping. Molecular markers or DNA markers are small segments of DNA sequence showing polymorphisms (differences) between individuals. They can be detected as specific sequences of nucleotides in the DNA molecule (Xu Y., 2010). They physically define localised genomic regions (gene location on the chromosome) and allow one to ask whether trait variation is associated with any particular location (Collard et al., 2005). Genetic markers can be classified into several groups including Single Nucleotide Polymorphism (SNP), Restriction fragment Length Polymorphism (RFLPs), Amplified Fragment Length Polymorphism (AFLPs), Random Amplification Polymorphic DNA (RAPD), Simple Sequence Repeat (SSRs. Two commonly used methods of analysis for QTL detection are simple interval mapping (SIM) and composite interval mapping (CIM) analyses. SIM uses linkage maps and measures intervals between adjacent pairs of linked markers along the chromosomes. More recently, CIM has gained popularity for mapping QTLs. It combines interval mapping with linear regression and

includes additional genetic markers in the statistical model and an adjacent pair of linked markers for interval mapping (Zeng,1994). In our study, the CIM method was used as it helps us to separate the individual QTL effects by combining interval mapping with multiple regression and is more precise and effective at QTL mapping (Collard *et al.*, 2005).

In contrast to nutrient responses, many molecular components and candidate genes are well known in vernalisation-related flowering time. VERNALISATION (VRN) genes involved in flowering time traits associated with vernalisation are well studied in Brassicaceae, Poaceae, and Amaranthaceae (Andrés & Coupland, 2012; Ream & Woods, 2012). In temperate grasses, three VRN genes are identified. FT and VRN1 are promoters of flowering in *Brachypodium* (Ream *et al*., 2014). Also, the wheat and barley flowering studies have suggested that the VRN1 gene is a MADS-box transcription factor consistent with FT levels and rapid flowering induced by the cold (Yan *et al*., 2004; Andrés & Coupland, 2012). Overexpressing the FT gene reduces VRN2 and increases VRN1, thus overexpressing transgene FT (Distelfeld *et al*., 2012). However, a recent study in *Brachypodium* showed the ability to flower without vernalisation and is directly linked to three significant loci, two of which colocalise with the homologs of VRN2 and FT in *B*. *distachyon* (Bettgenhaeuser *et al*., 2017).

5.1.2. Recombinant inbred line (RIL) population

A common approach in inbreeding cereals for QTL analysis by linkage mapping involves segregating populations such as recombinant inbred line (RIL). RILs are proven very effective in QTL analysis and are also known as immortal mapping populations. Such populations are derived from a cross between parental lines showing differences in the trait of interest, and therefore, RILs can be easily maintained by selfing as they are homozygous. RIL populations

are created by single seed descent from an F2 population produced by crossing a homozygous, inbred parental line. These initially heterozygous lines are allowed to pollinate over 6-8 generations self- to create a population comprising of homozygous lines, with approximately 50% of each parent in different combinations (Doerge, 2002). RIL populations are statistically considered better than F2 populations in the genetic mapping (Ferreira *et al*., 2006) as they can go through multiple meiotic cycles by allowing more recombinant events with better mapping resolution. The advantage of the RIL population is that it is homozygous true-breeding, so it can repeatedly grow without a change occurring within the population's genotypic makeup and show great variation for most phenotypic trait investigations (North *et al*., 2009).

5.1.2 Genetic maps

Van Ooijen (2011) define the genetic map as a representation of the relative positions of genes and genetic markers on the chromosomes for a given species. Therefore, linkage analysis determines genetic maps and is commonly known as linkage maps. Linkage analysis studies the co-segregation of genetic markers by observing how often loci alleles are inherited together or exchanged due to crossovers in meiosis. To be able to follow the co-segregation of alleles, we need to be able to distinguish the alleles. This depends on associated polymorphisms in or very close to the alleles. Otherwise, we cannot follow their segregation and measure their recombination rate. The recombination rate gives us a measure of the distance between any two loci. Genes or markers tightly linked will be transmitted with higher frequency to the progeny and have a lower recombination rate. The frequency of recombinant genotypes is used to calculate recombination fractions. Markers with a recombination frequency of 50% are assumed to be located far apart or in different

chromosomes. Using mapping functions, these recombination fractions can be converted to map units, centimorgans (cM) (Haldane, 1919; Kosambi, 1942). Since we need to follow inherited loci to construct a linkage map, we need a mapping population. The first step is to identify polymorphic markers in the parents of the mapping population that then need to be screened across the entire population. The DNA markers for each individual are then coded, and the linkage analysis of polymorphic markers is performed using computer algorithms (Van Ooijen, 2011). Genetic maps are constructed in two steps. First, we determine the linkage groups and establish the map order. This analysis outputs a set of linkage groups that represent chromosomal segments or entire chromosomes where markers are ordered (Collard *et al*., 2005).

5.1.3 Low nutrient availability related traits for QTL analyses

Nutrient tolerance is a relative term that can describe the ability of a plant to withstand low nutrient availability in the soil. Several studies have investigated the effects of nutrients on flowering traits suggesting that nutrient limitation can significantly affect the bud appearance in Arabidopsis (Kolář & Seňková,2008; Ye T. *et al*., 2019). Consequently, some studies have indicated that environmental mediated stress factors like N limitation induce early flowering, whereas P limitation delays flowering in plants (Rossiter, 1978; Vidal *et al*., 2014; Cho *et al*., 2017; Lin & Tsay, 2017). This further suggests an essential role of N and P in plant growth and development, as mentioned and discussed in part on nutrients in Chapter 1. Previous studies have reported N-related mechanisms, N and P availability on root architecture, stimulation of *Brachypodium* growth by high N availability, and N availability on grain production (Ingram *et al*., 2012; Poiré *et al*., 2014). However, no reported study investigated QTLs (for plant height, spikelet number, and flowering) and candidate gene

identification for a flowering time under nutrient limitation in *Brachypodium* accessions. Here, the study focuses on understanding low N and P tolerance associated phenotypic traits in the RIL population derived from ABR6 x Bd21 *Brachypodium* with a specific focus on flowering time, which will further help us in cereal crops breeding and selecting genotypes with better nutrient tolerant crop yields. Plants take up nitrate and ammonium from the soil to sustain many metabolic processes and N deficient plants tend to rebalance their growth, increasing root growth relative to above ground parts (Zhang H. *et al*., 2007; Ikram *et al*., 2012). NO_3^- and PO_4^{3-} availability is responsible for rapid foliage growth and affecting the quality of seed, and flower production in plants and therefore targeting them will potentially improve the production and yield of the temperate cereal crops (Liu *et al*., 2013). Phenotypically measurable traits associated with low nutrient availability in the crops can be measured as above ground biomass and morphological responses, such as leaf number, plant height, flowering time or various below-ground measurements like root architecture, relative roots growth, and numbers studied previously in Chapter 2. Furthermore, as mentioned above, these traits are associated with plant physiology and low nutrient availability relations.

Several studies have examined the responses of plants to single-defined stresses (Ingram *et al*., 2012; Poiré *et al*., 2014), but little is known under low N and P environments in *Brachypodium*. In the current study, the response of 113 RILs derived from the parental accessions, ABR6 and Bd21, to low N and P conditions was investigated in the phenotyping platform to explore the genetic variation in response to low nutrient availability.

This chapter introduces how two genotypically and phenotypically diverse *Brachypodium* accessions (ABR6 x Bd21) and the RIL population developed from these accessions

phenotypically respond to N and P limitations. The phenotypic variation results obtained using this F8 population helped to explore the genetic architecture of the traits measured. Seven QTLs are reported in the study under nutrient limitation, where two QTLs control the flowering time within this RIL population. Both the QTLs colocalize with well-described *B. distachyon* flowering time genes (VRN1 and VRN2), suggesting a conserved flowering time regulator effect in response to low nutrient tolerance. The present study provides a basis for molecular deciphering of low nutrient-related mechanisms in *Brachypodium* as a model for temperate cereal and forages crops in future studies.

5.2 Materials and methods

5.2.1 Plant material and growth conditions

A RIL population of *Brachypodium distachyon* was derived from an interspecific cross obtained from ABR6 and Bd21, with two contrasting and geographic origin ecotypes. The Iraqi accession Bd21 which does not require vernalization, whereas a Spanish accession ABR6 which requires 6-week vernalization period to induce flowering (Routledge *et al.*, 2004; Garvin *et al.*, 2008). The population was F8 generation and comprised of 113 RILs. The experiment was conducted to have a better understanding for phenological traits and QTL identification under low nutrient availability using this mapping population at the National Plant Phenomics Centre facilities (Aberystwyth University, UK). Three seeds were sown in each pot on 24th October 2018 in a 6 cm plastic pots containing 50 grams of 40 % silver sand /60% WI13 compost (Bulrush, Magherafelt, N Ireland, low nutrient compost). 10 days after sowing, pots were thinned to one seedling per pot followed by 6-week vernalisation under controlled environment growth conditions at 4 °C with a 16/8h photoperiod on 14th day from sowing. The plants were transferred into a glasshouse under controlled environmental

conditions at 18 °C (day) and 15 °C (night) with a 14/10h photoperiod. Each pot was weighed, and plants were watered automatically every two days above to 65% from gravimetric water content daily during their vegetative growth period at PlantScreen Phenotyping System (Photon System Instruments, PSI) without using the imaging acquisition. Plants were grown under LED lights at a light intensity of approximately 600 m mol $m^{2\ s\ -1}$ (200W GreenPower LED). Plants were moved to a neighbouring glasshouse compartment set to the same environmental conditions at their reproductive stage and transferred the experiment was given the code Bd021.

5.2.2 Nutrient limitation experimental design

The seedlings were planted in three replicates for each RIL population along with the parents (ABR6 and Bd21) into three specific nutrient treatments before and after vernalisation i.e., on the first and the last day of vernalisation as explained in Chapter 3. Nutrient limitation experiment was imposed by preparing reduced nitrate (N), and reduced phosphate (P) from the Hoagland solution recipe whereas for the control plants full Hoagland solution was used (Hoagland and Arnon 1950). Each tray comprising of 20 pots were soaked with 500 ml of the above three treatment solutions: a full Hoagland's nutrient solution (control), minus N, and minus P, respectively. Hoagland solution recipe for 2.5 L stock solution was prepared as mentioned in Chapter 2.

5.2.3 Phenotypic trait measurements

At the end of the growth stage, phenological measurements for the RIL population along with the parents under three different treatments were scored. The measurable traits and their abbreviations (abbr.) with the measurable units are listed in Table 5-1.

Table 5-1: Summary of measured phenological traits with their abbreviations and unit of measurements

Abbr.	Meaning	Unit
PHt	Plant height	cm
TN	Tiller number	No.
SN	Spike number	No.
SPM	Spikelet number on the main stem	No.
EWt	Ear weight	g
PWt	Above ground plant biomass	g
FT	Flowering time	days
HI	Harvest index	-

Plant height (PHt): the height (cm) of the plant was measured from the soil surface to the top of the inflorescence (excluding awns) at the maturity stage using a measuring stick. Tiller number (TN): primary branches growing from the main stem was termed as tiller, numbers were counted but secondary branches developing from primary branches were not. TN was counted between the beginning of physiological maturity and end of flowering time as the number of days after sowing (DAS) and the day on which the first inflorescence or heading appeared.

Spike number (SN): spike number was scored at the senescence stage for each fertile tiller. Spikelet number was counted on the main stem (SPM) for each plant at the senescence.

Ear weight (EWt): the inflorescence was harvested from each plant and the total ear biomass (seed and the awns) were weighed (g) by placing separately on a weighing balance. Plant biomass (PWt): was weighed (g) by harvesting aboveground biomass without the

inflorescence from each pot and were put separately into paper bags. Flowering time (FT): Plants were inspected daily, and FT was scored as the number of days between the sowing day and the day on which the first flower appeared. The day of flowering was recorded for each plant in a pot. At maturity, each plant was harvested individually and Harvest index (HI): was determined based on EWt and above ground PWt calculated as follows:

$$HI = EWt/PWt.$$

5.2.4 ABR6 x Bd21 F8 population and genetic map

A cross between geographically and phenotypically distinct *B*. *distachyon* accessions (ABR6 x Bd21) F1 individuals were generated for the creation of RIL population using single seed descent to the F8 generation and available at Aberystwyth University. The final genetic map comprising of 169 SNP markers with 1,999 cM spanned five linkage groups corresponding to five chromosomes of *Brachypodium distachyon* was used in the present study. RIL populations derived from ABR6 and Bd21 (F4 population) by Bettgenhaeuser *et al*. (2017) confirms the high rate of recombination amongst *B*. *distachyon* and other grass species (Huo *et al*., 2011; Woods *et al*., 2017). All the chromosomes were scanned for segregation distortion at F8 generation by using a χ2 test by Mathew J Moscou (Sainsbury laboratory, Norwich) (data not available).

5.2.5 Genotypic data analysis

All phenotypical data was analysed using the statistical software R (Team, 2020). A Shapiro-Wilk test was performed to test the normality of the obtained data from the RILs and parental accessions. Analysis of variance (ANOVA) and least squares mean of phenotypic

values of all traits for the three treatments were calculated. Transgressive segregation displayed all the phenotypic values (normalised by the control) and the RIL population along with both the parents were plotted. Correlation coefficients between all the phenotypic traits were calculated for each treatment using least squares means.

QTL analysis was performed using R studio and R/qtl package. Data for RIL population was converted into riself (data). The trait value was analysed using simple Harley-Knott linear regression and composite interval mapping (CIM) method (Zeng,1994) was performed as it has several advantages over traditional methods of regression analysis. The Standard Model 6 was used for scanning the genetic map and estimating the likelihood of a QTL. Results are presented using a logarithmic of odds (LOD) score. These profiles are used to identify the most likely position for a QTL in relation to a linkage map. Percentage variance explained (PVE) was calculated for all statistically significant QTL peaks:

$$\mathrm{PVE} = (1 - 10^{-2 \times \mathrm{LOD\,n}}) \times 100, \mathrm{n} = 117$$

Thresholds were determined by permutation tests using 1000 permutations controlled at $\alpha = 0.05$ (Doerge and Churchill 1996) with the significant peak exceeding the level that can be determined using permutation tests. Genes close to the most significantly associated SNP from each QTL region were identified, and gene annotations were retrieved using Phytozome (version 13; https://phytozome-next.jgi.doe.gov/).

5.3 Results

5.3.1 Phenotypic variation under different treatments of the parental ABR6 and Bd21 accessions

To determine the phenotypic variation of the parental lines of the RILs under nutrient stress, ABR6 and Bd21 accessions were exposed to three different treatments: full Hoagland's solution (control), minus N, and minus P. A one-way analysis of variance was performed for the means to compare the differences under the three treatments (Table 5-2). Except for flowering time, the minus N treatment significantly affected all the phenotypic traits measured in ABR6 and Bd21 when compared to the controls ($p< 0.05$). The minus P treatment had a more varied response on ABR6 with PHt, SN, PWt and EWt being significantly reduced in ABR6 ($p<0.001$) compared to controls while there was no effect on tiller number, spike number and flowering time on the main stem. For Bd21, the minus P treatment had a similar effect as minus N treatments with all traits except flowering time being affected (Table 5-2).

Comparison of plant height between the parental lines, measured at the senescence stage after the inflorescence had been removed, showed that Bd21 plants were significantly taller compared with ABR6 plants under control ($p<0.001$), minus N ($p<0.001$) and P treatments ($p<0.05$; Table 5-2). For Bd21, the P0% treatment resulted in a significant further reduction in plant height when compared with the reduction in plant height as a result of N0% treatment (Table 5-2). However, for ABR6 there was no significant effect on plant height reduction between the N0% and P0% treatments.

Although N0% treatment resulted in a significant reduction of the number of fertile tillers in both genotypes, a significant reduction in tiller number was only observed for Bd21 upon P0% treatment. For ABR6, there was no significant effect for this measure between P0% treated plants and control plants. Plant biomass measurements, not including the inflorescence was significantly reduced by both treatments in both genotypes with no statistical difference in reduction between the two treatments. The biomass measures following minus N stress conditions were only 15% and 17%, respectively for ABR6 and Bd21 when compared with their respective controls. For minus P stress condition, the biomass measures were 22% and 19%, respectively for ABR6 and Bd21 when compared with their controls (Table 5-2).

SN, and SPM were scored at the end of the experiment whereas ear weight (g) was measured by removing the inflorescence at the senescence stage. It was observed that the parental lines ABR6 and Bd21 when compared showed no statistically significant difference for SPM, PWt, and EWt under control, minus N and P conditions. However, a significant difference was obtained in the above traits when the effect of the treatments (control, minus N and P) was compared for each of the parental lines ($p< 0.001$), except for the spike number following P0% treatment in ABR6 (Table 5-2).

Treatments did not affect flowering time with Bd21 consistently flowering earlier compared to ABR6 under control, minus N and P conditions, whereas a significant difference was observed between the two parental accessions under control, minus N, and minus P treatments ($p< 0.001$, $p< 0.001$, $p<0.01$, respectively).

In summary, these results show that minus N and P treatments generally lead to similar and dramatic phenotypic effects in both genotypes. However, ABR6 appears less sensitive to P0% treatment with regards to tiller number and spike number when compared with Bd21.

Table 5-2: Analysis of variance for parental accessions ABR6 and Bd21 under different treatments. Mean ±SE (n= 3) values with letters signifying significant differences between the treatments within the genotype; ***, **, * significant difference at P<0.001, P<0.01, P<0.05, respectively, ns= not significant

Phenotype	Treatment	ABR6	Bd21	Sig diff within the treatment btw genotype
PHt	Hoagland	20.8 ±0.4 a	28.7±0.5 a	***
	Minus N	11.3 ±0.6 b	21.2 ±0.4 b	***
	Minus P	8.2 ±2.3 b	16.2 ±1.1 c	*
TN	Hoagland	3.6 ±0.3 a	3.7±0.3 a	ns
	Minus N	1.0 ±0.0 b	1.0 ±0.0 b	ns
	Minus P	3.0 ±0.0 a	1.0 ±0.0 b	***
SN	Hoagland	4.0 ±0.6 a	6.0 ±1.5 a	ns
	Minus N	1.0 ±0.0 b	1.0 ±0.0 b	ns
	Minus P	3.0 ±0.0 a	1.0 ±0.0 b	***
SPM	Hoagland	2.3 ±0.3 a	2.0 ±0.0 a	ns
	Minus N	1.0 ±0.0 b	1.0 ±0.0 b	ns
	Minus P	1.0 ±0.0 b	1.0 ±0.0 b	ns
PWt	Hoagland	0.4 ±0.6 a	0.5 ±0.07 a	ns
	Minus N	0.06 ±0.0 b	0.08 ±0.0 b	ns
	Minus P	0.1 ±0.03 b	0.1 ±0.0 b	ns
EWt	Hoagland	0.21 ±0.02 a	0.3 ±0.01 a	ns
	Minus N	0.03 ±0.0 b	0.03 ±0.0 b	ns
	Minus P	0.05 ±0.02 b	0.04 ±0.0 b	ns
FT	Hoagland	90.3 ±0.3 a	76.0 ±0.0 a	***
	Minus N	93.0 ±1.2 a	78.0 ±1.0 a	***
	Minus P	94.0 ±3.2 a	76.0 ±0.0 a	**

PHt: Plant height (cm), TN: Tiller number, SN: Spike number, SPM: Spikelet on main stem, PWt: Plant weight (g), EWt: Ear weight (g), FT: Flowering time (days)

5.3.2 Population response to low nutrient availability

A statistical analysis was performed to understand how nutrient stress affects F8-population of *Brachypodium* parental accessions and their underlying physiological and genetic mechanisms. ABR6 and Bd21 derived population to low nutrient stress response will further improve the selection efficiency by deciphering the complex network related nutrient tolerant traits and identify QTLs associated with these traits to enhance the agricultural production.

One way analysis of variance was performed and comparison between the mean trait values of the RIL population. The results reflected those from the parental accessions under the low nutrient conditions. A significant decrease was observed for all traits except FT when compared to the control under minus N, and P as shown in figure 1 ($P<0.01$, $P<0.001$, respectively). A statistically significant reduction on average of 21% PHt was observed in RIL population under minus N when compared to the control ($P<0.001$) (Table 5-3). P0% had an even more dramatic effect on PHt with 45% of reduction on the population when compared to the control ($P<0.001$).

Specifically, under N0% the values of TN, SN, and SPM ranged from 1 to 3 number, 1 to 2, 0 to 2, 0 under minus N and 1 to 3, 2 to 4, 1 to 3 under minus P, respectively. Also, a statistically significant treatment by genotype interaction was found in PHt, TN, SN, SPM, EWt, PWt as shown in Table 5-3 ($P<0.001$). The above ground plant biomass and ear weight showed a reduction of 83% under minus N when compared to the control and largely varied across the population ranging from 0.11 to 0.19 g, and 0.02 to 0.08 g, respectively (Table 5-3). Similarly, under P0% a fall of 76%, and 74% in the plant biomass and ear weight was found when compared to the control (Table 5-3). Both the above ground biomass and ear

weight measured largely varied from 0.12 to 0.20 g and 0.03 to 0.12 g, respectively (Figure 5-1 E, and F).

Table 5-3: Low nutrient effect on plant height (PHt), fertile tiller number (TN), spike number (SN), spikelets on the main stem (SPM), plant weight (PWt), ear weight (EWt), flowering time (FT) of *Brachypodium distachyon* recombinant inbred line (RIL) population

Phenotype	Hoagland	Minus N	Minus P	Treatment	Genotype	G x E
PHt (cm)	25.6± 0.18	20.3± 0.2	14.0± 0.19	***	***	***
TN	4.2± 0.03	1.2± 0.03	2.1± 0.04	***	***	***
SN	5.8± 0.15	1.4± 0.04	2.6± 0.07	***	***	***
SPM	2.86± 0.03	1.07± 0.01	1.27± 0.02	***	***	***
PWt (g)	0.6± 0.00	0.1± 0.00	0.14± 0.00	***	***	***
EWt (g)	0.31± 0.00	0.05± 0.00	0.08± 0.00	***	***	***
FT (days)	83.0± 0.3	83.0± 0.23	83.0± 0.3	ns	***	ns

*,**,***Significance at P<0.05, 0.01, and 0.001, respectively, ns, not significant

However, no statistically significant difference was observed in the FT under treatment effect and treatment by genotype interaction effect (Table 5-3). Therefore, low nutrient availability did not alter the flowering time in both the accessions of *Brachypodium*.

A.

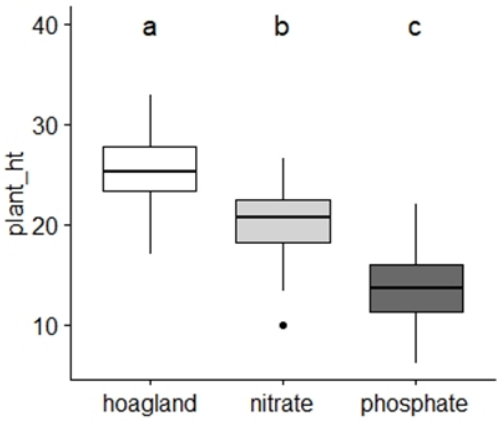
40
30
20
10
plant_ht
a
b
c
hoagland
nitrate
phosphate

B.

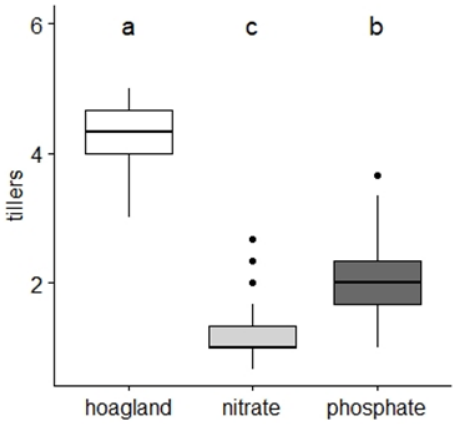
6
4
2
tillers
a
c
b
hoagland
nitrate
phosphate

C.

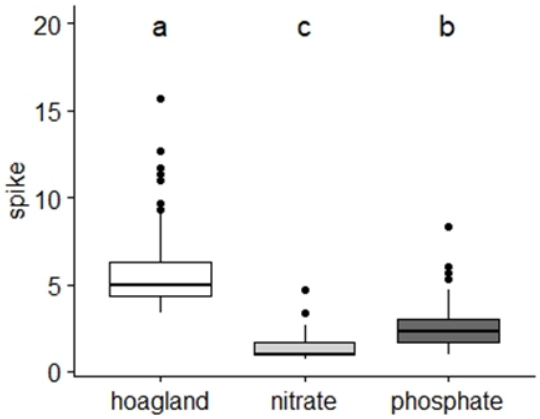
20
15
10
5
0
spike
a
c
b
hoagland
nitrate
phosphate

D.

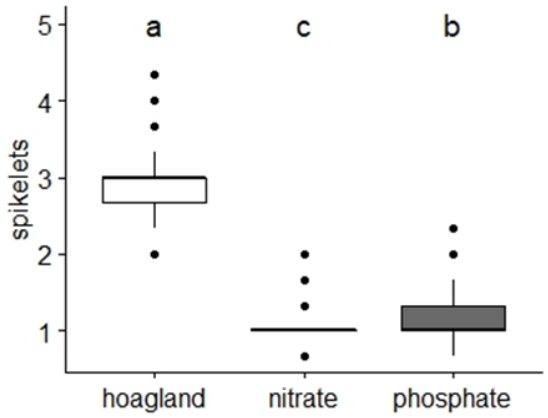
5
4
3
2
1
spikelets
a
c
b
hoagland
nitrate
phosphate

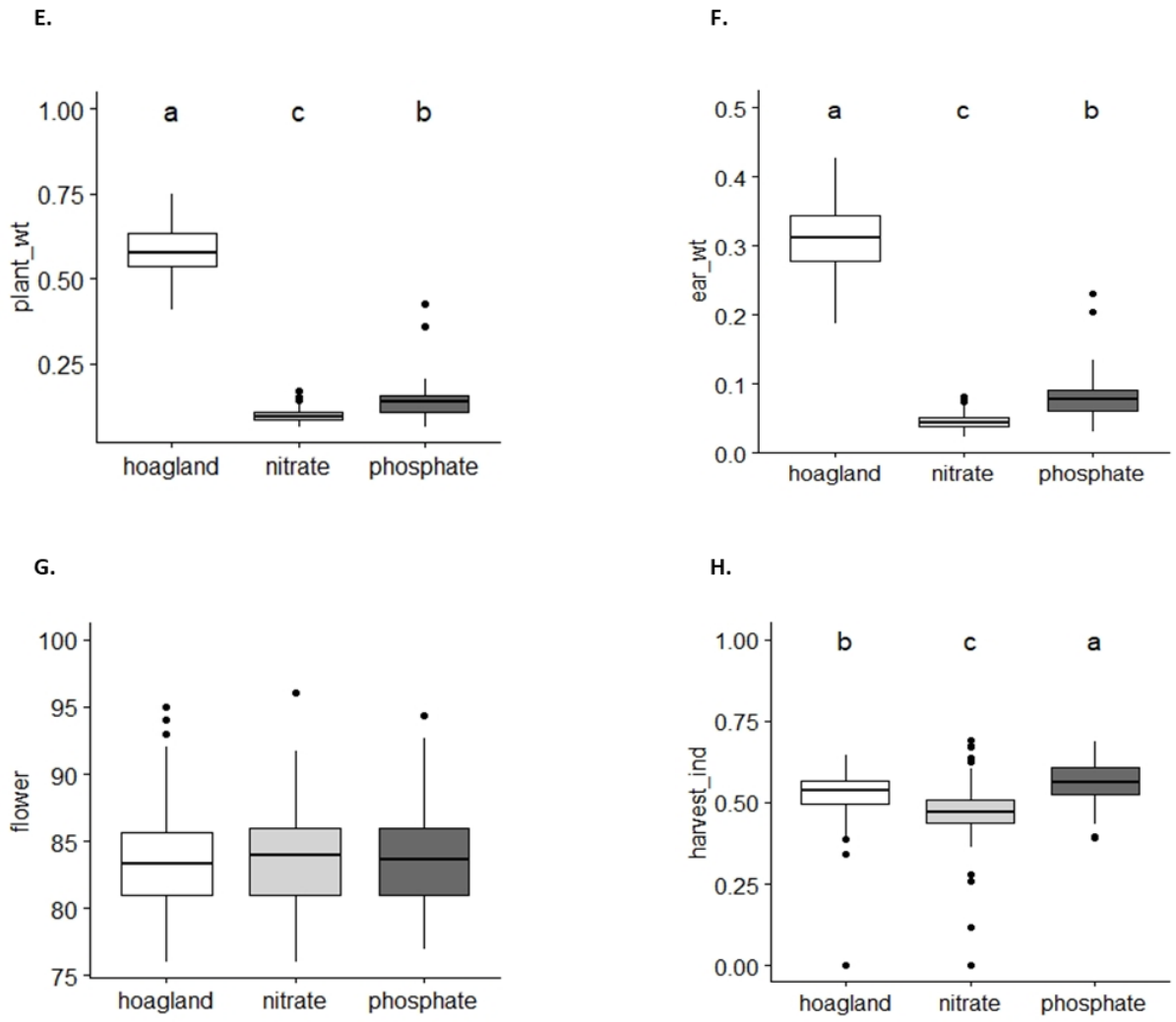

Figure 5-1: Variability of each trait per treatment of 113 RIL population with three replicates derived from ABR6 x Bd21 *Brachypodium* lines A. Plant height (cm), B. Tiller number, C. Spike number, D. Spikelet on the main stem, E. Plant weight (g), F. Ear weight (g,) G. Flowering time, H.Harvest Index (HI). Treatments are Hoagland (control), No nitrate and no phosphate. Mean ±SE (N = 113)

In summary, the mean values for all traits significantly decreased under minus N and P treatment when compared to their respective control except FT. Genotype effects were observed for all the phenotypic measured traits under all the treatments. Interestingly, significant effect was observed in treatment by genotype interactions in all the above-mentioned traits except for the FT phenotype.

5.3.3 Frequency distribution of phenotypic traits in ABR6 x Bd21 population under nutrient treatments

To establish a better understanding for the parental and RILs behaviour we evaluated the variation in phenotypic traits and focused on the transgressive segregation for the nutrient limitation treatment in *Brachypodium*.

Transgressive segregation was observed for all the phenotypic traits under control, and nutrient limited stressed conditions (Figure 5-2). All the phenotypic measurements were normally distributed as shown in figure 5-2 in response to minus N, and P treatments. A polygenic distribution was observed under control conditions suggesting many genes controlling for growth and physiological traits.

The shape of distribution changed dramatically, skewing towards lower values (left) in all the phenotypic traits compared to the Hoagland treatment (Figure 5-2). However, no change in the distribution of FT was found in both the parental accessions under Hoagland treatment. The parent ABR6 exhibited delayed flowering under both N and P limited treatments. Meanwhile, lower values for PHt were found ABR6 than Bd21 under Hoagland and nutrient limitation. Minus P treatment skewed the distribution of PHt even further towards lower values (Figure 5-2).

The RIL population showed a transgressive segregation for all measured traits suggesting significant genetic variability to cope with the effect of low nutrient treatment. Upon treatment with a Hoagland solution, the distribution of most traits like PHt, SN, PWt, EWt, FT within the RIL population followed a normal distribution with a wide transgressive segregation in both the directions.

In summary, normal distribution for most traits was involved and nutrient tolerance between the two parental lines further provided a foundation for a range of nutrient tolerant traits in segregating population to be identified for QTL analysis.

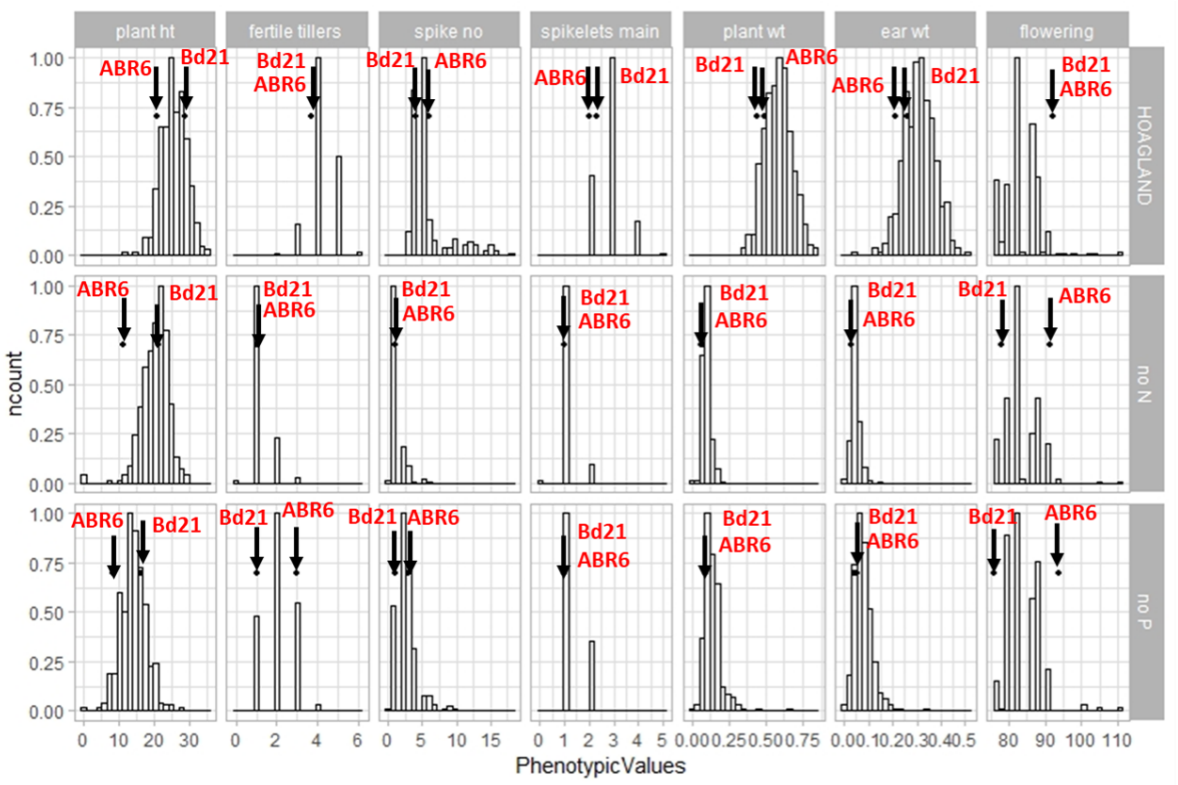

Figure 5-2: Frequency distribution of phenotypic traits measured in the RIL population derived from ABR6 X Bd21 under Hoagland (control), minus N and minus P treatments. Arrows suggesting the parents ABR6 and Bd21

5.3.4 Correlation analyses in the mapping population under all the treatments

Pearson's correlation analysis for all the three different treatments was performed to obtain pairwise correlation coefficients between the phenotypic traits using the corr command in R (Teams 2021). The data was used to establish if there is a significant correlation among the phenotypic traits under three different treatment conditions.

Based on the effects seen at the vegetative stage under low nutrient treatments, the total above ground biomass (PWt) and EWt was measured in g for each RILs with three technical replicates. Interestingly, the shoot growth and grain weight were found correlated. Results showed a significant strong positive correlation between plant weight and ear weight in segregating population of *Brachypodium distachyon* under all the treatments (r= 0.79, P<0.01 (Hoagland); r= 0.93, P<0.001 (minus N); r= 0.97, P<0.001 (minus P) as shown in table 4, 5, and 6, respectively.

Tiller number and spike number correlation

Both the traits were positively correlated to each other under the low nutrient treatment conditions. A positive correlation was found in Hoagland treatment (Table 5-4). Interestingly, a strong significant positive correlation was observed in minus N (r= 0.03; P<0.001), and minus P (r= 0.74; p<0.01), respectively (Table 5-5; 5-6).

Previous studies have suggested that flowering time can be modulated and is important for yield and quality while delayed flowering may be useful for leaf and forage crops (Distelfeld *et al.*, 2009; Jung and Muller 2009). The FT phenotype in ABR6 x Bd21 derived population were slightly skewed under minus N and P treatments and showed a negative correlation with the plant height. There were negative but not significant correlations (r= -0.25) between FT and PHt, FT and SN, FT and HI under Hoagland treatment. Positive but not significant correlations were found between FT and SPM, FT and PWt, FT and EWt under Hoagland treatment (Table 5-4).

A negative correlation was observed between flowering time and other phenotypic traits like tiller number, spike number, plant weight, ear weight under N0% (Table 5-5). Moreover, a significantly weak correlation (r= -0.48, P<0.01(minus N) was found between flowering

time and plant height in minus N as shown in table 5-5. However, a positive but not significant correlation was estimated between flowering time and spikelet on the main stem under low N stress (r= 0.04, P= 0.06).

Interestingly, a positive but not significant correlation was found between flowering time and measured phenotypes like tiller number, spike number, spikelet on the main stem, plant weight, ear weight, harvest index except plant height under P0% (Table 5-6). A significant negative correlation was obtained between flowering time and plant height (r= -0.30, P<0.05) under minus P treatment.

Table 5-4: Pearson correlation coefficients among 8 traits measured under Hoagland treatment (n= 113), PHt= Plant height, TN= fertile tillers, SN= Spikelet number, SPM= Spikelet on the main stem, PWt= Plant weight, EWt= Ear weight, HI= Harvest Index, FT= Flowering time

	PHt	TN	SN	SPM	PWt	EWt	H I	FT
PHt	1							
TN	-0.18	1						
SN	-0.24	0.20	1					
SPM	0.29	-0.04	-0.18	1				
PWt	0.33	0.37	-0.05	0.41	1			
EWt	0.16	0.24	-0.34	0.28	0.79 **	1		
H I	-0.05	-0.02	-0.37	0.03	0.04	0.36	1	
FT	-0.25	-0.01	-0.16	0.06	0.16	0.04	-0.15	1

** Significant at P<0.01

Table 5-5: Pearson correlation coefficients among 8 traits measured under minus nitrate treatment (n= 113). PHt= Plant height, TN= fertile tillers, SN= Spikelet number, SPM= Spikelet on the main stem, PWt= Plant weight, EWt= Ear weight, HI= Harvest Index, FT= Flowering time

	PHt	**TN**	**SN**	**SPM**	**PWt**	**EWt**	**H I**	**FT**
PHt	1							
TN	0.14	1						
SN	0.03	0.82 ***	1					
SPM	0.28	-0.06	-0.10	1				
PWt	0.54	0.48	0.33	0.46	1			
EWt	0.47	0.32	-0.15	0.51	0.93 ***	1		
H I	-0.26	-0.05	-0.07	0.29	0.28	0.48	1	
FT	-0.48 **	-0.13	-0.09	0.04	-0.11	-0.11	-0.03	1

*, **, *** Significant at P<0.05, P<0.01, and P<0.001, respectively

Table 5-6: Pearson correlation coefficients among 8 traits measured under minus phosphate treatment (N= 113). PHt= Plant height, TN= fertile tillers, SN= Spikelet number, SPM= Spikelet on the main stem, PWt= Plant weight, EWt= Ear weight, HI= Harvest Index, FT= Flowering time

	PHt	TN	SN	SPM	PWt	EWt	H I	FT
PHt	1							
TN	-0.06	1						
SN	-0.08	0.74 **	1					
SPM	0.27	0.01	-0.04	1				
PWt	0.28	0.59	0.49	0.34	1			
EWt	0.17	0.57	0.44	0.34	0.97 ***	1		
H I	-0.28	0.21	0.05	0.11	0.30	0.52	1	
FT	-0.30 *	0.17	0.26	0.05	0.14	0.16	0.16	1

*, **, *** Significant at P<0.05, P<0.01, and P<0.001, respectively

5.3.5 Genotypic analysis

Having established that the most traits display variation in the F8 RIL population including transgressive segregation, that there is significant genotype-treatment effect for all except FT, and that the correlations between most traits are relatively weak, I next explored the genetic architecture underlying this variation. The diagrammatic scheme for genetic map along with summary, and histograms with the measured phenotypes for this data are presented in Appendix Figure A5.1.

5.3.5.1 QTL identification

This section explores QTL analysis to identify regions of the *Brachypodium* genome to the observed phenotypic variation in the RIL population derived from ABR6 and Bd21 for nutrient treatments. R/qtl package using CIM analysis was used in detecting QTL region

controlling the phenotypic traits under nutrient limitation. Seven significant QTLs were detected under these treatment conditions (Figure 5-3). Genes close to the most significantly associated SNP from each QTL region were identified, and gene annotations were retrieved using Phytozome tool.

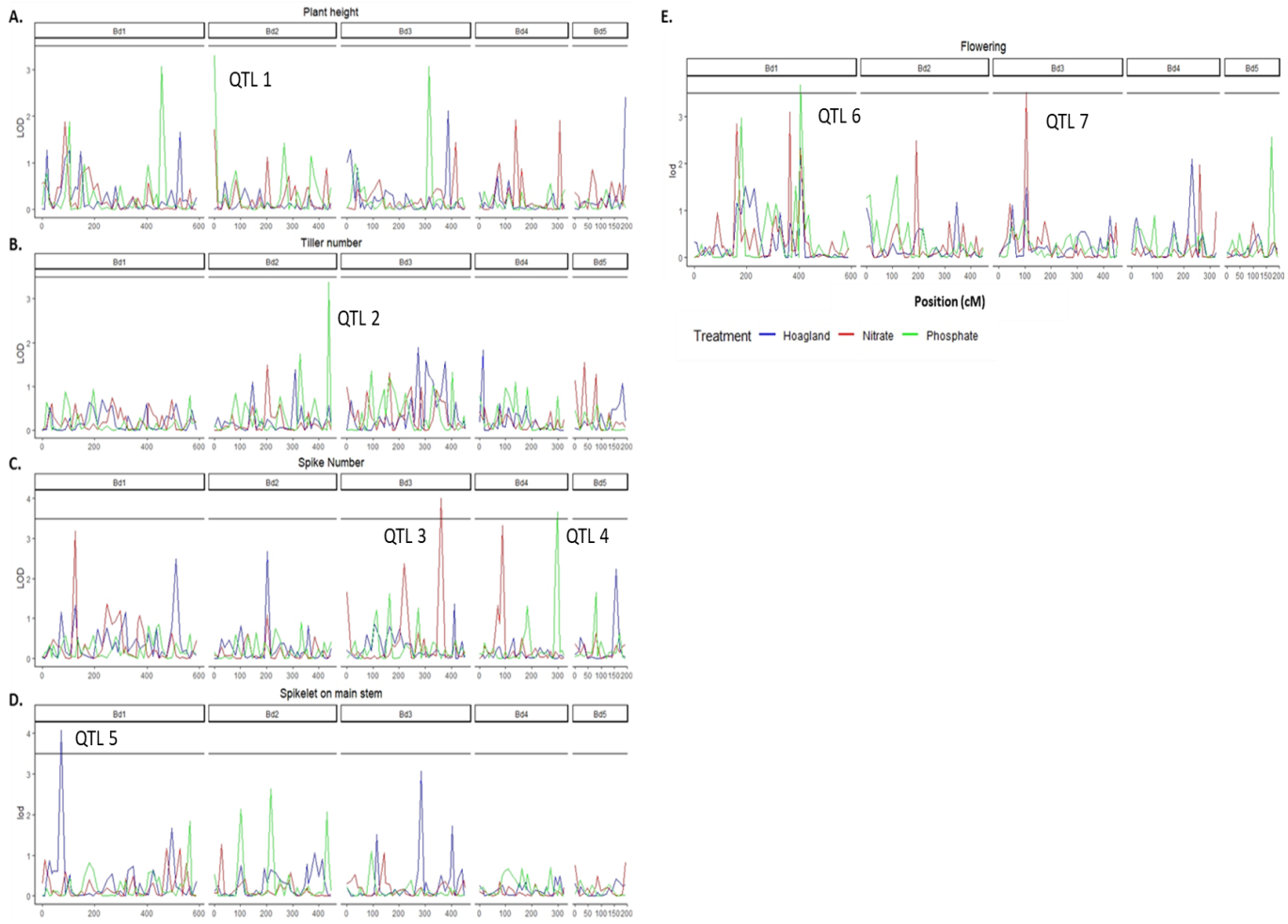

Figure 5-3: Location of QTLs under three different treatment conditions A. Plant height, B. Tiller number, C. Spike number, D. Spikelet on the main stem, E. Flowering time in the ABR6 x Bd21 F8 populations. QTL analysis was performed using composite interval mapping under an additive model hypothesis test (H_0:H_1) and plotted based on permutation thresholds. The black horizontal line represents the threshold p=0.1, based on 1,000 permutations. Blue= Hoagland (control), red= minus nitrate, and green= minus phosphate. See table 7 for full QTL details under different conditions.

3 QTL peaks under P0% condition was identified for plant height where all of them did not have a significant contribution where it correlates with flowering time. The highest peak for plant height in ABR6 x Bd21 population was found on chromosome 2 (QTL 1) with the LOD value 3.3. Peak marker Bd2_6789_60_F explains 13% phenotypic variance in this RIL population (Figure 5-3. A).

Tiller number was scored under all the three above mentioned conditions and interestingly a QTL peak under P0% was observed on chromosome Bd2 (QTL 2) (Figure 5-3. B). The observed peak for tiller number was not significant in minus P treatment (Table 5.7). No QTLs were found under control, and minus N conditions.

Additionally, spike number showed two major significant QTL, identified under minus N and P treatments, whereas no other QTL were identified under control conditions (Figure 5-3. C). A QTL on Bd3 (QTL 4, marker Bd3_52074165_60_R) explained 15% variation under N0% and Bd4 (QTL 5, marker Bd4_46441435_60_F) accounting 13% PVE in P0%. Additionally, QTL on Bd4 did not have a significant contribution identified and explained 13.7% variance under minus N (p= 0.1) (Table 5-7).

A significant QTL on chromosome 1 (QTL5, peak marker Bd1_5510069_60_F, 71.6) appeared to be the major locus governing the spikelet on the main stem in control environments, explaining the most phenotypic variation (phenotypic variance explained; PVE) 15 % compared to any other QTL (Table 5-7). Whereas, no significant QTL peaks were observed under minus N, and P treatments (Figure 5-3 D).

Flowering time: two major flowering time QTLs were found on chromosome 3 (QTL 6) under N starvation environment and chromosome 1 (QTL7) under P starvation environmental

conditions (Figure 5-3. E). Depending on the treatment QTL 6 (marker Bd3_11328451_60_R) explains 14% and QTL7 (marker Bd1_ Bd1_52521087_60_F) 13.9% of the phenotypic variance observed in this mapping population, respectively (Table 5-7).

In addition, most significant QTLs with highest LOD were identified for SPM, SN and FT under different treatment conditions in the RIL population. The QTLs specific to minus N, and P treatments are particularly interesting and may provide a route by which to further dissect nutrient responses. The QTL peaks and markers associated for that region under both the treatments are depicted in Appendix A5.2.

Table 5-7: Significant QTLs in three different conditions were identified using R/qtl package. Each QTL includes the interval region of the QTL, SNP position, and amount of variation explained by each QTL. Plant height (PHt), tiller number (TN), spikelet number (SN), spikelet on the main stem (SPM), flowering time (FT)

Treatment	Phenotypic trait	Chromosome/ cM	LOD	Marker	Lowest cM value	Highest cM value	PVE %
Hoagland	SPM	Bd1/ 71.6	4.1	Bd1_5510069_60_F	57.8	86.2	15.3
Minus N	SN	Bd3/361.5	4.1	Bd3_52074165_60_R	220	376	14
	FT	Bd3/105.5	3.5	Bd3_11328451_60_R	92.9	113	14
Minus P	PHt	Bd2/0	3.3	Bd2_6789_60_F	0	0	13
	TN	Bd2/436.9	3.0	Bd2_58536533_60_F	430	446.2	10
	SN	Bd4/299.2	3.68	Bd4_46441435_60_F	289.7	308	14
	FT	Bd1/405	3.7	Bd1_52521087_60_F	160	423	13.9

5.3.5.2 Candidate genes analysis

In this section, an overview is given for candidate gene identification that was carried out for the region closest to the QTL peak associated with the flowering time (FT) phenotypic

trait only. Candidate genes were within 0.3 to 0.5 Mb interval around the SNP peak for FT phenotypic trait and were identified using adjacent markers on the genetic maps and searched against the *Brachypodium distachyon* (v3.1) genome. The list of remaining genes close to the SNP peak are shown in Table A5-1. Therefore, searching for candidate genes for nutrient tolerance on chromosome 3 and 1 was conducted in the region spanning up to 1 Mb. In previous studies homologs for flowering time regulating FT in Arabidopsis, wheat, barley and rice in *B*. *distachyon* (Higgins *et al*., 2010; Ream *et al*., 2012; Bettgenhaeuser J. *et al*., 2017). The annotated genes found under N and P limitation for the flowering trait are reported and discussed below:

N stress environment: Four candidate genes related to FT and corresponding to N limitation on chromosome 3 could be identified. All the important candidate genes identified in the QTL region, including the genes involved in flowering time regulation are shown in Appendix Table A5-1. The selected SNPs present on chromosome 3 closest to the peak is shown in Appendix Figure 5.2A. The candidate gene *VRN2* (Bradi3g10010) encoding for CCT domain protein was found closest to the SNP peak marker (Location: Bd3_8185831_R) as shown in Table 5.8. *VRN2* gene a floral repressor and is responsible for eliminating vernalization requirement have also been previously studied as a homolog in cereals like barley, wheat. CCT domain protein containing CCT genes play a vital role in regulating FT in cereal crops. In addition, some CCT gene demonstrates pleiotropic effect by controlling plant height, grain number in response to environmental stresses (Li and Xu, 2017). Furthermore, *VRN2* (Bradi3g10010) allows us to understand the genetic variation between the ABR6 and Bd21 accessions and is coexpressed with genes in cold stress specific coexpression subnetwork (Bettgenhaeuser J. *et al*., 2017).

The gene closest to the SNP peak in chromosome 3 corresponds to Bradi3g09750 which encodes a F-box protein and has been reported to influence flowering time as it is known to be expressed in the vegetative or seed developmental stages (Jeong Hong M. *et al*., 2020). Bradi3g09510 represents another candidate gene on chromosome 3 in the FT QTL region close to the peak marker (Bd3_7843999_R; Table 5-8). This gene is encoding VQ Motif-Containing Protein Family is involved in plant growth and development like seed development in response to salinity in maize (Song W. *et al*., 2016). Another candidate gene Bradi3g10820, encodes for a protein with a TIFY domain Divergent CCT motif (CCT_2). CCT_2 proteins modulate flowering time along with playing an important role in plant development in response to abiotic stress (Li and Xu, 2017).

P stress environment: Two candidate genes Bradi1g55041 and Bradi1g55051 encoding MADs-box family proteins which corresponds to *VRN1* were found on chromosome 1. The selected SNPs present on chromosome 1 closest to the peak is shown in Appendix Figure 5-2 B. These genes are reported in promoting inflorescence development during vernalization by repressing the transcription of *VRN2* (Lv Bo *et al*., 2014; Li and Xu, 2017). Both the genes were found spanned within 0.1 Mb close to the SNP peak marker (Table 5-8). Bradi1g52330 encodes for a Glycyl-tRNA synthetase and has found to be coexpressed with the genes involved functions in flower specific coexpression (Bd1_50813465_F). Another gene found in chromosome 1 close to SNP peak was Bradi1g52390 encoding for U-Box protein which functions in response to environmental stress (Young Ryu M. *et al*., 2019) (Table 5-8). Bradi1g54139 encoding zinc finger FYVE domain containing protein was found involved to be involved in abiotic stress tolerance in Arabidopsis and wheat (Zang *et al*., 2016).

Table 5-8: SNP peak and closest gene from each QTL identified for FT under nutrient limitation condition where Chr: chromosome, gene identified on the chromosome, location of the SNP, function of the gene, orthologous species, gene & function

Treatment	Chr	Gene identified	Location	Function	Orthologue gene & function	Orthologous species
N treatment	Bd3	Bradi3g09750	Bd3_7950638_F	F-box protein	At3g61590 (Kelch-repeat protein)	*Oryza sativa* J.
		Bradi3g10010	Bd3_8184940_R	CCT motif domain		
		Bradi3g10820	Bd3_9075866_R	TIFY domain/Divergent CCT motif	LOC123425321 (TIFY 10b)	*Hordeum vulgare*
		Bradi3g09510	Bd3_7635705_R	VQ motif	LOC123447105 (uncharacterised)	*Hordeum vulgare*
P treatment	Bd1	Bradi1g55041	Bd1_53602248_R	MADs Box protein	Traes_3B_FEE0CF773	*Triticum aestivum*
		Bradi1g55051	Bd1_53607712_R	MADs Box protein		
		Bradi1g52390	Bd1_50836678_R	U-Box domain containing protein	ZmB84.09G064400	*Zea mays*
		Bradi1g52330	Bd1_50813465_F	Glycyl- tRNA synthetase	Traes_7AS_23D2CB8A0	*Triticum aestivum*
		Bradi1g54139	Bd1_52724577_F	Zinc Finger FYVE domain containing protein		

5.4 Discussion

Distinct genotypes from different geographic origins can be exploited to explore grass's natural variation. Previous studies have explained the molecular basis of vernalisation and

the range of flowering behaviour in *Brachypodium distachyon* (Schwartz *et al*., 2010; Ream *et al*., 2014; Tyler *et al*., 2014). Several homologs' genes for the flowering pathway have been labelled in *B*. *distachyon,* which has the highest rate of recombination known in plants (Higgins et al., 2010; Brkljacic *et al*., 2011; Woods *et al*., 2017). N limiting nutrient is selected in the present study due to its response, independent of vernalization pathways and functions in controlling various biological processes (Liu *et al*., 2013; Vidal *et al*., 2014). On the other hand, few studies have shown that P deficiency delays the flowering time in plants (Cho *et al*., 2017). Interestingly most of the genes mapped for a novel flowering time under vernalisation, but little is known about low N and P availability in cereal crops.

Flowering time involves five genetically identified pathways: vernalization, photoperiod, gibberellin, autonomous, and endogenous/ageing pathways (Lin & Tsay, 2017). Previous studies have focused on how nutrient availability alters the flowering time (Wada & Takeno, 2010). Meanwhile, the regulation of flowering time has already been studied extensively in *Brachypodium*, and the exact location of chromosome position range of marker was observed, which could let us have an idea to locate orthologous genes in the present study (Bettgenhaeuser *et al*., 2017). In cereal crops like wheat, barley it has been suggested that majorly epistatic interactions are present where the VRN1 promoter likely turns off VRN2 promoter directly or indirectly by activating flowering in the leaves under cold treatment or vernalisation (L Yan *et al*., 2003; Shimada *et al*., 2009; Chen & Dubcovsky, 2012). However, some genotypes flower quickly without vernalisation, like Bd21 suggesting the deletions or point mutations of the VRN2 locus. This further indicates that it acts as a flowering repressor and VRN2 presence usually requires vernalisation, which was found in the present study.

Phenotypic measurements

Morphological traits are significantly affected by nutrient limitations in crops. The present study helps us to understand the morphological behaviour in geographic diverse parental accessions and segregating populations to the low nutrient response. In this research plant, phenotypic measurements for parental genotypes and RIL population of *Brachypodium* under nutrient limitation were evaluated. Overall, a significant reduction in both accessions was observed under low nutrient availability. ABR6 ecotypes showed a considerable decrease in PHt, SPM, PWt, and EWt under nitrate and phosphate limitations compared to the control conditions. SN and TN showed no significant effect under minus phosphate; however, low nitrate treatment showed a significant reduction compared to the control. Bd21, on the other hand, showed a substantial reduction in all the measured phenotypic traits under nutrient limitation compared to the control.

Interestingly, no significant effect in flowering time was observed under nitrate and phosphate limitation compared to the control in both the genotypes (Table 5-2). Flowering time (FT) is a relatively stable trait and therefore, it did not alter across the treatments. Nutrient deficiency and poor nutrient availability in the soil can promote or delay FT (Hyeon Cho *et al*., 2016). However, it was found that RILs variously respond to N availability by promoting flowering time (not significant) or not changing flowering time, which agrees with the previous findings (Kolář & Seňková, 2008; Vidal *et al*., 2014). The other possible reason for no significant differences in FT under nutrient starvation could be due to the plant's adaptive or coping mechanism. The plants start to remobilise the nutrients from the phloem mobile nutrients and leaves to developing tissues and storage organs like spikelet formation or grain development in response to stress thus leading to early senescence.

Here in the study, reduction in all measured phenotypic traits in the parental accessions was much more pertinent in Bd21 than ABR6 under the low nutrient treatment. A similar effect on RILs was found under nutrient limitation, while no significant impact was noted for flowering time compared to the control.

Segregation distortion in the ABR6 x Bd21 population and Correlation under nutrient limitation

Segregation distortion is one of the common observations studied previously in the development of mapping populations in rice, maize, and barley (Xu *et al*., 1997; Li *et al*., 2010). Transgressive segregation is a classic phenomenon in plant breeding in which specific phenotypes of recombinant offspring are outside the parental range. This phenomenon is distinct from heterosis in that the novel phenotypes in transgressive segregants are transmitted stably through generations (true-breeding), whereas the hybrid vigour observed in heterotic F1 hybrids is due to heterozygosity at multiple loci, thus the vigour properties segregate through generations. In the present study, the ABR6 x Bd21 population showed a significant deviation and did not lie at the extremes of the population distribution under nutrient limitations. Therefore, it is likely to deduce that these loci are linked to the phenotypic trait during population development based on genetic or environmental conditions (Bettgenhaeuser *et al*., 2017). Furthermore, the distribution of susceptibility and resistance of only a few RILs more than ABR6 and Bd21 demonstrate transgressive segregation for the measured phenotypic traits (Figure 5-2).

The results show an expected positive phenotypic correlation with yield component traits and biomass traits under control and low P treatment with previous studies. HI is the best strategy for improving crop yield under abiotic stress, which can be determined by

measuring the total above-ground biomass allocated to the grain. In the present study positive correlation was found between HI and EWt under nutrient limitations. The results were confirming previous reports where HI and grain yield showed a positive correlation under drought in bean plants (Beebe *et al*., 2008; Assefa *et al*., 2015).

FT showed a positive correlation with SN, SPM, PWt, EWt, and HI under low P, however, under low N a positive correlation was only found between FT and SPM. Therefore, the present study showed a harvest time indicator that is also studied in the alfalfa RIL population (Adhikari *et al*., 2019). A significant negative correlation between days to flowering and plant height was detected under minus N, and P treatments, while a non-significant correlation between FT and PHt was observed under control conditions. Falconer and Mackay (1996) revealed that the genetic correlations among traits may not be fully understood using only phenotypic correlations and therefore it will be important to evaluate genetic correlations in future.

QTL analysis and candidate genes

Many studies have focused on nutrient uptake in cereals like rice where QTL identification was studied using different mapping populations for growth and yield traits under nutrient deficiency (Su *et al*., 2006; Feng *et al*., 2010). Available RIL population derived from ABR6 x Bd21 *Brachypodium* accessions were evaluated under a low nutrient stress environment to determine the effect of these environments on classical quantitative genetic parameters and QTL identification for plant morphology. Significant QTL for SPM was characteristic on chromosome 1 under control conditions. SN and FT detected QTLs under low nitrate treatment during the analysis on the same chromosome 3. Consequently, PHt, TN, SN, and FT showed significant QTLs on chromosomes 1, 2, and 4 under reduced phosphate

treatment (Figure 4). The marker associated with PHt was Bd2_6789_60_F, and the QTL analysis of plant height has often been studied in important agricultural crops such as maize (Zhang *et al*., 2006) and prominent research has been performed in biomass crops like switchgrass (Serba *et al*., 2015). A QTL linked to the same chromosome 2 under reduced phosphate treatment was found in TN and is related to the marker Bd2_58536533_60_F. The most robust QTL on chromosomes 1 and 4 for FT and SN, with 13.8% and 14% of the total variance, is explained by genetic factors.

The genetic and genomic source of flowering time has been investigated extensively in cereal crops (Adhikari *et al*., 2019); however, the flowering time under nutrient starvation is poorly understood. Previous studies have suggested that ABR6 is more tolerant accession and require 6-week vernalisation to flower than Bd21. Thus, the results from the study support earlier investigations of the *Brachypodium* population (Ream *et al*., 2014; Bettgenhaeuser *et al*., 2017; Woods *et al*., 2017). Previous studies have identified QTL and focused on flowering-time in ABR6, and Bd21 derived mapping RIL population of *B. distachyon* (Ream *et al*., 2014; Bettgenhaeuser *et al*., 2016; Woods *et al*., 2017), and this lends support to the two QTLs (QTL6 and QTL7) identified for flowering time. However, in this study, the amount of variation explained by the QTL was low compared with the QTLs found in the previous studies. This may be due to various reasons like a lower number of markers, different mapping populations and treatment used, which can have implications in the QTL analysis. M. Gomez *et al*. (2006) suggested that the few identified QTLs in the stressful environment might correlate to lower heritability or a broader signal spread across more loci, leading to less significant peaks.

The two flowering time QTLs were detected under nutrient limitation, suggesting that the genetic control of flowering within this F8 population is robust. Interestingly, VRN1 and VRN2 loci were found in the two significant QTLs identified (Table 5-8). These candidate genes identified in undomesticated *B*. *distachyon* colocalize with loci identified as flowering regulators in the domesticated crops wheat and barley (Woods D. *et al*., 2016; Woods and Amasino, 2015). Thus, this study suggested that another set of candidate genes identified broadly found within the Poaceae also controlled the variation in flowering time. Kant *et al*. (2011) suggested that nitrate and phosphate show opposite effects on flowering, whereas lower N and P concentrations in Arabidopsis promote early or delayed flowering. However, some studies have suggested that severe N deficiency leads to a negative effect on flowering than those grown under higher N conditions which resemble the present study (Yuan *et al*., 2016).

Flowering time is a crucial trait to study in cereal and bioenergy crops. *Brachypodium*, a non-domesticated model specie, contains orthologs of all the vital flowering time pathways already defined in grasses like rice (Table 5-8). Due to the small size and easy growth conditions, *Brachypodium* was used to understand flowering time variation under nutrient limitations. As described above, the previously identified vernalization gene, Bradi3g10010 (VRN2), colocalised to QTL7 (Bettgenhaeuser *et al*., 2017) and significant QTLs from composite interval mapping of transformed flowering time phenotypes (T3) in the ABR6 x Bd21 F4:5 families (Appendix Table A5.2). In the present investigation, VRN1 previously identified flowering time-loci was found in QTL6 intervals under P limitation (Table 5-8). It has been suggested that vernalisation pathways differ between Arabidopsis (FLC) and grasses (VRN2) due to the critical flowering repressors (Higgins *et al*., 2010). Therefore, flowering time-related genes identified in the present study provided an excellent system to

test if flowering time variation between wild ecotypes of *Brachypodium* involves the same genes that have been selected in domesticated cereal crops. The work presented here clearly demonstrates a significant degree of variation in flowering time among natural accessions of *Brachypodium*. Moreover, flowering time regulation involves a complex multigenic trait in *Brachypodium*, and it can be concluded that it is also relevant to crop plants.

QTLs were missed in the significant gaps between the markers, and therefore, no marker was further linked with the respective gene, which did not give us a considerable peak (M. Lynch & Walsh, 1998; Hackett, 2002). Therefore, composite interval mapping was performed over standard interval mapping to combine interval mapping with regression analyses on several background markers, which act as alternatives for other QTLs influencing the measured phenotypic traits under nutrient stress (Jansen *et al*., 1994; Zeng, 1994). The size of the population also has an effect, as it has been studied previously that screening larger populations is more successful at detecting phenotypes with more negligible effects (Collard *et al*., 2005; Doerge, 2002).

Notably, seven novel QTLs were identified on chromosomes Bd1, Bd2, Bd3, and Bd4, with four QTLs found under minus P and two under minus N treatment. Two QTLs for spike number and flowering time were reported on the same chromosome under the minus N treatment. QTLs for spikelet on the main stem were associated with Hoagland (control) treatment.

5.5 Conclusion

In summary, N and P limitations are among the significant constraints affecting the production of cereal crops. Understanding which traits are associated with productivity

under nutrient limitations could guide research for selecting desirable traits in cereal crops. The QTLs detected in the present study will provide the bases for candidate gene identification for other measured traits like plant height, spikelet number, and ear weight in response to nutrient limitation. The data will also provide natural variability to identify molecular analysis affecting N and P availability in *Brachypodium*. Therefore, the data provided in this chapter will allow plant breeders to develop new strategies in temperate C3 cereals to improve yield and productivity under nutrient limitations.

Chapter 6 : Overexpression of a pectin methyl-esterase inhibitor (PMEI) in *Brachypodium distachyon* and its response to abiotic stress

6.1 Introduction

Cereal crops are majorly affected by abiotic stresses resulting in global agricultural losses. Previous chapters of my thesis focused on nutrient limitation, one of the significant abiotic interactors that can limit plant growth and productivity. In addition to nutrient stress, this chapter will also focus on water deficit stress caused by drought due to erratic monsoon and rainfall distribution witnessed every year, thus, leading to fluctuations in crop yields and productivity. Drought stress is expected to increase in frequency in future as a result of decreased precipitation and increased evaporation which can further lead to the reduction in plant biomass and seed production, ultimately leading to 90% water loss via stomatal pores during the transpiration process (Bartels & Sunkar, 2005, 2005; Schroeder *et al*., 2013; Marchin *et al*., 2020).

Water is one of the elements with a significant influence on the life of plants; even the slightest deficiency can cause severe damage to many cellular processes. Water potential in the plant (Ψw) strongly influences cell growth, photosynthesis, and crop productivity. Ψw is controlling the concentration, pressure, and gravity.

$$\Psi w = \Psi s + \Psi s + \Psi g$$

Where Ψs is the osmotic potential and represents the effect that dissolved solutes (independent of the specific nature of the solute) have on water potential. Dissolved solutes reduce the water potential of a solution relative to the reference state of pure water. Ψp refers to the hydrostatic pressure. The hydrostatic pressure can be positive such as the

pressure within the cells, also called turgor pressure, or damaging as in the xylem and the space between cells; this is termed tension. Turgor pressure is essential for many physiological processes such as cell enlargement, gas exchange in leaves, phloem transport, and membrane transport processes. It contributes to the rigidity and mechanical stability of non-lignified plant tissues. Ψg is the gravitational component, which affects the cell level and is negligible.

Previous studies have reported that plants evolved many mechanisms to cope with environmental stresses, including drought and nutrient stress, via physiological, morphological, and molecular alterations (Todaka *et al*., 2012; Verelst *et al*., 2013). Plants usually maximise the water and nutrient uptake while minimising water loss by stomatal closure and reducing stomatal density under dehydration stress conditions (Yu *et al*., 2017). Plants experiencing water deficit show stunted shoot growth, decreased transpiration, and foliar senescence (Buchanan-Wollaston *et al*., 2002; Scarpeci *et al*., 2017). Drought has a similar limitation to cereal crop production as nutrient stress, with an estimated yearly depreciation of up to 70% compared to the yield from favourable conditions (Burke *et al*., 2009; Tollenaar & Lee, 2002. Because of poorly irrigated or rainfed lands, genetic improvement of crops for increased adaptations to water deficit stress has become vital in agricultural research. Therefore, it has become a global challenge for plant breeders to develop drought-resilient crops that can retain water by reducing transpiration and enhancing yield and biomass quality.

It is generally the outer layer or plant cell wall of plants that determines the shape and size of the cell. The plant cell wall enacts as a primary protective barrier, is involved in growth and development processes, and is closely interlinked with responding to environmental

stresses (Wormit & Usadel, 2018; Marchin *et al*., 2020). Cell wall architecture is believed to reinforce rigidity and strength, which plays a pivotal role in resisting internal turgor pressure and protecting against abiotic stresses (Le Gall *et al*., 2015). The cell wall is a complex dynamic structure composed of high molecular weight polysaccharides, including cellulose, hemicellulose, pectin, and several structural proteins, phenolic and aliphatic polymers, as discussed in Chapter 1 (Ivakov & Persson, 2012). Pectins are the primary and most complicated polysaccharide that helps control cell wall porosity, elongation, adhesion, and plant development in response to environmental stresses. Previous studies have reported that grass's primary wall is composed of cellulose and hemicellulose with minimal amounts of pectin (Biswal *et al*., 2018). It is rich in galacturonic acid polysaccharides in the cell wall, and the main domains include non-branched and most abundant- homogalacturonan (HG), rhamnogalacturonan-I, and rhamnogalacturonan-II, which are covalently attached (Bosch & Hepler, 2005; Pelloux *et al*., 2007) (Figure 6-1). It has been concluded that grasses reflect a lower number of HG in grasses (2-10%) than dicots (Wormit & Usadel, 2018).

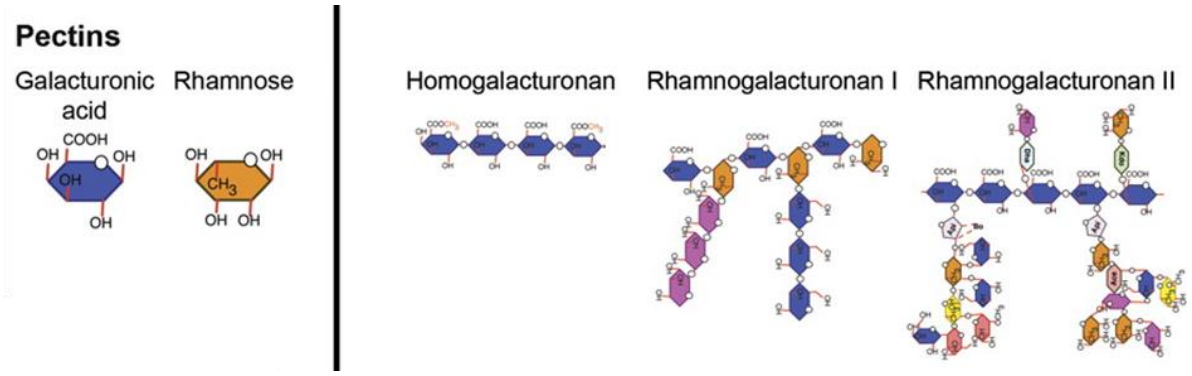

Figure 6-1: Pectin structure and its components (Sarkar P. *et al*.,2009)

They are majorly synthesised in the Golgi apparatus and transported to the cell wall in a highly methylesterified state. Additionally, the methylesterification of HG is regulated by pectin methylesterases (PME) which alter the methylesterification status by removing

methyl groups from HG, consequently affecting the properties of the cell wall, as shown in Figure 6-2

HG secreted into the cell wall is highly methylesterified at the C6 atom of the galacturonic acid (GalA) residue. It is acknowledged that pectin methyltransferase alters the methyl-esterification localized in the Golgi apparatus (Mouille *et al*., 2007). This degree of modification is further selectively modified by pH, charge, and crosslinking factors. Pectin methylesterase (PME) enzyme belongs to Carbohydrate Esterase Family 8 (PMEs; E.C. 3.1.11; Cazy group CE8) and is classified based on their primary structure (Pelloux *et al*., 2007; Wolf *et al*., 2009). It catalyzes de-methylesterification of HG, releasing protons and methanol as shown in Figure 6-2 (Jolie *et al*.,2010) and releasing negatively charged carboxyl groups. Thus, PMEs play a vital role in diverse physiological processes, including vegetative and reproductive plant development, and control the degree of HG's methylesterification. Two alternative pectin modification processes can achieve de-methylesterification. It can be either followed by stiffening of the cell wall by releasing blocks of unesterified carboxyl groups that form a bond with calcium ions, thus creating a Ca^{2+} pectate gel, also known as blockwise de-methylesterification. The HG-Ca^{2+} complex acts as a hydrophilic filter, thus preventing the collapse of the cellulose/hemicellulose network. On the other hand, it can lead to a random methylesterification pattern by de-esterifying single gala residue and thus resulting in cell wall loosening by stimulating the activity of hydrolases. These domains become more susceptible to hydrolytic degradation (Hong *et al*., 2010).

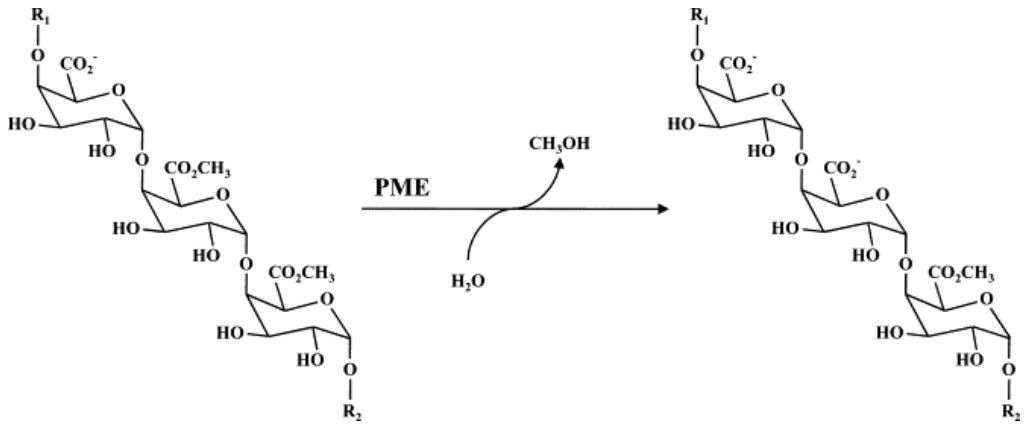

Figure 6-2: PME catalyses the hydrolysis of the methyl ester group at C-6 of pectin (HG) by demethylesterification of the methyl ester group with the production of methanol, generating free carboxyl groups and releasing protons (Jolie *et al*.,2010)

Furthermore, PME activity is regulated by specific endogenous proteinaceous PME inhibitors (PMEIs). PMEIs were first discovered and isolated from kiwi fruit (*Actinidia chinensis* Planch) which comprises a single polypeptide chain with an N-terminal Ala residue with 152 amino acids. It belongs to a multigene encoding protein family that inhibits PME activity by forming a reversible 1:1 non-covalent complex of which stability is dependent on pH (BALESTRIERI *et al*., 1990). Later studies revealed 71 PMEI members in Arabidopsis, pepper, and tomato (Raiola *et al*., 2004; An *et al*., 2008; Reca *et al*., 2012). PMEI stability dramatically depends on pH, disulphide bond, an ionic interaction. Di Matteo *et al*. (2005) studied the crystallographic analysis and suggested that the PME-PMEI complex in plants vividly varies from bacterial PMEI. Consequently, PMEIs mainly inhibit plant endogenous PMEs, unlike other inhibitor proteins. A mature, active protein at the N-terminal extension of PME is usually observed and known as PRO regions. These regions have structural similarities to PMEI and serve as molecular chaperones for PME folding or inhibitors to PME or regulators of PME, which focus on the cell wall. Thus, PRO regions end up sharing the same homology with PMEIs (Huang *et al*., 2017).

Many such genes have been reported in model plants that are involved in drought tolerance, and Bradi3g45080, encoding a PMEI, was previously shown to be upregulated by drought in the cell wall formation and expansion zone of *Brachypodium* Bd21 leaf tissue (Verelst *et al*., 2013; Lenk I *et al*., 2019). Interestingly, little is known about how changes in the extent of methyl esterification of cell wall pectin affect *Brachypodium* under typical and various environmental stress factors. Many studies have shown how PMEIs are involved in plant development and cell wall stiffening.

Therefore, this study overexpressed a gene encoding PMEI in *Brachypodium* lines using a *Zea mays* ubiquitin (ZmUbi1) promoter, studied the growth phenotype, and conducted biochemical and molecular analysis under drought and nutrient stress. Thus, aberrant growth phenotype and sugar composition of the cell walls of drought-tolerant lines were also reported in the present study. Therefore, transgenic *Brachypodium* plants with increased expression levels of PMEI (PMEI-OE) were generated to understand the inadequacy of water and low nutrient availability. These abiotic stresses are a significant limiting factor to cereal crop yields and productivity and are further studied in this chapter for a better understanding of the demand for sustainable agriculture. Results presented in this chapter describe the molecular analysis of the transgenic plants, followed by an evaluation of phenotypic and biomass properties under drought and nutrient stress.

6.2 Materials and methods

6.2.1 Vector construction via gateway cloning (performed by the previous researcher)

Subsequent semi-quantitative PCR results in the host laboratory at Aberystwyth University indeed confirmed higher expression levels of this PMEI in *Brachypodium* leaves after

drought treatments (Bosch M., personal communication). A highly efficient gateway expression vector, pANIC 6A (Mann *et al*., 2012), in which the PMEI gene of interest was cloned (Figure 6-3), was used for *Agrobacterium*-mediated transformation *Brachypodium* kindly provided by Sue Dalton at IBERS, Gogerddan, Aberystwyth. The pANIC 6A plasmid contains the ZmUbi1 promoter for the ubiquitous expression of the PMEI target gene. Hygromycin (hph) and red fluorescent protein (RFP) were used as selectable screening makers to improve the transformation efficiency. The expression of RFP was used to screen the seedlings using a fluorescence dissection microscope and select those that were RFP positive lines (RFP+).

The host laboratory, Aberystwyth University, amplified the target gene from cDNA isolated from *Brachypodium distachyon* inbred line (Bd21-3). Two different constructs were prepared for the overexpression of Bradi3g45080, one that included the PMEI stop codon and one lacking the stop codon and instead of exhibiting an in-frame fusion with an AcV5 epitope tag. This tag encodes a small peptide of 9 amino acid residues (SWKDASGWS) with the OCS T (Octopine synthase terminator sequence) used as a terminator region (Figure 6.3). The overexpression of the PMEI gene (Brachy-214: PMEI and Brachy-217: PMEI-AcV5) was achieved in the inbred *Brachypodium distachyon* line (Bd21-3).

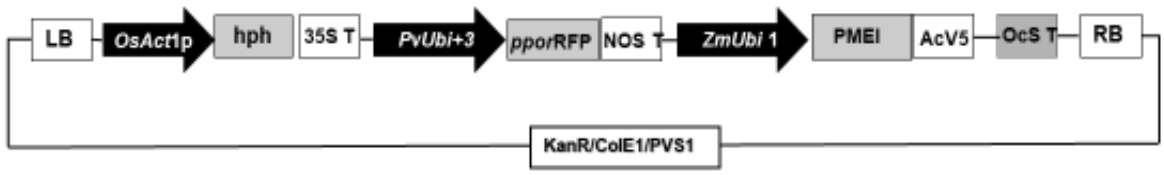

Figure 6-3: The Gateway pANIC 6A expression vector used for the overexpression of PMEI in *Brachypodium*. The overexpression vector contains the PMEI (gene of interest) under the control of the maize ubiquitin promoter ZmUb1 with a terminator to end the transcription, PvUbi+3 (switchgrass polyubiquitin promoter), OsAct1 (rice actin 1 promoter and intron), hph

(hygromycin phosphotransferase coding region), pporRFP (Porites porites red fluorescent protein-coding region), 35S T (35S terminator sequence), OCST (octopine synthase terminator sequence), AcV5 (epitope tag), PVS1 (origin of replication in *A*. *tumefaciens*), Kan (Kanamycin as a bacterial resistance marker), ColE1 (origin of replication in E. coli), LB (left border), RB (right border)

6.2.2 Plant material, growth conditions and identification of transgenic seeds

The seeds of transgenic *Brachypodium* lines were provided by Sue Dalton at IBERS (Aberystwyth). In this study, 21 seeds of independent transgenic lines were used to identify the homozygous lines by using a fluorescence microscope. Florets of the independent transgenic lines were peeled from the lemma and palea. These seeds were double surface-sterilized once with 10% bleach for 60 minutes in a laminar flow bench with thorough rinsing using autoclaved distilled water. The above-sterilized seeds were incubated at 4 °C overnight and second sterilisation was performed for another 15 mins with 10% bleach followed by thorough rinsing with sterilized distilled water. The sterilised seeds were then placed onto a moistened Whatman filter paper onto the Petri plates and sealed with micropore tape for germination. The plates were incubated in dark for 48 h at 24 °C. Subsequently, the plates were transferred to the growth room, with 16 h light at 24 °C and 55% relative humidity, where the seeds germinated synchronously.

A fluorescence microscope was used to screen the above germinated transgenic seedlings followed by a selection of RFP+ lines. The selected transgenic PMEI-overexpressing (PMEI-OE) lines along with two null-segregants (RFP- lines) and wild-type (Bd21-3) seedlings were sown into a pot with 80% F2 levington compost and 20% grit sand as a substrate under controlled greenhouse conditions of 16/8h; 21-22 °C/18-20 °C Day/night-controlled environment. Following are the selected lines and their initials used throughout the experiment in this chapter:

PMEI-OE=PMEI_3363=PMEI_1; PMEI_3571=PMEI_2; PMEI_3610=PMEI_3;

PMEI_3649=PMEI_4; PMEI_3663= PMEI_5

NULL SEGREGANTS= PMEI_3655=PMEI_6; PMEI_3664=PMEI_7

WILD-TYPE= Bd21-3= WT

Molecular analysis

6.2.3 RNA extraction

For molecular analysis, leaves of 35-old plant leaves were harvested from selected RFP+, RFP- and wild type *Brachypodium distachyon* (Bd21-3) control plants. The sample was frozen in liquid nitrogen and subsequently stored at -80 °C. For RNA isolation and purification, leaf tissue was homogenised into a fine talc powder using a pestle and mortar and by the addition of liquid nitrogen and combination with Trizol reagent (Invitrogen). Qiagen RNAeasy Plant Mini Kit was used for further RNA extraction according to the manufacturer's instructions.

Finally, RNA was eluted and dissolved in RNase free water diethylpyrocarbonate (DEPC). The quantity and purity of isolated RNA were checked on an EPOCH spectrophotometer (BioTEK). The A260/230 and A260/280 ratios were used for RNA extracted samples. The nucleic acid is detected at 260 nm, whereas protein, salt and solvents are detected at 230 and 280 nm. Good quality RNA has a value of 1.8 or greater for the A260/230 ratio and between 1.8 and 2 for A260/280. Also, the quality and integrity of isolated and purified RNA were checked by performing agarose gel electrophoresis (0.8% agarose in TAE buffer) (Appendix Figure A6.1).

Isopropanol precipitation of RNA samples

For samples with too low RNA yield or purity, isopropanol precipitation was performed. An equal volume of 100% isopropanol was added to the RNA samples and mixed well by vortexing and incubated at -20°C overnight. The samples were then centrifuged for 15 min at 14,000 rpm at 4°C and the supernatant was removed without disruption of the pellet. The pellet was washed with 1 mL of 75% ethanol prepared with RNase free water followed by vigorous vortexing. The samples were then centrifuged at max speed for 5 min at 4°C and ethanol was removed. The pellet was left with caps open at room temperature for 5-10 min to air-dry. Finally, the pellet was re-suspended in 200 µL of RNase free water, and RNA was isolated using the Qiagen RNAeasy Plant Mini Kit columns.

6.2.4 Reverse transcription for real-time PCR analysis

For cDNA synthesis, 800 ng of RNA was converted to cDNA using the superscript III first-strand synthesis supermix according to the manufacturer's protocol (Invitrogen). Briefly, obtained RNA was converted into the first-strand cDNA using 800 ng total RNA, 1 µl of 50 µM oligo (dT)20 primer and annealing buffer and RNAse free water to a total reaction volume of 8µL. The reaction was conducted in aseptic conditions in 100 µl PCR tubes on ice. After preparing the mix, samples were incubated in a preheated thermal cycler at 65°C for 5 min to anneal template with oligo (dT) 20 primers. The reaction was terminated by placing tubes on ice for a few minutes immediately after incubation. Subsequently, 10 µl of 2X First-Strand Reaction Mix and 2 µl of Superscript III/RNase OUT Enzyme Mix were then added to the PCR tube on ice. Samples were mixed by vortexing, and the PCR tube contents were collected by brief centrifugation and incubated in the thermal cycler at 50 °C for 50 min. The reaction was terminated at 85 °C for 5 min and stored at -20 °C until use.

6.2.5 Conventional PCR using RFP and hygromycin primers

To confirm the RFP+ lines are overexpressing the endogenous PMEI gene a conventional PCR examination was performed. PCR reactions consisted of 10 µl of Quick load Taq (2xmm) 0.4 µl of each RFP and hygromycin primers (10 µM) (Forward, Reverse), 1 µl of cDNA template and 8.2 µl DEPC treated water. The PCR thermal cycling conditions were followed by using My Taq™ Red Mix with initial denaturation at 95 °C for 1 minute, denaturation at 95 °C for 15 seconds, annealing at 55 °C for 15 seconds, and extension at 72 °C for 15 seconds for 33 cycles. Non-specific amplification, product integrity and specificity, were confirmed by 1% agarose gel with 1x TAE Buffer at an electric field set at 80 Volt.

Real-time PCR was performed to confirm the differential expression of genes and was performed by using Roche Light Cycler 480 and fluorescent DNA binding dye SYBR Green PCR Master Mix (Applied Biosystems). Briefly, AmpliTaq Gold® DNA polymerase and dNTPs present in the SYBR® Green PCR Master Mix along with gene-specific primers amplify a target sequence/amplicon as PCR progresses or after each following PCR cycle, the PCR product/amplicon doubles. Since SYBR Green I is a double-stranded DNA (dsDNA) fluorescent binding dye, the fluorescence intensity detected by the Roche Light Cycler® 480 at 530 nm after each PCR cycle simultaneously increases proportionately to the amount of PCR product/amplicon generated. Hence, real-time PCR monitors the amplification of products in real-time and calculates the amplification efficiency of the products to perform quantitative analysis of gene expression.

There are two main types of analysis techniques/methods to quantify gene expression by real-time PCR:

To evaluate gene-specific primer amplification efficiencies for the target gene, absolute quantification was performed. This quantifies a target DNA sequence/amplicon and expresses the result as an absolute crossing point (Cp) value using (i) a standard curve created by serial dilutions of known concentration of cDNA and (ii) the unknown sample's Cp falling on the standard curve. Cp is the cycle number at which the fluorescence of a sample rises above the background fluorescence in an amplification reaction or above the point at which the amplified PCR product becomes firstly visible by the Roche Light Cycler® 480. The Cp will depend on the initial concentration of DNA i.e. a low initial concentration of target DNA requires more amplification cycles to reach the Cp, and a high concentration of target DNA requires fewer amplification cycles. Melting peak and amplification curves were generated during absolute quantification suggesting the absence of primer-dimer formation primer-dimer (Figure 6-4 A&B). Moreover, Figure 6.4C shows the amplification curves obtained during the primer selection with an efficiency of 2.13 suggesting high G-C content of cDNA. The error was 0.113 which showed the accuracy of the quantification followed by a slope value (-3.045) which explains the kinetics of the PCR amplification.

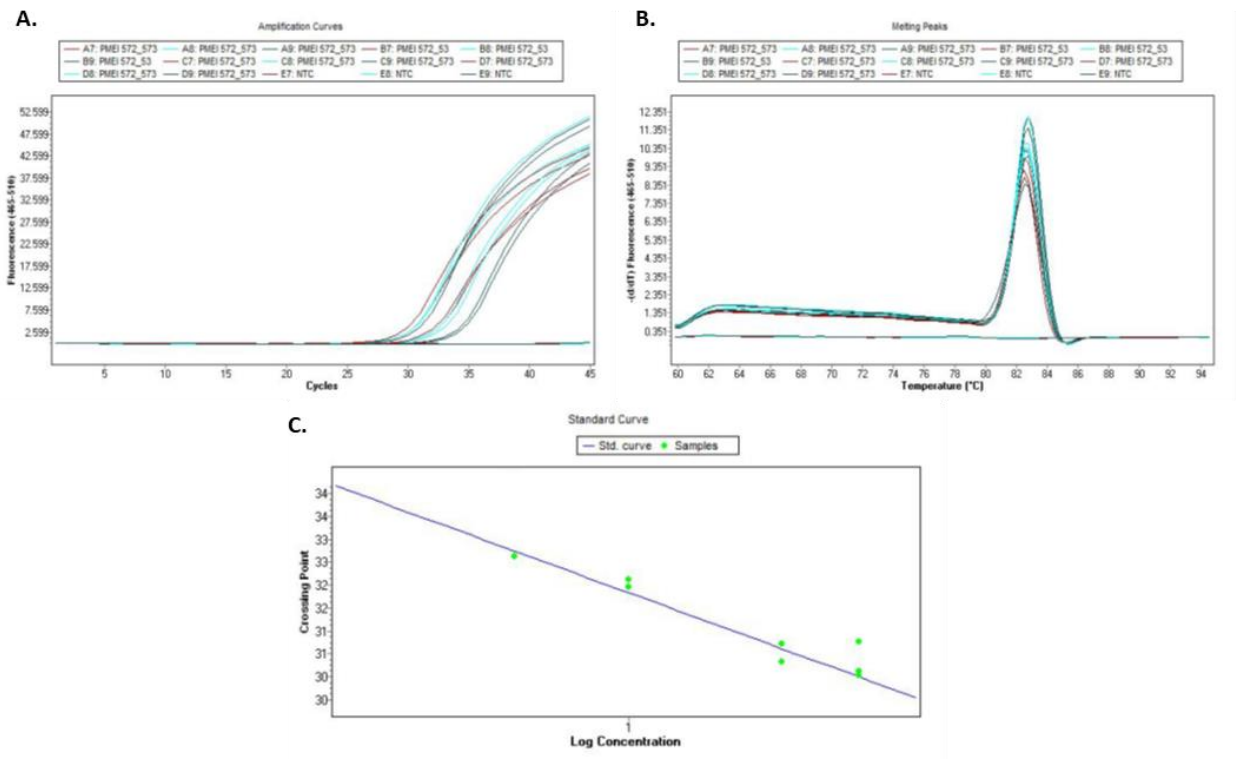

Figure 6-4: Real-time PCR analysis on gene-specific primer amplification efficiency A: Standard curve B. Melt curve, C. Amplification curves

(b) The relative quantification method which compares the Cp of two different DNA sequences (i.e. a reference and target gene of interest) within a sample and expresses the result as a normalised ratio. A reference gene found at a constant Cp in all samples serves as endogenous control and provides a basis for normalizing sample-to-sample differences. Real-time PCR reactions were set up in 96-well plates (Roche), and each reaction contained 10 µl of SYBR Green I Master Mix (Applied Biosystems), forward and reverse primer concentrations and cDNA template from pooled samples diluted to 1:10 (~10ng cDNA). The final reaction volume was adjusted with DEPC nuclease-free water to 20µl. Three reaction replicates were prepared per sample. The plate was sealed with an optical adhesive cover and centrifuged to position PCR reactions into the bottom of the well. 96-well plates with reaction components were assembled on ice until ready to load onto the Light Cycler® 480. Thermal cycling conditions were composed of an initial denaturation step at 95 °C for 10

minutes for polymerase activation, followed by 45 cycles of denaturation at 95 °C for 15 sec, annealing/extension at 60 °C for 1 min/72 °C for 15 sec, and a melting peak analysis step (1 cycle) at 95 °C for 15 sec. Results from absolute quantification for selecting gene-specific primer amplification efficiencies are reported in Appendix Table A6.1.

Biochemical analysis

6.2.6 Protein extraction and total protein determination by the Bradford method

Proteins were extracted using leaf material (35-day old) from the transgenic PMEI and control (Bd21-3) *Brachypodium* accessions following a protocol based on Pinzon-Latorre & Deyholos (2014) with slight modifications. Total protein extract was obtained by grinding tissue in liquid nitrogen and then transferred to an extraction buffer containing 1 M NaCl, 12.5 mM Citric Acid, 50 mM Na_2HPO_4 plus one tablet per 10 mL of cOmplete ULTRA protease inhibitor (Roche), pH 6.5 (1 mL of extraction buffer per 1 g of plant tissue). The homogenate was then shaken for 2 h at 4 °C, subsequently centrifuged at 14,000 rpm for 15 min, and the supernatant was collected. A standard curve was prepared from six points with final protein concentrations of serum albumin (BSA) of 0, 1, 2, 3, 5, and 10 µg/µl. The phosphate extraction buffer was used as a blank. For protein extracts, 2 µL of each extract was added to a cuvette well and adjusted to 160 µl with phosphate buffer. Next, 40 µl of Bradford reagent was added to each well and incubated for 5 min at room temperature. The absorbance was measured at 595 nm using a BioTek PowerWave Microplate spectrophotometer and the protein concentration was determined (Bradford,1976).

6.2.7 Pectin methylesterase activity assay

The esterified PME activity was quantified by using a radial gel diffusion assay. A 2% (w/v) agarose gel containing 0.1% (w/v) of 85% methyl esterified pectin from citrus fruit (P9561,

Sigma-Aldrich); 12.5 mM citric acid, and 50 mM Na_2HPO_4, was dissolved (pH= 6.5). Approximately, 25 mL was poured into square 90 mm Petri plates and allowed to polymerise at room temperature. Wells with a diameter of 4 mm was obtained by using a 200 µl micropipette tip with a diameter of 4mm, and equal amounts of protein samples were dispensed into each well (200 µg of total protein) and plates were sealed with parafilm. The experiment was performed in three technical replicates and plates were incubated at 30 °C for 16 h. The gel was finally stained with an aqueous solution of 0.05% (w/v) ruthenium red for 1 h and washed several times with sterile distilled water. The binding of ruthenium red to pectin increases as the degree of pectin methyl esterification decreases (Downie *et al*.,1998). The development of a stained zone that developed when 0.1% (w/v) of 85% esterified pectin was digested with PME was identical regardless of the buffer. The halo resulting from the hydrolysis of esterified pectin in the gel was photographed immediately, and the area of the halo was measured by using ImageJ software. A standard curve was prepared using commercial orange peel PME (Sigma-Aldrich) with an activity range going from 0.005 to 0.05 units (1unit= 16.67 nanokatals) (Appendix A6.3). PME activity was calculated based on the standard curve.

6.2.8 Evaluation of drought stress tolerance

The selected PMEI-OE, null segregants, and wild-type lines were grown under normal conditions with F2-levington as substrate under standard growth conditions operated at 16 h/8 h; 21-22 °C /18-20 °C Day/night. To eliminate the influence of temperature and humidity on plant development between treatments, temperature and humidity were maintained throughout the experiment. The weight of the plant was monitored and the plants were weighed before water deficit treatment. All the plants were initially watered to

75% soil water content (SWC) for 10 days. For drought treatment, 30-day old seedlings were subjected to drought stress reaching SWC of 15% for 10 days while the control plants were watered to 75% SWC. Re-watering treatment was subjected on day 6 of withholding water from the plants and 75% SWC was maintained at this level. Thereafter, SMC was maintained at 20% under re-watering treatment to access the ability of stressed plants to recover from drought conditions. To summarise, the ability of PMEI-OE plants to tolerate water-deficit stress was examined by exposing 3-week-old plants to 10 days of dehydration, with another set of 6 days without water followed by re-watering and control plants with 75% SWC (Verelst *et al*., 2013). Phenotypical and physiological measurements were recorded at the end of the experiment on day 10 which included plant height, tiller number, leaf number, fresh weight, dry weight, and plant water content.

6.2.9 Evaluation of nutrient stress and phenotypic measurements

Another set of experiments was conducted under low nutrient stress conditions in selected PMEI-OE, null segregants and control (Bd21-3) lines of *Brachypodium*. The treatments were selected based on previous chapters of my thesis. The seeds were sown in an ultralow nutrient substrate (Bulrush compost) under controlled conditions as mentioned in Section 6.3.8. The low nutrient solution was prepared as mentioned in Chapter 2 Section 2.1.1. under nutrient composition (Hoagland & Arnon,1950). The photoperiod in the glasshouse was maintained at 16 h of light and 8 h of dark. Temperature and humidity were controlled in the greenhouse using TinyTag datalogger (Gemini Dataloggers). 40-day old plants were treated with nutrient-deprived Hoagland solution (25 ml/pot) i.e., Control (Hoagland 100%), no nitrate (N0%), no phosphate (P0%), no potassium (K0%), and no boron (B0%), respectively.

Phenotypic measurements help us to improve our understanding of plant responses under environmental stress conditions, therefore, the measurements were taken at the end of the experiment (2 weeks after the treatment or 54-old day plants). Photographs and detailed measurements were conducted at the end of the experiment. Plant height (cm) was measured from the base of the soil to the last node of the main stem. Tiller number (number of branches excluding the main stem) and total leaf number present on the plant were measured on the initial and final days of the experiment. The data presented represents the final day measurements only. At the time of harvest fresh weight (g) was noted. Dry weight (g) was determined by drying the above-ground biomass at 72 °C for 3days. Fresh and dry weight measures were used to calculate the plant water content (PWC).

$$PWC\ (\%)\ =\ (FWt - DWt)/FWt\ *100$$

Where, FWt = Fresh weight (g),

DWt = Dry weight (g)

Each sample was measured in biological replicates (n=5)

At the time of senescence, seeds were harvested from basal florets of spikelets from the main stem. Total spikelet number present on the plant, spikelet weight (present on the main stem), and spikelet length (present on the main stem) were measured for all the PMEI-OE, null segregant and control plants treated under low-nutrient stress (n=5) (Boden *et al.*, 2013).

6.2.10 Cell wall preparation

The cell wall was prepared as described in Chapter 2 Section 2.2.6 and 2.2.7.

6.2.11 Total sugar release content

Monosaccharide content of the cell wall was determined as described in Chapter 2 Section 2.2.8.

6.2.12 Saccharification efficiency

This was determined as described in Chapter 2 Section 2.2.9.

6.2.13 Statistical analysis

Statistical analyses were performed by using R software (R Core Team, 2021). Morphological and chemical measurement data were analyzed with ANOVA and Tukey's HSD test at the 0.05 level of significance to determine posthoc pairwise comparison. Results of the statistical analysis were visualized following (Tufte, 2001) and using the ggplot package (Wickham & Chang, 2016).

6.3 Results

Pectin methylesterases (PMEs) along with their proteinaceous inhibitors (PMEIs) are usually intricate in the regulation of plant development which includes tissue growth to fruit ripening. Recent studies have suggested that overexpressing endogenous PMEIs majorly affects the cell wall properties thereby playing an important role in drought stress tolerance (Zhang *et al*., 2019; Lenk *et al*., 2019). PMEIs play an important role in controlling the properties of cell wall pectins by playing an important role in the degree of methylesterification (Pelloux *et al*., 2007). Previous studies have suggested that overexpressing PMEIs could further regulate plant abiotic stress resistance in rice, wheat, and Arabidopsis (Wormit and Usadel, 2018; Zhang *et al*., 2019). However, reduced PMEI

gene expression showing lower sensitivity to salinity can mitigate the stress by enhancing root growth, fresh weight (Chen *et al*., 2018). Consequently, genetic evidence supporting the role of pectins in drought and nutrient tolerance in *Brachypodium* is still lacking. The expression of Bradi3g45080, encoding a PMEI, was upregulated in *Brachypodium* lines exposed to drought stress suggesting an improved drought tolerance (Verelst *et al*., 2013).

6.3.1 Screening and expression analysis of transgenic lines overexpressing PMEI in *Brachypodium*

To explore the function of PMEI, the overexpression construct illustrated in Figure 3 was introduced into *Brachypodium* lines by *Agrobacterium tumefaciens* transformation in the Bosch lab. PMEI expression was constitutively driven under the control of the maize ubiquitin promoter (ZmUbi1). The transformed independent lines were further screened for red fluorescence positive (RFP+) to obtain and select positive transgenic lines from F1 segregating population for further detailed analysis.

Red fluorescent protein (RFP) for rapid and convenient screening during seed germination

The pANIC6A plasmid contains a ppRFP reporter gene isolated from the coral *Porite porites* which produce a red fluorescent protein under the control of the switchgrass Ubi1 promoter (PvUBI1, Figure 6-3). Therefore, a red fluorescence emitted by RFP was utilized to screen the transgenic lines and to distinguish between the positive (transgenic) and negative (null segregant) lines in germinated seedlings. A strong red fluorescent signal was observed in the roots, confirming RFP to be a strong visual screening marker for the rapid identification of seedlings expressing the transgene during early growth stages.

Conventional PCR

35-day-old plant leaves of the selected independent RFP+, RFP-, and WT plants were harvested for RNA extraction and cDNA construction was performed to identify the presence of the target gene in all the selected independent lines. As shown in Figure 6.3 sequencing demonstrates the insertion of RFP and hygromycin markers which are included in the construct. Conventional PCR was run using primer sets (forward and reverse) and the bands were shown in Figure 6-5. This method identified the transgenic, non-transgenic and wild type lines by showing the intensity of the presence of the target gene present in RFP+ lines (band 1-5), whereas smaller bands RFP- or negative control lines (6 and 7 smaller bands), and no bands for WT (Bd21-3).

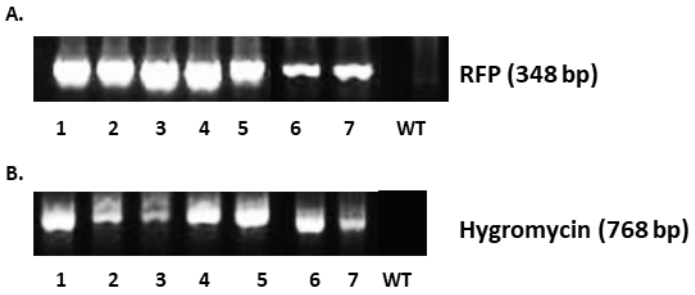

Figure 6-5: Image showing gel electrophoresis by using conventional PCR suggesting that the selected lines are transgenic A: RFP marker (348 bp product) B: Hygromycin marker (768 bp product). 1= PMEI_1, 2= PMEI_2, 3= PMEI_3, 4= PMEI_4, 5= PMEI_5, 6= PMEI_6, 7= PMEI_7, WT= Wild-type

Table 6-1: Target and reference sequence of gene specific primers used for real time quantitative PCR analysis

Gene	Target/Reference genes	Designated primers	Sequence	Amplicon size(bp)
Bradi3g45080	PMEI	MB572 MB573	F: 5'- CCATCACCAACCTCATCCAC-3' R: 5'- TCCAGAGACACGACGAACAC-3'	100
Bradi4g00660	UBC18	LF74 LF75	F 5'-GGAGGCACCTCAGGTCATTT -3' F 5'- CGAGCTAGACAGCATGGACA-3'	193

The RFP and hygromycin markers suggested the presence of the screening markers between RFP+ and control lines. Therefore, conventional PCR with the selected target gene primers (Table 6-1) was performed so as to examine primer specificity, as shown in Figure 6-6 A. Based on the Image J analysis, the band area (mm^2) was quantified, and the graph suggested the presence of the target gene in RFP+ selected lines (Figure 6-6 B).

However, reverse transcriptase PCR was not enough to confirm that the selected lines were overexpressing the endogenous PMEI gene, or transgene, causing gene expression, and therefore, quantitative PCR was performed to quantify the expression level of the wild-type compared to the wild type plants.

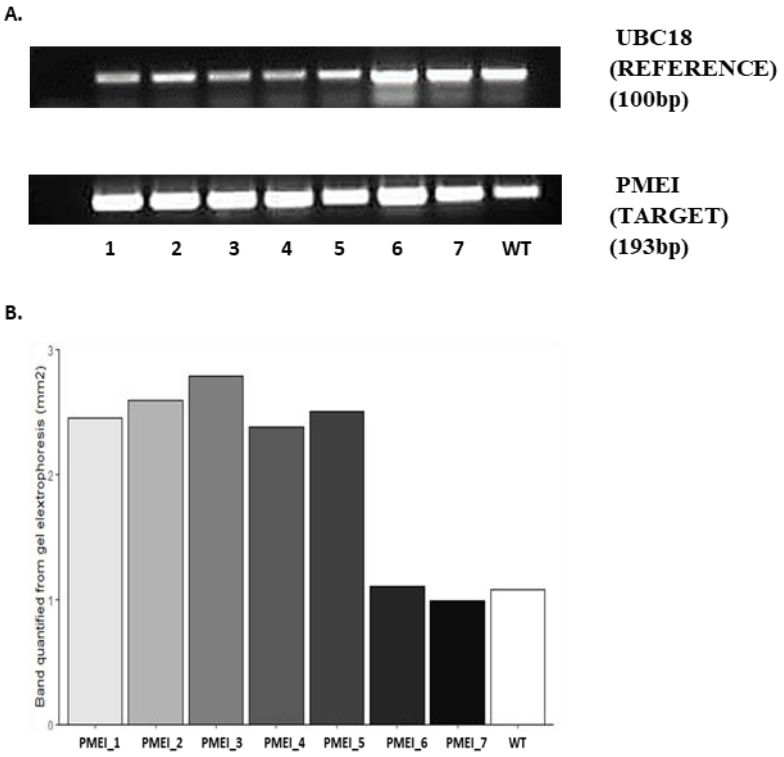

Figure 6-6: A PCR analysis using ubiquitin (UBC18) and PMEI gene specific primers. NTC= no template control; PMEI_1-PMEI_5= independent RFP+ transgenic lines; PMEI_6-7= independent negative RFP transgenic lines; WT= wild-type (control) showing the UBC18 reference gene on top and the PMEI target gene at the bottom.100 ng cDNA as PCR template B. Quantification of the band was performed based on the relative expression from the target PMEI() to the UBC control by using Image J analysis

Confirmation of PMEI transgene overexpression by performing real-time PCR

Genetic analysis with the use of Real-Time PCR was performed to compare PMEI gene expression levels between RFP+, RFP- and wild type (control) plants. Gene expression was calculated using Bradi3g45080 encoding PMEI, and expression was calculated compared with the wild type. The above experiments suggested the presence of transgenic gene in RFP+ lines thereby, five selected RFP+ lines along with two RFP- lines, and a wild-type (WT or control) were further investigated for the integration of the PMEI transgene.

Real-time PCR was performed to check the expression level of the transgene has critical importance in the application of genetically engineered grasses encoding particular traits

with gene specific primers as shown in table 6-1 (Zhang *et al*., 2015). Leaf tissues from three biological replications were collected from positive, negative transgenic lines along with the control plants for RNA isolation. PMEI integration and generation of transgenic PMEI overexpression lines was achieved in RFP+ lines by expression analysis from leaf tissue by Real-time PCR. From the previously selected RFP positive lines, overexpression levels of PMEI ranged between ~2.1-fold to ~4-fold, with PMEI_5 displaying the lowest and PMEI_3 the highest expression (Table 6-2). No differences in the expression levels were found for selected PMEI lines except PMEI_3 which showed a significant increase in the expression level compared to the control (Table 6-2). Moreover, the negative RFP lines showed marginal overexpression in PMEI_6 (~1.55-fold), and PMEI_7 (~0.67-fold) which was lower than the RFP+ selected transgenic lines. The results indicate that we have identified five independent transgenic *Brachypodium* lines showing increased levels of PMEI expression.

Table 6-2: : Estimation of fold change in PMEI expression level based on the ratio of PMEI/UBC18 shown in A and measured using B. Results expressed as means ± SE and letters showing post-hoc statistically significant difference from control (n=3 experiments)

Gene expression level by real-time PCR		
Selected lines	**Fold change**	**Significance**
PMEI_1	3.06 ± 0.39	abc
PMEI_2	2.98 ± 0.45	abc
PMEI_3	3.87 ± 0.59	a
PMEI_4	3.62 ± 1.2	ab
PMEI_5	2.07 ± 0.6	abc
PMEI_6	1.55 ± 0.23	abc
PMEI_7	0.67 ± 0.14	c
Wild type (control)	1.0 ± 0	bc

6.3.2 PMEI-OE reduces PME activity in transgenic *Brachypodium* lines

In order to understand the inhibition role of the PMEI gene and explore the overall PME activity in leaf tissues, a radial diffusion assay was performed. This assay was detected by the development of fuchsia-stained haloes which was caused by de-methylesterification of

highly methylesterified pectin present in the agarose gel (Downie *et al*., 1998). PME assay was accessed by using two biological replicates, which were each measured in three technical replicates, which further allows the quantification of PME activity in biological samples. The results showed a reduction in the diameter of the halo of various transgenic lines compared to the wild type (Figure 6-7 A). We used a standard curve with different concentrations of orange peel pectin esterase (Appendix Figure 6.2) to allow the quantification of the PME activity in the samples. The results suggested a reduced halo formation when compared to the wild type. A reduction in the formed haloes were found in PMEI-OE and null segregant lines compared with the WT (Bd21-3) (Figure 6-7 B). Interestingly, only two PMEI-OE lines showed a statistically significant difference in PMEI_1 with 71 % (0.26nkat, $p<0.001$), and PMEI_3 with 40 % reduction (0.6nkat, $p<0.05$) of PME activity when compared to the WT. However, PME activity in the PMEI-OE (PMEI_2, PMEI_4 & PMEI_5) and null segregants (PMEI_6 & PMEI_7) were not significantly different when compared to the WT (Figure 6-7 B).

Overall, the results suggested that the overexpression of PMEI showed a modest decrease of PME activity in leaf tissues compared with the control lines, hence suggesting more esterified pectin in the cell wall.

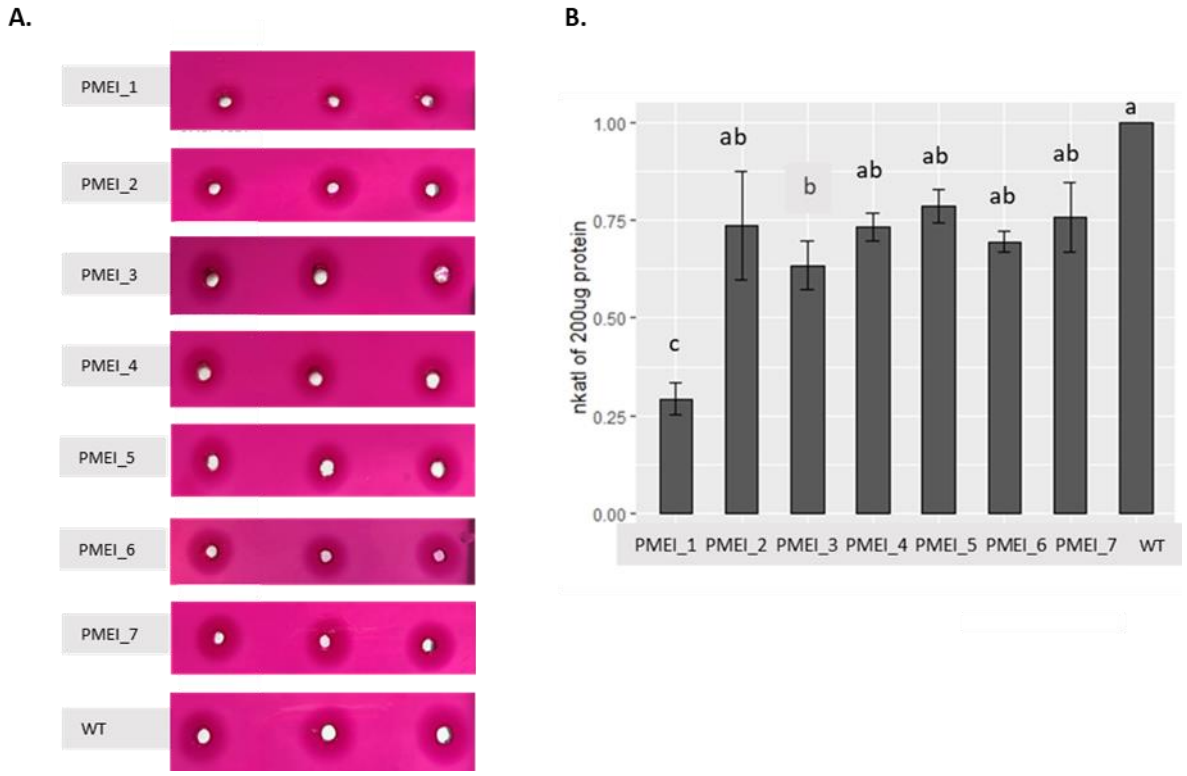

Figure 6-7: A PCR analysis using ubiquitin (UBC18) and PMEI gene specific primers. NTC= no template control; PMEI_1-PMEI_5= independent RFP+ transgenic lines; PMEI_6-7= independent negative RFP transgenic lines; WT= wild-type (control) showing the UBC18 reference gene on top and the PMEI target gene at the bottom.100 ng cDNA as PCR template B. Qunatification of the band from the gel electrophoresis by using Image J analysis

6.3.3 Phenotypic and morphological assessment of selected PMEI overexpressing *Brachypodium* lines under drought

Brachypodium originating from Iraq is an interesting specie to study as it is considered a drought-tolerant grass. Consequently, previous studies reported and identified that *Brachypodium* possesses specific tolerance mechanisms and grass cell wall traits which can be implemented in other closely related grass crops like wheat, barley, sorghum, and maize (K. Yordem *et al*., 2011; Wu *et al*., 2012). Thereby, the PMEI gene was overexpressed in the study to attain highly drought tolerant grass species. The potential to make grass crops

more drought tolerant and phenotypic assessment was evaluated. The selected PMEI-OE (A=PMEI_1, B=PMEI_2, C=PMEI_3, D=PMEI_4, E=PMEI_5), null-segregants (F=PMEI_6, G=PMEI_7) and WT lines (H=Bd21-3) were exposed to different treatments as explained in section 6.2.7.

Above ground physio-morphological parameters were measured at the end of the 10-day treatment period to evaluate if transgenic plants with high levels of PMEI expression would cope better under drought compared to the WT. Representative photographs show the plant stature and phenotypic differences between different treatments and suggested no obvious differences in plant stature observed in PMEI-OE, null-segregants and wild-type plants when compared to each other as shown in Figure 6-8.

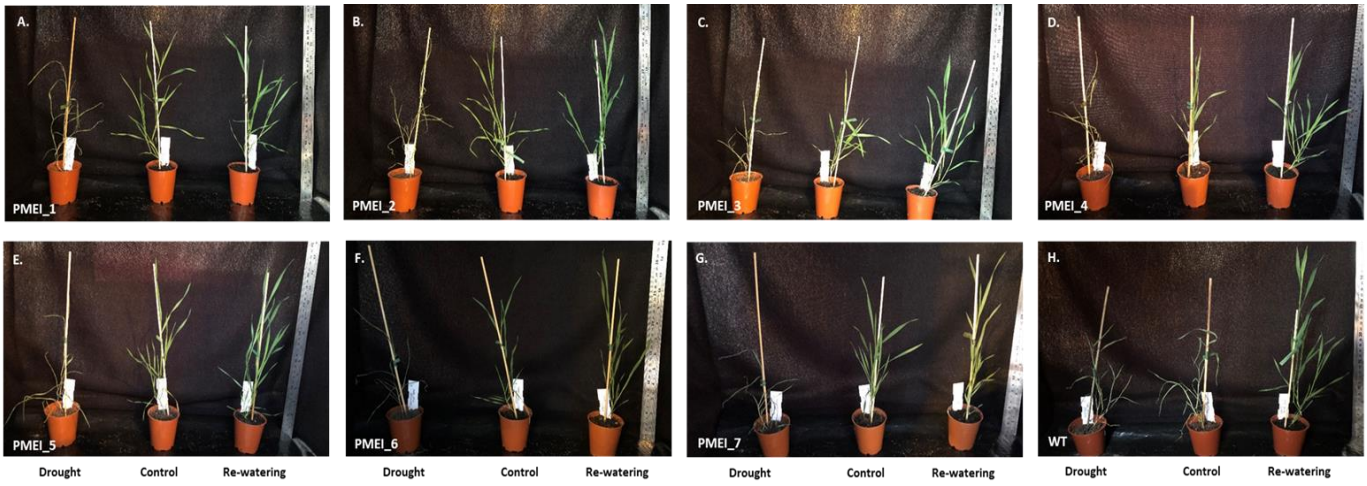

Figure 6-8: Images of transgenic PMEI *Brachypodium* plants taken at the end of 10-day drought treatment stage. Treatments include drought, well-watered (control), and re-watering for all PMEI-OE lines, null-segregant control and wild-type. A=PMEI_1, B=PMEI_2, C=PMEI_3, D=PMEI_4, E=PMEI_5 (PMEI-OE lines); F=PMEI_6, G=PMEI_7 (Null segregants), H=WT (Bd21-3). Scale bar= 1meter

With the above representative images of three different treatments taken at the end of 10-day drought experiment it was quite difficult to compare the PMEI-OE, null segregant and wild type lines. Therefore, phenotypic measurements were followed with some statistical analysis in the following results section.

PHENOTYPIC TRAITS

To obtain deeper insights into the potential effects of PMEI-OE, phenotypic analysis was undertaken to observe the differences in visual traits as a result of the stress treatments in the selected PMEI overexpressing plants compared to the Bd21-3 *Brachypodium* lines. Thereafter, plant height, leaf number, tiller number, fresh weight, dry weight, and plant water content data will be presented.

PLANT HEIGHT

The plant height was measured from the base of the soil to the last node of the main stem of each *Brachypodium* line as described in section 6.9. When comparing measurements between the three treatments for each individual line, plant height showed no significant differences according to to *post hoc* analysis under re-watering conditions when compared to the optimal well-watered (control) conditions except PMEI_3 ($p<0.01$) (Figure 6-9 A). However, treatment with a 10-day water deficit resulted in a significant reduction in plant height in all the PMEI-OE transgenic, null segregant and wild-type line in comparison to the control conditions (Figure 6-9 A). Line PMEI_3 showed the most prominent effect with a 31% reduction ($p<0.001$) in plant height after drought treatment compared to the control plants. Statistical analysis was also performed for each of the treatments amongst transgenic PMEI-OE, non-segregant and wild-type lines as shown in Table 6-3. Under control conditions a significant 20% reduction in plant height was observed for PMEI_4 when compared to the wild type. Drought treatment resulted in a significant plant height reduction in PMEI_3 (35%, $p<0.001$) followed by PMEI_1 (25.8%, $p<0.01$), and PMEI_7 (22.6%, $p<0.01$) in comparison to the wild type (Table 6-3). Moreover, plant height measures for PMEI_3 and PMEI_4 were significantly reduced by 21.5% ($p<0.001$) and 20%

(p<0.01), respectively, after re-watering when compared to the wild-type lines of *Brachypodium*.

TOTAL LEAF NUMBER

Total leaf number on the plant was another classical growth measurement which was determined by counting the number of leaves at the end of the 10-day experiment for all the treatments. When comparing leaf numbers between re-watering and control treatments, a significant difference could only be observed for PMEI_5 plants, with re-watering resulting in significantly lower leaf number (p<0.01) at day 10 compared to those measured under control conditions. Drought treatment revealed a significant reduction in all the PMEI-OE, and null segregant lines except WT in comparison to the well-watered conditions (Figure 6.9 B). *Post-hoc* analysis suggested no significant difference in PMEI-OE, null segregant and wild-type lines in well-watered treatment (Table 6-3). Leaf number was significantly reduced in PMEI_5 (21.7%, p<0.01) upon drought treatment compared to wild-type plants. Under re-watering conditions only PMEI_5 exhibited no recovery in leaf number and showed a significant decrease in leaf number when compared to the wild type (25%, p<0.01) as shown in Table 6-3.

TILLER NUMBER

Results obtained for tiller number were not consistent with those of total leaf number as a significant reduction was observed in PMEI_2, PMEI_3, PMEI_4, and PMEI_5 plants after re-watering when compared to well-watered conditions (Figure 6-9 C). However, no significant difference was observed in PMEI_1, null-segregants and WT under re-watering treatment when compared to the control treatment. Interestingly, tiller numbers in drought treated plants showed no significant difference in PMEI_4 and Bd21-3 when compared to their well-

watered controls but a significant reduction in tiller number was observed in all the PMEI-OE and null segregant lines of *Brachypodium* (Figure 6-9 C). When PMEI-OE and null segregant lines were compared to the wild-type under optimal control conditions, no significant difference was revealed in those plants. However, drought triggered a significant reduction in tiller number for PMEI_3 (33%, $p<0.001$) in comparison to wild-type plants followed by PMEI_7 (30%, $p<0.01$) and PMEI_1 (30%, $p<0.01$), respectively. Interestingly, under re-watering treatment only PMEI_7 (null-segregant) showed a significantly decreased tiller number (20%, $p<0.01$) when compared to Bd21-3 (Table 6-3).

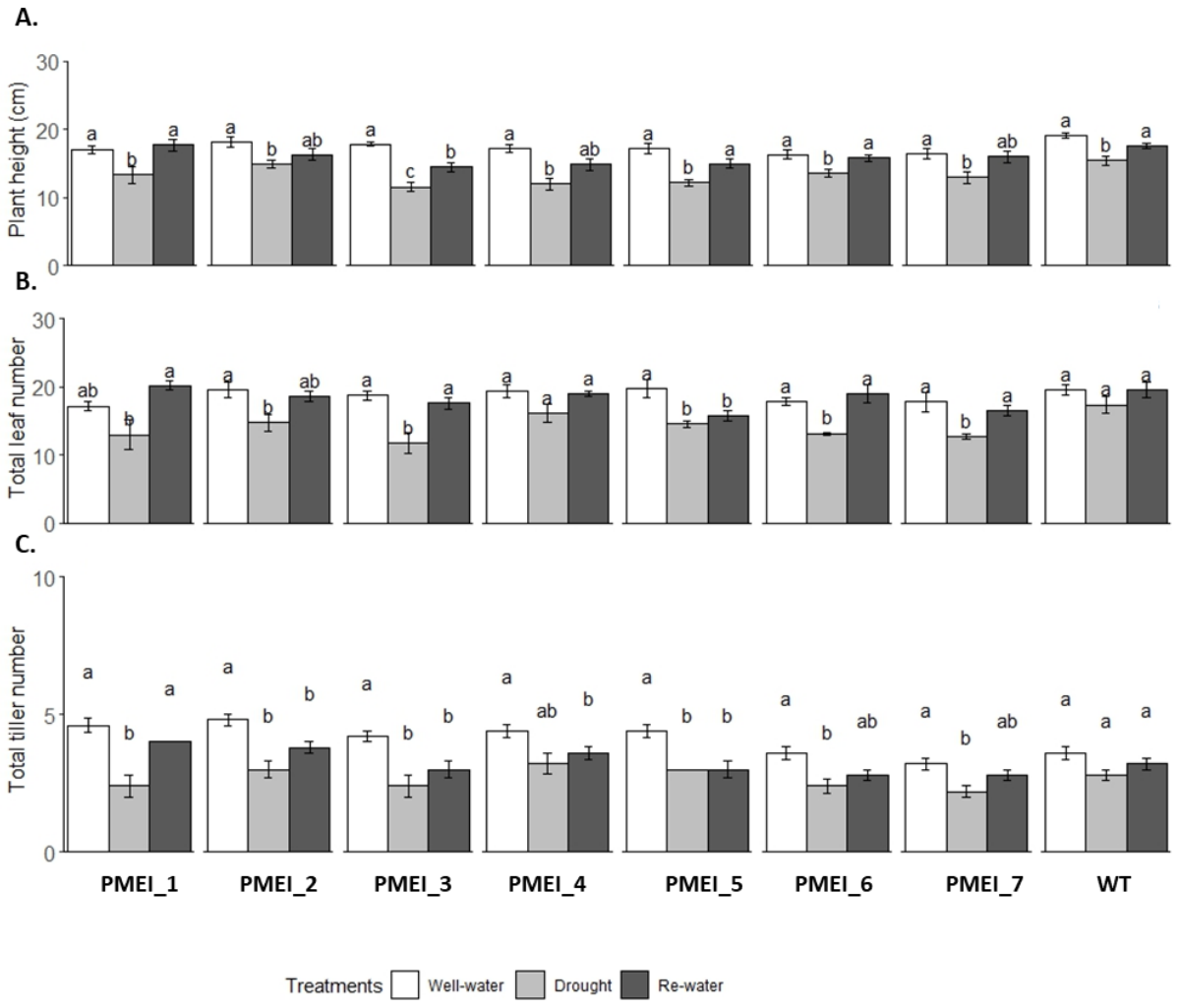

Figure 6-9: Measurements of phenotypic traits: A- plant height (cm), B- total leaf number, C- tiller number. Data represent the means of five replicates with bars indicating ±SE. Lower

case letters indicate post-hoc analysis significant differences ($p < 0.05$) between the treatments for each individual line

In summary, heterozygous transgenic and null segregant control *Brachypodium* plants evaluated for plant morphology following the three treatments revealed no significant changes in plant height, leaf number, and tiller number compared to wild-type lines of *Brachypodium distachyon*.

Table 6-3: Transgenic independent PMEI-OE lines, null segregant and wild-type with three different treatments of well-watered or control conditions, drought, and re-watering. Mean value and letters showing statistical significant difference by post-hoc analysis plant height, total leaf number, tiller number, fresh weight, dry weight, and plant water content

Treatment	*Brachypodium* lines	Plant height	Leaf number	Tiller number	FWt	DWt	PWC
Well-watered	PMEI_3363	14.5 ab	14.5 a	3.3 a	0.6 a	0.1 b	77.8 a
	PMEI_3571	15.4 ab	16.3 a	3.5 a	0.9 a	0.2 ab	76.6 a
	PMEI_3610	14.5 ab	15.5 a	3.1 a	0.8 a	0.2 ab	73 a
	PMEI_3649	13.5 b	16 a	3.2 a	0.8 a	0.2 ab	77.1 a
	PMEI_3663	14.8 ab	16.5 a	3.3 a	0.8 a	0.2 ab	76.6 a
	PMEI_3655	13.8 ab	15 a	3 a	0.9 a	0.2 ab	76 a
	PMEI_3664	14.5 ab	14.3 a	2.6 a	0.7 a	0.16 ab	76 a
	Bd21-3	16.8 a	16.5 a	3 a	0.9 a	0.23 a	75.4 a
Deficit	PMEI_3363	11.5 bc	16 ab	2.1 bc	0.08 ab	0.08 ab	3 a
	PMEI_3571	14 ab	15 ab	2.7 abc	0.1 ab	0.08 ab	11 a
	PMEI_3610	10 c	14 ab	2 c	0.05 b	0.05 b	18.7 a
	PMEI_3649	14 ab	14.3 ab	3 ab	0.08 ab	0.08 ab	3 a
	PMEI_3663	13.1 ab	13 b	2.6 abc	0.08 ab	0.08 ab	3 a
	PMEI_3655	12.4 abc	15 ab	2.4 abc	0.09 ab	0.09 ab	9.5 a
	PMEI_3664	12 bc	13.3 ab	2.1 bc	0.05 b	0.05 b	15.5 a
	Bd21-3	15.5 a	16.6 a	3 a	0.12 a	0.1 a	11.4 a
Re-water	PMEI_3363	15.2 ab	15.9 a	3.5 a	0.6 a	0.15 a	73 a
	PMEI_3571	13.8 abc	14.9 ab	3.1 ab	0.5 a	0.13 a	61 a
	PMEI_3610	12.2 c	14 ab	2.7 bc	0.4 a	0.1 a	71.8 a
	PMEI_3649	12.4 bc	14.3 ab	2.9 abc	0.4 a	0.1 a	75.7 a
	PMEI_3663	12.6 abc	12.5 b	2.5 bc	0.4 a	0.1 a	76.8 a
	PMEI_3655	13.2 abc	14.8 ab	2.7 bc	0.6 a	0.14 a	75.6 a
	PMEI_3664	13.2 abc	13.3 ab	2.4 c	0.6 a	0.13 a	78.5 a
	Bd21-3	15.54 a	16.7 a	3 ab	0.6 a	0.17 a	66.7 a

FRESH WEIGHT

To investigate aspects that relate to the phenotypic measurements, fresh biomass, dry biomass, and plant water content was analysed under the water deficit, re-watering, and well-watered conditions. Above ground fresh weight was measured and statistical analysis

was performed within the genotype to understand the effect of different treatments as shown in Figure 6-10 A. No significant differences were noted for PMEI_1 ($p= 0.9$), PMEI_3664 ($p= 0.7$), and wild type ($p= 0.09$) when comparing re-watering treatment with well-watered conditions (Figure 6-10 A). However, a significant reduction in fresh weight following re-watering conditions was found for PMEI_2 ($p< 0.01$), PMEI_3 ($p< 0.05$), PMEI_4 ($p<0.001$), PMEI_5 ($p<0.001$), and PMEI_6 ($p<0.01$) compared with well-watered plants. A significant reduction in the fresh weight under drought treatment was observed in PMEI-OE, null segregant, and wild-type ($p<0.001$) compared with well-watered conditions (Figure 6-10 A).

Statistical analysis was also performed within each treatment between PMEI-OE, null segregant and control lines of *Brachypodium*. None of the PMEI-OE lines showed a significant difference in fresh weight compared to wild type plants for well-watered and re-watered treatments. Whereas a significant reduction in fresh weight in PMEI_3 ($p<0.01$) and PMEI_7 ($p<0.01$) under water deficit treatment was noted when compared to the wild type plants (Table 6-3).

DRY WEIGHT

The dry weight of the treated plants showed similar trend to fresh shoot biomass under re-watered conditions with a significant reduction for PMEI_2 ($p<0.05$), PMEI_3 ($p<0.01$), PMEI_4 ($p<0.01$), PMEI_5 ($p<0.001$), and PMEI_6 ($p<0.01$) while no significant effect was observed for PMEI_1 ($p= 0.8$), PMEI_7 ($p= 0.34$), and wild-type ($p= 0.07$) when compared to the well-watered conditions (Figure 6-10 B). Water deficit resulted in a significant reduction ($p<0.001$) in dry weight for all the PMEI-OE, null segregant, and wild-type plants in comparison to the well-watered conditions. The exception was the PMEI-OE line PMEI_1)

which showed no significant difference ($p= 0.15$) compared with the well-watered plants (Figure 6-10 B).

Notably, the dry biomass of PMEI_1 was significantly lower (by 39%, $p<0.01$) under well-watered conditions when compared with control plants (Table 6-3). Under drought treatment a significant reduction in dry weight was noted for PMEI_3 (PMEI-OE) and PMEI_7 (null segregant) by 58% ($p<0.01$) and 57% ($p<0.01$), respectively, compared with the wild-type line. No significant difference was found under re-watering conditions in PMEI-OE and null segregant lines when compared to the wild-type (Table 6-3).

PLANT WATER CONTENT

Plant water content (PWC) percent was calculated using fresh, and dry weight biomass. PWC showed a significant reduction in PMEI_1 (5%, $p<0.05$) in re-watered conditions compared with the well-watered plants. However, drought treatment resulted in a drastic significant reduction PWC in PMEI-OE, null segregant, and wild-type ($p<0.001$) lines of *Brachypodium* compared with the well-watered conditions (Figure 6-10 C).

No significant difference under all the three treatment was observed in all the genotypes when compared to the wild-type lines (Table 6-3).

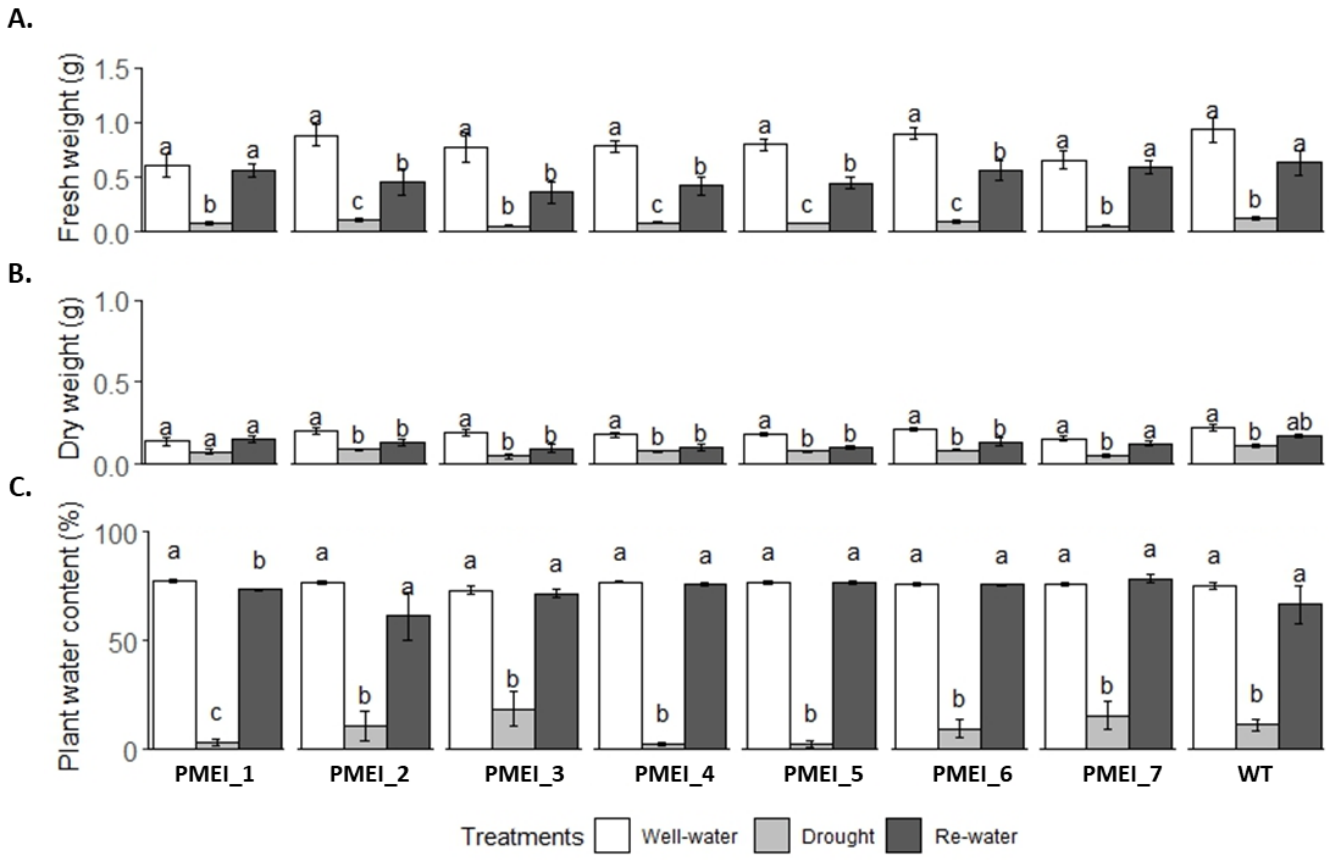

Figure 6-10: A. Fresh weight, B. dry weight and C. plant water content measurement following three different treatments. Data represent the means ±SE (n= 5). Letters show significant difference p <0.05 within the genotype between the treatment [Treatments: Well- watered, Drought and Re-watering]

6.3.4 Phenotypic assessment and biomass quality of selected PMEI-OE *Brachypodium* lines under nutrient stress

Plant growth

Based on previous studies it has been suggested that drought stress elevates the expression of some genes which are involved in cell wall synthesis and modification (Ingo *et al*., 2007; Verelst *et al*., 2013; Andrade *et al*., 2019). Therefore, we increased the expression of PMEI in the present study to observe if these transgenic *Brachypodium* lines exhibited morpho-physiological changes in under drought stress that would make them more tolerant to these conditions. Low nutrient availability is a major factor determining plant distribution and

productivity which can negatively affect the development, yield and biomass quality of plants (Chapin, 1983). Therefore, we treated the independent PMEI-OE, null segregant and wild-type lines of *Brachypodium* with nutrient deprived solution to study the phenotypic behaviour and saccharification efficiency. Phenotypic measurements like plant height, total leaf number and tiller number was scored in the greenhouse at the senescence growth stage.

Table 6-4: Transgenic independent PMEI-OE lines, null segregant and wild-type with five different nutrient treatments of 100% Hoagland or control conditions, N0%, P0%, K0%, and B0%. Mean value and letters showing statistical significant difference by post-hoc analysis plant height, total leaf number, and tiller number

Treatment	***Brachypodium lines***	***Plant height***	***Leaf number***	***Tiller number***
100% H.S.	*PMEI_3363*	*21.14 a*	*16.6 a*	*3.4 a*
	PMEI_3571	*18.58 ab*	*17.2 a*	*4.2 a*
	PMEI_3610	*16.78 abc*	*16 a*	*3.6 a*
	PMEI_3649	*16.54 bc*	*15.6 a*	*3.8 a*
	PMEI_3663	*15.76 bcd*	*15.8 a*	*3.8 a*
	PMEI_3655	*11.98 d*	*13.4 a*	*3 a*
	PMEI_3664	*13.70 cd*	*15.2 a*	*3.4 a*
	Bd21-3	*19.16 ab*	*17.2 a*	*4 a*
N0%	*PMEI_3363*	*20.66 a*	*7.6 ab*	*ns*
	PMEI_3571	*18.62 ab*	*8.2 a*	*ns*
	PMEI_3610	*17.46 abc*	*8 ab*	*ns*
	PMEI_3649	*15.4 abcd*	*7.4 ab*	*ns*
	PMEI_3663	*14.72 bcd*	*7.6 ab*	*ns*
	PMEI_3655	*12.04 cd*	*7 ab*	*ns*
	PMEI_3664	*11.36 d*	*6.8 b*	*ns*
	Bd21-3	*17.1 abc*	*7.2 ab*	*ns*
P0%	*PMEI_3363*	*19.42 ab*	*9.2 abc*	*1 ab*
	PMEI_3571	*23.64 a*	*11.24 a*	*1.8 a*
	PMEI_3610	*21.34 ab*	*9.8 abc*	*1 ab*
	PMEI_3649	*15.96 bc*	*10.6 ab*	*1.4 ab*
	PMEI_3663	*17.74 bc*	*8.4 bc*	*0 b*
	PMEI_3655	*16.24 bc*	*8.6 bc*	*0.2 b*
	PMEI_3664	*12.9 c*	*8 c*	*0 b*
	Bd21-3	*18.3 abc*	*7.6 c*	*0 b*
K0%	*PMEI_3363*	*21.34 ab*	*17 ab*	*3.6 a*
	PMEI_3571	*23.84 a*	*18.8 a*	*4 a*
	PMEI_3610	*19.2 bc*	*14.6 b*	*3.4 a*
	PMEI_3649	*15.64 c*	*17.4 ab*	*3.6 a*
	PMEI_3663	*17.72 bc*	*18.6 a*	*4 a*
	PMEI_3655	*18.24 bc*	*17.6 ab*	*3.4 a*
	PMEI_3664	*10.76 d*	*10.8 c*	*1.6 b*
	Bd21-3	*18.14 bc*	*14.8 b*	*3.4 a*
B0%	*PMEI_3363*	*21.04 ab*	*18.2 a*	*4 a*
	PMEI_3571	*22.54 a*	*19 a*	*4.6 a*
	PMEI_3610	*17.98 abc*	*16.8 a*	*3.6 a*
	PMEI_3649	*18.2 abc*	*18 a*	*4 a*
	PMEI_3663	*22.78 a*	*20.2 a*	*4.2 a*
	PMEI_3655	*16.16 bc*	*19.4 a*	*4 a*
	PMEI_3664	*12.86 c*	*11.8 a*	*1.8 b*
	Bd21-3	*18.66 ab*	*16.8 a*	*3.8 a*

PLANT HEIGHT

Results presented in Figure 6-11 A are from the end of the experiment. No reduction in plant height was observed for any of the lines under N0%, when compared to the Hoagland treated plants. However, P0% treatment resulted in an increase in plant height for a number of lines, but this was only significant for one of the PMEI_OE lines (PMEI_2) when compared to the Hoagland control (Figure 6-11 A).

A significant reduction in plant height was observed in null segregants (PMEI_6= 37%, $p<0.001$and PMEI_7= 28%, $p<0.001$) under Hoagland when compared to the wild-type lines of *Brachypodium* (Appendix A6.3). N0% treatment triggered a significant reduction in plant height by 34% in one of the null segregants (PMEI_7, $p<0.01$) when compared to the wild-type plants. Furthermore, P0% showed no significant effect in PMEI-OE, and null segregants for plant height when compared to the wild-type lines of *Brachypodium*. However, in K0% only PMEI_7 (41%, $p<0.01$) showed a significant reduction plant height compared to the WT (Table 6-4). B0% showed a similar effect like K0% where the PMEI-7 showed a significant decrease in plant height compared to the wild-type (Table 6-4). Interestingly, the results showed a consistently increase in plant height in PMEI_1, and PMEI_2 (PMEI-OE) lines under all nutrient environment when compared to the wild-type (results not significant).

TOTAL LEAF NUMBER

Total leaf number varied most significantly amongst all the transgenic, null segregant and wild-type lines under no nitrate and phosphate treatment when compared to the Hoagland solution plants (Figure 6.11 B). No significant differences in leaf number were observed under no potassium treatment except PMEI_5 ($p<0.01$) where a significant increase was found compared to the Hoagland plants. Whereas a significant reduction in PMEI_7 ($p<0.01$)

was shown in leaf number compared with the control plants (Figure 6.11 B). Boron treatment resulted a significant increase in leaf number in PMEI_5 ($p<0.001$) and PMEI_6 ($p<0.001$) whereas a reduction was observed in PMEI_7 ($p<0.01$) when compared to the control plants (Figure 6-11 B).

PMEI-OE and null segregant lines showed no significant difference in Hoagland control and no nitrate conditions when compared to the wild-type plants (Table 6-4). PMEI-2 (48%, $p<0.001$) and PMEI_4 (40%, $p<0.01$) showed a significant increase in leaf number when compared to wild type plants under no phosphate stress conditions (Table 6-4). A similar trend to plant height was noted in leaf number under K0% with a significant increase for PMEI_2 (27%) and PMEI_5 (26%) when compared to the wild type. However, PMEI_7 showed a significant ($p<0.01$) reduction by 27% was noted in K0% compared with the control. Moreover, boron stress resulted in no significant difference in leaf number compared to Bd21-3 plants. Overall, the results suggest that P0% and K0% increased the leaf number in transgenic lines overexpressing PMEI while Hoagland and B0% had no effect.

TILLER NUMBER

The plot in Figure 8C represents the tiller number at the end of the experiment. No nitrate and phosphate resulted in a dramatic and significant reduction on the tiller number for all genotypes including wild type when compared to the control nutrient condition. However, K0% treatment did not significantly affect the tiller number for overexpressing PMEI- plants and PMEI_6 however wild-type plants showed a significant reduction compared with control conditions (Figure 6-11 C). Boron deprivation had no significant effect on tiller number except PMEI_7 ($p<0.01$) which showed a significant reduction compared to the control plants (Figure 6-11 C).

Statistical analysis was performed to compare the PMEI-OE and null segregant lines with the wild-type under individual nutrient stress conditions. No significant difference was noted in Hoagland control conditions for these lines when compared to the wild-type plants. Interestingly, for all the plants no tillers could be observed under N0% (Table 6.4). Furthermore, under P0% no tillering was observed in null segregant and wild-type (Bd21-3) lines while PMEI-OE lines (apart from PMEI_5) showed some tillers. Except for one null segregant (PMEI_3664, $p<0.01$), K0% and B0% treatment showed no significant effect on tiller numbers when compared to the wild type. In summary, the results suggest that tillering is less effected in PMEI-OE lines following P0% treatment when compared to wild-type and null segregant lines.

Summarizing the phenotypic results, it appears that plant growth and development in the PMEI overexpression lines PMEI_1, and PMEI_2 was less affected by low nutrient environment conditions when compared to the wild-type *Brachypodium* plants.

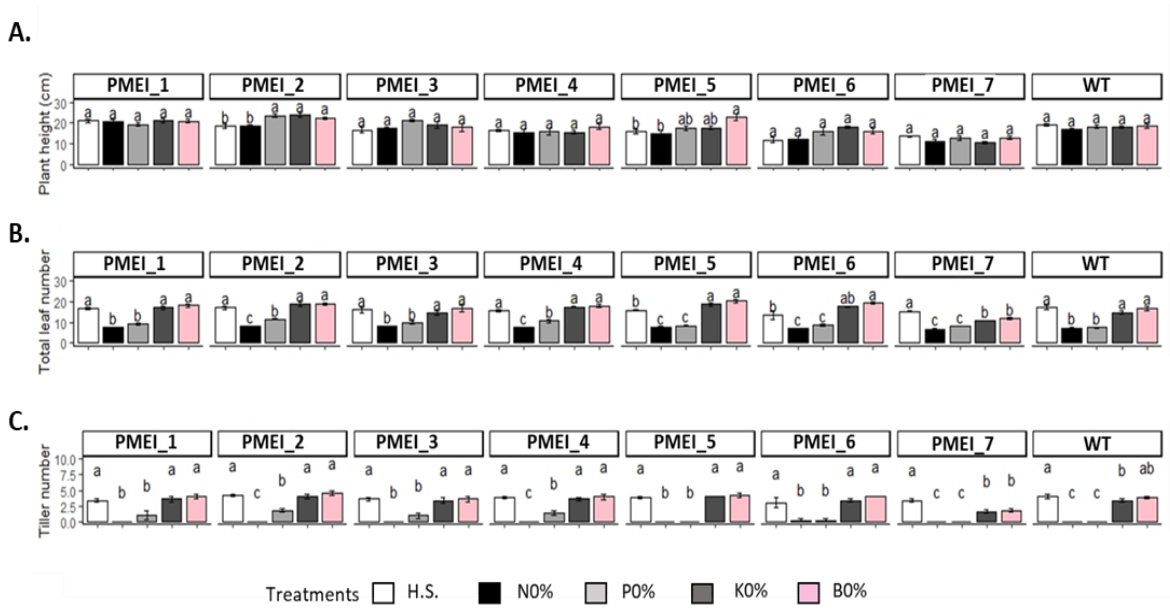

Figure 6-11: Plants growing under low nutrient compost at the greenhouse. Phenotypic traits were observed under low nutrient stress in selected upregulated PMEI, null segregant

and wild-type lines of *Brachypodium*. Statistical analysis within the selected lines amongst the treatments A. plant height (cm), B. total leaf number, and C. tiller number. Data represent the mean values ±SE (n=5) with letters showing significant difference P <0.05 [Treatments: Hoagland solution (H.S. 100%), N0%, P0%, K0% and B0%]

TOTAL SPIKELET NUMBER

To determine if spikelet number, length, and weight were affected by low nutrient availability, five plants from each treatment were scored and analysed (Figure 6.12). The number of spikelets present on the plant was counted at senescence stage. No significant difference was found in the total spikelet number under Hoagland and N0% treatment when PMEI-OE and null-segregant lines were compared to the wild-type (Figure 6-12 A). Under no phosphate condition only PMEI_4 ($p<0.05$) (PMEI-OE) showed a significant increase in spikelet number compared with the wild-type. However, no significant difference in PMEI-OE and null segregants were found in spikelet number in comparison with the wild-type under P0% (Figure 6-12 A). Potassium limitation had no significant effect on PMEI-OE lines however a significant decrease in total spikelet number was observed in PMEI_6 (null segregant, $p<0.001$). Furthermore, total spikelet number was significantly reduced ($p<0.001$) by boron limitation in the two null segregant lines (PMEI_7, $p<0.001$ and PMEI_6, $p<0.01$) compared with the wild type (Figure 6-12 A). Generally, the response of plants exposed to Hoagland, N0%, K0%, and B0% treatment showed no significant difference in PMEI-OE lines in comparison to wild-type *Brachypodium* plants, while P0% showed a significant spikelet number increase in one of the PMEI-OE lines (PMEI_4, $p<0.05$) (Figure 6-12 A).

SPIKELET LENGTH, AND WEIGHT

Treatment with full Hoagland did not result in significant differences in spikelet length for PMEI-OE and null segregants when compared with control plants, except for PMEI_1 ($p<0.01$). No significant difference was observed under nitrate limitation (Figure 6-12 B). In

addition, no significant difference in PMEI-OE lines under phosphate limitation was observed, with one of the null segregants (PMEI_6, $p<0.05$) showing a significant reduction in spikelet length. K0% also showed a significant decrease in spikelet length for one of the null segregants (PMEI_7, $p<0.001$) with no significant difference in PMEI-OE lines compared with the control (Figure 6-12 B). Boron deprivation treated plants also, resulted a significant reduction in null-segregant lines (PMEI_6, $p<0.05$; PMEI_7, $p<0.001$, respectively) while no significant difference in spikelet length was noted in PMEI-OE lines compared to the wild-type (Figure 6-12 B).

Spikelets harvested from the main stem of each genotype (n=5) from each treatment were weighed, and data was analysed (unit= g). Hoagland and no nitrate treatment suggested no significant difference in spikelet weight in all the genotypes compared with the control (Figure 6-12 C). A significant increase in spikelet weight was observed for two PMEI-OE lines after P0% treatment compared with the Bd21-3 line (PMEI_1, $p<0.01$; PMEI_3, $p<0.01$, respectively). Potassium limitation resulted in a significant reduction in spikelet weight in one null segregant line (PMEI_7, $p< 0.01$), however no significant difference was observed in the PMEI-OE lines compared with the control. A similar effect in boron limitation was observed with a slight reduction in weight in null segregant PMEI_7 ($p>0.05$) compared to the wild type as shown in Figure 6-12 C.

Therefore, the results are consistent across the PMEI-OE lines showing no significant difference in spikelet length and weight in comparison to the control lines of *Brachypodium* after low nutrient treatments.

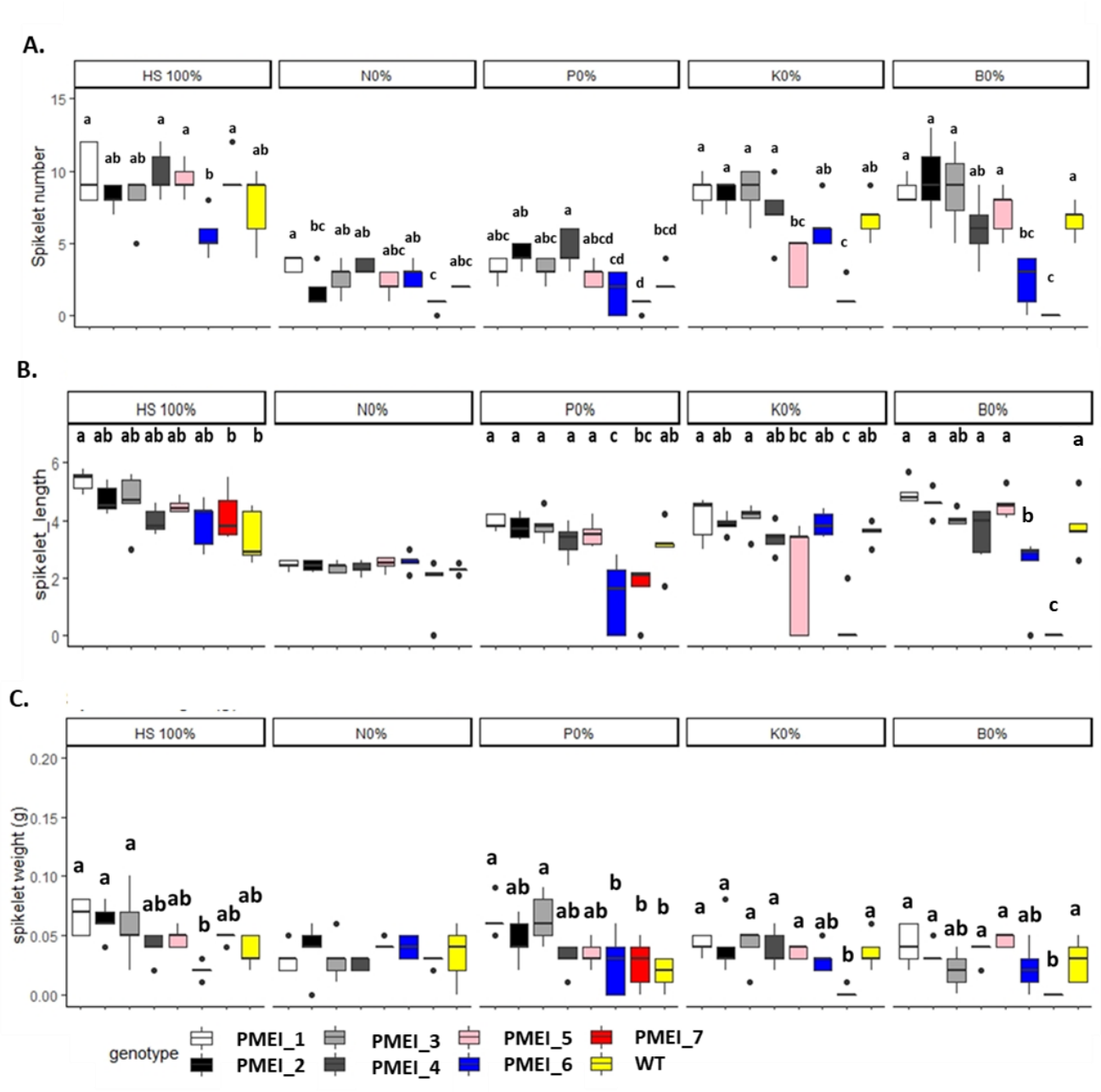

Figure 6-12: A.Total spikelet number, B. Spikelet length (cm), C. Spikelet weight (g) measured under low nutrient stress conditions (100% H.S, N0%, P0%, K0%, and B0%) in the selected PMEI-OE (A-E), null segregant (F-G) and wild-type (H) lines of *Brachypodium*. Mean values ±SE (n=5) and letters showing post-hoc analysis (P<0.05). No letters suggests that the values are not significant

6.3.5 Biomass quality analysis

It has been speculated that by overexpressing endogenous PMEI increases the saccharification efficiency by reducing cross-linking in the cell wall due to higher degree of

esterification (Lionetti *et al*., 2010; Wormit & Usadel, 2018a). However, little is known that how modifications in pectin made by genetic engineering approach can affect cell wall polymers under low nutrient availability in grasses. Therefore, this section aimed to assess if increased expression of PMEI in the PMEI-OE lines affected cell wall related traits under low nutrient environment. To address this, the biomass of the above selected lines was subjected to cell wall composition analysis and saccharification efficiency determination. Saccharification efficiency was performed by determining the amount of monosaccharides released from the cell wall upon an enzymatic treatment. The cell wall composition was determined by quantifying the most abundant monosaccharides reported in the cell wall which includes arabinose, galactose, glucose, mannose, and xylose.

6.3.6 Total monosaccharide content in PMEI-OE lines under nutrient limitation

Total amount of monosaccharides was quantified as a percentage of the cell wall weight using the AIR stem biomass material under low nutrient availability. The effect of nutrient stress on selected PMEI-OE, null segregant, and control lines for arabinose, galactose, glucose, mannose, and xylose were determined and quantified. Two-way ANOVA and post-hoc Tukey HSD test revealed the significant differences between the *Brachypodium* lines within each treatment as shown in Table 6-5. Glucose content was overall increased in PMEI-OE lines when compared to wild type plants, however this increment was only significant for PMEI_1 (56%; $p<0.001$), PMEI_2 (39%; $p<0.01$), PMEI_3 (29.1%; $p<0.05$) showed under Hoagland treatment. There was no significant effect in glucose content for most of the PMEI-OE and null segregant lines following N0%, P0%, and B0% treatment compared with the Bd21-3 lines of *Brachypodium*. (Table 6-5). However, K0% showed

significantly high in glucose content in PMEI-OE lines (PMEI_1, and PMEI_5, ranging from 45 to 39%) in comparison to the wild-type lines.

Xylose content caused significant decrease in one PMEI-OE lines ($p<0.05$) and null segregant ($p<0.001$) under Hoagland treatment compared with the control (PMEI_1= -18%, PMEI_6= -26%, respectively). Interestingly, an increased xylose content was observed as that of glucose content under nitrate limitation in PME_1 (24%, $p<0.05$) compared with the control. Phosphate limitation resulted in a significantly lower xylose content in five PMEI-OE lines (PMEI_1= -30%, $p<0.001$; PMEI_2= -29%, $p<0.001$; PMEI_3= -31%, $p=0.001$; PMEI_4= -31%, $p<0.001$, PMEI_5= -22%, $p<0.05$, respectively) compared with wild-type lines (control). However, no significant difference was found in K0%, except PMEI_6 ($p<0.05$) showing an increase by 44% in xylose content compared with the control (Table 6.4). A significant increase in PMEI_1 (66%, $p<0.001$) and PMEI_6 (55%, $p<0.05$) was found under B0% compared to the wild type.

After 100% Hoagland and nitrate limitation treatment, the arabinose content was not significantly different between PMEI-OE, null segregant and wild-type lines. P0% significantly lowered the arabinose content in three PMEI-OE lines ($p<0.001$) (PMEI_1, 62%; PMEI_3, 58%; PMEI_4, 60%) compared with the wild-type. K0% and B0% showed no significant difference in arabinose content in all the genotypes. Interestingly, galactose content showed a significant reduction in PME_1 (52%, $p<0.001$), PMEI_3 (36%, $p<0.05$), and PMEI_4 (50%, $p<0.001$) in comparison to the wild-type lines of *Brachypodium* after treatment with full Hoagland. PMEI-OE lines showed no significant difference in galactose content under N0% and K0% compared with the control lines (Table 6-5). Treatment with P0% showed a statistically significant reduction ($p<0.001$) in galactose content in four

selected PMEI-0E lines (PMEI_1=77%, PMEI_2=83%, PMEI_3=80%, PMEI_4=86%, and PMEI_5=31%, respectively) compared with the control. Galactose content after boron treatment was significantly increased by ~3-fold in PMEI_1 ($p<0.05$) and the null segregant PMEI_6 ($p<0.05$) compared with the control (Table 6-5).

Mannose content showed no significant difference in PMEI-OE under Hoagland, P0%, and K0% treatment compared with the control. A significant increase (>3-fold) occurred in the PMEI_1 ($p<0.01$) line under nitrate limitation while 0% boron treatment resulted in a >5-fold increase in PMEI_3 ($p<0.01$) compared with the wild-type line (Table 6-5).

Table 6-5: Values expressed as a percentage of cell wall material dry weight (%CWM) for low nutrient treatment in PMEI-OE, null segregant, and wild-type lines of *Brachypodium* and are presented as mean values ±S E (n=2 biological and n=3 technical replicates). For statistical significance ANOVA test ($p<0.05$) and post-hoc Tukey's test for statistical difference was also performed. '***' $p<0.001$, '**' $p<0.01$, '*' $p<0.05$

Treatment	*Brachypodium* lines	Glucose (wt% CWM)	Xylose (wt% CWM)	Arabinose (wt% CWM)	Galactose (wt% CWM)	Mannose (wt% CWM)
100% H.S.	PMEI_1	38.1 ±2.6***	23.5 ±0.5*	6.0 ± 1.2	3.12 ±0.06***	0.67 ±0.02
	PMEI_2	33.8 ±0.5**	26.0 ±1.6	7.7 ±1.4	5.22 ±0.6	0.92 ±0.2
	PMEI_3	31.5 ±0.7*	24.5 ±1.3	7.0 ±1.3	4.14 ±0.5*	0.73 ±0.21
	PMEI_4	29.7 ±1.8	24.0 ±1.2	7.3 ±1.5	3.29 ±0.12***	0.61 ±0.12
	PMEI_5	27.0 ±0.6	29.0 ±0.3	7.7 ±1.1	6.76 ±0.1	2.21 ±0.45
	PMEI_6	24.9 ±2.8	21.2 ±0.7***	6.1 ±0.5	8.42 ±0.2	1.06 ±0.02
	PMEI_7	23.1 ±1.5	26.8 ±1.2	9.4 ±1.0	6.94 ±0.9	0.78 ±0.1
	Bd21-3	24.4 ±1.0	28.8 ±1.6	7.4 ±0.8	6.53 ±0.22	1.83 ±0.54
N0%	PMEI_1	29.6 ±1.5	35.0 ±1.0*	9.1 ±1.6	7.05 ±0.7	3.63 ±0.4 **
	PMEI_2	18.3 ±1.1	30.4 ±1.1	8.0 ±1.5	4.94 ±0.7	1.04 ±0.32
	PMEI_3	22.8 ±1.4	32.9 ±1.7	7.8 ±1.0	5.86 ±0.8	2.21 ±0.4
	PMEI_4	27.5 ±3.4	34.0 ±0.8	7.8 ±1.2	5.20 ±0.9	0.96 ±0.04
	PMEI_5	24.0 ±1.3	33.0 ±1.9	7.9 ±1.1	4.85 ±0.12	0.86 ±0.4
	PMEI_6	23.5 ±1.5	32.8 ±1.5	7.2 ±1.0	5.76 ±1	1.20 ±0.3
	PMEI_7	20.1 ±1.4	23.6 ±2.2	6.5 ±1.0	7.85 ±0.41	2.63 ±0.4
	Bd21-3	22.0 ±1.3	28.2 ±1.4	7.6 ±1.5	4.42 ±0.8	1.11 ±0.01
P0%	PMEI_1	29.9 ±1.2	23.5 ±0.9***	2.5 ±0.2**	1.40 ±0.2***	0.36 ±0.07
	PMEI_2	25.2 ±1.5	23.7 ±2.5***	3.7 ±0.1	1.05 ±0.03***	0.24 ±0.02
	PMEI_3	28.2±1.9	23.3 ±1.9***	2.8 ±0.3*	1.22 ±0.05***	0.38 ±0.06
	PMEI_4	26.3 ±0.4	23.1 ±1.3***	2.7 ±0.3*	0.84 ±0.21***	0.22 ±0.8
	PMEI_5	28.5 ±3.1	26.2 ±1.1*	5.7 ±0.6	4.23 ±0.48**	2.71 ±1.0
	PMEI_6	24.1 ±1.7	29.7 ±2.1	5.0 ±0.6	7.22 ±0.29	3.05 ±1.4
	PMEI_7	20.0 ±2.8	32.2 ±0.9	6.0 ±0.6	6.32 ±0.43	6.29 ±0.3**
	Bd21-3	30.5 ±3.3	33.6 ±0.7	6.7 ±1.2	6.15 ±0.34	1.43 ±0.05
K0%	PMEI_1	32.9 ±2.0***	29.6 ±1.7	10.6 ±3.0	2.86 ±0.14	0.65 ±0.05
	PMEI_2	27.3 ±1.9	26.6 ±0.9	6.2 ±1.2	3.10 ±0.09	0.64 ±0.03
	PMEI_3	27.0 ±2.4	22.7 ±1.7	6.0 ±1.1	3.55 ±1.2	15.27 ±32
	PMEI_4	22.2 ±1.5	22.5 ±0.9	5.8 ±0.9	2.28 ±0.23	2.24 ±1.8
	PMEI_5	31.6 ±1.6*	30.1 ±1.4	5.2 ±0.4	5.37 ±0.5	3.85 ±1.2
	PMEI_6	29.1 ±1.6	35.6 ±1.6*	6.3 ±0.1	4.83 ±0.05	0.84 ±0.01
	PMEI_7	20.2 ±1.7	23.1 ±1.2	5.9 ±0.6	1.95 ±0.9	0.33 ±0.16
	Bd21-3	22.7 ±0.7	24.7 ±1.9	4.6 ±0.3	2.91 ±0.53	2.31 ±0.16
B0%	PMEI_1	29.1 ±1.9	30.0 ±1.0***	5.9 ±1.3	4.66 ±0.8*	0.63 ±0.07
	PMEI_2	21.0 ±4.4	23.8 ±0.8	6.4 ±0.9	1.16 ±0.04	0.47 ±0.03
	PMEI_3	26.3 ±4.6	24.1 ±1.5	5.7 ±0.9	2.63 ±0.46	3.76 ±0.7**
	PMEI_4	26.3 ±0.5	18.9 ±1.3	2.36 ±0.12	2.98 ±1.2	0.61 ±0.04
	PMEI_5	28.5 ±2.7	19.7 ±1.2	2.36 ±0.03	1.77 ±0.02	0.48 ±0.08
	PMEI_6	24.1 ±1.7	27.9 ±4.1*	2.91 ±0.12	4.90 ±0.1*	0.88 ±0.1
	PMEI_7	20.0 ±2.8	21.0 ±0.7	2.24 ±0.03	4.25 ±0.9	2.76 ±1.1
	Bd21-3	22.7 ±0.7	18.0 ±1.6	2.24 ±0.03	1.48 ±0.03	0.71 ±0.02

In summary, the effect of nutrient stress on the monosaccharide content seems specific according to the nutrient limitation condition applied. Overall, Hoagland treatment showed

increased glucose and reduced xylose, arabinose, galactose and mannose in PMEI-OE compared to the wild type lines (Bd21-3). P0% treatment dramatically decreased the xylose and arabinose content in PMEI-OE lines however, increased sugar composition in Bd21-3 plants. While in PMEI-OE lines the levels of these monosaccharide remained closer to those observed when plants were treated with N0%, K0%, and B0%.

6.3.7 Effect of nutrient stress on biomass saccharification efficiency

Enzymatic saccharification assays were performed on the stem biomass samples harvested at the end of nutrient stress treatment. The saccharification potential was quantified as the amount of monosaccharides released as D-arabinose (AraE), D-glucose (GluE) and D-xylose (XylE) from the leaf CWM by performing enzymatic digestion (da Costa et al., 2014). The released monosaccharides in the supernatant were quantified and expressed as a percentage of the available sugar. The enzymatic saccharification efficiency for GluE, XylE and AraE was calculated for stem samples of the PMEI-OE, null-segregants, and WT lines are shown in Table 6.6. The experiment was performed in two biological and three technical replicates for each PMEI-OE, null segregant and wild-type (control) line. Values are calculated and presented as mean ± standard error between the replicates in Table 6-6.

The full Hoagland treatment resulted in an overall increase in enzymatic glucose release in the PMEI-OE lines, whereas a significant increase in GluE was only found in PMEI_1 (57%) and PMEI_2 (62%) compared with the Bd21-3 lines of *Brachypodium* (Table 6.6). GluE following N0%, P0%, K0%, and B0% treatment resulted in an increase GluE, however, no significant difference was noted in PMEI-OE lines when compared to the control (Table 6-6).

There was a general tendency for a decrease of enzymatic xylose release in the transgenic lines following Hoagland treatment compared to wild-type plants. XylE release following by 45% and B0% by 50% treatment showed a significant increase in one PMEI-OE line (PMEI_5, $p<0.01$) compared with the control lines (Table 6-6). Consequently, no significant difference was obtained in XylE release under nitrate and phosphate limitation compared to the control plants.

Hoagland treatment resulted in a significant increase in AraE from stem biomass of PMEI-OE lines when compared to the wild-type. OE line PMEI_3 showed a 3-fold increase in AraE in comparison to the wild-type ($p<0.001$). N0% induced treatment condition resulted in no significant difference in all the PMEI-OE, and null segregant lines in comparison to the wild-type as shown in Table 6-6. Following no phosphate treatment, four PMEI-OE lines showed a significant increase in AraE by ~1-fold (PMEI_1, and PMEI_2, $p<0.001$ for both, PMEI_3=$p<0.01$, and PMEI_4 =$p<0.05$) when compared to the wild type (Table 6-6). Potassium and boron limitation gave similar results to N0% as no significant difference in AraE release was found when compared to the wild-type plants.

The results of this experiment suggested that the overexpression of PMEI generally does not affect the enzymatic sugar release from stem material when plants are exposed to nutrient stress. However, under conditions where nutrients are not limiting, it appears that the increased expression of PMEI can enhance the enzymatic release of glucose and arabinose from stem biomass.

Table 6-6: Enzymatic saccharification efficiency in stem samples of PMEI-OE, null segregant and wild-type lines of *Brachypodium* under low nutrient availability. Mean values ± SE, letters show post-analysis (Tukey's test). Statistical significance difference in comparison to the wild-type lines under each treatment (n= 2 biological and n=3 technical replicates)

Treatment	*Brachypodium* lines	Glucose	Xylose	Arabinose (AraE)
100% H.S.	PMEI_1	26.6 ±1.7ab	16.8 ±2.7a	0.8 ±0.06ab
	PMEI_2	27.3 ±0.8 a	20.8 ±1.0a	0.7 ±0.03 ab
	PMEI_3	23.7 ±0.8 abc	17.8 ±0.7a	1.2 ±0.40a
	PMEI_4	23.6 ±2.4abc	18.1 ±0.8a	0.7 ±0.04ab
	PMEI_5	19.8 ±0.05bcd	18.4 ±0.6a	0.8 ±0.05ab
	PMEI_6	15.6 ±2.4d	15.2 ±1.2a	0.9 ±0.10ab
	PMEI_7	13.4±0.9d	19.5 ±2.4a	0.3±0.06b
	Bd21-3	16.9±0.8cd	16.9 ±1.4a	0.3±0.0b
N0%	PMEI_1	13.6 ±2.7a	17.2 ±1.9a	0.26 ±0.05a
	PMEI_2	8.4 ±0.5a	17.4 ±1.5a	0.28 ±0.04a
	PMEI_3	13.3 ±1.5a	17.7 ±2.3a	0.28 ±0.03a
	PMEI_4	7.3 ±0.7a	20.5 ±1.1a	0.34 ±0.04a
	PMEI_5	14.1 ±3.9a	19.6 ±2.8a	0.24 ±0.02a
	PMEI_6	6.5 ±1.0a	16.3 ±2.3a	0.4 ±0.11a
	PMEI_7	10.7 ±1.2a	16.2 ±2.1a	0.4 ±0.06a
	Bd21-3	6.5 ±10.5a	18.5 ±2.0a	0.34 ±0.06a
P0%	PMEI_1	13.4±4.1a	12.3 ±1.9b	1.6 ±0.04a
	PMEI_2	12.6 ±2.4a	12.2 ±1.9b	1.7 ±0.13a
	PMEI_3	15.9 ±1.4a	14.6 ±0.8b	1.46 ±0.13ab
	PMEI_4	11.8 ±2.7a	13.0 ±1.5b	1.26 ±0.1abc
	PMEI_5	11.0 ±2.7a	11.8 ±1.2b	0.44 ±0.03d
	PMEI_6	16.1 ±2.7a	15.9 ±0.9ab	0.91 ±0.2bcd
	PMEI_7	7.8 ±1.0a	24.1 ±4.1a	0.7 ±0.17cd
	Bd21-3	5.7 ±1.0a	17.3 ±1.6ab	0.6 ±0.06d
K0%	PMEI_1	11.1 ± 3.0a	15.5 ±0.8ab	1.6 ±0.5a
	PMEI_2	12.3 ±3.3a	15.0 ±1.7ab	0.6 ±0.1a
	PMEI_3	11.0 ±3.5a	14.8 ±1.1ab	0.8 ±0.3a
	PMEI_4	12.4 ±2.7a	13.1 ±1.9b	0.5 ±0.1a
	PMEI_5	5.4 ±0.4a	19.6 ±1.0a	6.5 ±5.8a
	PMEI_6	4.8 ±1.3a	15.2 ±0.8ab	0.48 ±0.2a
	PMEI_7	4.9 ±0.9a	12.5 ±0.8b	7.6 ±7.0a
	Bd21-3	4.5 ±0.3a	13.5 ±0.9b	0.4 ±0.04a
B0%	PMEI_1	16.5 ±5.6a	10.3 ±0.8b	4.5 ±3.9a
	PMEI_2	15.7 ±3.1a	12.2 ±1.1ab	0.4 ±0.04a
	PMEI_3	14.9 ±5.1a	11.7 ±1.3b	0.8 ±0.3a
	PMEI_4	11.0 ±3.5a	10.9 ±0.4b	0.7 ±0.2a
	PMEI_5	16.0 ±4.1a	16.8 ±1.3a	0.9 ±0.2a
	PMEI_6	10.7 ±2.3a	12.4 ±1.0ab	0.6 ±0.1a
	PMEI_7	10.1 ±2.0a	11.3 ±1.1b	0.5 ±0.0a
	Bd21-3	13.3 ±0.5a	11.2 ±1.2b	0.4 ±0.02a

6.4 Discussion

Plant cell wall is the first line of defensive barriers where pectin comprises of only 5% of the cell wall content in grasses (Vogel J., 2008); however, they play a very essential part in the complex cell wall matrix. Pectins have been shown to be involved in many diverse processes, including plant growth, development, morphogenesis, defence, cell-cell adhesion, wall structure, signalling, cell expansion, wall porosity, binding of ions, growth factors and enzymes, pollen tube growth, seed hydration, leaf abscission, and fruit development (Mohnen, 2008; Ridley *et al*., 2001). There are three main structural classes of pectin in cell walls, including those of grasses, namely homogalacturonan (HG), rhamnogalacturonan II (RG-II), and rhamnogalacturonan I (RG-I). In functional terms, RG-I is not well defined, although both galactan and arabinan polymers are implicated in contributing to cell wall mechanical properties and to cell wall flexibility (L. Jones *et al*., 2003; Louise Jones *et al*., 2005; Moore *et al*., 2008; Ulvskov *et al*., 2005).

Brachypodium is a temperate wild grass and an emerging, very promising model system for studying grain, energy, forage (Luo *et al*., 2011). Phylogenetic surveys consider *Brachypodium* most closely related to wheat, barley, maize, sorghum, rice. This makes the undomesticated crop an interesting grass specie to understand environmental stress tolerance mechanisms that have been lost during domestication of cereal crops. Previous studies have suggested that cell wall formation and expansion related Bradi3g45080 gene functioning for pectinesterase inhibitor was elevated by water deficit stress in *Brachypodium* plants (Verelst *et al*., 2013). Therefore, in this chapter, we investigated the overexpression of the cell wall-related PMEI gene in selected transgenic lines of *Brachypodium* under drought stress to validate observations made by a previous researcher.

Screening of the independent transgenic lines using RFP marker was performed and the selection of homozygous lines, null segregants and wild type were made. The expression of selected overexpressing lines was measured using real-time PCR and showed an increased expression level compared to wild-type ones. At the molecular level, PMEI overexpression was measured by real-time PCR analysis to determine the expression of the gene in transformed transgenic lines (PMEI_1-5), null segregants (PMEI6 and PMEI_7) and wild-type *Brachypodium* lines. In particular, the PMEI_3 transgenic line showed a significant increase in the expression of the target gene compared with the control (Lionetti *et al*., 2007; Huang *et al*., 2017; Wu *et al*., 2018).

This was followed by a PME radial gel diffusion assay for the selected transgenic PMEI overexpressing lines (Figure 6-7). In enzymatic assays, PMEI_1 and PMEI_3 significantly inhibited activity of pectin methylesterase (PME) by showing a reduction in halo formation when compared to the wild type (6-7 B). The decrease in PME activity was likely due to the interaction between the overexpressed inhibitor and endogenous enzyme. It is commonly known that pectin methylesterification plays a vital role in plant growth, it is maximal during cell expansion stage and gradually decreases as cell elongation stops (Lionetti *et al*., 2007). Also, the degree of methylesterification of pectins related to PME and PMEI can influence the cell wall mechanism (Peaucelle *et al*., 2012). The similar results were found in Arabidopsis with functionally characterized and isolated pepper gene, $CaPMEI_1$ proteins which inhibited PME activity (An *et al*., 2008). Therefore, in this study, it was inferred that PMEI gene affects the pectin methylesterification and thereby, it's essential to study cell wall porosity by methylesterification in future studies.

Overall this chapter aimed to investigate the influence of drought and re-watering treatment on the overexpressing PME inhibitors transformed lines of *Brachypodium*. Another aim was to evaluate phenotypic and saccharification efficiency in transformed and wild-type lines in response to nutrient limitation.

Phenotypic trait evaluation under drought treatment

Taking real-time PCR and radial assay activity into consideration, it was decided to perform a more extensive examination of physiological measurements in PMEI-OE and wild-type lines of *Brachypodium* under drought and re-watering treatment. This study observed a substantial effect on various phenological traits under drought stress even when the Bradi3g45080 gene was up-regulated. Five genetically modified events, two null events, and one control line were exposed to three treatments which included water deficit, re-watered treatment, and well-irrigated conditions during the experiment. The treatment affected plant's productivity as measured by above-ground parameters across the treatments. The fact that this study tested PMEI upregulated lines in the controlled environment is particularly important, considering that few studies have reported results from cell wall-related PMEI gene overexpressing under drought in *Brachypodium*. An *et al*. (2008) showed the overexpression of PME inhibitor (CaPMEI1) demonstrated drought tolerance in pepper plants during post-germination growth.

Conversely, the observations made in this study for phenotypic measurements in drought-stressed treatment were reduced in the transformed lines compared to the wild-type (Bd21-3). Unfortunately, there was a pronounced reduction in plant height in two transgenic lines, PMEI_1, PMEI_3, and one null segregant PMEI_7 under water deficiency compared to the wild-type lines. Some plants can escape drought stress by changing their phenology and

accelerating their life cycle to reproduce to mitigate severe stress known as escape strategy (Kooyers 2015). Drought escape can also refer to the artificial adjustment of plant's growth period, life cycle, or planting time to prevent them from encountering local seasonal or climatic droughts (Fang & Xiong, 2015).

Interestingly, under re-watering condition PMEI_1 maintained its stability and showed no significant effect in plant height compared with control (Table 6-3). Leaf and tiller number had no significant effect under well-watered conditions; however, dehydration caused a significant reduction in PMEI_5 for leaf number, and PMEI_1, PMEI_3 and PMEI_7 (null segregant) for tiller number compared with the wild type. PMEI_5 did not recover after 4 days re-watering condition, whereas no difference in tiller number was found in the modified lines when compared to the control. In this study we also found PMEI_3 and PMEI_7 (null segregant) was significantly showing lower fresh and dry biomass when compared with wild type under drought. In contrast, transgene overexpression did not cause any obvious phenotypic difference under drought stress compared with the wild type. Successful overexpression of PMEI was accomplished in the present study, however not leading to detectable phenotype. It is thus most likely that this strategy was not functional in *Brachypodium* and the level of overexpression was insufficient for phenotype detection under drought treatment. *Brachypodium* recognized as a model system by Draper *et al*. (2001) followed by first publication of successful overexpression and downregulation of genes of interest after a decade was published by Vain P. (2011) suggesting its close relationship to the major cereal and bioenergy crops like Wheat, Maize, Sorghum, Miscanthus, Switchgrass (Vogel *et al*., 2010). Therefore, further evaluation of phenotypic

and biomass quality in *Brachypodium* lines under nutrient limitation was made during this study.

Phenotypic trait evaluation under reduced nutrient treatment

Brachypodium, a model system, enables the study of the genetics and genomics of nutrient stress responses affecting major cereal and bioenergy crops. Nutrient limitation is of great importance and majorly experienced by agriculture, thus affecting the biomass quality of the growing crops. Therefore, in the present study, we were interested in understanding if transgenic lines show adaption traits and can alter the quality of biomass conversion to low nutrient stress conditions. Previous studies have shown that the PMEI overexpressing gene inhibits cold, drought, salinity, and pathogen stress (Verelst *et al*., 2013; Chen *et al*.,2018; Jeong *et al*., 2018). It is interesting to investigate the role of PMEI in plant nutrient response. In this chapter, Hoagland treatment showed no reduction measured in plant height in modified PMEI-OE lines of *Brachypodium*.

In contrast, a similar effect was found in reduced nitrate, phosphate, and boron treatments compared to wild-type treatments. Interestingly, potassium starvation showed a significant increase in plant height in PMEI_2 compared with the wild type. A similar result was observed in leaf and tiller numbers for Hoagland and reduced nitrate and boron conditions comparable to the wild type. A significant increase was observed in PMEI_2 and PMEI_4 transgenic lines for leaf number under low phosphate treatment and PMEI_2 under potassium limitation compared with the control. Therefore, the phenotypic results suggested that PMEI_2 and PMEI_4 showed tolerance to induced low phosphate and potassium treatment compared to the wild type (Table 6-4). The results were consistent with the previous studies where seed germination, root growth, and survival rate were

enhanced under cold and salt stress and improved cell wall immunity against the pathogen in Arabidopsis (Lionetti *et al*., 2007).

Total monosaccharide content in PMEI-OE lines of *Brachypodium* under nutrient limitation

Phenotyping of the PMEI overexpressing lines revealed similar or no significant differences in plant height, leaf and tiller number, exceptions being PMEI_2 showed increased height and leaf number compared with WT under P0%. In addition, *Brachypodium's* phylogenetic and sequenced genome has collinearity with agronomically major grasses thus, making it a suitable model for biomass grasses (Garvin *et al*., 2010). The modification of the monosaccharide composition of the cell wall for all the PMEI-OE, null segregants, and wild type lines of *Brachypodium* induced by nutrient stress was estimated. Complete Hoagland treatment resulted in an increased glucose content and no difference in arabinose and mannose monosaccharides in PMEI-OE lines of *Brachypodium*. The results are in agreement to da Costa *et al*. (2019). The results further showed a significant reduction of xylose (PMEI_1), and galactose (PMEI_1, PMEI_3, PMEI_4) under hoagland treatment. PMEI_1 showed a significant increase in xylose and mannose with reduced nitrogen treatment but no significant effect in glucose, arabinose, and galactose content. The result on total monosaccharide content under nitrogen limitation is in contrast with what found by da Costa *et al*. (2019) in Micanthus genotypes. In PMEI-OE lines a reduced saccharification yield under phosphate limitation was found which resulted in a significantly lower amount of xylose and galactose compared to the wild type. Potassium limitation showed a significant increase in glucose content only in PMEI_1 with no effect in monosaccharide content in PMEI-OE lines of *Brachypodium*. Boron limitation showed a similar trend to nitrogen limitation where a significant increase in xylose and galactose was found in PMEI_1. It also

caused a significantly higher amount of mannose in PMEI_3 line when compared to the control.

Saccharification efficiency in PMEI-OE lines of *Brachypodium* under nutrient limitation

Previous studies have suggested that the cell wall is the key component and plays a vital role in plant resistance to abiotic stress conditions, which can cause alterations in cell wall architecture (Le Gall *et al*., 2015). This alteration in the cell wall could increase or decrease cell wall stiffness or loosening. Previous studies have suggested that *Brachypodium distachyon* portrays its ability in various spheres of grass research, among other cell wall and saccharification potential (Gomez *et al*., 2008; Kellogg, 2015; Głazowska *et al*., 2018). PMEI overexpression under disease resistance is well documented in the literature, although the demethylesterification role under nutrient limitation remains elusive (Lionetti *et al*., 2007; Wormit & Usadel, 2018). Enzymatic saccharification was determined as a percentage of reducing sugars released on the total sugar content measured. The present study showed an increased saccharification efficiency in PMEI-OE (PMEI_1, PMEI_2, and PMEI_3) under control conditions suggesting a reduction of de-methylesterification of HG. To summarise, the results showed an increased enzymatic saccharification efficiency, as has been demonstrated in the previous study (Lionetti *et al*., 2007). However, PMEI-OE lines showed cell wall recalcitrance in response to nutrient stress by showing no effect on saccharification efficiency.

6.5 Conclusion

In the present research, five independently transformed lines, null segregants, and wild type lines were screened for transgene expression levels and evaluated phenotypically to nutrient limitation. The selected lines were treated with nutrient stress treatment and the

efficiency of enzymatic conversion of cell wall material into fermentable monosaccharides was assessed. The cell walls contain high amounts of cell wall polymers which resist the plant cell wall destruction under nutrient limitation and are thus a desirable trait for biomass quality of cereal crops. This resistance of plant cell walls to deconstruct monomeric sugars is known as recalcitrance, measured by saccharification yield, which is the total sugar released by enzymatic treatment of cell wall polysaccharides.

On the other side, this study's altered or upregulated cell wall-related gene resulted in a higher recalcitrance to enzymatic treatment under nutrient limitation. This is the first report of differences in saccharification efficiency related to the PMEI-OE lines of *Brachypodium* under nutrient limitation. In this study, under 100% Hoagland treatment in bulrush compost resulted in the highest saccharification yield from stems in PMEI-OE lines when compared to the wild type suggesting the plants were less recalcitrant under complete nutrient conditions also agrees with previous studies in Miscanthus (da Costa *et al*., 2019), wheat (H. Zhang *et al*., 2013) and switchgrass (Crowe *et al*., 2017). However, to my knowledge, this is the first report of nutrient limitation in PMEI-OE lines of *Brachypodium distachyon* on saccharification efficiency measurement and provides information that could be used to enhance biomass bioenergy-related traits in cereal crops. Therefore, a more detailed study on cell wall architecture should be conducted under nutrient limitations.

Chapter 7 : General discussion

The present experimental work of my thesis aimed to screen and select low nutrient effects on phenotypic traits using *Brachypodium distachyon* genotypes. This hypothesis was tested by investigating the phenotypic and biomass quality measurements and assessing natural variation in response to nutrient limitation. The experiments in the previous chapters showed phenological change in Brachypodium populations along the gradient in response to nutrient limitation. However, flowering phenology revealed as an adaptation to nitrate and phosphate treatments in RIL population, regardless of the F8 segregated population derived from ABR6 and Bd21.

Brachypodium distachyon, a model organism, was selected due to its dynamic research tool availability that offers small physical stature, fully sequenced smallest diploid genome with a high recombination rate and natural variation (Ream *et al*., 2015; Woods D. *et al*., 2016). *Brachypodium* has developed new concepts for improving cereal and bioenergy grasses for food, feed, and biofuel production. The environmental diversity associated with the more extensive geographic range in which *Brachypodium* genotypes can be further found facilitates the transfer of findings from a model species to crops like wheat, barley, Miscanthus, and switchgrass.

Today *B*. *distachyon* is considered an ideal and robust model species based on research on plant development, abiotic stress, plant-microbe interactions, evolutionary biology, ecology research etc. However, species like *B*. *stacei* is a small diploid and *B*. *hybridum* allotetraploid annual grass form a part of trio of Brachypodium species i.e. *B*. *distachyon* (2n= 10), *B*. *stacei* (2n=20) and *B*. *hybridum* (2n=30). It has been suggested that *B*. *hybridum* is derived from *B*. *distachyon* and *B*. *stacei* or their ancestors. The small stature of *B*. *hybridum* and *B*. *stacei*

with soon completed genome will provide an exceptional opportunity to study genetic variation and gene analysis on molecular level (https://jgi.doe.gov/our-science/science-programs/plant-genomics/brachypodium/).

Due to short lifecycle and high recalcitrance trait in response to nutrient limitation *Brachypodium* specie found in the study suggested that it could have not been used to study biomass quality in grasses. In the higher yield development of biofuel crops, delayed flowering is considered an essential trait; however, with the nutrient stress conditions, *Brachypodium distachyon* species flowered early and completed its lifecycle quickly, thus suggesting that other *Brachypodium* species would have been ideal for studying nutrient limitation. In addition, it's thought that grasses like wheat, barley, and sorghum lose some variability in flowering time through domestication. Therefore, *Brachypodium* species selection was justified in the present study due to the considerable variation found amongst natural accessions for flowering time traits.

Chapter 2 involved screening low nutrient concentrations in two geographical and genetic distant ABR6 and Bd21 *Brachypodium* genotypes. These two genotypes were selected primarily due to the availability of resources present at IBERS, Aberystwyth. The hypothesis was rejected regarding K, the third most crucial macronutrient and the micronutrient B, as no significant results as a function of different dose-response in above-ground and root length measurements compared to the control were found. B is involved in many physiological processes, which can affect plants grown in toxicity and deficiency; however, no significant response was found for boron doses in the present study (Shireen *et al*., 2018). Further investigations on B deficiency in hydroponics would have been an ideal system to work in future to obtain precise results. K and B stressed plants followed the same trend in

both the accessions and showed a clear adaptive response to these stressors (Thornburg *et al*., 2020). The study unravelled the answer to low nutrient treatment in the model specie for grasses – *Brachypodium distachyon*.

ABR6 x Bd21 *Brachypodium* population has since been published by Bettgenhaeuser *et al*. (2017) to identify genetic loci associated with flowering time previously and due to its easy availability with existing RIL F8 population at Aberystwyth University led to the detailed analysis using the above genotypes. However, chapter 4 provided evidence that based on biomass and spikelet morphology, Iraqi and Turkish parental genotypes of *Brachypodium* are ideal candidates for future studies if sufficient resources become available.

Chapter 3 explored using the semi-automated platform, also called 'smart-glasshouse', to monitor the response of ABR6 and Bd21 plants under selected nutrient dosage. These plants were grown under the same controlled and monitored conditions, including temperature, humidity, light, and watering, which allowed maintenance of a homogenous environment across the experiment. The reduction in uncontrolled environmental variation, especially in watering, enabled more accurate measurements of the effect of the various nutrient limitation treatments. However, complete automation of image analysis on this platform is not available in the present study. Despite these technical shortcomings in the experiment, it was clear that N and P limitations would be interesting to evaluate available *Brachypodium* accessions for further analysis. Chapter 3 and chapter 2 showed similar effects under nutrient limitation by showing species-specific responses. Potassium and boron limitations showed identical results in physio-morphological measurements in chapters 2 and 3 despite varied nutrient-deprived treatments.

Chapter 4 evaluated 17 *Brachypodium* ecotypes of different origins and plants exposed to low nutrient environmental conditions. *Brachypodium* accessions showed tolerance and susceptibility, thus suggesting potential parental ecotypes implications for the future application of the genetic basis of nutrient tolerance in other important crop species.

The study aimed to detect P and N efficiency-related QTLs regulating phenotypic traits, including flowering time, using the RIL population of Brachypodium distachyon derived from a cross between ABR6 and Bd21 and to associate QTLs with functional genes involved in nutrient resistance. Findings in chapter 5 lead to the identification of significant but minor QTLs using mapping RIL population influenced by nutrient starvation. One possible reason for QTL with minor effects found in the study could be fewer SNP genetic markers available for the F8 RIL population. However, a considerable phenotyping strategy should be applied to select QTLs in future experiments by repeating the experimental setup. Furthermore, flowering time candidate genes such as VRN1 and VRN2 may be expected, given the vernalisation strategy. Interestingly, the study showed that these genes work experimentally under nutrient limitations.

Chapter 6 describes a comprehensive genotypic and phenotypic analysis of PMEI-OE lines under abiotic stress. Drought escape strategy was employed in wild-type plants to mitigate the water stress. Phenological traits like flowering and senescence timing, play a vital adaptive role under drought and should be measured in future studies. As PMEs are essential in cell elongation, leaf size measurements and root phenotyping might be valuable. Previous studies also suggested that root growth analysis is considered an ideal system to study cell growth; therefore, investigation of root architecture should be investigated in the future (Lionetti *et al*., 2007). It would have been interesting to conduct parallel research by

developing knockout mutant lines or down-regulation of *Brachypodium* species to regulate cell wall thickening and thus helping to understand the growth dynamics in grasses in response to abiotic stresses.

Key findings

- Nitrate and phosphate significantly reduced above-ground and below-ground measurements.
- ABR6 genotype showed a significant reduction in enzymatic sugar release impacting biomass recalcitrance under nutrient treatment in both glasshouse and automated PSI system
- Bd30-1 x Bd21, Luc1 x Jer1, and Bd29-1 x Koz-3 were the potential candidates found after phenotypic measurements
- Seven significant QTLs were reported in the present study under control and nutrient limitation in the RIL population derived from ABR6 and Bd21 genotypes
- VRN1 and VRN2 flowering time genes were found under nitrate and phosphate limitation
- PMEI_1 and PMEI_3 showed significant reduction in radial diffusion assay thus inhibiting the methylesterification
- PMEI_1, PMEI_2, and PMEI_3 showed a significant increase in saccharification efficiency by increasing the enzymatic sugar release compared to the wild-type under control conditions

Conclusions and future work

This study focused on studying phenotypic, molecular and genetic effects for agriculturally relevant traits on different *Brachypodium* accessions, or transgenic lines, for example, under nutrient and drought stress. The results and experimental work presented in the present research serve as a starting point for a better understanding of nutrient-limiting stress tolerance, thereby leading to the sustainable improvement of crop species. The preliminary

study presented in this thesis could be complemented with investigations on nutrient uptake mechanisms, nutrient translocations and nutrient measurement in the above and below-ground biomass.

The preliminary screening information of nutrient dose-response by studying phenotypic measurements in ABR6 and Bd21 accessions at both glasshouse and PlantScreen Phenotyping (Photon System Instruments, PSI) levels allowed for the selection of the nutrients. Further studies of the response of *Brachypodium* genotypes to nutrient limitation should include detailed micro-nutrients like B for a more extended period. It would be interesting to perform experiments where nutrient-deprived conditions are imposed at different growth stages and for a more extended period along with good quality measurements by using computational imaging to speed up genomics studies. Approaches like machine learning will have a great potential to evaluate other traits further and facilitate the analysis of biological datasets (Atkinson et al., 2017).

The present research increased our knowledge necessary for developing strategies to produce new varieties that are more resistant to nutrient limitations to supply the food and feed the growing population's demand. A more detailed analysis for candidate gene identification and expression analysis is essential for the complex traits to nutrient tolerance. Cell wall composition and fine architecture should be conducted to elucidate the differences in the cell wall structure under abiotic stress conditions. Especially it would be of interest to perform experiments on the two PMEI-OE lines of *Brachypodium* under B limitation as this micro-nutrient plays a vital role in pectin cross-linking and cell wall formation.

In conclusion, *Brachypodium* is a promising model species for grass research. Its high genetic variability can be exploited to develop grass crops more tolerant to nutrient limitation and drought. Overall, the QTL results and candidate genes identified here could be used to obtain more information on the genetic basis of nutrient tolerance in cereal and bioenergy crops.

Appendix

Table A2. 1: Mineral composition for the complete Hoagland solution, reduced N, and P dose response solutions (0%, 4%, 20% of 100% Hoagland). For reduced Nitrate, KCl was substituted in N dose response treatment to balance K in the prepared solution for above-ground measurements

		Hoagland	**N20%**	**N4%**	**N0%**	**P20%**	**P4%**	**P0%**
Salt g	Stock g/L	Amount mL/2.5L	Amount mL/2.5 L	Amount mL/2.5 L	Amount mL/2. 5L	Amount mL/2.5 L	Amount mL/2.5L	Amount mL/2.5L
NH4NO3	80 g/L	2.5	0.5	0.1	0	2.5	2.5	2.5
KNO3	202 g/L	6.25	1.25	0.25	0	6.25	6.25	6.25
NaH2PO4	119.9 g/L	1.25	1.25	1.25	1.25	0.25	0.05	0
KCl	74.6 g/L	0	5	6	6.25	0	0	0
MgSO4.7H2O	246 g/L	5	5	5	5	5	5	5
CaCl2*6H2O	147 g/L	6.25	6.25	6.25	6.25	6.25	6.25	6.25
ZnSO4.7H2O	0.22 g/L	2.5	2.5	2.5	2.5	2.5	2.5	2.5
H3MoO4.H2O	0.09 g/L	2.5	2.5	2.5	2.5	2.5	2.5	2.5
CuSO4.5H2O	0.51 g/L	2.5	2.5	2.5	2.5	2.5	2.5	2.5
H3BO3	2.86 g/L	2.5	2.5	2.5	2.5	2.5	2.5	2.5
MnCl2.4H2O	1.81 g/L	2.5	2.5	2.5	2.5	2.5	2.5	2.5
FeSO4.7H20	4.77 g/L	2.5	2.5	2.5	2.5	2.5	2.5	2.5

Table A2. 2: Mineral composition prepared for the complete Hoagland, reduced K, and B nutrient dose response solution (0%, 4%, 20% of 100% Hoagland). For reduced Potassium, NaNO3 was substituted to balance nitrate level in the solution to observe only K limitation for above-ground measurements

		Hoagland	**K20%**	**K4%**	**K0%**	**B20%**	**B4%**	**B0%**
Salt g	Stock g/L	Amount mL/2.5L	Amount mL/2.5L	Amount mL/2.5L	Amount mL/2.5L	Amount mL/2.5L	Amount mL/2.5L	Amount mL/2.5L
NH4NO3	80 g/L	2.5	0.5	0.1	0	2.5	2.5	2.5
KNO3	202 g/L	6.25	1.25	0.25	0	6.25	6.25	6.25
NaH2PO4	119.9 g/L	1.25	1.25	1.25	1.25	1.25	1.25	1.25
NaNO3		0	5	6	6.25			
MgSO4.7H2O	246 g/L	5	5	5	5	5	5	5
CaCl2*6H2O	147 g/L	6.25	6.25	6.25	6.25	6.25	6.25	6.25
ZnSO4.7H2O	0.22 g/L	2.5	2.5	2.5	2.5	2.5	2.5	2.5
H3MoO4.H2O	0.09 g/L	2.5	2.5	2.5	2.5	2.5	2.5	2.5
CuSO4.5H2O	0.51 g/L	2.5	2.5	2.5	2.5	2.5	2.5	2.5
H3BO3	2.86 g/L	2.5	2.5	2.5	2.5	0.5	0.1	0
MnCl2.4H2O	1.81 g/L	2.5	2.5	2.5	2.5	2.5	2.5	2.5
FeSO4.7H20	4.77 g/L	2.5	2.5	2.5	2.5	2.5	2.5	2.5

Table A2. 3: Stock nutrient solution preparation for each element to further use it in the preparation of Murashige and Skoong (MS) media using gelrite to prepare nutrient limiting MS media for the growth of ABR6 and Bd21 seedlings

Major minerals or macronutrients (x10)

Component	**mgs per litre**	**gm in x10 stock solution i.e. 10l worth**
KNO3	1900	19.0g **OMIT**
NH4NO3	1650	16.5g **OMIT**
NaH2PO4	195	1.95g **OMIT**
CaCl2.2H2O	441	4.41g
MgSO4.7H2O	370	3.7g
Myo-inositol	100	1g
H2O		500mls (add 50ml/L)

Minor minerals or micronutrients (x100)

Component	**mgs/L**	**mg or gm in x100 stock**
FeNaEDTA	36.7	3.67g
MnSO4.4H2O	22.3	2.23g
ZnSO4.7H2O	8.6	860mg
H3BO3	6.2	620mg **OMIT**
KI	0.83	83mg
Na2MoO4.2H2O	0.25	25mg
CoCl2.6H2O	0.025	25ml of 10mg/100ml stock
CuSO4.5H2O	0.025	25ml of 10mg/100ml stock
H2O		500mls (add 5ml/L)

Vitamins (x100)

Component	**mgs/l**	**mg in x100 stock**
Glycine	2	200
Thiamine HCl	1	100
Pyridoxine HCl	0.5	50
Nicotinic acid	0.5	50
H2O		100mls (add 1ml/L)

Stocks of OMITTED and substitute components

Component	**mgs/l**	**gm and mg in x10 stocks**
KNO3	1900 = 18.79mM	19g in 200ml
NH4NO3	1650=20.61mM (+752 if replace KNO3)	16.5g in 200ml
NaH2PO4	195= 1.25mM	1.95g in 100ml
H3BO3	6.2=100.27mM	62mg in 100ml
KCl	1402 to replace KNO3 =18.79mM	14.02 g in 200ml
NaH2PO4.2H2O	195=1.25mM	1.95g in 100ml

Table A2. 4: MS nutrient medium preparation with pH=5.8 (double strength according to 500ml bottle) and 1.6g of gelrite was added in 250ml media bottle (concentration 0.32% gelrite)

Component	**Amount per litre**	**Amount per 500ml (20 petri-dish)**
Major minerals	50ml	25ml
Minor minerals	5ml	2.5ml
Vitamins	1ml	0.5ml
Sucrose (3%)	30g	15g
KNO3	20ml	10ml
NH4NO3	20ml	10ml
NH4NO3	29.12ml to substitute N for KNO3	14.56ml
NaH2PO4	10ml	5ml
H3BO3	10ml	5ml
KCl	20ml to substitute K for KNO3	10ml
H2O	Made up to 500ml	Made up to 250ml
Component	**Amount per litre**	**Amount per 5 litre**
Major minerals	50ml	250ml
Minor minerals	5ml	25ml
Vitamins	1ml	5ml
Sucrose (3%)	30g	150g
H2O	Made up to 400ml	Made up to 2000ml

Table A2. 5: A. Molarity calculations used for preparing low nutrient concentrations solution calculation. MS media preparation with NPKB limited dose response B. 20% of 100% Hoagland solution C. 4% of 100% Hoagland solution D. 0% of 100% Hoagland solution. Enough for 20 petri square petri plates

A.

Compound	**molarity**	**zero**	**4%**	**20%**
KNO3	**18.79mM**	**0 K and 0 N**	**0.75mM**	**3.758mM**
NH4NO3	**20.61mM**	**0 N**	**1.64mM**	**4.122mM**
NaH2PO4	**1.25mM**	**0 P**	**0.05mM**	**0.25mM**
H3BO3	**100.27uM**	**0 H**	**4uM**	**20uM**
KCl Substitute K	**20.04mM**	**18.79mM=100% K In no N**	**19.24mM = 96% K**	**16.032mM = 80% K**
NH4NO3 Substitute N	**9.395mM**	**9.395mM =100% N(2N) In no K (equiv 18.79mM N 1N)**	**9.02mM = 96% N**	**7.52mM = 80% N**
Total K	**18.79mM**	**0mM**	**0.75mM**	**3.76mM**
Total P	**1.25**	**0mM**	**0.05mM**	**0.25mM**
Total N (2 N's)	**60.01mM**	**0mM**	**2.39mM**	**12mM**

B. Table with low 20% compounds

Component	**Normal MS medium**	**20% K**	**20% NO3/NH4**	**20% P**	**20% B**
Murashige and Skoog stock	200ml	200ml	200ml	200ml	200ml
KNO3 stock	10ml	**2ml**	**2ml**	10ml	10ml
NH4NO3 stock	10ml	**13.6ml**	**2ml**	10ml	10ml
NaH2PO4 stock	5ml	**1ml**	5ml	**1ml**	5ml
H3BO3 stock	5ml	5ml	5ml	5ml	**1ml**
KCl stock	0	0	**8ml**	**0.5ml**	0
H2O	Made up to 250ml (500ml final)	Made up to 250ml (500ml final)	Made up to 250ml (500ml final)	Made up to 250ml (500ml final)	Made up to 250ml (500ml final)

C. Table with low 4% compounds

Component	**Normal MS medium**	**4% K**	**4% NO3/NH4**	**4% P**	**4% B**
Murashige and Skoog stock	200ml	200ml	200ml	200ml	200ml
KNO3 stock	10ml	**0.4ml**	**0.4ml**	10ml	10ml
NH4NO3 stock	10ml	**14.4ml**	**0.4ml**	10ml	10ml
NaH2PO4 stock	5ml	**0.2ml**	5ml	**0.2ml**	5ml
H3BO3 stock	5ml	5ml	5ml	5ml	**0.2ml**
KCl stock	0	0	**9.6ml**	**0**	0
H2O	Made up to 250ml (500ml final)	Made up to 250ml (500ml final)	Made up to 250ml (500ml final)	Made up to 250ml (500ml final)	Made up to 250ml (500ml final)

D. Table with zero compounds

Component	**Normal MS medium**	**No K**	**No NO3/NH4**	**No P**	**No B**

Murashige and Skoog stock	200ml	200ml	200ml	200ml	200ml
KNO3 stock	10ml	**0**	**0**	10ml	10ml
NH4NO3 stock	10ml	**14.56ml**	**0**	10ml	10ml
NaH2PO4 stock	5ml	**0**	5ml	**0**	5ml
H3BO3 stock	5ml	5ml	5ml	5ml	**0**
KCl stock	0	0	**10ml**	**0**	0
H2O	Made up to 250ml (500ml final)	Made up to 250ml (500ml final)	Made up to 250ml (500ml final)	Made up to 250ml (500ml final)	Made up to 250ml (500ml final)

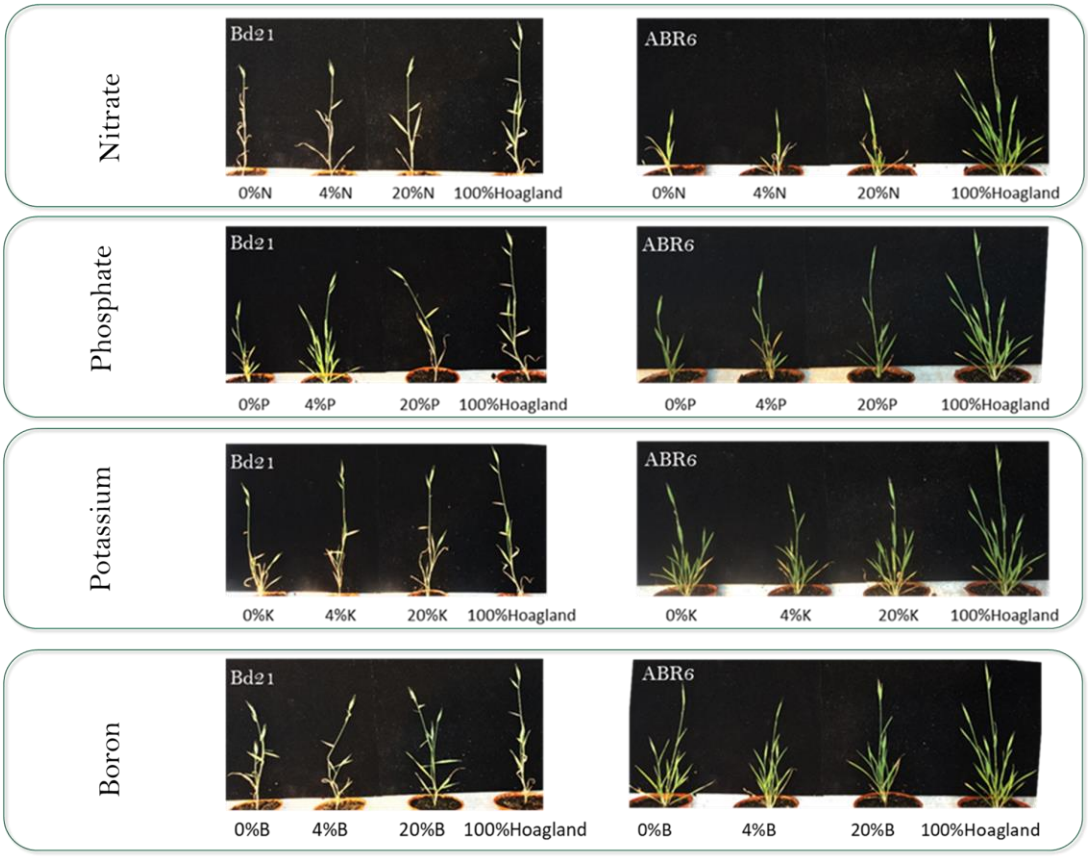

Figure A2. 1: Representative images of two genotypes, ABR6 and Bd21 under low nitrate(N), phosphate(P), potassium(K) and boron(B) dose-response

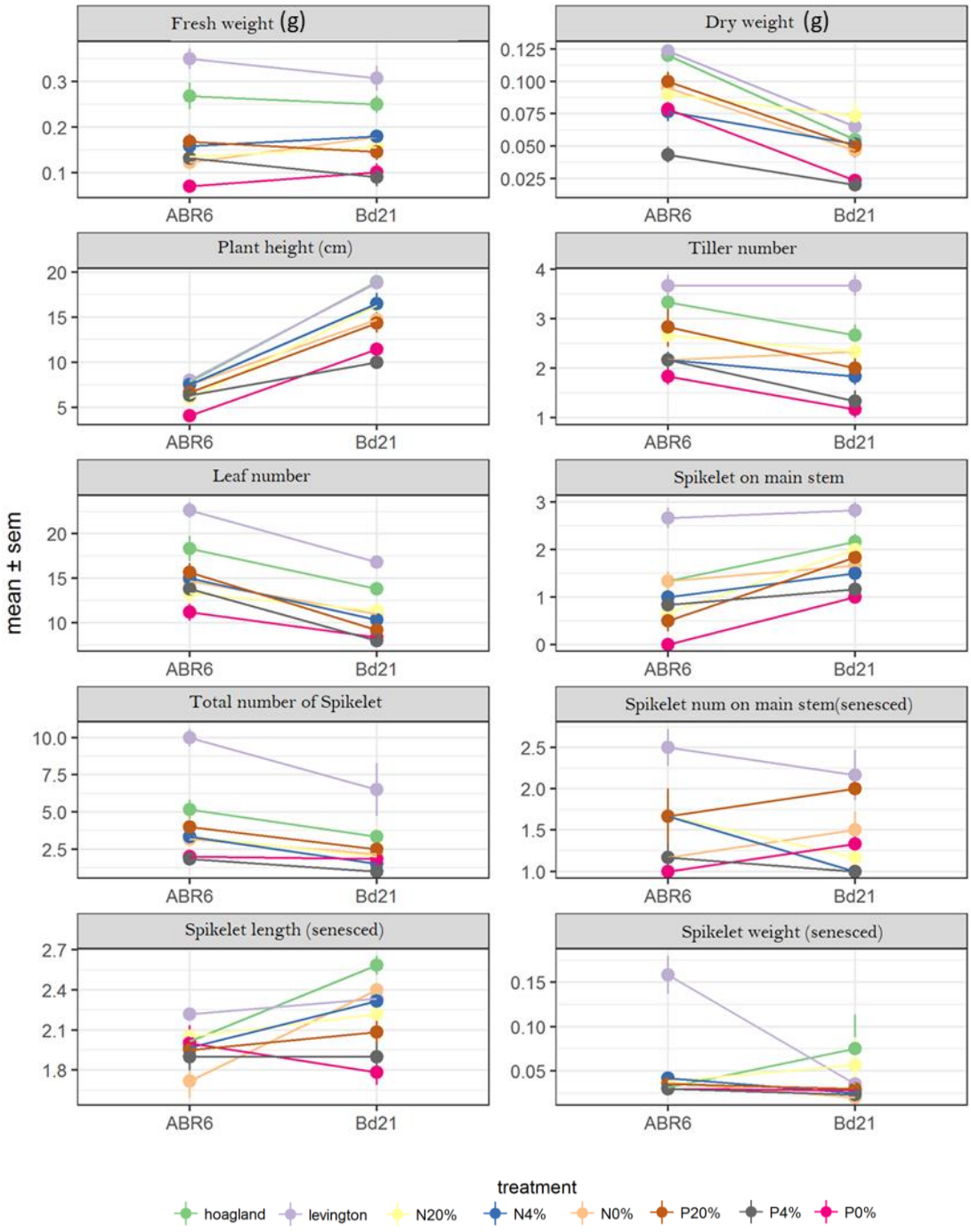

Figure A2. 2: Fresh weight, dry weight, plant height, tiller number, leaf number, spikelet on the main stem, the total number of spikelet and spikelet number, length, the weight of spikelet (senesced) of the two genotypes under nitrate and phosphate dose-response was measured, (n=6)

A.


Control
N20%
N4%
N0%
Bd21

B.

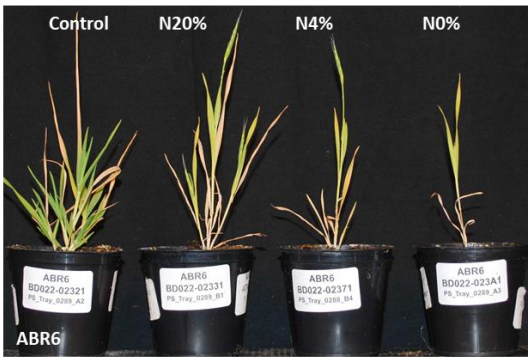
Control
N20%
N4%
N0%
ABR6

C.


Control
P20%
P4%
P0%
Bd21

D.

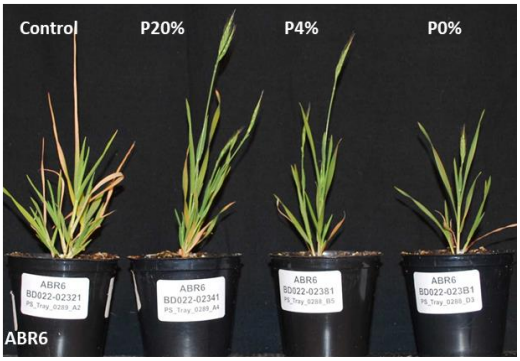
Control
P20%
P4%
P0%
ABR6

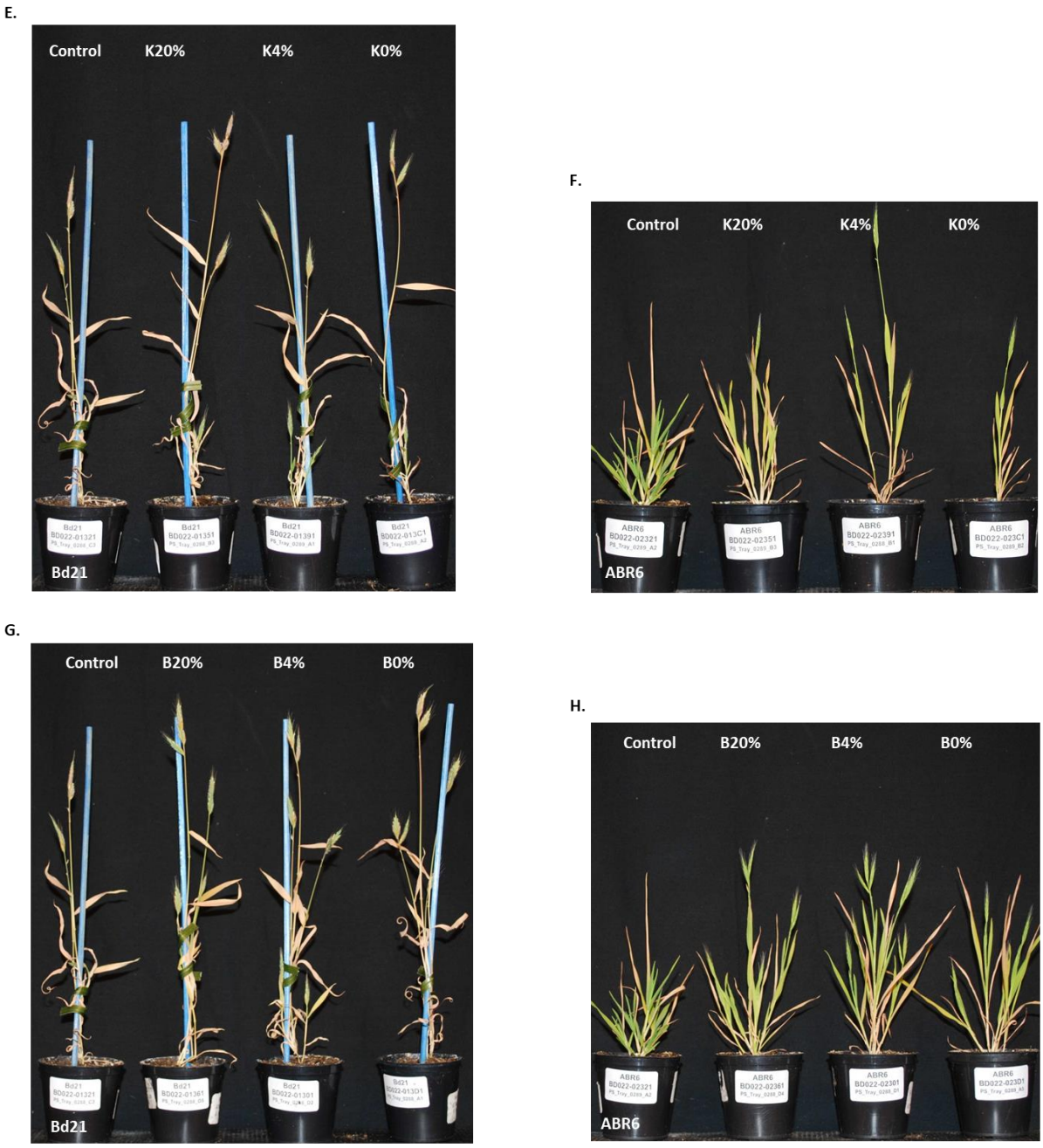

Figure A3. 1: The photographs taken at the end of the experiment from the front view against the black background. Both the accessions ABR6 and Bd21 under low nutrient dose-response (NPKB) were photographed along with control (100%) at the senescence stage

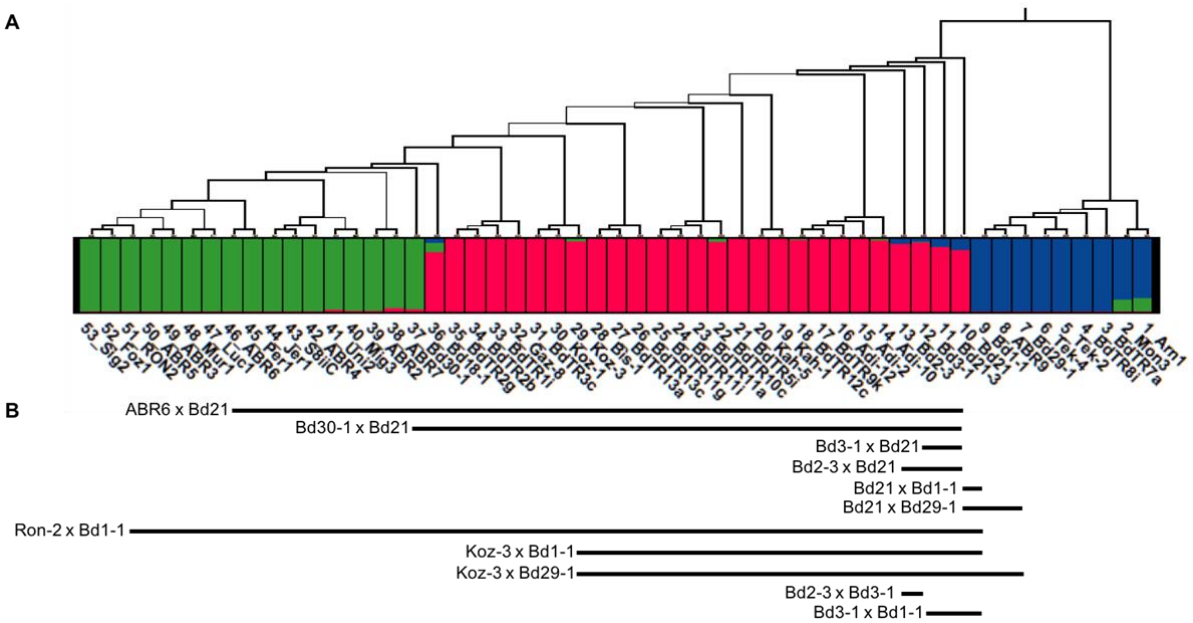

Figure A4. 1: Diagrammatic scheme of population structure of resequenced *Brachypodium distachyon* accessions of RIL population A. Phylogenetic tree and population structure analysis based on 4.5 million SNPs in coding sequence space (provided by Gordon and Vogel unpublished data) B. Relationship of parental accessions of RIL populations

Figure A4. 2: Photographs taken before the samples were harvested for biomass weight measurements (10 days after nutrient deprived treatment). Front view with black background and a scale for all the Brachypodium parental ecotypes of the RIL populations under H.S. 100% (control), N0%, and P0%

Table A4. 1: Ranking of the phenotypic traits by standardising the mean value (n=6) from control to the nutrient deprived treatment [(control-treatment)/control] followed by using *Brachypodium distachyon*, where control=0; [(Control-Control)/Control]

Brachypodium accessions	Nutrient limitation	Plant height	Leaf number	Fresh weight	Dry weight	Spikelet weight	Spikelet number (m.s.)	Spikelet length	Total spikelet
ABR6	N0%	13	15	6	9	17	6	9	11
	P0%	9	17	15	15	14	4	9	8
Adi-9									
	N0%	10	7	5	5	13	7	5	7
	P0%	7	9	11	7	10	13	6	11
Bd21									
	N0%	1	10	2	2	2	1	2	1
	P0%	8	15	7	9	9	17	15	16
Bd1-1									
	N0%	5	3	4	4	5	3	1	3
	P0%	10	2	8	6	17	10	11	7
Bd2-3									
	N0%	6	5	1	1	7	15	10	12
	P0%	15	11	1	2	3	3	3	5
Bd21-3	N0%	17	12	14	10	4	12	3	6
	P0%	13	14	6	3	4	15	5	12
Bd29-1	N0%	12	4	11	8	14	14	14	15
	P0%	12	10	13	13	15	12	12	17
Bd3-1	N0%	4	11	8	11	12	4	4	2
	P0%	2	4	10	10	12	1	2	1
Bd30-1	N0%	11	14	7	12	8	17	7	14
	P0%	1	8	5	5	7	7	1	6
BdTR10h	N0%	16	9	15	17	11	12	15	16
	P0%	5	16	4	4	2	2	4	3
BdTR11F	N0%	14	13	16	16	10	11	13	13
	P0%	3	12	12	12	6	8	7	15
BdTR13k	N0%	15	2	17	15	16	10	16	10
	P0%	14	**6**	14	14	16	11	14	13
Foz-1	N0%	2	16	3	3	1	2	6	8
	P0%	11	3	3	11	11	9	16	10
Jer	N0%	3	8	13	7	15	5	8	5
	P0%	16	13	17	17	5	6	8	9
Koz-3	N0%	8	17	9	6	6	8	11	9
	P0%	4	1	2	1	8	5	13	4
Luc-1	N0%	9	6	10	13	9	16	17	17
	P0%	17	5	17	16	13	14	17	14
Tek-4	N0%	7	1	12	14	3	8	12	4
	P0%	**6**	7	9	8	1	16	10	2

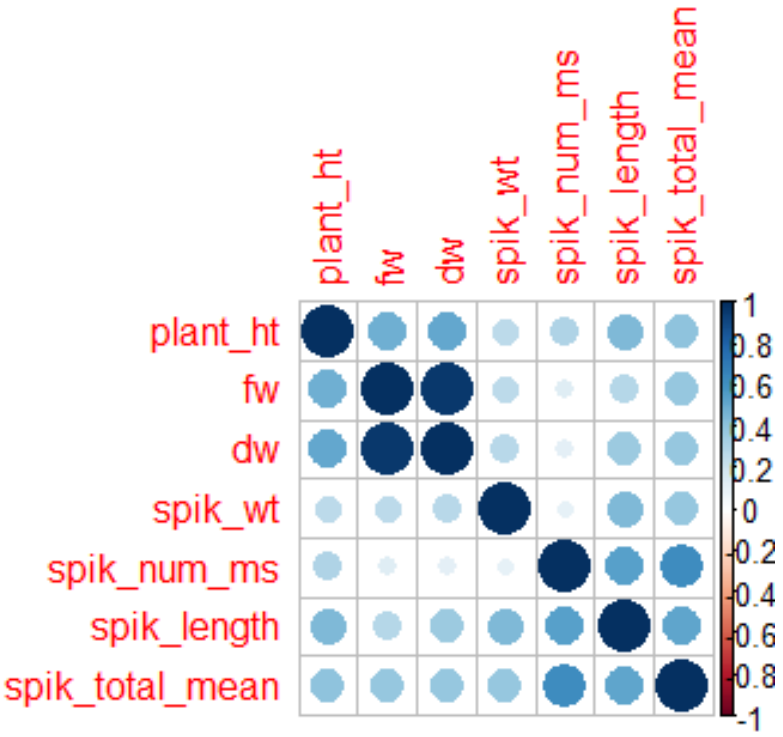

Figure A4. 3: Spearman correlation coefficients between average of the traits evaluated for the accessions of Brachypodium. For both N (bottom) and P (top) limitation treatments. plant_ht: plant height, fw: fresh weight (g), dw: dry weight (g), spik_wt: ear weight, spik_num_ms: spikelet on the main stem, spik_length: spikelet length (cm), spik_total_mean: total number of spikelets. Light blue circles are coefficients with a $p > 0.01$

A.

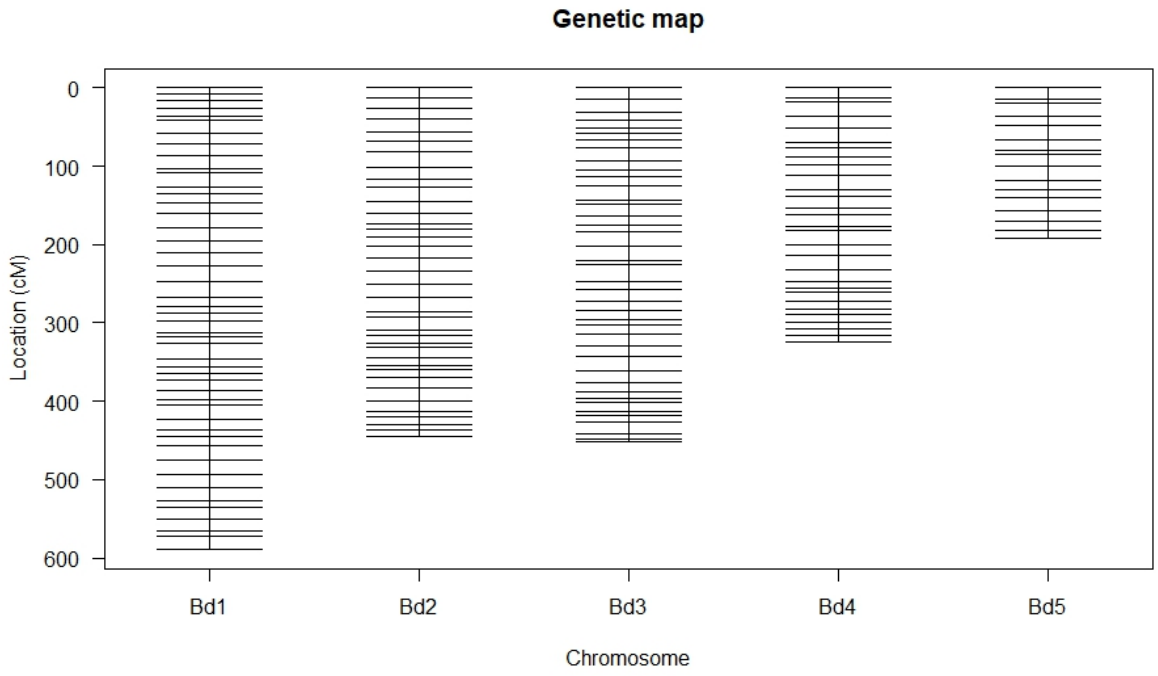

B.

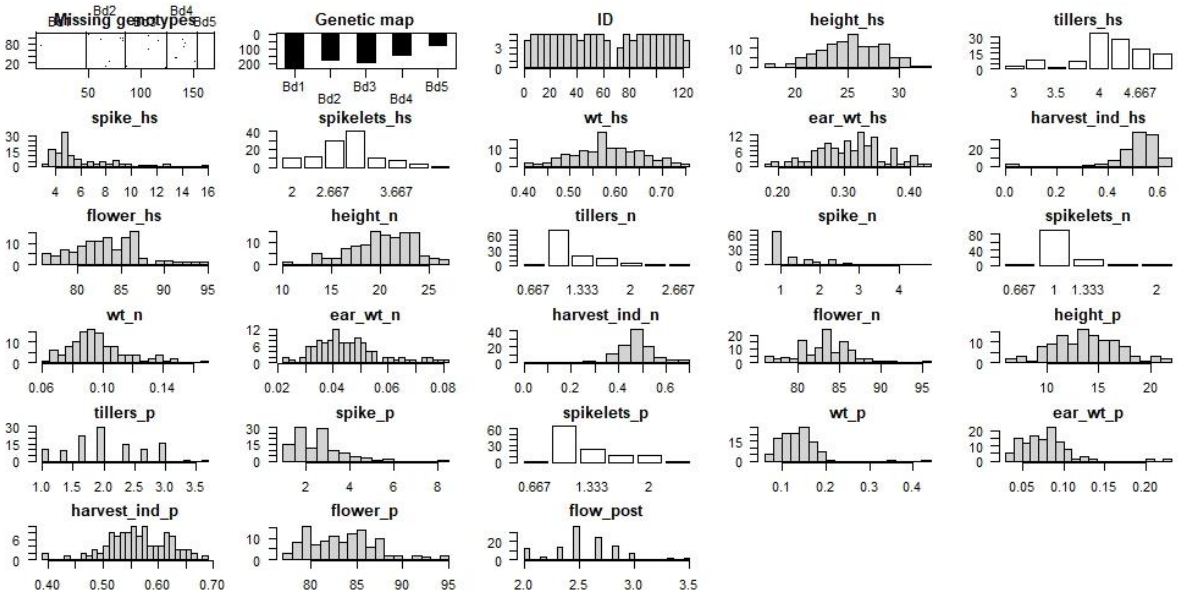

Figure A5. 1: A: Graphical representation of genetic map of selected markers, where y-axis and x-axis shows marker numbers (cM= centimorgans), along with B. distachyon chromosomes, B: Summary of the RIL population derived from ABR6 and Bd21 comprising of missing data plot along with histograms of measured phenotypes for the RIL population under nutrient limitation

A.

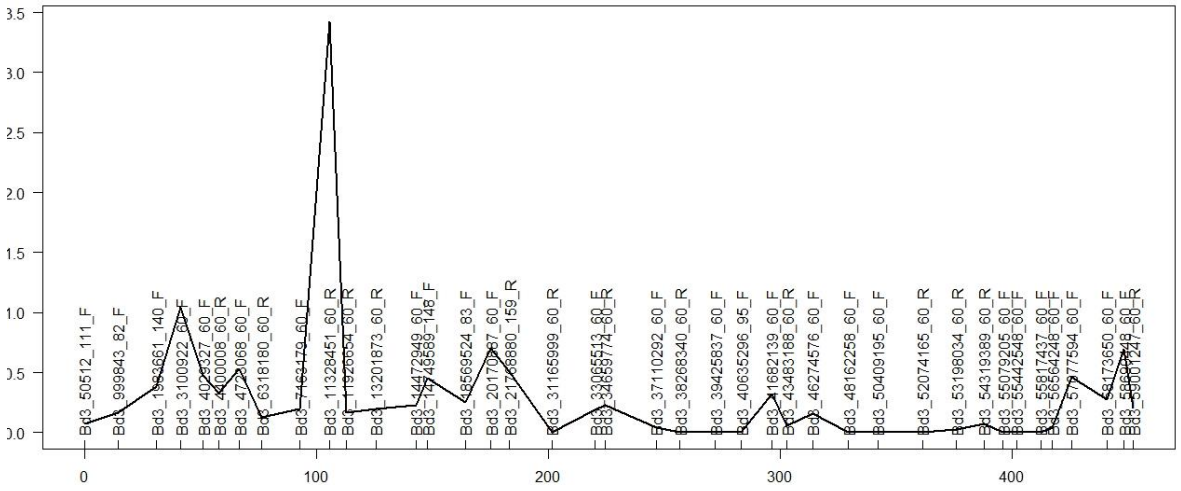

B.

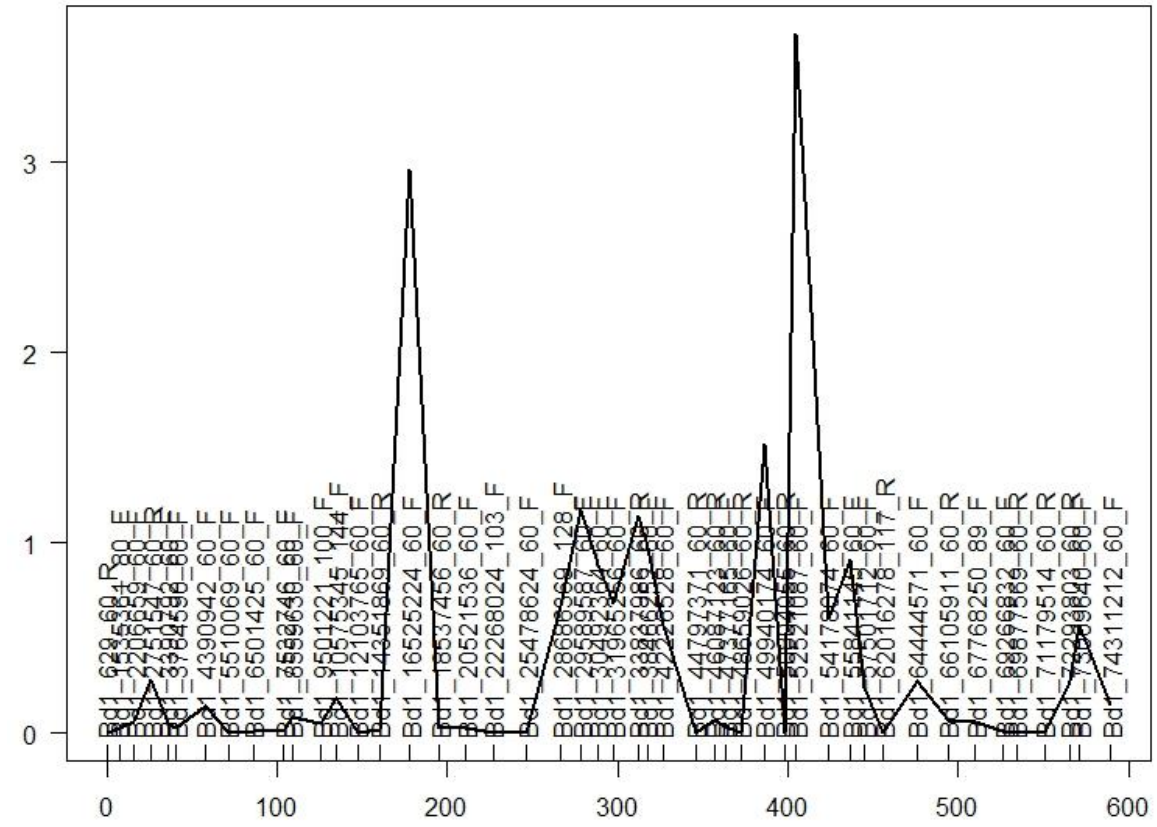

Figure A5. 2: A. Bd3 chromosome maker positions (cM) B. Bd1 chromosome marker positions (cM) for QTL6 and 7 for flowering time under N and P limitation environmental conditions

Table A5. 1: List of gene identified at/close to SNP peak along with location and function

Treatment	Chr	Gene identified	Location	Function
N limitation	Bd3	Bradi3g12590	Bd3_11321594_F	MFS transporter, PHS family, inorganic phosphate transporter
		Bradi3g12610	Bd3_11329724_R	ABC transporter family member 1
		Bradi3g12600	Bd3_11325948_F	OTU Domain containing protein
		Bradi3g13440	Bd3_11915782_R	SNARE proteins
		Bradi3g13275	Bd3_11796863_R	Plant invertase/pectin methylesterase inhibitor (PMEI)
		Bradi3g13450	Bd3_11921734_R	I-Branching enzyme
P limitation	Bd1	Bradi1g52320	Bd1_50805200_F	Peroxisomal Acyl-Coenzyme A oxidase 2
		Bradi1g52330	Bd1_50813465_F	Glycyl-tRNA synthetase
		Bradi1g52390	Bd1_50836678_R	U-Box Domain containing protein
		Bradi1g52407	Bd1_50855442_F	TPL-binding domain in jasmonate signalling
		Bradi1g52490	Bd1_50900133_F	C2H2-type zinc finger

Bradi1g53747	Bd1_52230813_F	Glycerol-3-phosphate dehydrogenase, chloroplastic
Bradi1g53940	Bd1_52515651_R	Leucine-rich repeat containing protein
Bradi1g53980	Bd1_52526543_R	Trypsin-like peptidase domain
Bradi1g54139	Bd1_52724577_F	Zinc finger FYVE domain containing protein

Table A5. 2: Significant QTLs from composite interval mapping of transformed flowering time phenotypes (T3) in the ABR6 x Bd21 F4:5 families (Bettgenhaeuser et al., 2017)

ENVa	Locus	Chrb	cM	EWTc	LOD	AEEd	PVEe	1-LOD	SIf
1	qFLT1	Bd1	297.6	3.06	12.96	2.87	36.30%	296.1	305.6
1	qFLT6	Bd3	91.2	3.06	4.51	1.64	11.80%	ND	
2	qFLT1	Bd1	297.6	3.09	7.59	0.82	20.00%	296.1	305.6
2	qFLT4	Bd2	409	3.09	3.2	0.47	6.70%	403.2	411
2	qFLT6	Bd3	93.2	3.09	6.64	0.79	18.20%	72.9	97
3	qFLT1	Bd1	297.6	3.2	8.61	1.5	31.10%	292.1	303.6
3	qFLT6	Bd3	91.2	3.2	5.69	1.2	18.70%	74.9	97
4	qFLT1	Bd1	297.6	3.19	3.49	1.77	15.90%	292.1	305.6
4	qFLT7	Bd3	294.6	3.19	3.79	1.59	14.00%	273.9	300.7
5	qFLT1	Bd1	297.6	3.17	8.62	3.43	37.50%	294.1	301.6

a Environment b Chromosome c Experiment-wide permutation threshold d Additive effect estimate for transformed phenotypes e Percent of phenotypic variance explained f One-LOD support interval (cM); ND denotes QTLs not detected using standard interval mapping.

A.

Sample	Independent lines	Concentration (ng/µl)	260/280
PMEI_1	3363	238.8	2.23
PMEI_2	3571	423.5	2.24
PMEI_3	3610	532.6	2.25
PMEI_4	3649	512.5	2.25
PMEI_5	3663	476.4	2.25
PMEI_6	3655	588.56	2.25
PMEI_7	3664	152.8	2.19
WT	Bd21-3	386.16	2.23

B.

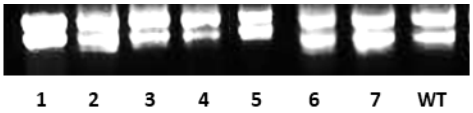

Figure A6. 1: A: RNA concentration and 260/280 ratio measured using EPOCH B: RNA integrity on agarose gel (0.8%) where an equal amount of RNA from all the samples was taken along with loading dye. 1= PMEI_1, 2=PMEI_2, 3= PMEI_3, 4= PMEI_4, 5= PMEI_5, 6= PMEI_6, 7= PMEI_7, WT= Wild type

Table A6. 1: Results obtained from absolute quantification for the evaluation of gene specific primer amplification efficiencies and other parameters like slope, efficiency and error

Target/reference gene	Family	Gene	Designed primer	Slope	Efficiency	Error
Target	PMEI	Bradi3g45080	PMEI 566_567	-1.757	3.709	0.305
	PMEI	Bradi3g45080	PMEI 568_567	-3.944	1.793	0.033
	PMEI	Bradi3g45080	PMEI 568_569	-3.638	1.883	1.104
	PMEI	Bradi3g45080	PMEI 572_573	-3.045	2.133	0.113
Reference	UCB18	Bradi4g00660	LF 70_71	-4.117	1.749	0.556
	UCB18	Bradi4g00660	LF 74_75	-3.872	2.113	0.110
	UCB18	Bradi4g00660	LF 74_76	-3.448	1.950	0.002

Red highlighted pairs of primer fulfilled the criteria required for further detailed analysis

A.

Concentration [U]					[mm2]
0.05	Area	245.677	250.834	233.651	
	Hole	11.001	13.054	13.113	
	Halo	234.676	237.78	220.538	230.998
0.025	Area	150.417	151.755	145.312	
	Hole	12.05	11.914	11.989	
	Halo	138.367	139.841	133.323	137.177
0.01	Area	89.635	86.105	97.771	
	Hole	11.603	11.925	12.55	
	Halo	78.032	74.18	85.221	79.14433
0.005	Area	37.917	34.188	40.889	
	Hole	12.193	11.454	10.314	
	Halo	25.724	22.734	30.575	26.34433

Concentration	Area [mm2]
0.05	230.998
0.025	137.177
0.01	79.144
0.005	26.344

B.

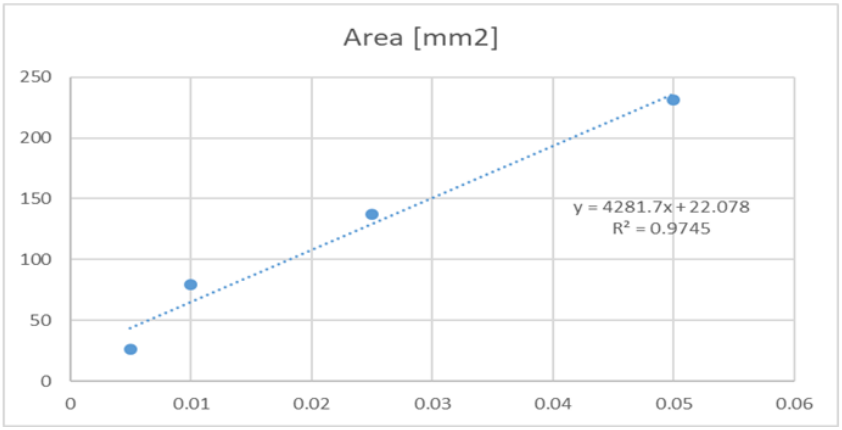

Figure A6. 2: Standard curve using Bradford method for protein extraction for PME assay analysis

References

A Ebringerová, 2005. (2005). Structural diversity and application potential of hemicelluloses. *Wiley Online Library*, *232*, 1–12. https://doi.org/10.1002/masy.200551401

Adhikari, L., Makaju, S. O., & Missaoui, A. M. (2019). QTL mapping of flowering time and biomass yield in tetraploid alfalfa (Medicago sativa L.). *BMC Plant Biology*, *19*(1). https://doi.org/10.1186/S12870-019-1946-0

Adolf, V., Jacobsen, S., Experimental, S. S.-E. and, & 2013, undefined. (n.d.). Salt tolerance mechanisms in quinoa (Chenopodium quinoa Willd.). *Elsevier*. Retrieved April 3, 2022, from https://www.sciencedirect.com/science/article/pii/S0098847212001554?casa_token=aY1W0pr0E5kAAAAA:qVydcveaxC4Ino6yn3S79Em3DU-FQ4tLmHiPJ96rDn_EZ4UxbMK2WfVbLfwL3SvkrzlsYtD4NQ

Ahmad et al.,2012, U. (n.d.). Boron Deficiency in soils and crops: a review. *Books.Google.Com*. Retrieved April 5, 2022, from https://books.google.com/books?hl=en&lr=&id=gIefDwAAQBAJ&oi=fnd&pg=PA77&dq=AHMAD+ET+AL+2012+BORON+&ots=HbCwxd37zo&sig=wYBAD8TcTCuZ0kyCpBlV3K4PZFQ

Albersheim, P., Darvill, A., Roberts, K., & Sederoff, R. (2010). *Plant cell walls*. https://books.google.com/books?hl=en&lr=&id=vCsWBAAAQBAJ&oi=fnd&pg=PP1&dq=ALBERSHEIM+ET+AL+2011&ots=Qi16wViUig&sig=b4w-k_Qar6hL_rkY8hiJSrrkkmE

Amtmann, A., Troufflard, S., & Armengaud, P. (2008). The effect of potassium nutrition on pest and disease resistance in plants. *Physiologia Plantarum*, *133*(4), 682–691. https://doi.org/10.1111/J.1399-3054.2008.01075.X

An, S. H., Sohn, K. H., Choi, H. W., Hwang, I. S., Lee, S. C., & Hwang, B. K. (2008). Pepper pectin methylesterase inhibitor protein CaPMEI1 is required for antifungal activity, basal disease resistance and abiotic stress tolerance. *Planta*, *228*(1), 61–78. https://doi.org/10.1007/S00425-008-0719-Z

Andrés & Coupland, 2012, U. (n.d.). The genetic basis of flowering responses to seasonal cues. *Nature.Com*. Retrieved April 6, 2022, from https://idp.nature.com/authorize/casa?redirect_uri=https://www.nature.com/articles/nrg3291&casa_token=b_HF9r9FbmsAAAAA:X64f19lPIm7tVf0BQt2A6OPFLckLaSq7BEJ-C71fAFXPCGfc8ZFWTCRIZn3DwnsTWJYnErKakq_6WOsh

Assefa, T., Wu, J., Beebe, S. E., Rao, I. M., Marcomin, D., & Claude, R. J. (2015). Improving adaptation to drought stress in small red common bean: phenotypic differences and predicted genotypic effects on grain yield, yield components and harvest index. *Euphytica*, *203*(3), 477–489. https://doi.org/10.1007/S10681-014-1242-X

Aziz, T., Lambers, H., Nicol, D., & Ryan, M. H. (2015). Mechanisms for tolerance of very high tissue phosphorus concentrations in Ptilotus polystachyus. *Plant, Cell & Environment*, *38*(4), 790–799. https://doi.org/10.1111/PCE.12450

BALESTRIERI, C., CASTALDO, D., GIOVANE, A., QUAGLIUOLO, L., & SERVILLO, L. (1990). A glycoprotein inhibitor of pectin methylesterase in kiwi fruit (Actinidia chinensis). *European Journal of Biochemistry*, *193*(1), 183–187. https://doi.org/10.1111/J.1432-1033.1990.TB19321.X

Bänziger M, Edmeades GO, Beck D, B. M. (2000). (n.d.). *Bänziger M, Edmeades GO, Beck D, Bellon M (2000) Breeding for drought and nitrogen stress tolerance in maize: from theory to practice. Breeding strategies. CIMMYT, Mexico - Google Search*. Retrieved April 3, 2022, from https://www.google.com/search?q=Bänziger+M%2C+Edmeades+GO%2C+Beck+D%2C+Bellon+M+(2000)+Breeding+for+drought+and+nitrogen+stress+tolerance+in+maize%3A+from+theory+to+practice.+Breeding+strategies.+CIMMYT%2C+Mexico&rlz=1C1GGRV_enGB764GB764&oq=Bänziger+M%2C+

Barnes & Anderson, 2018. (2018). Cytosolic invertases contribute to cellulose biosynthesis and influence carbon partitioning in seedlings of Arabidopsis thaliana. *Plant Journal*, *94*(6), 956–974. https://doi.org/10.1111/TPJ.13909

Barrero, J. M., Jacobsen, J. V., Talbot, M. J., White, R. G., Swain, S. M., Garvin, D. F., &

Gubler, F. (2012). Grain dormancy and light quality effects on germination in the model grass Brachypodium distachyon. *New Phytologist*, *193*(2), 376–386. https://doi.org/10.1111/J.1469-8137.2011.03938.X

Bartels & Sunkar, 2005, U. (2005). Drought and salt tolerance in plants. *Taylor & Francis*, *24*(1), 23–58. https://doi.org/10.1080/07352680590910410

Beebe, S. E., Rao, I. M., Cajiao, C., & Grajales, M. (2008). Selection for drought resistance in common bean also improves yield in phosphorus limited and favorable environments. *Crop Science*, *48*(2), 582–592. https://doi.org/10.2135/CROPSCI2007.07.0404

Bekeko & Mulualem, 2016, U. (n.d.). Genetics of plant–pathogen interactions and resistance. *Researchgate.Net*. Retrieved April 6, 2022, from https://www.researchgate.net/profile/Zelalem-Erena/publication/304626852_Genetics_of_plant-pathogen_interactions_and_resistance/links/57754b4508aead7ba06ffcae/Genetics-of-plant-pathogen-interactions-and-resistance.pdf

Bellaloui, N., & Brown, P. H. (1998). Cultivar differences in boron uptake and distribution in celery (Apium graveolens), tomato (Lycopersicon esculentum) and wheat (triticum aestivum). *Plant and Soil*, *198*(2), 153–158. https://doi.org/10.1023/A:1004343031242

Bergelson & Roux, 2010, U. (n.d.). Towards identifying genes underlying ecologically relevant traits in Arabidopsis thaliana. *Nature.Com*. Retrieved April 7, 2022, from https://idp.nature.com/authorize/casa?redirect_uri=https://www.nature.com/articles/nrg2896&casa_token=WNTlRPUoPTwAAAAA:SzrZTBye3hFX3u4Eqqz4LO9xN9lhx0-ZwoQokopK5-ftbzOSfPY3ucsDxbiwslpfzViUsvrGp-It6Pnh

Bernardo, 2008, U. (2008). Molecular markers and selection for complex traits in plants: learning from the last 20 years. *Wiley Online Library*, *48*(5), 1649–1664. https://doi.org/10.2135/cropsci2008.03.0131

Bettgenhaeuser, J. (2016). *Deciphering the genetic basis of quantitative traits in Brachypodium distachyon*. *September*.

Bettgenhaeuser, J., Corke, F. M. K., Opanowicz, M., Green, P., Hernández-Pinzón, I., Doonan, J. H., & Moscou, M. J. (2017). Natural variation in brachypodium links vernalization and flowering time loci as major flowering determinants. *Plant Physiology*, *173*(1), 256–268. https://doi.org/10.1104/pp.16.00813

Bevan, M., Garvin, D., Biotechnology, J. V.-C. O. in, & 2010, undefined. (n.d.). Brachypodium distachyon genomics for sustainable food and fuel production. *Elsevier*. Retrieved April 4, 2022, from https://www.sciencedirect.com/science/article/pii/S0958166910000455?casa_token=ZdFmMqJwlUYAAAAA:F1ZWwl3qxyj96CXfez4CG5XVmjSm5XBY2-d3E6ooCEOyolX7NWJd3WI6ANI2L7DxAcPQDrO2AQ

Beyaz, R. (2020). Impact of gamma irradiation pretreatment on the growth of common vetch (Vicia sativa L.) seedlings grown under salt and drought stress. *International Journal of Radiation Biology*, *96*(2), 257–266. https://doi.org/10.1080/09553002.2020.1688885

Bhaskar R. et al., 2003. (2003). Leaf chlorophyll, net gas exchange and chloroplast ultrastructure in citrus leaves of different nitrogen status. *Tree Physiology*, *23*(8), 553–559. https://doi.org/10.1093/TREEPHYS/23.8.553

Bhatia, R., Gallagher, J. A., Gomez, L. D., & Bosch, M. (2017). Genetic engineering of grass cell wall polysaccharides for biorefining. *Plant Biotechnology Journal*, *15*(9), 1071–1092. https://doi.org/10.1111/pbi.12764

Bianco, M., Filho, A. C., one, L. de C.-P., & 2015, undefined. (n.d.). Nutritional status of the cauliflower cultivar 'Verona'grown with omission of out added macronutrients. *Journals.Plos.Org*. Retrieved April 3, 2022, from https://journals.plos.org/plosone/article?id=10.1371/journal.pone.0123500

Biswal, A. K., Atmodjo, M. A., Li, M., Baxter, H. L., Yoo, C. G., Pu, Y., Lee, Y. C., Mazarei, M., Black, I. M., Zhang, J. Y., Ramanna, H., Bray, A. L., King, Z. R., Lafayette, P. R., Pattathil, S., Donohoe, B. S., Mohanty, S. S., Ryno, D., Yee, K., … Mohnen, D. (2018). Sugar release and growth of biofuel crops are improved by downregulation of pectin biosynthesis.

Nature Biotechnology, *36*(3), 249–257. https://doi.org/10.1038/nbt.4067

Biswal, A. K., Hao, Z., Pattathil, S., Yang, X., Winkeler, K., Collins, C., Mohanty, S. S., Richardson, E. A., Gelineo-Albersheim, I., Hunt, K., Ryno, D., Sykes, R. W., Turner, G. B., Ziebell, A., Gjersing, E., Lukowitz, W., Davis, M. F., Decker, S. R., Hahn, M. G., & Mohnen, D. (2015). Downregulation of GAUT12 in Populus deltoides by RNA silencing results in reduced recalcitrance, increased growth and reduced xylan and pectin in a woody biofuel feedstock. *Biotechnology for Biofuels*, *8*(1). https://doi.org/10.1186/s13068-015-0218-y

Bita, C. E., & Gerats, T. (2013). Plant tolerance to high temperature in a changing environment: Scientific fundamentals and production of heat stress-tolerant crops. *Frontiers in Plant Science*, *4*(JUL). https://doi.org/10.3389/FPLS.2013.00273/FULL

Blevins, D. G. (1989). An Overview of Nitrogen Metabolism In Higher Plants. *Plant Nitrogen Metabolism*, 1–41. https://doi.org/10.1007/978-1-4613-0835-5_1

Blevins, D. G., & Lukaszewski, K. M. (1998). Boron in Plant Structure and Function. *Annual Review of Plant Physiology and Plant Molecular Biology*, *49*(1), 481–500. https://doi.org/10.1146/annurev.arplant.49.1.481

Boden, S. A., Kavanová, M., Finnegan, E., Wigge, P. A., Wardlaw, I., Dawson, I., Wallwork, M., Jenner, C., Logue, S., Sedgley, M., Battisti, D., Naylor, R., Lobell, D., Schlenker, W., Costa-Roberts, J., Porter, J., Gawith, M., Peacock, J., Parsons, A., … Kumar, S. (2013). Thermal stress effects on grain yield in *Brachypodium distachyon* occur via H2A.Z-nucleosomes. *Genome Biology*, *14*(6), R65. https://doi.org/10.1186/gb-2013-14-6-r65

Bonser, et al., 1996. (1996). Effect of phosphorus deficiency on growth angle of basal roots in Phaseolus vulgaris. *New Phytologist*, *132*(2), 281–288. https://doi.org/10.1111/J.1469-8137.1996.TB01847.X

Bosch & Hepler, 2005, U. (n.d.). Pectin methylesterases and pectin dynamics in pollen tubes. *Academic.Oup.Com*. Retrieved April 5, 2022, from https://academic.oup.com/plcell/article-abstract/17/12/3219/6114682

Bossdorf, O., & Pigliucci, M. (2009). Plasticity to wind is modular and genetically variable in *Arabidopsis thaliana*. *Evolutionary Ecology*, *23*(5), 669–685. https://doi.org/10.1007/s10682-008-9263-3

Bouain, N., Krouk, G., Lacombe, B., Science, H. R.-T. in P., & 2019, undefined. (n.d.). Getting to the root of plant mineral nutrition: combinatorial nutrient stresses reveal emergent properties. *Elsevier*. Retrieved April 4, 2022, from https://www.sciencedirect.com/science/article/pii/S1360138519300779?casa_token=111SvqpMAQIAAAAA:L1M-3BzygCi0_b3uPEEjZqNGcD7BjHYGRk1pd70sRO6zOAg6DrtRVqoMrgtnjkz19_oi2IUr8w

Bouvier D'Yvoire, M., Bouchabke-Coussa, O., Voorend, W., Antelme, S., Cezard, L., Legee, F., Lebris, P., Legay, S., Whitehead, C., McQueen-Mason, S. J., Gomez, L. D., Jouanin, L., Lapierre, C., & Sibout, R. (2013). Disrupting the cinnamyl alcohol dehydrogenase 1 gene (BdCAD1) leads to altered lignification and improved saccharification in *Brachypodium distachyon*. *Plant Journal*, *73*, 496–508. https://doi.org/10.1111/tpj.12053

Bradford,1976, U. (1976). A rapid and sensitive method for the quantitation of microgram quantities of protein utilizing the principle of protein-dye binding. *Elsevier*, *72*, 248–254. https://www.sciencedirect.com/science/article/pii/0003269776905273

Bradshaw, A. D. (2006). Unravelling phenotypic plasticity - Why should we bother? *New Phytologist*, *170*(4), 644–648. https://doi.org/10.1111/J.1469-8137.2006.01761.X

Brkljacic et al., 2011. (n.d.). Brachypodium as a model for the grasses: today and the future. *Academic.Oup.Com*. Retrieved April 4, 2022, from https://academic.oup.com/plphys/article-abstract/157/1/3/6108811

Buckler, E. S., Holland, J. B., Bradbury, P. J., Acharya, C. B., Brown, P. J., Browne, C., Ersoz, E., Flint-Garcia, S., Garcia, A., Glaubitz, J. C., Goodman, M. M., Harjes, C., Guill, K., Kroon, D. E., Larsson, S., Lepak, N. K., Li, H., Mitchell, S. E., Pressoir, G., … McMullen, M. D. (2009). The genetic architecture of maize flowering time. *Science*, *325*(5941), 714–718. https://doi.org/10.1126/SCIENCE.1174276

Cai, H., Chu, Q., Yuan, L., Liu, J., Chen, X., Chen, F., Mi, G., & Zhang, F. (2012). Identification

of quantitative trait loci for leaf area and chlorophyll content in maize (Zea mays) under low nitrogen and low phosphorus supply. *Molecular Breeding*, *30*(1), 251–266. https://doi.org/10.1007/S11032-011-9615-5

Cakmak, I. (2005). The role of potassium in alleviating detrimental effects of abiotic stresses in plants. *Journal of Plant Nutrition and Soil Science*, *168*(4), 521–530. https://doi.org/10.1002/JPLN.200420485

Camacho-Cristóbal, 2015, U. (n.d.). Boron deficiency inhibits root cell elongation via an ethylene/auxin/ROS-dependent pathway in Arabidopsis seedlings. *Academic.Oup.Com*. Retrieved April 5, 2022, from https://academic.oup.com/jxb/article-abstract/66/13/3831/514588

Carlsson, M., Merten, M., Kayser, M., Agriculture, J. I.-, Ecosystems, undefined, & 2017, undefined. (n.d.). Drought stress resistance and resilience of permanent grasslands are shaped by functional group composition and N fertilization. *Elsevier*. Retrieved April 4, 2022, from https://www.sciencedirect.com/science/article/pii/S0167880916305461?casa_token=cdBH7oU_of4AAAAA:gmvbYRtXw-4iTp-Q_GrGAODqjRCLNiH_UuhT3R0i8l8IFWF6ie83o2RczNgMaDT59JZb6fkokg

Carpita, N. C., & Gibeaut, D. M. (1993). Structural models of primary cell walls in flowering plants: Consistency of molecular structure with the physical properties of the walls during growth. *Plant Journal*, *3*(1), 1–30. https://doi.org/10.1111/J.1365-313X.1993.TB00007.X

Carpita, N., science, M. M.-T. in plant, & 2008, undefined. (n.d.). Maize and sorghum: genetic resources for bioenergy grasses. *Elsevier*. Retrieved April 4, 2022, from https://www.sciencedirect.com/science/article/pii/S1360138508001817?casa_token=ybOjwTYHzyAAAAAA:fHDB-lwtorAUUCJHU3nxGUQ1fGPSNFvsOtM5b_Csw0H7-FACPJwUuVMGwIaSWr8U4CDGclIKCQ

Catalán, P et al., 2012, U. (n.d.). Evolution and taxonomic split of the model grass Brachypodium distachyon. *Academic.Oup.Com*. Retrieved April 4, 2022, from

https://academic.oup.com/aob/article-abstract/109/2/385/124920

Chen, J et al.,2018. (n.d.). A cold-induced pectin methyl-esterase inhibitor gene contributes negatively to freezing tolerance but positively to salt tolerance in Arabidopsis. *Elsevier*. Retrieved April 5, 2022, from https://www.sciencedirect.com/science/article/pii/S0176161718300129?casa_token=IAyi89puzMkAAAAA:30_gFmiM77fPFTOPd9ueKmj2aUq9ythYoiawdXcfPR9fjkuqlz4rPSfkJyHdbL5Xa9HroaSRvQ

Chen & Dubcovsky, 2012. (2012). Wheat TILLING Mutants Show That the Vernalization Gene VRN1 Down-Regulates the Flowering Repressor VRN2 in Leaves but Is Not Essential for Flowering. *PLoS Genetics*, *8*(12). https://doi.org/10.1371/JOURNAL.PGEN.1003134

Chen, F., & Dixon, R. A. (2007). Lignin modification improves fermentable sugar yields for biofuel production. *Nature Biotechnology*, *25*(7), 759–761. https://doi.org/10.1038/nbt1316

Cho, L. H., Yoon, J., & An, G. (2017). The control of flowering time by environmental factors. *The Plant Journal*, *90*(4), 708–719. https://doi.org/10.1111/TPJ.13461

Ciereszko, I., Szczygła, A., & Zebrowska, E. (2011). PHOSPHATE DEFICIENCY AFFECTS ACID PHOSPHATASE ACTIVITY AND GROWTH OF TWO WHEAT VARIETIES. *Http://Dx.Doi.Org/10.1080/01904167.2011.544351*, *34*(6), 815–829. https://doi.org/10.1080/01904167.2011.544351

Citadirin, Y., Hidaka, K., Sago, Y., Wajima, T., & Kitano, M. (2011). Application of temperature stress to root zone of spinach II. Effect of the high temperature pre-treatment on quality. In *Environmental Control in Biology* (Vol. 49, Issue 4, pp. 157–164). https://doi.org/10.2525/ecb.49.157

Cleveland & Deeb et al., 2012. (2012). Selecting markers and evaluating coverage. *Methods in Molecular Biology*, *871*, 55–71. https://doi.org/10.1007/978-1-61779-785-9_5

Cobb et al., 2013. (2013). Next-generation phenotyping: Requirements and strategies for enhancing our understanding of genotype-phenotype relationships and its relevance to

crop improvement. *Theoretical and Applied Genetics*, *126*(4), 867–887. https://doi.org/10.1007/S00122-013-2066-0

Collard, B. C.Y., Jahufer, M. Z. Z., Brouwer, J. B., & Pang, E. C. K. (2005). An introduction to markers, quantitative trait loci (QTL) mapping and marker-assisted selection for crop improvement: The basic concepts. *Euphytica*, *142*(1–2), 169–196. https://doi.org/10.1007/S10681-005-1681-5

Collard, Bertrand C.Y., & Mackill, D. J. (2008). Marker-assisted selection: An approach for precision plant breeding in the twenty-first century. *Philosophical Transactions of the Royal Society B: Biological Sciences*, *363*(1491), 557–572. https://doi.org/10.1098/RSTB.2007.2170

Coomey, J. H., Sibout, R., & Hazen, S. P. (2020). Grass secondary cell walls, Brachypodium distachyon as a model for discovery. *New Phytologist*, *227*(6), 1649–1667. https://doi.org/10.1111/NPH.16603

Corradini & Cavazza, 2012, U. (n.d.). High-performance anion-exchange chromatography coupled with pulsed electrochemical detection as a powerful tool to evaluate carbohydrates of food interest. *Downloads.Hindawi.Com*. Retrieved April 4, 2022, from https://downloads.hindawi.com/archive/2012/487564.pdf

Crowe, J. D., Feringa, N., Pattathil, S., Merritt, B., Foster, C., Dines, D., Ong, R. G., & Hodge, D. B. (2017). Identification of developmental stage and anatomical fraction contributions to cell wall recalcitrance in switchgrass. *Biotechnology for Biofuels*, *10*(1). https://doi.org/10.1186/S13068-017-0870-5

Cui, Y., Lee, M. Y., Huo, N., Bragg, J., Yan, L., Yuan, C., Li, C., Holditch, S. J., Xie, J., Luo, M. C., Li, D., Yu, J., Martin, J., Schackwitz, W., Gu, Y. Q., Vogel, J. P., Jackson, A. O., Liu, Z., & Garvin, D. F. (2012). Fine mapping of the Bsr1 barley stripe mosaic virus resistance gene in the model grass brachypodium distachyon. *PLoS ONE*, *7*(6). https://doi.org/10.1371/JOURNAL.PONE.0038333

D'Ovidio, R., Mattei, B., Roberti, S., Biophysica, D. B.-B. et, & 2004, undefined. (n.d.). Polygalacturonases, polygalacturonase-inhibiting proteins and pectic oligomers in

plant–pathogen interactions. *Elsevier*. Retrieved April 4, 2022, from https://www.sciencedirect.com/science/article/pii/S1570963903003340?casa_token=rWsbpQl3KhkAAAAA:DdR_hrPqGYWbl88aIu9saHSjf6nOoabxIlzAntNt015Ct6uhDXYjw6bG9S8tpqCMBHtlD6hEkw

da Costa et al.,2019. (n.d.). Nutrient and drought stress: implications for phenology and biomass quality in miscanthus. *Academic.Oup.Com*. Retrieved April 4, 2022, from https://academic.oup.com/aob/article-abstract/124/4/553/5077397

da Costa, R. M. F., Lee, S. J., Allison, G. G., Hazen, S. P., Winters, A., & Bosch, M. (2014). Genotype, development and tissue-derived variation of cell-wall properties in the lignocellulosic energy crop Miscanthus. *Annals of Botany*, *114*, 1265–1277. https://doi.org/10.1093/aob/mcu054

de Bang, T. C., Husted, S., Laursen, K. H., Persson, D. P., & Schjoerring, J. K. (2021). The molecular–physiological functions of mineral macronutrients and their consequences for deficiency symptoms in plants. *New Phytologist*, *229*(5), 2446–2469. https://doi.org/10.1111/NPH.17074

de Oliveira Maia Júnior, S., de Andrade, J. R., dos Santos, C. M., Silva, A. L. J., Endres, L., Silva, J. V., & dos Santos Silva, L. K. (2020). Osmoregulators' accumulation minimizes the effects of drought stress in sugarcane and contributes to the recovery of photochemical efficiency in photosystem II after rewatering. *Acta Physiologiae Plantarum*, *42*(4), 1–11. https://doi.org/10.1007/s11738-020-03050-y

Dear, B.S. & Weir, 2004. (n.d.). *Dear, B.S., Weir, R.G. 2004. Boron deficiency in... - Google Scholar*. Retrieved April 4, 2022, from https://scholar.google.com/scholar?hl=en&as_sdt=0%2C5&q=Dear%2C+B.S.%2C+Weir%2C+R.G.+2004.+Boron+deficiency+in+pastures+and+field+crops&btnG=

Dell & Huang,1997, U. (n.d.). Physiological response of plants to low boron. *Springer*. Retrieved April 5, 2022, from https://idp.springer.com/authorize/casa?redirect_uri=https://link.springer.com/article/10.1023/A:1004264009230&casa_token=7VRLZnZdrncAAAAA:QKD2W9XRnLrVpzQMR

nQYjU5mRyxZLhjpuWqGFrb8OIK2CsxFsWaTcwdpCjYZiezvaJCg6IJRnivXIzRc

Di Matteo et al.,2005, U. (n.d.). Structural basis for the interaction between pectin methylesterase and a specific inhibitor protein. *Academic.Oup.Com*. Retrieved April 6, 2022, from https://academic.oup.com/plcell/article-abstract/17/3/849/6114493

Ding, S. Y., & Himmel, M. E. (2006). The maize primary cell wall microfibril: A new model derived from direct visualization. *Journal of Agricultural and Food Chemistry*, *54*(3), 597–606. https://doi.org/10.1021/JF051851Z

Distelfeld et al., 2009, U. (n.d.). Genetic and Molecular Characterization of the VRN2 Loci in Tetraploid Wheat. *Academic.Oup.Com*. Retrieved April 7, 2022, from https://academic.oup.com/plphys/article-abstract/149/1/245/6107716

Distelfeld et al., 2012, U. (n.d.). Divergent functions of orthologous NAC transcription factors in wheat and rice. *Springer*. Retrieved April 6, 2022, from https://idp.springer.com/authorize/casa?redirect_uri=https://link.springer.com/article/10.1007/s11103-012-9881-6&casa_token=10-lmF-hnfoAAAAA:3QKmHG68pdURK7wGE71J1pUqJyX2JAKtwm58_JD9_hBnQ8zosyyucWS0azVXZUYV_JgNsfqkca3qHi9u

Doerge, 2002, U. (n.d.). Mapping and analysis of quantitative trait loci in experimental populations. *Nature.Com*. Retrieved April 6, 2022, from https://idp.nature.com/authorize/casa?redirect_uri=https://www.nature.com/articles/nrg703&casa_token=rahz1SVXA2YAAAAA:fb6jT8NuVMWErfpnw-ILfJBuLOLFRSjVLS1ZOT3XMTfCwmHNfzs5nLH_hNRvYTschfkEZfZ5hh06r9CF

Downie et al., 1998, U. (n.d.). A gel diffusion assay for quantification of pectin methylesterase activity. *Elsevier*. Retrieved April 6, 2022, from https://www.sciencedirect.com/science/article/pii/S0003269798928470

Draper et al.,2001, U. (n.d.). Brachypodium distachyon. A New Model System for Functional Genomics in Grasses. *Academic.Oup.Com*. Retrieved April 4, 2022, from https://academic.oup.com/plphys/article-abstract/127/4/1539/6103642

Draper, J., Mur, L., … G. J.-P., & 2001, undefined. (n.d.). Brachypodium distachyon. A New Model System for Functional Genomics in Grasses. *Academic.Oup.Com*. Retrieved April 4, 2022, from https://academic.oup.com/plphys/article-abstract/127/4/1539/6103642

EA Kellogg,2001, U. (n.d.). Evolutionary history of the grasses. *Academic.Oup.Com*. Retrieved April 4, 2022, from https://academic.oup.com/plphys/article-abstract/125/3/1198/6109905

Eaton, S. V. (1952). Effects of Phosphorus Deficiency on Growth and Metabolism of Black Mustard. Contributions from the Hull Botanical Laboratory 631. *Botanical Gazette*, *113*(3), 301–309. https://doi.org/10.1086/335722

Eeuwijk, F. van, Bink, M., … K. C.-C. opinion in plant, & 2010, undefined. (n.d.). Detection and use of QTL for complex traits in multiple environments. *Elsevier*. Retrieved April 7, 2022, from https://www.sciencedirect.com/science/article/pii/S136952661000004X?casa_token=DIdD_f83XmsAAAAA:hAXbd4rgbJVZNK9lg-FJJaGHDOrFzhGc8CuLjLR6OKlHg_zJ2D0fUMskq5li47VY4NToE3E7PA

Fageria, N. K., & Moreira, A. (2011). The Role of Mineral Nutrition on Root Growth of Crop Plants. *Advances in Agronomy*, *110*(C), 251–331. https://doi.org/10.1016/B978-0-12-385531-2.00004-9

Feng, Y., Cao, L. Y., Wu, W. M., Shen, X. H., Zhan, X. D., Zhai, R. R., Wang, R. C., Chen, D. B., & Cheng, S. H. (2010). Mapping QTLs for nitrogen-deficiency tolerance at seedling stage in rice (Oryza sativa L.). *Plant Breeding*, *129*(6), 652–656. https://doi.org/10.1111/J.1439-0523.2009.01728.X

Ferreira et al., 2006, U. (n.d.). Estimating the effects of population size and type on the accuracy of genetic maps. *SciELO Brasil*. Retrieved April 6, 2022, from https://www.scielo.br/pdf/gmb/v29n1/28190.pdf

Fiji, U. . image j. (n.d.). *Fiji, U.S image j - Google Search*. Retrieved April 4, 2022, from https://www.google.com/search?q=Fiji%2C+U.S+image+j&sxsrf=APq-WBtjRX0jXXjnQcGnNFSZSGUSn9XGjA%3A1649106108341&ei=vFxLYs-

zFIjXgQbBo4AI&ved=0ahUKEwjPgaP-pvv2AhWIa8AKHcERAAEQ4dUDCA4&uact=5&oq=Fiji%2C+U.S+image+j&gs_lcp=Cgdnd3Mtd2l6EAMyCAgAEBYQChAeMgYIABAWEB46

Food, & (FAO), A. O. (2019). *FAOSTAT statistical database of the United Nation Food and Agriculture Organization (FAO) statistical division*.

Foster, C. E., Martin, T. M., & Pauly, M. (2010). Comprehensive compositional analysis of plant cell walls (Lignocellulosic biomass) Part I: Lignin. *Journal of Visualized Experiments*, *37*, e1745. https://doi.org/10.3791/1745

Fredeen et al.,1989, U. (n.d.). Influence of Phosphorus Nutrition on Growth and Carbon Partitioning in Glycine max. *Academic.Oup.Com*. Retrieved April 4, 2022, from https://academic.oup.com/plphys/article-abstract/89/1/225/6083595

Fritsche-Neto, R., Miranda, G., DeLima, R., Rural, H. S.-C., & 2010, undefined. (2010). Factor analysis and SREG GGE biplot for the genotype× environment interaction stratification in maize. *SciELO Brasil*, *5*, 1043–1048. https://www.scielo.br/j/cr/a/pqG4pZg4ZDBwSMTtpsrfz4G/abstract/?lang=en

García-Sánchez, F., … S. S.-G.-J. of hazardous, & 2020, undefined. (n.d.). Multiple stresses occurring with boron toxicity and deficiency in plants. *Elsevier*. Retrieved April 4, 2022, from https://www.sciencedirect.com/science/article/pii/S0304389420307020?casa_token=ZJbKwwJoJtEAAAAA:Wo5iuaEj-Uhs_EWSG7cYiBfKPLt7xnb7fecRGUMFHrjLWgIBOaq9YnbvPWQHh6dZF-eSHe0F3Q

Garvin, 2015. (2015). *Brachypodium distachyon Genetic Resources*. 183–195. https://doi.org/10.1007/7397_2015_5

Garvin, D. F., Gu, Y. Q., Hasterok, R., Hazen, S. P., Jenkins, G., Mockler, T. C., Mur, L. A. J., & Vogel, J. P. (2008). Development of genetic and genomic research resources for Brachypodium distachyon, a new model system for grass crop research. *Crop Science*, *48*(SUPPL. 1). https://doi.org/10.2135/CROPSCI2007.06.0332TPG

Garvin, D. F., McKenzie, N., Vogel, J. P., Mockler, T. C., Blankenheim, Z. J., Wright, J., Cheema, J. J., Dicks, J., Huo, N., Hayden, D. M., Gu, Y., Tobias, C., Chang, J. H., Chu, A., Trick, M., Michael, T. P., Bevan, M. W., Snape, J. W., Garvin, D., … Bevan, M. (2010). An SSR-based genetic linkage map of the model grass Brachypodium distachyon. *Genome*, *53*(1), 1–13. https://doi.org/10.1139/G09-079

Garvin et al., 2008, U. (n.d.). Development of Genetic and Genomic Research Resources for Brachypodium distachyon, a New Model System for Grass Crop Research. *Wiley Online Library*. Retrieved April 4, 2022, from https://acsess.onlinelibrary.wiley.com/doi/abs/10.2135/cropsci2007.06.0332tpg?casa_token=_n9z2gwaolAAAAAA:Sgwk6OaHFrWIe66vWJ2Vu9uDHxhCBR9tmPbvTEZOea5m-tpyaOkCg1l8AuW7ZoqD5S0dfYcwdGHM6_o

Giffordet al., 2013, U. (n.d.). Plasticity regulators modulate specific root traits in discrete nitrogen environments. *Journals.Plos.Org*. Retrieved April 7, 2022, from https://journals.plos.org/plosgenetics/article?id=10.1371/journal.pgen.1003760

Gimeno, V., Simón, I., Nieves, M., Trees, V. M.-, & 2012, undefined. (2012). The physiological and nutritional responses to an excess of boron by Verna lemon trees that were grafted on four contrasting rootstocks. *Springer*, *26*(5), 1513–1526. https://doi.org/10.1007/s00468-012-0724-5

Girin et al., 2014, U. (n.d.). Brachypodium: a promising hub between model species and cereals. *Academic.Oup.Com*. Retrieved April 6, 2022, from https://academic.oup.com/jxb/article-abstract/65/19/5683/546694

Głazowska, S., Baldwin, L., Mravec, J., Bukh, C., Hansen, T. H., Jensen, M. M., Fangel, J. U., Willats, W. G. T., Glasius, M., Felby, C., & Schjoerring, J. K. (2018). The impact of silicon on cell wall composition and enzymatic saccharification of Brachypodium distachyon. *Biotechnology for Biofuels*, *11*(1), 1–18. https://doi.org/10.1186/S13068-018-1166-0/FIGURES/7

Glover-Cutter, et al., 2014, U. (n.d.). Enhanced Oxidative Stress Resistance through Activation of a Zinc Deficiency Transcription Factor in Brachypodium distachyon.

Academic.Oup.Com. Retrieved April 7, 2022, from https://academic.oup.com/plphys/article-abstract/166/3/1492/6111194

Godfray, H. C. J., Beddington, J. R., Crute, I. R., Haddad, L., Lawrence, D., Muir, J. F., Pretty, J., Robinson, S., Thomas, S. M., & Toulmin, C. (2010). Food security: The challenge of feeding 9 billion people. *Science*, *327*(5967), 812–818. https://doi.org/10.1126/SCIENCE.1185383

Gomez, L. D., Bristow, J. K., Statham, E. R., & McQueen-Mason, S. J. (2008). Analysis of saccharification in Brachypodium distachyon stems under mild conditions of hydrolysis. *Biotechnology for Biofuels*, *1*. https://doi.org/10.1186/1754-6834-1-15

Gomez, M., Kumar, S., … P. J.-A. J. of, & 2006, undefined. (2006). Mapping QTLs linked to physio-morphological and plant production traits under drought stress in rice (Oryza sativa L.) in the target environment. *Researchgate.Net*. https://doi.org/10.3844/ajbbsp.2006.161.169

Gondwe, R. L., Kinoshita, R., Suminoe, T., Aiuchi, D., Palta, J. P., & Tani, M. (2020). Available Soil Nutrients and NPK Application Impacts on Yield, Quality, and Nutrient Composition of Potatoes Growing during the Main Season in Japan. *American Journal of Potato Research*, *97*(3), 234–245. https://doi.org/10.1007/S12230-020-09776-2/TABLES/5

González-Fontes, A., Herrera-Rodríguez, M. B., Martín-Rejano, E. M., Navarro-Gochicoa, M. T., Rexach, J., & Camacho-Cristóbal, J. J. (2016). Root responses to boron deficiency mediated by ethylene. *Frontiers in Plant Science*, *6*(JAN2016), 1103. https://doi.org/10.3389/FPLS.2015.01103/BIBTEX

Gottlieb, A., Müller, H. G., Massa, A. N., Wanjugi, H., Deal, K. R., You, F. M., Xu, X., Gu, Y. Q., Luo, M. C., Anderson, O. D., Chan, A. P., Rabinowicz, P., Devos, K. M., & Dvorak, J. (2013). Insular Organization of Gene Space in Grass Genomes. *PLoS ONE*, *8*(1). https://doi.org/10.1371/JOURNAL.PONE.0054101

Greenup et al., 2009, U. (n.d.). The molecular biology of seasonal flowering-responses in Arabidopsis and the cereals. *Academic.Oup.Com*. Retrieved April 7, 2022, from https://academic.oup.com/aob/article-abstract/103/8/1165/178792

Greiner & I Egli, 2003. (2003). Determination of the activity of acidic phytate-degrading enzymes in cereal seeds. *ACS Publications*, *51*(4), 847–850. https://doi.org/10.1021/jf0204405

Großkinsky & Svensgaard, 2015, U. (n.d.). Plant phenomics and the need for physiological phenotyping across scales to narrow the genotype-to-phenotype knowledge gap. *Academic.Oup.Com*. Retrieved April 6, 2022, from https://academic.oup.com/jxb/article-abstract/66/18/5429/482901

Gruber, B. D., Giehl, R. F. H., Friedel, S., & von Wirén, N. (2013). Plasticity of the Arabidopsis Root System under Nutrient Deficiencies. *Plant Physiology*, *163*(1), 161–179. https://doi.org/10.1104/PP.113.218453

Gupta et al., 2013, U. (n.d.). Impact of boron deficiency on plant growth. *Researchgate.Net*. Retrieved April 4, 2022, from https://www.researchgate.net/profile/Hitesh-Solanki-3/publication/249335637_Impact_of_boron_deficiency_on_plant_growth/links/0c96051e5265734620000000/Impact-of-boron-deficiency-on-plant-growth.pdf

Hackett, C. A. (2002). Statistical methods for QTL mapping in cereals. *Plant Molecular Biology*, *48*(5–6), 585–599. https://doi.org/10.1023/A:1014896712447

Haldane, 1919, U. (n.d.). The probable errors of calculated linkage values, and the most accurate method of determining gametic from certain zygotic series. *Ias.Ac.In*. Retrieved April 6, 2022, from https://www.ias.ac.in/describe/article/jgen/008/04/0291-0297

Harholt, J., Suttangkakul, A., & Scheller, H. V. (2010). Biosynthesis of pectin. *Plant Physiology*, *153*(2), 384–395. https://doi.org/10.1104/PP.110.156588

Hatfield, R. D., Rancour, D. M., & Marita, J. M. (2017). Grass cell walls: A story of cross-linking. *Frontiers in Plant Science*, *7*. https://doi.org/10.3389/FPLS.2016.02056/FULL

Havlin, J., Systems, A. S.-S., & 2021, undefined. (n.d.). Review of Phosphite as a Plant Nutrient and Fungicide. *Mdpi.Com*. Retrieved April 3, 2022, from https://www.mdpi.com/2571-8789/5/3/52

Higgins, J. A., Bailey, P. C., & Laurie, D. A. (2010). Comparative genomics of flowering time pathways using brachypodium distachyon as a model for the temperate Grasses. *PLoS ONE*, *5*(4). https://doi.org/10.1371/JOURNAL.PONE.0010065

Hindhaugh, R., Bosch, M., botany, I. D.-A. of, & 2021, undefined. (n.d.). Mechanical stimulation in wheat triggers age-and dose-dependent alterations in growth, development and grain characteristics. *Academic.Oup.Com*. Retrieved April 4, 2022, from https://academic.oup.com/aob/article-abstract/128/5/589/6294076

Hirel, B., Gouis, J. Le, … B. N.-J. of experimental, & 2007, undefined. (n.d.). The challenge of improving nitrogen use efficiency in crop plants: towards a more central role for genetic variability and quantitative genetics within integrated. *Academic.Oup.Com*. Retrieved April 4, 2022, from https://academic.oup.com/jxb/article-abstract/58/9/2369/543374

Hoagland & Arnon,1950, U. (n.d.). The water-culture method for growing plants without soil. *Cabdirect.Org*. Retrieved April 4, 2022, from https://www.cabdirect.org/cabdirect/abstract/19500302257

Hong et al., 2010, U. (n.d.). Functional characterization of pectin methylesterase inhibitor (PMEI) in wheat. *Jstage.Jst.Go.Jp*. Retrieved April 5, 2022, from https://www.jstage.jst.go.jp/article/ggs/85/2/85_2_97/_article/-char/ja/

Houle, D., Govindaraju, D., genetics, S. O.-N. reviews, & 2010, undefined. (n.d.). Phenomics: the next challenge. *Nature.Com*. Retrieved April 4, 2022, from https://idp.nature.com/authorize/casa?redirect_uri=https://www.nature.com/articles/nrg2897&casa_token=BYvhglCzawoAAAAA:-JRbQmz5F2ZwnehVkU8CP5PZ1yscKzW53vxQtdJFYJw29O8Fu5yB1ARkWeZ3eOyQRuuAdGxcgKKyVLfF

Howell, 1954, U. (1950). Phosphorus nutrition of soybeans. *Ncbi.Nlm.Nih.Gov*, *6*, 0. https://www.ncbi.nlm.nih.gov/pmc/articles/PMC540562/

Hu et al., 2020, U. (n.d.). The reduction in leaf area precedes that in photosynthesis under potassium deficiency: the importance of leaf anatomy. *Wiley Online Library*. Retrieved

April 7, 2022, from https://nph.onlinelibrary.wiley.com/doi/abs/10.1111/nph.16644

Hu, Y., & Schmidhalter, U. (2005). Drought and salinity: A comparison of their effects on mineral nutrition of plants. *Journal of Plant Nutrition and Soil Science*, *168*(4), 541–549. https://doi.org/10.1002/JPLN.200420516

Huang, Y. C., Wu, H. C., Wang, Y. Da, Liu, C. H., Lin, C. C., Luo, D. L., & Jinn, T. L. (2017). PECTIN METHYLESTERASE34 contributes to heat tolerance through its role in promoting stomatal movement. *Plant Physiology*, *174*(2), 748–763. https://doi.org/10.1104/pp.17.00335

Huo, N., Garvin, D. F., You, F. M., McMahon, S., Luo, M. C., Gu, Y. Q., Lazo, G. R., & Vogel, J. P. (2011). Comparison of a high-density genetic linkage map to genome features in the model grass Brachypodium distachyon. *Theoretical and Applied Genetics*, *123*(3), 455–464. https://doi.org/10.1007/S00122-011-1598-4

Hussain et al., 2017, U. (n.d.). Genotyping-by-sequencing derived high-density linkage map and its application to QTL mapping of flag leaf traits in bread wheat. *Nature.Com*. Retrieved April 6, 2022, from https://www.nature.com/articles/s41598-017-16006-z

Ikram et al., 2012, U. (n.d.). Natural variation of Arabidopsis response to nitrogen availability. *Academic.Oup.Com*. Retrieved April 6, 2022, from https://academic.oup.com/jxb/article-abstract/63/1/91/552676

Ingram, P. A., Zhu, J., Shariff, A., Davis, I. W., Benfey, P. N., & Elich, T. (2012). High-throughput imaging and analysis of root system architecture in Brachypodium distachyon under differential nutrient availability. *Philosophical Transactions of the Royal Society B: Biological Sciences*, *367*(1595), 1559–1569. https://doi.org/10.1098/RSTB.2011.0241

Ishii, T & T Matsunaga, 2001. (n.d.). Pectic polysaccharide rhamnogalacturonan II is covalently linked to homogalacturonan. *Elsevier*. Retrieved April 4, 2022, from https://www.sciencedirect.com/science/article/pii/S0031942201000474?casa_token=nJ3Ne47mfSwAAAAA:W-kgmwfxOn_kL8xPOcYp-jKfrY3QvBdIFpVGBFEQxGd16HzhhS3COaEcuRKrU-8xw2gWfmp-wA

Ishii, T, research, T. M.-C., & 1996, undefined. (n.d.). Isolation and characterization of a boron-rhamnogalacturonan-II complex from cell walls of sugar beet pulp. *Elsevier*. Retrieved April 4, 2022, from https://www.sciencedirect.com/science/article/pii/0008621596000109

Ishii, Tadashi. (1997). Structure and functions of feruloylated polysaccharides. *Plant Science*, *127*(2), 111–127. https://doi.org/10.1016/S0168-9452(97)00130-1

Ivakov & Persson, 2012. (2012). Plant Cell Walls. *ELS*. https://doi.org/10.1002/9780470015902.A0001682.PUB2

Jansen, R., Genetics, P. S.-, & 1994, undefined. (1994). High resolution of quantitative traits into multiple loci via interval mapping. *Academic.Oup.Com*. https://academic.oup.com/genetics/article-abstract/136/4/1447/6012230

Jeong, H. Y., Nguyen, H. P., Eom, S. H., & Lee, C. (2018). Integrative analysis of pectin methylesterase (PME) and PME inhibitors in tomato (Solanum lycopersicum): Identification, tissue-specific expression, and biochemical characterization. *Plant Physiology and Biochemistry*, *132*, 557–565. https://doi.org/10.1016/J.PLAPHY.2018.10.006

Jewel et al., 2019, U. (n.d.). Identification of quantitative trait loci associated with nutrient use efficiency traits, using SNP markers in an early backcross population of rice (Oryza sativa L.). *Mdpi.Com*. Retrieved April 6, 2022, from https://www.mdpi.com/414348

Jia, Z., Giehl, R. F. H., & Von Wirén, N. (2020). The Root Foraging Response under Low Nitrogen Depends on DWARF1-Mediated Brassinosteroid Biosynthesis. *Plant Physiology*, *183*(3), 998–1010. https://doi.org/10.1104/PP.20.00440

Johannsen, W. (1911). The Genotype Conception of Heredity. *The American Naturalist*, *45*(531), 129–159. https://doi.org/10.1086/279202

Jolie et al.,2010, U. (n.d.). Pectin methylesterase and its proteinaceous inhibitor: a review. *Elsevier*. Retrieved April 5, 2022, from https://www.sciencedirect.com/science/article/pii/S0008621510004350?casa_token=

B_OWjV_cMBkAAAAA:ZastWhgY8lGIxaDKbSmoMLQf0m2ryA4Q02y3NKbZpF9ORcVtnxNWYqdA_Q4cX-LZdyQta3ohbw

Jones, L., Milne, J. L., Ashford, D., & McQueen-Mason, S. J. (2003). Cell wall arabinan is essential for guard cell function. *Proceedings of the National Academy of Sciences*, *100*(20), 11783–11788. https://doi.org/10.1073/pnas.1832434100

Jones, Louise, Milne, J. L., Ashford, D., McCann, M. C., & McQueen-Mason, S. J. (2005). A conserved functional role of pectic polymers in stomatal guard cells from a range of plant species. *Planta*, *221*(2), 255–264. https://doi.org/10.1007/s00425-004-1432-1

JP Lynch, 2013. (n.d.). Steep, cheap and deep: an ideotype to optimize water and N acquisition by maize root systems. In *academic.oup.com*. Retrieved April 3, 2022, from https://academic.oup.com/aob/article-abstract/112/2/347/162759

Kamal, N., Gorafi, Y., … M. A.-I. J. of, & 2019, undefined. (n.d.). Stay-green trait: A prospective approach for yield potential, and drought and heat stress adaptation in globally important cereals. *Mdpi.Com*. Retrieved April 4, 2022, from https://www.mdpi.com/578180

Kang, M. S., & Banga, S. S. (2013). Global Agriculture and Climate Change. *Journal of Crop Improvement*, *27*(6), 667–692. https://doi.org/10.1080/15427528.2013.845051

Kant, S, Kafkafi, U., Pasricha, N., crop, S. B.-P. for sustainable, & 2002, undefined. (n.d.). Potassium and abiotic stresses in plants. *Citeseer*. Retrieved April 4, 2022, from https://citeseerx.ist.psu.edu/viewdoc/download?doi=10.1.1.575.4024&rep=rep1&type=pdf

Kant, Surya, Peng, M., & Rothstein, S. J. (2011). Genetic regulation by NLA and microRNA827 for maintaining nitrate-dependent phosphate homeostasis in Arabidopsis. *PLoS Genetics*, *7*(3). https://doi.org/10.1371/JOURNAL.PGEN.1002021

Kellogg, E. A. (2015). Brachypodium distachyon as a Genetic Model System. *Annual Review of Genetics*, *49*, 1–20. https://doi.org/10.1146/ANNUREV-GENET-112414-055135

Khan, M. A., Gemenet, D. C., & Villordon, A. (2016). Root system architecture and abiotic

stress tolerance: Current knowledge in root and tuber crops. *Frontiers in Plant Science*, *7*(NOVEMBER2016). https://doi.org/10.3389/FPLS.2016.01584/FULL

Kohorn, B. D., Johansen, S., Shishido, A., Todorova, T., Martinez, R., Defeo, E., & Obregon, P. (2009). Pectin activation of MAP kinase and gene expression is WAK2 dependent. *Plant Journal*, *60*(6), 974–982. https://doi.org/10.1111/J.1365-313X.2009.04016.X

Kolář & Seňková, 2008, U. (n.d.). Reduction of mineral nutrient availability accelerates flowering of Arabidopsis thaliana. *Elsevier*. Retrieved April 6, 2022, from https://www.sciencedirect.com/science/article/pii/S0176161708000229?casa_token=N7ElSYW_ILsAAAAA:qeFqW05CW7kfgv1kuKmeNsyq-bvSZiA2RsIO5QOX0Vz4jGrjjNkFZBsrjeTNyjtTQXKxMEH2Xg

Kosambi, 1942, U. (n.d.). On valid tests of linguistic hypotheses. *Repository.Ias.Ac.In*. Retrieved April 6, 2022, from http://repository.ias.ac.in/99262/1/Valid_tests_of_linguistic_hypothesis.pdf

Krapp et al., 2011, U. (n.d.). Arabidopsis roots and shoots show distinct temporal adaptation patterns toward nitrogen starvation. *Academic.Oup.Com*. Retrieved April 7, 2022, from https://academic.oup.com/plphys/article-abstract/157/3/1255/6108845

Kvakić, M., Pellerin, S., Ciais, P., Achat, D. L., Augusto, L., Denoroy, P., Gerber, J. S., Goll, D., Mollier, A., Mueller, N. D., Wang, X., & Ringeval, B. (2018). Quantifying the Limitation to World Cereal Production Due To Soil Phosphorus Status. *Global Biogeochemical Cycles*, *32*(1), 143–157. https://doi.org/10.1002/2017GB005754

Le Gall, H., Philippe, F., Domon, J.-M., Gillet, F., Pelloux, J., & Rayon, C. (2015a). Cell wall metabolism in response to abiotic stress. *Plants*, *4*, 112–166. https://doi.org/10.3390/plants4010112

Le Gall, H., Philippe, F., Domon, J. M., Gillet, F., Pelloux, J., & Rayon, C. (2015b). Cell Wall Metabolism in Response to Abiotic Stress. *Plants 2015, Vol. 4, Pages 112-166*, *4*(1), 112–166. https://doi.org/10.3390/PLANTS4010112

Leghari, S. et al., & 2016. (n.d.). Role of nitrogen for plant growth and development: A

review. *Go.Gale.Com*. Retrieved April 3, 2022, from https://go.gale.com/ps/i.do?id=GALE%7CA472372583&sid=googleScholar&v=2.1&it=r&linkaccess=abs&issn=19950756&p=AONE&sw=w

Lenk I et al., 2019, U. (n.d.). Transcriptional and metabolomic analyses indicate that cell wall properties are associated with drought tolerance in Brachypodium distachyon. *Mdpi.Com*. Retrieved April 6, 2022, from https://www.mdpi.com/442692

Li, H., Kilian, A., Zhou, M., Wenzl, P., Huttner, E., Mendham, N., McIntyre, L., & Vaillancourt, R. E. (2010). Construction of a high-density composite map and comparative mapping of segregation distortion regions in barley. *Molecular Genetics and Genomics*, *284*(5), 319–331. https://doi.org/10.1007/S00438-010-0570-3

Li, X., Mu, Y., Cheng, Y., Liu, X., & Nian, H. (2013). Effects of intercropping sugarcane and soybean on growth, rhizosphere soil microbes, nitrogen and phosphorus availability. *Acta Physiologiae Plantarum*, *35*(4), 1113–1119. https://doi.org/10.1007/S11738-012-1148-Y

Lichtenthaler & Buschmann, 2001. (2001). Chlorophylls and Carotenoids: Measurement and Characterization by UV-VIS Spectroscopy. *Current Protocols in Food Analytical Chemistry*, *1*(1), F4.3.1-F4.3.8. https://doi.org/10.1002/0471142913.FAF0403S01

Lichtenthaler, H. K. (1987). Chlorophylls and Carotenoids: Pigments of Photosynthetic Biomembranes. *Methods in Enzymology*, *148*(C), 350–382. https://doi.org/10.1016/0076-6879(87)48036-1

Liebig, J. von, & Playfair, L. (1843). *Chemistry in its application to agriculture and physiology*. https://books.google.com/books?hl=en&lr=&id=ccE1AQAAMAAJ&oi=fnd&pg=PA9&dq=Justus+von+Liebig+1843&ots=ubtvYwRiqc&sig=8frkseqG9MjYu4V1cBH-fQXKRJo

Lin & Tsay, 2017, U. (n.d.). Influence of differing nitrate and nitrogen availability on flowering control in Arabidopsis. *Academic.Oup.Com*. Retrieved April 6, 2022, from https://academic.oup.com/jxb/article-abstract/68/10/2603/3091696

Lionetti, V., Francocci, F., Ferrari, S., Volpi, C., Bellincampi, D., Galletti, R., D'Ovidio, R., De

Lorenzo, G., & Cervone, F. (2010). Engineering the cell wall by reducing de-methyl-esterified homogalacturonan improves saccharification of plant tissues for bioconversion. *Proceedings of the National Academy of Sciences of the United States of America*, *107*(2), 616–621. https://doi.org/10.1073/pnas.0907549107

Lionetti, V., Raiola, A., Camardella, L., Giovane, A., Obel, N., Pauly, M., Favaron, F., Cervone, F., & Bellincampi, D. (2007). Overexpression of pectin methylesterase inhibitors in Arabidopsis restricts fungal infection by Botrytis cinerea. *Plant Physiology*, *143*(4), 1871–1880. https://doi.org/10.1104/pp.106.090803

Liu et al., 2013. (2013). Nitrate or NaCl regulates floral induction in Arabidopsis thaliana. *Biologia (Poland)*, *68*(2), 215–222. https://doi.org/10.2478/S11756-013-0004-X

Liu, H. Y., Sun, W. N., Su, W. A., & Tang, Z. C. (2006). Co-regulation of water channels and potassium channels in rice. *Physiologia Plantarum*, *128*(1), 58–69. https://doi.org/10.1111/J.1399-3054.2006.00709.X

Liu Y. et al., 2019. (n.d.). Boron and calcium deficiency disturbing the growth of trifoliate rootstock seedlings (Poncirus trifoliate L.) by changing root architecture and cell wall. *Elsevier*. Retrieved April 5, 2022, from https://www.sciencedirect.com/science/article/pii/S0981942819304085?casa_token=PV5FwRK81lsAAAAA:tVyxXaMGa260jTlQo5S207OsRZC2c_IfUJiuFMbvnHj1g50HZKVJl08TxpBc2n6igYKmhdAf7w

LM Condron & H Tiessen 2005. (n.d.). Interactions of organic phosphorus in terrestrial ecosystems. In *cabdirect.org*. Retrieved April 3, 2022, from https://www.cabdirect.org/cabdirect/abstract/20073011537

Lobos, G. A., Camargo, A. V., Del Pozo, A., Araus, J. L., Ortiz, R., & Doonan, J. H. (2017). Editorial: Plant phenotyping and phenomics for plant breeding. *Frontiers in Plant Science*, *8*. https://doi.org/10.3389/FPLS.2017.02181/FULL

López-Bucio,2003, U. (n.d.). The role of nutrient availability in regulating root architecture. *Elsevier*. Retrieved April 4, 2022, from https://www.sciencedirect.com/science/article/pii/S1369526603000359?casa_token=

OE84d8_G70AAAAAA:Yxl09KIW0rbRQ-84Ss2Mg_SOx2lxqWICNux2hXvFAr2U8w1iDwhwZhQnLwQIgeZs-GkkLYk6yw

Louw-Gaume et al., 2010. (2010). A comparative study on plant growth and root plasticity responses of two Brachiaria forage grasses grown in nutrient solution at low and high phosphorus supply. *Plant and Soil*, *328*(1), 155–164. https://doi.org/10.1007/S11104-009-0093-Z

Luo, N., Liu, J., Yu, X., & Jiang, Y. (2011). Natural variation of drought response in Brachypodium distachyon. *Physiologia Plantarum*, *141*(1), 19–29. https://doi.org/10.1111/j.1399-3054.2010.01413.x

Lynch & Brown, 2001. (2001). Topsoil foraging - An architectural adaptation of plants to low phosphorus availability. *Plant and Soil*, *237*(2), 225–237. https://doi.org/10.1023/A:1013324727040

Lynch, J., Läuchli, A., & Epstein, E. (1991). Vegetative Growth of the Common Bean in Response to Phosphorus Nutrition. *Crop Science*, *31*(2), 380–387. https://doi.org/10.2135/CROPSCI1991.0011183X003100020031X

Lynch, J. P., & Lynch, J. P. (2007). Roots of the Second Green Revolution. *Australian Journal of Botany*, *55*(5), 493–512. https://doi.org/10.1071/BT06118

Lynch, M., & Walsh, B. (1998). *Genetics and analysis of quantitative traits*. http://www.invemar.org.co/redcostera1/invemar/docs/RinconLiterario/2011/febrero/AG_8.pdf

M Brdar-Jokanović , 2020, U. (n.d.). Boron toxicity and deficiency in agricultural plants. *Mdpi.Com*. Retrieved April 4, 2022, from https://www.mdpi.com/645690

Mahajan, S., & Tuteja, N. (2005). Cold, salinity and drought stresses: An overview. *Archives of Biochemistry and Biophysics*, *444*(2), 139–158. https://doi.org/10.1016/j.abb.2005.10.018

Mahmoud Seleiman, 2014. (n.d.). *(PDF) Towards sustainable intensification of feedstock production with nutrient cycling*. Retrieved April 3, 2022, from

https://www.researchgate.net/publication/261685396_Towards_sustainable_intensification_of_feedstock_production_with_nutrient_cycling

Makino, Y., & Ueno, O. (2018). Structural and physiological responses of the C4 grass Sorghum bicolor to nitrogen limitation. *Plant Production Science*, *21*(1), 39–50. https://doi.org/10.1080/1343943X.2018.1432290

Malhotra, H., Vandana, Sharma, S., & Pandey, R. (2018). Phosphorus Nutrition: Plant Growth in Response to Deficiency and Excess. *Plant Nutrients and Abiotic Stress Tolerance*, 171–190. https://doi.org/10.1007/978-981-10-9044-8_7

Mann, D. G. J., Lafayette, P. R., Abercrombie, L. L., King, Z. R., Mazarei, M., Halter, M. C., Poovaiah, C. R., Baxter, H., Shen, H., Dixon, R. A., Parrott, W. A., & Neal Stewart, J. (2012). Gateway-compatible vectors for high-throughput gene functional analysis in switchgrass (Panicum virgatum L.) and other monocot species. *Plant Biotechnology Journal*, *10*(2), 226–236. https://doi.org/10.1111/J.1467-7652.2011.00658.X

Marchin, R. M., Ossola, A., Leishman, M. R., & Ellsworth, D. S. (2020). A Simple Method for Simulating Drought Effects on Plants. *Frontiers in Plant Science*, *10*. https://doi.org/10.3389/FPLS.2019.01715/FULL

Marriott, P. E., Sibout, R., Lapierre, C., Fangel, J. U., Willats, W. G. T., Hofte, H., Gómez, L. D., & McQueen-Mason, S. J. (2014). Range of cell-wall alterations enhance saccharification in *Brachypodium distachyon* mutants. *Proceedings of the National Academy of Sciences of the United States of America*, *111*(40), 14601–14606. https://doi.org/10.1073/pnas.1414020111

Marschner, H. (1986). *Mineral nutrition of higher plants, Horst Marschner*. http://www.sidalc.net/cgi-bin/wxis.exe/?IsisScript=sibur.xis&method=post&formato=2&cantidad=1&expresion=mfn=006259

Martín-Rejano, E. M., Camacho-Cristóbal, J. J., Herrera-Rodríguez, M. B., Rexach, J., Navarro-Gochicoa, M. T., & González-Fontes, A. (2011). Auxin and ethylene are involved in the responses of root system architecture to low boron supply in Arabidopsis seedlings.

Physiologia Plantarum, *142*(2), 170–178. https://doi.org/10.1111/J.1399-3054.2011.01459.X

Matoh, T. (1997). Boron in plant cell walls. *Plant and Soil 1997 193:1*, *193*(1), 59–70. https://doi.org/10.1023/A:1004207824251

Matoh, T., & Kobayashi, M. (2002). Boron Function in Plant Cell Walls. *Boron in Plant and Animal Nutrition*, 143–155. https://doi.org/10.1007/978-1-4615-0607-2_13

Mehmood, M., Ibrahim, M., Rashid, U., … M. N.-S. P., & 2017, undefined. (n.d.). Biomass production for bioenergy using marginal lands. *Elsevier*. Retrieved April 2, 2022, from https://www.sciencedirect.com/science/article/pii/S2352550916300197?casa_token=XeD4n6IB4tsAAAAA:BoQKsGFxT7iaiVJN89y4mEmr9A0DYDOgeQfVnb5DUA_OE7NgJchAd_63RaoE1kApm79BbJ6ZIg

Mei et al., 2016, U. (n.d.). Boron deficiency affects root vessel anatomy and mineral nutrient allocation of Poncirus trifoliata (L.) Raf. *Springer*. Retrieved April 7, 2022, from https://link.springer.com/article/10.1007/s11738-016-2099-5

Mei, L., Li, Q., Wang, H., Sheng, O., & Peng, S. ang. (2016). Boron deficiency affects root vessel anatomy and mineral nutrient allocation of Poncirus trifoliata (L.) Raf. *Acta Physiologiae Plantarum*, *38*(4). https://doi.org/10.1007/S11738-016-2099-5

Meng, X., Yoo, C., Li, M., & A. R.-J. of A. B., & 2016, undefined. (n.d.). Physicochemical structural changes of cellulosic substrates during enzymatic saccharification. *Osti.Gov*. Retrieved April 4, 2022, from https://www.osti.gov/biblio/1343547

Mengel, K., Kirkby, E. A., Kosegarten, H., & Appel, T. (2001). Nitrogen. *Principles of Plant Nutrition*, 397–434. https://doi.org/10.1007/978-94-010-1009-2_7

Merrill, J. Z., & Cornwell, J. C. (2005). The Role of Oligohaline Marshes in Estuarine Nutrient Cycling. *Concepts and Controversies in Tidal Marsh Ecology*, 425–441. https://doi.org/10.1007/0-306-47534-0_19

Mohnen, D. (2008). Pectin structure and biosynthesis. *Current Opinion in Plant Biology*, *11*(3), 266–277. https://doi.org/10.1016/j.pbi.2008.03.006

Moore, J. P., Farrant, J. M., & Driouich, A. (2008). A role for pectin-associated arabinans in maintaining the flexibility of the plant cell wall during water deficit stress. *Plant Signaling and Behavior*, *3*(2), 102–104. https://doi.org/10.4161/psb.3.2.4959

Mouille et al., 2007. (2007). Homogalacturonan synthesis in Arabidopsis thaliana requires a Golgi-localized protein with a putative methyltransferase domain. *Plant Journal*, *50*(4), 605–614. https://doi.org/10.1111/J.1365-313X.2007.03086.X

Munns & Gilliham, 2015, U. (2015). Salinity tolerance of crops–what is the cost? *Wiley Online Library*, *208*(3), 668–673. https://doi.org/10.1111/nph.13519

Munson, S. M., & Long, A. L. (2017). Climate drives shifts in grass reproductive phenology across the western USA. *New Phytologist*, *213*(4), 1945–1955. https://doi.org/10.1111/NPH.14327

Mur, L., Allainguillaume, J., … P. C.-N., & 2011, undefined. (n.d.). Exploiting the Brachypodium Tool Box in cereal and grass research. *Wiley Online Library*. Retrieved April 4, 2022, from https://nph.onlinelibrary.wiley.com/doi/abs/10.1111/j.1469-8137.2011.03748.x

Murren, C. J., & Pigliucci, M. (2005). Morphological responses to stimulated wind in the genus *Brassica* (Brassicaceae): Allopolyploids and Their Parental Species. *American Journal of Botany*, *92*(5), 810–818. https://doi.org/10.3732/ajb.92.5.810

Myers, S. S., Smith, M. R., Guth, S., Golden, C. D., Vaitla, B., Mueller, N. D., Dangour, A. D., & Huybers, P. (2017). Climate Change and Global Food Systems: Potential Impacts on Food Security and Undernutrition. *Annual Review of Public Health*, *38*, 259–277. https://doi.org/10.1146/ANNUREV-PUBLHEALTH-031816-044356

North et al., 2009, U. (n.d.). Natural variation in Arabidopsis adaptation to growth at low nitrogen conditions. *Elsevier*. Retrieved April 6, 2022, from https://www.sciencedirect.com/science/article/pii/S0981942809001624?casa_token=xgEa9gB5yYcAAAAA:NVvUZFq3ot_BoKuOhVMYzaL-Z8pDdAnvhbNyfoz1igCAUc3HbdvralFWPVh1eh0jF2PQJmjSiA

O'Neill, M., Warrenfeltz, D., Kates, K., … P. P.-J. of B., & 1996, undefined. (n.d.). Rhamnogalacturonan-II, a pectic polysaccharide in the walls of growing plant cell, forms a dimer that is covalently cross-linked by a borate ester: in vitro. *ASBMB*. Retrieved April 4, 2022, from https://www.jbc.org/article/S0021-9258(19)61839-9/abstract

Ogden, M., Hoefgen, R., Roessner, U., … S. P.-I. journal of, & 2018, undefined. (n.d.). Feeding the walls: how does nutrient availability regulate cell wall composition? *Mdpi.Com*. Retrieved April 4, 2022, from https://www.mdpi.com/337706

Opanowicz, M et al., 2008. Undefined. (n.d.). Brachypodium distachyon: making hay with a wild grass. *Elsevier*. Retrieved April 4, 2022, from https://www.sciencedirect.com/science/article/pii/S1360138508000800?casa_token=bNI7wc48D_0AAAAA:tcssNlfn81Uj-XdIcTQ4c3t5i5YfUCsWRGjVb3mCV-8O41nbE0Bz1xCWC1BMpIhm8ApuEDmFKg

Oscarson, 2000, U. (n.d.). The strategy of the wheat plant in acclimating growth and grain production to nitrogen availability. *Academic.Oup.Com*. Retrieved April 7, 2022, from https://academic.oup.com/jxb/article-abstract/51/352/1921/538868

Pacheco-Villalobos, D., & Hardtke, C. S. (2012). Natural genetic variation of root system architecture from Arabidopsis to Brachypodium: Towards adaptive value. *Philosophical Transactions of the Royal Society B: Biological Sciences*, *367*(1595), 1552–1558. https://doi.org/10.1098/rstb.2011.0237

Pan et al., 2017, U. (n.d.). Effects of low sink demand on leaf photosynthesis under potassium deficiency. *Elsevier*. Retrieved April 7, 2022, from https://www.sciencedirect.com/science/article/pii/S0981942817300396?casa_token=m3B-46qmkUIAAAAA:Wn52ZD0G419-NESQ_FgndRVXJbTBiJi8ZaXDRSMtXyzNthO0su7HVvBQ_8eSefj4AbZkeaujzA

Pancaldi, F., & Trindade, L. M. (2020). Marginal Lands to Grow Novel Bio-Based Crops: A Plant Breeding Perspective. *Frontiers in Plant Science*, *11*. https://doi.org/10.3389/FPLS.2020.00227/FULL

Pauly, M., Gille, S., Liu, L., Mansoori, N., de Souza, A., Schultink, A., & Xiong, G. (2013). Hemicellulose biosynthesis. *Planta*, *238*(4), 627–642. https://doi.org/10.1007/S00425-013-1921-1

Pauly, M., & Keegstra, K. (2010). Plant cell wall polymers as precursors for biofuels. *Current Opinion in Plant Biology*, *13*(3), 304–311. https://doi.org/10.1016/J.PBI.2009.12.009

Peaucelle, A., Braybrook, S., & Höfte, H. (2012). Cell wall mechanics and growth control in plants: The role of pectins revisited. *Frontiers in Plant Science*, *3*(JUN). https://doi.org/10.3389/FPLS.2012.00121/FULL

Pelloux et al., 2007, U. (n.d.). New insights into pectin methylesterase structure and function. *Elsevier*. Retrieved April 5, 2022, from https://www.sciencedirect.com/science/article/pii/S1360138507000969?casa_token=TP_Fj73rcG0AAAAA:ziElFBjaYR17JqVGbw_DdLORhlHEQEe_4B4iOS-IBmAxJg_9Fx6BwfWUBcCD8-mxwt6WpvuYBQ

Perchlik, M., Physiology, M. T.-P., & 2018, undefined. (n.d.). Leaf amino acid supply affects photosynthetic and plant nitrogen use efficiency under nitrogen stress. *Academic.Oup.Com*. Retrieved April 3, 2022, from https://academic.oup.com/plphys/article-abstract/178/1/174/6116507

Pettigrew, W. T. (2008). Potassium influences on yield and quality production for maize, wheat, soybean and cotton. *Physiologia Plantarum*, *133*(4), 670–681. https://doi.org/10.1111/J.1399-3054.2008.01073.X

Pieruschka R & H Poorter 2012, U. (n.d.). Phenotyping plants: genes, phenes and machines. *CSIRO Publishing*. https://doi.org/10.1071/FPv39n11_IN

Pinzon-Latorre, D., & Deyholos, M. K. (2014). Pectinmethylesterases (PME) and Pectinmethylesterase Inhibitors (PMEI) enriched during phloem fiber development in flax (*Linum usitatissimum*). *PLoS ONE*, *9*(8), e105386. https://doi.org/10.1371/journal.pone.0105386

Ploeg, R. Van der, … W. B.-S. S. S. of, & 1999, undefined. (1999). On the origin of the theory

of mineral nutrition of plants and the law of the minimum. *Wiley Online Library*, *63*(5), 1055–1062. https://doi.org/10.2136/sssaj1999.6351055x

Poiré et al., 2014, U. (n.d.). Digital imaging approaches for phenotyping whole plant nitrogen and phosphorus response in Brachypodium distachyon. *Wiley Online Library*. Retrieved April 5, 2022, from https://onlinelibrary.wiley.com/doi/abs/10.1111/jipb.12198?casa_token=Q9M6QGrADA8AAAAA:lchRp_dahRsyuB1FPPc10kCBDcCoGDxJRFtgqFyfdh0uyxiPpIVjywThOAB8s-r0_HtTXWHedx7wLMY

Poiré, R., Chochois, V., Sirault, X. R. R., Vogel, J. P., Watt, M., & Furbank, R. T. (2014). Digital imaging approaches for phenotyping whole plant nitrogen and phosphorus response in Brachypodium distachyon. *Journal of Integrative Plant Biology*, *56*(8), 781–796. https://doi.org/10.1111/JIPB.12198

Raiola et al., 2004, U. (n.d.). Two Arabidopsis thaliana genes encode functional pectin methylesterase inhibitors. *Elsevier*. Retrieved April 6, 2022, from https://www.sciencedirect.com/science/article/pii/S0014579303014911

Ralph, J., Guillaumie, S., Grabber, J., … C. L.-C. R., & 2004, undefined. (n.d.). Genetic and molecular basis of grass cell-wall biosynthesis and degradability. III. Towards a forage grass ideotype. *Elsevier*. Retrieved April 4, 2022, from https://www.sciencedirect.com/science/article/pii/S1631069104000769

Rancour, D. M., Marita, J. M., & Hatfield, R. D. (2012). Cell wall composition throughout development for the model grass Brachypodium distachyon. *Frontiers in Plant Science*, *3*(DEC), 1–14. https://doi.org/10.3389/fpls.2012.00266

Ream & Woods, 2012, U. (n.d.). The molecular basis of vernalization in different plant groups. *Symposium.Cshlp.Org*. Retrieved April 6, 2022, from http://symposium.cshlp.org/content/77/105.short

Ream et al., 2014, U. (n.d.). Interaction of Photoperiod and Vernalization Determines Flowering Time of Brachypodium distachyon. *Academic.Oup.Com*. Retrieved April 6, 2022, from https://academic.oup.com/plphys/article-abstract/164/2/694/6112903

Reca, I. B., Lionetti, V., Camardella, L., D'Avino, R., Giardina, T., Cervone, F., & Bellincampi, D. (2012). A functional pectin methylesterase inhibitor protein (SolyPMEI) is expressed during tomato fruit ripening and interacts with PME-1. *Plant Molecular Biology*, *79*(4–5), 429–442. https://doi.org/10.1007/S11103-012-9921-2

Reddy, N. R., Sathe, S. K., & Salunkhe, D. K. (1982). Phytates in Legumes and Cereals. *Advances in Food Research*, *28*(C), 1–92. https://doi.org/10.1016/S0065-2628(08)60110-X

Rerkasem & Jamjod, 2004, U. (n.d.). Boron deficiency in wheat: a review. *Elsevier*. Retrieved April 5, 2022, from https://www.sciencedirect.com/science/article/pii/S0378429004000656?casa_token=-kgDx9da_OwAAAAA:2JXbEPhId4nKHjuaDJbpOFFURqp3y-t4FA6uM5KG_-rknRiywT3kxCBhUHFzWNqRpqTimA-v7A

Ridley, B. L., O'Neill, M. A., & Mohnen, D. (2001). Pectins: Structure, biosynthesis, and oligogalacturonide-related signaling. *Phytochemistry*, *57*, 929–967. https://doi.org/10.1016/S0031-9422(01)00113-3

Römheld, V., & Kirkby, E. A. (2010). Research on potassium in agriculture: Needs and prospects. *Plant and Soil*, *335*(1), 155–180. https://doi.org/10.1007/S11104-010-0520-1/FIGURES/6

Rosolem A. et al., 1994. (1994). Root growth and mineral nutrition of corn hybrids as affected by phosphorus and lime. *Communications in Soil Science and Plant Analysis*, *25*(13–14), 2491–2499. https://doi.org/10.1080/00103629409369202

Rossiter, 1978. (n.d.). Phosphorus Deficiency and Flowering in Subterranean Clover (T. subterraneum L.). *Academic.Oup.Com*. Retrieved April 6, 2022, from https://academic.oup.com/aob/article-abstract/42/2/325/174506

Routledge, A. P. M., Shelley, G., Smith, J. V., Talbot, N. J., Draper, J., & Mur, L. A. J. (2004). Magnaporthe grisea interactions with the model grass Brachypodium distachyon closely resemble those with rice (Oryza sativa). *Molecular Plant Pathology*, *5*(4), 253–265. https://doi.org/10.1111/J.1364-3703.2004.00224.X

RStudio, C. T. (2021). *R: A language and environment for statistical computing. R Foundation for Statistical Computing, Vienna, Austria. 2014*.

Sarkar P. et al.,2009, U. (n.d.). Plant cell walls throughout evolution: towards a molecular understanding of their design principles. *Academic.Oup.Com*. Retrieved April 5, 2022, from https://academic.oup.com/jxb/article-abstract/60/13/3615/533649

Scheller, 2010, U. (n.d.). Hemicelluloses. *Annualreviews.Org*. Retrieved April 4, 2022, from https://www.annualreviews.org/doi/abs/10.1146/annurev-arplant-042809-112315?casa_token=DIdf-lErjE8AAAAA:M2_VBoU2cYfDrMkxvP3l_1XL32s14KIZm0Pf33TOHS_qxJZYtVsDzK7syOXgf4QMTw9qXcHJwKo9

Schlegel, A. J., Grant, C. A., & Havlin, J. L. (2005). Challenging approaches to nitrogen fertilizer recommendations in continuous cropping systems in the Great Plains. *Agronomy Journal*, *97*(2), 391–398. https://doi.org/10.2134/AGRONJ2005.0391

Scholthof, K., Irigoyen, S., … P. C.-T. P., & 2018, undefined. (n.d.). Brachypodium: A Monocot Grass Model Genus for Plant Biology. *Academic.Oup.Com*. Retrieved April 4, 2022, from https://academic.oup.com/plcell/article-abstract/30/8/1673/6099156

Schroeder et al.,2013, U. (n.d.). Using membrane transporters to improve crops for sustainable food production. *Nature.Com*. Retrieved April 5, 2022, from https://idp.nature.com/authorize/casa?redirect_uri=https://www.nature.com/articles/nature11909&casa_token=YYXqFsIkR90AAAAA:Jp9gObXqFvxx6lqfgUJ7sSK9YKCWkwz4aPr9q_V8hSmTORMmrsfbtlCoH53NXKg7d2dr7BGwYFc4Gu5T

Schuster, 2011, U. (n.d.). Marker-assisted selection for quantitative traits. *SciELO Brasil*. Retrieved April 6, 2022, from https://www.scielo.br/pdf/cbab/v11nspe/08.pdf

Schwartz & Amasino, 2013, U. (n.d.). Nitrogen recycling and flowering time in perennial bioenergy crops. *Frontiersin.Org*. Retrieved April 7, 2022, from https://www.frontiersin.org/articles/10.3389/fpls.2013.00076/full

Schwartz, C. J., Doyle, M. R., Manzaneda, A. J., Rey, P. J., Mitchell-Olds, T., & Amasino, R. M.

(2010). Natural variation of flowering time and vernalization responsiveness in Brachypodium distachyon. *Bioenergy Research*, *3*(1), 38–46. https://doi.org/10.1007/S12155-009-9069-3

Seeley, 1950, U. (n.d.). Potassium deficiency of greenhouse roses. *Cabdirect.Org*. Retrieved April 7, 2022, from https://www.cabdirect.org/cabdirect/abstract/19510303889

Serba, D. D., Daverdin, G., Bouton, J. H., Devos, K. M., Brummer, E. C., & Saha, M. C. (2015). Quantitative Trait Loci (QTL) Underlying Biomass Yield and Plant Height in Switchgrass. *BioEnergy Research*, *8*(1), 307–324. https://doi.org/10.1007/S12155-014-9523-8

Shaar-Moshe et al., 2017. (n.d.). Unique physiological and transcriptional shifts under combinations of salinity, drought, and heat. *Academic.Oup.Com*. Retrieved April 7, 2022, from https://academic.oup.com/plphys/article-abstract/174/1/421/6116735

Shabala, S., & Pottosin, I. (2014). Regulation of potassium transport in plants under hostile conditions: Implications for abiotic and biotic stress tolerance. *Physiologia Plantarum*, *151*(3), 257–279. https://doi.org/10.1111/ppl.12165

Sheikh, B. A. (2006). Hydroponics: Key to sustain agriculture in water stressed and urban environment. *Pakistan Journal of Agriculture Agricultural Engineering and Veterinary Sciences*, *22*(2), 53–57.

Shimada, S., Ogawa, T., Kitagawa, S., Suzuki, T., Ikari, C., Shitsukawa, N., Abe, T., Kawahigashi, H., Kikuchi, R., Handa, H., & Murai, K. (2009). A genetic network of flowering-time genes in wheat leaves, in which an APETALA1/FRUITFULL-like gene, VRN1, is upstream of FLOWERING LOCUS T. *Plant Journal*, *58*(4), 668–681. https://doi.org/10.1111/J.1365-313X.2009.03806.X

Simon et al., 2008, U. (n.d.). Quantitative Trait Loci Mapping in Five New Large Recombinant Inbred Line Populations of Arabidopsis thaliana Genotyped With Consensus Single-Nucleotide. *Academic.Oup.Com*. Retrieved April 7, 2022, from https://academic.oup.com/genetics/article-abstract/178/4/2253/6073925

Singh, B., & Singh, A. (2015). *Marker-assisted plant breeding: principles and practices*.

https://link.springer.com/content/pdf/10.1007/978-81-322-2316-0.pdf

Singh S. K. et al., 2017. (2017). Relationship between photosynthetic pigments and chlorophyll fluorescence in soybean under varying phosphorus nutrition at ambient and elevated CO2. *Photosynthetica*, *55*(3), 421–433. https://doi.org/10.1007/S11099-016-0657-0

Sluiter, A., Hames, B., Ruiz, R., Scarlata, C., Sluiter, J., Templeton, D., & Crocker, D. (2012). Determination of structural carbohydrates and lignin in biomass. *Laboratory Analytical Procedure (LAP)*, *April 2008*, 1–17. https://doi.org/NREL/TP-510-42618

Smith BG & PJ Harris, 1999. (n.d.). The polysaccharide composition of Poales cell walls: Poaceae cell walls are not unique. *Elsevier*. Retrieved April 4, 2022, from https://www.sciencedirect.com/science/article/pii/S0305197898000684?casa_token=28eoNI4UwbcAAAAA:I6q_4ieUkwkg6gzbg2RN-SFIGPTbWvWNQ-DH4Zv1ZMrDX9M8aOomDz357S46VMrzm1RpSxKPUA

Srinivasarao C. et al., 2016, U. (n.d.). Chlorophyll fluorescence induction kinetics and yield responses in rainfed crops with variable potassium nutrition in K deficient semi-arid alfisols. *Elsevier*. Retrieved April 5, 2022, from https://www.sciencedirect.com/science/article/pii/S1011134415300798

Starnes, D., Padmanabhan, P., biochemistry, S. S.-P. physiology and, & 2008, undefined. (n.d.). Effect of P sources on growth, P accumulation and activities of phytase and acid phosphatases in two cultivars of annual ryegrass (Lolium multiflorum L.). *Elsevier*. Retrieved April 3, 2022, from https://www.sciencedirect.com/science/article/pii/S0981942807001258?casa_token=pOuiU_R7CyUAAAAA:FbMnIPubA7OqXZ2ytRQAbl9MoypAFalihrWGNZBVLDOmBiCqXnR4QKONZuTvsnxWpzUxzXvaww

Steingrobe, B., & Claassen, N. (2000). Potassium Dynamics in the Rhizosphere and K Efficiency of Crops 1. *J. Plant Nutr. Soil Sci*, *163*, 101–106. https://doi.org/10.1002/(SICI)1522-2624(200002)163:1

Studer, M. H., DeMartini, J. D., Davis, M. F., Sykes, R. W., Davison, B., Keller, M., Tuskan, G.

A., Wyman, C. E., & . (2011). Lignin content in natural *Populus* variants affects sugar release. *Proceedings of the National Academy of Sciences*, *108*(15), 6300–6305. https://doi.org/10.1073/pnas.1009252108

Su, J., Xiao, Y., Li, M., Liu, Q., Li, B., Tong, Y., Jia, J., Soil, Z. L.-P. and, & 2006, undefined. (2006). Mapping QTLs for phosphorus-deficiency tolerance at wheat seedling stage. *Springer*, *281*(1–2), 25–36. https://doi.org/10.1007/s11104-005-3771-5

Swadesh, J. (2001). *HPLC : practical and industrial applications*. 461.

Swift et al., 2020, U. (n.d.). Nutrient dose-responsive transcriptome changes driven by Michaelis–Menten kinetics underlie plant growth rates. *National Acad Sciences*. Retrieved April 4, 2022, from https://www.pnas.org/content/117/23/12531.short

Team, R. C. (2020). *R: A language and environment for statistical computing. R Foundation for Statistical Computing, Vienna, Austria.*

Thuynsma et al., 2016, U. (n.d.). The effects of limiting phosphate on photosynthesis and growth of Lotus japonicus. *Elsevier*. Retrieved April 7, 2022, from https://www.sciencedirect.com/science/article/pii/S0254629915325783

Trethewey, J. A. K., Campbell, L. M., & Harris, P. J. (2005). (1→3),(1→4)-β-D-glucans in the cell walls of the Poales (sensu lato): An immunogold labeling study using a monoclonal antibody. *American Journal of Botany*, *92*(10), 1660–1674. https://doi.org/10.3732/AJB.92.10.1660

Tscharntke, T., Clough, Y., Wanger, T. C., Jackson, L., Motzke, I., Perfecto, I., Vandermeer, J., & Whitbread, A. (2012). Global food security, biodiversity conservation and the future of agricultural intensification. *Biological Conservation*, *151*(1), 53–59. https://doi.org/10.1016/J.BIOCON.2012.01.068

Tyler, L., Fangel, J. U., Fagerström, A. D., Steinwand, M. A., Raab, T. K., Willats, W. G. T., & Vogel, J. P. (2014). Selection and phenotypic characterization of a core collection of Brachypodium distachyon inbred lines. *BMC Plant Biology*, *14*(1). https://doi.org/10.1186/1471-2229-14-25

Ulvskov, P., Wium, H., Bruce, D., Jørgensen, B., Qvist, K. B., Skjøt, M., Hepworth, D., Borkhardt, B., & Sørensen, S. O. (2005). Biophysical consequences of remodeling the neutral side chains of rhamnogalacturonan I in tubers of transgenic potatoes. *Planta*, *220*(4), 609–620. https://doi.org/10.1007/s00425-004-1373-8

Vain P., 2011, U. (n.d.). Brachypodium as a model system for grass research. *Elsevier*. Retrieved April 5, 2022, from https://www.sciencedirect.com/science/article/pii/S0733521011000804?casa_token=CeufXgnvepIAAAAA:der66dOWsbrYIKVNLKiHaES0hIN54CQxCPckIo1OrluKa_sl4HcpIjTL8IlbzgW8lYwK418R_Q

Van Ooijen, 2011, U. (n.d.). Multipoint maximum likelihood mapping in a full-sib family of an outbreeding species. *Cambridge.Org*. https://doi.org/10.1017/S0016672311000279

Vance, C. P., Uhde-Stone, C., & Allan, D. L. (2003). Phosphorus acquisition and use: critical adaptations by plants for securing a nonrenewable resource. *New Phytologist*, *157*(3), 423–447. https://doi.org/10.1046/J.1469-8137.2003.00695.X

Verelst, W., Bertolini, E., De Bodt, S., Vandepoele, K., Demeulenaere, M., Pè, M. E., & Inzé, D. (2013). Molecular and physiological analysis of growth-limiting drought stress in brachypodium distachyon leaves. *Molecular Plant*, *6*(2), 311–322. https://doi.org/10.1093/mp/sss098

Vidal et al., 2014, U. (n.d.). Nitrogen control of developmental phase transitions in Arabidopsis thaliana. *Academic.Oup.Com*. Retrieved April 6, 2022, from https://academic.oup.com/jxb/article-abstract/65/19/5611/2877503

Vogel J., 2008. (2008). Unique aspects of the grass cell wall. *Current Opinion in Plant Biology*, *11*(3), 301–307. https://doi.org/10.1016/j.pbi.2008.03.002

Vogel, J. (2016). *Genetics and genomics of Brachypodium*. https://link.springer.com/content/pdf/10.1007/978-3-319-26944-3.pdf

Vogel, J. P., Garvin, D. F., Mockler, T. C., Schmutz, J., Rokhsar, D., Bevan, M. W., Barry, K., Lucas, S., Harmon-Smith, M., Lail, K., Tice, H., Grimwood, J., McKenzie, N., Huo, N., Gu,

Y. Q., Lazo, G. R., Anderson, O. D., You, F. M., Luo, M. C., … Baxter, I. (2010). Genome sequencing and analysis of the model grass Brachypodium distachyon. *Nature*, *463*(7282), 763–768. https://doi.org/10.1038/NATURE08747

Wada, K. C., & Takeno, K. (2010). Stress-induced flowering. *Plant Signaling and Behavior*, *5*(8), 944–947. https://doi.org/10.4161/PSB.5.8.11826

Wakeel, A. (2013). Potassium–sodium interactions in soil and plant under saline-sodic conditions. *Journal of Plant Nutrition and Soil Science*, *176*(3), 344–354. https://doi.org/10.1002/JPLN.201200417

Wang, M., Zheng, Q., Shen, Q., molecular, S. G.-I. journal of, & 2013, undefined. (n.d.). The critical role of potassium in plant stress response. *Mdpi.Com*. Retrieved April 4, 2022, from https://www.mdpi.com/1422-0067/14/4/7370

Wang, W., Vinocur, B., & Altman, A. (2003). Plant responses to drought, salinity and extreme temperatures: Towards genetic engineering for stress tolerance. *Planta*, *218*(1), 1–14. https://doi.org/10.1007/S00425-003-1105-5

Wang, Y., Chen, Y. F., & Wu, W. H. (2021). Potassium and phosphorus transport and signaling in plants. *Journal of Integrative Plant Biology*, *63*(1), 34–52. https://doi.org/10.1111/JIPB.13053

Wang Y. et al., 2019, U. (n.d.). Research progress on heat stress of rice at flowering stage. *Elsevier*. Retrieved April 7, 2022, from https://www.sciencedirect.com/science/article/pii/S1672630818300829

Wang, Z., Wu, X., Ren, Q., Chang, X., Li, R., & Jing, R. (2010). QTL mapping for developmental behavior of plant height in wheat (Triticum aestivum L.). *Euphytica*, *174*(3), 447–458. https://doi.org/10.1007/S10681-010-0166-3/TABLES/5

Warington,1923, U. (n.d.). The effect of boric acid and borax on the broad bean and certain other plants. *JSTOR*. Retrieved April 5, 2022, from https://www.jstor.org/stable/43236455?casa_token=MaBSbeKP1lgAAAAA:5uGMTmdvMjEgmG-

rUbJobg_YL5OJwTPHQFAFBkokhJk5jilf8odDc2vU1GZAdWFYGXYDAGic8jFnoN_6z17icsfKij8g1SXmpCbmza-1UrTQVJ8eCsw

Wasaya A. et al., 2017, U. (n.d.). Influence of varying tillage systems and nitrogen application on crop allometry, chlorophyll contents, biomass production and net returns of maize (Zea mays L. *Elsevier*. Retrieved April 5, 2022, from https://www.sciencedirect.com/science/article/pii/S0167198717300375?casa_token=bAy8MoCofgQAAAAA:lDAYJGbq9NmNlBhTj3vBNH437hXII6O7LEImrqNDPDFmY8dAwM5biS8SVu-EvwOnhVgUzG9rqA

Watt, M., Magee, L., Phytologist, M. M.-N., & 2008, undefined. (2008). Types, structure and potential for axial water flow in the deepest roots of field-grown cereals. *Wiley Online Library*, *178*(1), 135–146. https://doi.org/10.1111/j.1469-8137.2007.02358.x

White, P. J., George, T. S., Gregory, P. J., Bengough, A. G., Hallett, P. D., & McKenzie, B. M. (2013). Matching roots to their environment. *Annals of Botany*, *112*(2), 207–222. https://doi.org/10.1093/AOB/MCT123

Wickham & Chang, 2016, U. (n.d.). Package "ggplot2." *Cran.Microsoft.Com*. Retrieved April 6, 2022, from https://cran.microsoft.com/snapshot/2015-01-06/web/packages/ggplot2/ggplot2.pdf

Wolf, S., Mouille, G., & Pelloux, J. (2009). Homogalacturonan methyl-esterification and plant development. *Molecular Plant*, *2*(5), 851–860. https://doi.org/10.1093/mp/ssp066

Woods & Amasino et al., 2015. (2015). *Dissecting the Control of Flowering Time in Grasses Using Brachypodium distachyon*. 259–273. https://doi.org/10.1007/7397_2015_10

Woods, D. P., Bednarek, R., Bouché, F., Gordon, S. P., Vogel, J. P., Garvin, D. F., & Amasino, R. M. (2017). Genetic architecture of flowering-time variation in Brachypodium distachyon. *Plant Physiology*, *173*(1), 269–279. https://doi.org/10.1104/pp.16.01178

Wormit, A., & Usadel, B. (2018a). The multifaceted role of pectin methylesterase inhibitors (PMEIs). *International Journal of Molecular Sciences*, *19*(10), 1–19. https://doi.org/10.3390/ijms19102878

Wormit, A., & Usadel, B. (2018b). The Multifaceted Role of Pectin Methylesterase Inhibitors (PMEIs). *International Journal of Molecular Sciences 2018, Vol. 19, Page 2878*, *19*(10), 2878. https://doi.org/10.3390/IJMS19102878

Wu, D., Sun, Y., Wang, H., Shi, H., Su, M., Shan, H., Li, T., & Li, Q. (2018). The SlNAC8 gene of the halophyte Suaeda liaotungensis enhances drought and salt stress tolerance in transgenic Arabidopsis thaliana. *Gene*, *662*, 10–20. https://doi.org/10.1016/J.GENE.2018.04.012

Wuebbles, D., Fahey, D., & Hibbard, K. (2017). *Climate science special report: fourth national climate assessment, volume I*. https://repository.library.noaa.gov/view/noaa/19486/noaa_19486_DS1.pdf

Xu, C., Gao, J., Du, Z., Li, D., Wang, Z., Li, Y., reports, X. P.-S., & 2016, undefined. (n.d.). Identifying the genetic diversity, genetic structure and a core collection of Ziziphus jujuba Mill. var. jujuba accessions using microsatellite markers. *Nature.Com*. Retrieved April 4, 2022, from https://www.nature.com/articles/srep31503

Xu et al., 1997, U. (n.d.). Chromosomal regions associated with segregation distortion of molecular markers in F2, backcross, doubled haploid, and recombinant inbred populations in rice. *Springer*. Retrieved April 6, 2022, from https://idp.springer.com/authorize/casa?redirect_uri=https://link.springer.com/article/10.1007/s004380050355&casa_token=HAQfpycbJfEAAAAA:eZ798Uv7GcMDNGbKhbZmQVB0R9k2DknaORgCey1wxY2mKQTAJ0NhcW-op-jy96VILkDzY5y4WpixBIlu

Xu Y., 2010. (2010). *Molecular plant breeding*. https://books.google.com/books?hl=en&lr=&id=PRGM-iHuJcMC&oi=fnd&pg=PR5&dq=Xu,+2010+DNA+MOLECULES+IN+PLANTS&ots=FQTHsRAPcE&sig=5cmYoK7JHBhz193WsgyktNpfxFA

Yan et al., 2006, U. (n.d.). The wheat and barley vernalization gene VRN3 is an orthologue of FT. *National Acad Sciences*. Retrieved April 7, 2022, from https://www.pnas.org/content/103/51/19581.short

Yan, L, Loukoianov, A., Tranquilli, G., Helguera, M., Fahima, T., & Dubcovsky, J. (2003). MADS

box genes control vernalization-induced flowering in cereals. *National Acad Sciences*, *100*, 6263. https://www.pnas.org/content/100/22/13099.short

Yan, Liuling, Loukoianov, A., Blechl, A., Tranquilli, G., Ramakrishna, W., SanMiguel, P., Bennetzen, J. L., Echenique, V., & Dubcovsky, J. (2004). The Wheat VRN2 Gene Is a Flowering Repressor Down-Regulated by Vernalization. *Science*, *303*(5664), 1640–1644. https://doi.org/10.1126/SCIENCE.1094305

Yano & Tuberosa, 2009, U. (n.d.). Genome studies and molecular genetics—from sequence to crops: genomics comes of age. *Researchgate.Net*. Retrieved April 7, 2022, from https://www.researchgate.net/profile/Roberto-Tuberosa/publication/24002394_Genome_studies_and_molecular_genetics-from_sequence_to_crops_genomics_comes_of_age/links/5a304602458515a13d8545d1/Genome-studies-and-molecular-genetics-from-sequence-to-crops-genom

Yaseen & Malhi, 2011. (2011). Exploitation of genetic variability among wheat genotypes for tolerance to phosphorus deficiency stress. *Journal of Plant Nutrition*, *34*(5), 665–699. https://doi.org/10.1080/01904167.2011.540623

Ye T. et al., 2019, U. (n.d.). Nitrogen, phosphorus, and potassium fertilization affects the flowering time of rice (Oryza sativa L.). *Elsevier*. Retrieved April 6, 2022, from https://www.sciencedirect.com/science/article/pii/S2351989419303221

Yuan et al., 2016, U. (n.d.). Arabidopsis cryptochrome 1 functions in nitrogen regulation of flowering. *National Acad Sciences*. Retrieved April 6, 2022, from https://www.pnas.org/content/113/27/7661.short

Zeng,1994, U. (n.d.). Precision mapping of quantitative trait loci. *Academic.Oup.Com*. Retrieved April 6, 2022, from https://academic.oup.com/genetics/article-abstract/136/4/1457/6012232

Zhang & Lee, 2002, U. (n.d.). High-performance anion-exchange chromatography of carbohydrates on pellicular resin columns. *Elsevier*. Retrieved April 4, 2022, from https://www.sciencedirect.com/science/article/pii/S0301477002800318

Zhang H. et al., 2007, U. (n.d.). Signalling mechanisms underlying the morphological responses of the root system to nitrogen in Arabidopsis thaliana. *Academic.Oup.Com*. Retrieved April 6, 2022, from https://academic.oup.com/jxb/article-abstract/58/9/2329/544342

Zhang, H., Fangel, J., Willats, W., … M. S.-G., & 2014, undefined. (2013). Assessment of leaf/stem ratio in wheat straw feedstock and impact on enzymatic conversion. *Wiley Online Library*, *6*(1), 90–96. https://doi.org/10.1111/gcbb.12060

Zhang, J., Klueva, N. Y., Wang, Z., Wu, R., Ho, T. H. D., & Nguyen, H. T. (2000). Genetic engineering for abiotic stress resistance in crop plants. *In Vitro Cellular and Developmental Biology - Plant*, *36*(2), 108–114. https://doi.org/10.1007/S11627-000-0022-6

Zhong, S., Ali, S., Leng, Y., Wang, R., & Garvin, D. F. (2015). Brachypodium distachyon-cochliobolus sativus pathosystem is a new model for studying plant-fungal interactions in cereal crops. *Phytopathology*, *105*(4), 482–489. https://doi.org/10.1094/PHYTO-08-14-0214-R

Zhu et al., 2014, U. (n.d.). Effect of different levels of nitrogen deficiency on switchgrass seedling growth. *Elsevier*. Retrieved April 7, 2022, from https://www.sciencedirect.com/science/article/pii/S221451411400035X

Zhu, J., Kaeppler, S., Biology, J. L.-F. P., & 2005, undefined. (2005). Topsoil foraging and phosphorus acquisition efficiency in maize (Zea mays). *CSIRO Publishing*. https://doi.org/10.1071/FP05005